DISCOVERY OF PROTEIN-PROTEIN INTERACTIONS OF THE LYSYL OXIDASE ENZYME: IMPLICATIONS FOR CARDIOVASCULAR DISEASE, CANCER, AND FIBROSIS.

A DISSERTATION SUBMITTED TO THE GRADUATE DIVISION OF THE UNIVERSITY OF HAWAII
IN PARTIAL FULFILLMENT OF THE REQUIREMENTS FOR THE DEGREE OF

DOCTOR OF PHILOSOPHY

IN

BIOMEDICAL SCIENCES (CELL AND MOLECULAR BIOLOGY)

MAY 2005

By
Benjamin C. Fogelgren

Dissertation Committee:

Katalin Csiszar, Chairperson
Tom Humphreys
Alan Lau
Lon White
Athula Wikramanayake

ACKNOWLEDGEMENTS

I would like to acknowledge many people that helped make this dissertation research not only possible, but also enjoyable. First and foremost, I would like to express my deepest gratitude to Dr. Katalin Csiszar for being such a supportive mentor and such a fantastic scientist. She has always been encouraging, and she has greatly contributed to my scientific and professional growth. Over the years, she has protected my independence when I needed it, but was always there to provide direction when I had trouble finding the right path. I would also like to thank my other doctoral committee members, Tom Humphreys, Alan Lau, Lon White, and Athula Wikramanayake, for all their support, advice, and time.

I need to thank several members of Katalin's laboratory who contributed directly to this work. I am grateful to Keith Fong for teaching me the yeast two-hybrid screening technique and for being a great overall intellectual partner in the laboratory. I am grateful to have been able to work with three amazing students, Noémi Polgár, Kornélia Molnárné Szauter, and Zsuzsa Újfaludi, who all contributed to this work. Also, I am grateful to other members of Katalin's laboratory, including Sheri Fong, Janos Molnar, Tongyu Cao, and Lloyd Asuncion, for helpful discussions over the years that have generated many of the ideas in this dissertation. I am particularly thankful that this laboratory has always had a utopian atmosphere for students, filled with very kind people who always take the time to offer help and friendship.

The Cardiovascular Research Center of Hawaii (and formerly The Laboratory of Matrix Pathobiology), has been an excellent environment to allow the free exchange of scientific ideas, collaboration among scientists, and friendship among colleagues. I would like to thank its Director, Charles Boyd, and many other past and present members of the Center, including Johann Urschitz, Zsolt Urban, Zoltan Szabo, and Olivier Le Saux, for their support and help over the years.

I need to thank Herb Kagan for generously providing purified bovine LOX enzyme, and Deane Mosher for generously providing the embryonic fibroblast cell lines from the fibronectin knockout mice. I would also like to thank Dawn Kirschmann for providing polyclonal anti-LOX antibody, and Qingping He and Rose Laczko for their histology assistance. I would also like to thank Bob Mecham and Phil Trackman for helpful discussions and advice regarding this project. I also wish to thank Gert De Couet for allowing me to use his lab and equipment for the yeast two-hybrid screening. I would like to acknowledge the funding of the National Institutes of Health and the American Heart Association, which made this research possible.

I would especially like to thank my wonderful wife and best friend, Yvonne Tatsumura, for being incredibly supportive during these demanding years of research. I am grateful to her for helping keep my life in the proper perspective and balance. Her extensive knowledge of genetics and molecular biology research was also very helpful. I would like to thank her family here in Hawaii for welcoming me with so much warmth and aloha. I also thank my friend and fellow graduate student Matt Tuthill for many great scientific discussions during our Sunday morning surfing sessions.

I am extremely thankful for my parents and family, who always providing love, support and encouragement throughout my life. My parents always said that the key to happiness in life was to find something that you love to do, and then find a way to make a living at doing it. This principle is what led me into science, and is why I still love to come to the lab everyday.

ABSTRACT

Lysyl oxidase (LOX) is a copper-containing amine oxidase known to catalyze the covalent cross-linking of fibrillar collagens and elastin at peptidyl lysine residues. In addition, its involvement in cancer, wound healing, cell motility, chemotaxis, and differentiation reflect a remarkable functional diversity of LOX. To investigate novel mechanisms of LOX regulation and function, we performed a yeast two-hybrid screen to identify LOX-interacting proteins. From the 58 sequenced positive cDNAs, we identified placental lactogen (PL), fibronectin (FN), and fibulin-1 (FBLN1) as putative LOX-binding proteins. In this study, we present an extensive characterization of the interaction between LOX and FN, as well as evidence suggesting an important biological function in human physiologic and disease processes. GST pull-downs and solid phase binding assays confirmed the LOX-FN interaction. LOX bound to the cellular form of FN (cFN) with a dissociation constant (K_d) of 2.5 nM. This was comparable to our measured K_d of LOX binding to tropoelastin (1.9 nM) and type I collagen (5.2 nM), but LOX demonstrated a much lower binding affinity for the plasma form of FN (pFN). Immunofluorescent microscopy revealed co-localization of FN and LOX in normal human tissues where these proteins may interact *in vivo*. LOX enzymatic activity assays showed that cFN does not seem to be a substrate of LOX. However, cFN can act as a scaffold for enzymatically active 30-kD LOX. Furthermore, in FN-null mouse embryonic fibroblasts, we observed dramatically decreased proteolytic processing of the 45-kD LOX proenzyme to the 30-kD active form, with a corresponding decrease in LOX enzyme activity. Our results suggest that the FN matrix provides specific microenvironments to regulate LOX catalytic activity.

TABLE OF CONTENTS

Acknowledgements iv
Abstract vi
List of Tables x
List of Figures xi
List of Abbreviations xiv

CHAPTER 1. INTRODUCTION 1

LYSYL OXIDASE (LOX) 1
Lysyl Oxidase Enzyme Family 3
Protein Biosynthesis 10
Biological Functions of LOX 11
Collagen and Elastin Crosslinking 11
Novel Functions 13
LOX in Mammalian Development 14
LOX IN HUMAN PATHOLOGIES 16
Diseases of Copper Metabolism 16
Cardiovascular Disease 18
Cancer 19
Cutis Laxa 21
Fibrosis 22
DISSERTATION HYPOTHESIS AND SPECIFIC AIMS 24

CHAPTER 2. YEAST TWO-HYBRID SCREENING WITH LOX 27

INTRODUCTION 27
RESULTS 30
Generation of the LOX Yeast Bait Plasmid Constructs 30
Amplification of the Yeast Two-Hybrid Library 35
Screening the Yeast Two-Hybrid Library with LOX 36
Verifying the Interactions in Yeast 41
DISCUSSION 48
MATERIALS AND METHODS 59
Polymerase Chain Reaction (PCR) 59
Agarose Gel Electrophoresis 61
DNA Purification From Agarose 62
Measurement of DNA Concentration 62
Restriction Enzyme Digestions 62
DNA Ligations 63
Bacteria Media and Plates 63

Bacterial Transformations 63
Plasmid Purifications from Bacteria 64
DNA Sequencing 65
Yeast Media and Plates 65
Yeast Transformations 66
Polyacrylamide Gel Electrophoresis (PAGE) of Proteins 67
Western Blot Analysis 68
Amplification of Two-Hybrid Library 69
Screening of Two-Hybrid Library 70
Assay for LacZ Activity in Yeast 70
Plasmid Purifications from Yeast 71

CHAPTER 3. CHARACTERIZATION OF LOX'S INTERACTION WITH FIBRONECTIN 72

INTRODUCTION 72
RESULTS 77
Generation of Expression Constructs for Recombinant LOX 77
Expression and Purification of Recombinant GST-LOX Fusion Proteins 79
In Vitro Binding Analysis using Pull-down and Far-Western Assays 85
Co-immunoprecipitation of LOX and FN from Cultured Cells 90
Solid Phase Binding Assays to Measure the Equilibrium Disassociation Constant (K_d) 91
DISCUSSION 96
MATERIALS AND METHODS 102
Cloning of GST-LOX Expression Constructs 102
Bacterial Expression of GST-LOX Fusion Proteins 103
Extraction and Purification of GST-LOX Fusion Proteins 104
Measurement of Protein Concentration in Solutions 106
Protein-Staining of SDS-PAGE Gels 106
Western Blot Analysis 107
GST Pull-down Assays 107
Far-Western Blot Analysis 108
Cell Culturing of Human Dermal Fibroblasts 109
Co-immunoprecipitations (Co-IPs) 110
Solid Phase Binding Assays 110

CHAPTER 4. INVESTIGATION OF THE BIOLOGICAL ROLE OF THE LOX-FIBRONECTIN INTERACTION 112

INTRODUCTION 112
RESULTS 117

Effects of FN on LOX's Catalytic Activity 117
Immunofluorescent Co-staining of Human Cells and Tissues 120
Analysis of LOX in FN-null Conditions 129
DISCUSSION 132
MATERIALS AND METHODS 140
Lysyl Oxidase Activity Assays 140
Measurement of Protein Concentration 141
Immunofluorescent Staining 141
Cell Culturing of Mouse Embryonic Fibroblasts 142
Western Blot Analysis 143

CHAPTER 5. FUTURE DIRECTIONS AND FINAL DISCUSSION 144

FUTURE DIRECTIONS 144
Other Candidate Interactions Identified in the LOX Yeast Two-Hybrid Screen 144
LOX-like enzymes and FN 149
Downstream of the LOX-FN Interaction 151
FINAL DISCUSSION 154
Current Working Hypothesis 158
Implications for Human Disease 160

REFERENCES 162

LIST OF TABLES

TABLE		PAGE
1.	Members of the Mammalian Amine Oxidase Family	3
2.	Mammalian Copper-dependent Enzymes	16
3.	LOX Plasmid Constructs Designed for Yeast Two-Hybrid Expression	31
4.	Positive cDNAs Identified in the LOX Yeast Two-Hybrid Screen	40
5.	Fibulin-1 and Fibronectin cDNA Fragments Isolated from in the Screen	41
6.	Sequence of PCR Primers used for Cloning LOX cDNAs into pGBKT7	60
7.	LOX Plasmid Constructs Designed for Bacterial Expression with GST	79
8.	Summary of GST-LOX Fusion Protein Expression and Fraction Analysis	83
9.	Human Tissue Macroarrays Co-stained for LOX and Fibronectin	122

LIST OF FIGURES

FIGURE		PAGE
Chapter 1		
1.	Genomic Organization of the Lysyl Oxidase Gene Family	4
2.	Annotated Amino Acid Sequence of Human LOX	5
3.	Domain Organization of the Mammalian Lysyl Oxidase Family	6
4.	Sequence Alignment of the Lysyl Oxidase Copper Binding Motifs	7
5.	The Lysyl-Tyrosylquinone Cofactor of the Lysyl Oxidase Family	8
6.	The Cytokine Receptor-Like Domain of the Lysyl Oxidase Family	9
7.	Diagram of the Catalytic Activity of the Lysyl Oxidase Enzymes	12
Chapter 2		
8.	The Principle of the Yeast Two-Hybrid Screening Technique	28
9.	The pGBKT7 Yeast Two-Hybrid Bait Vector	31
10.	Sequence from the pGBKT7-LOX Expression Construct	33
11.	Western Blot of Yeast Extracts to Detect Bait Protein Expression	34
12.	The pACT2 Yeast Two-Hybrid Library Vector	35
13.	Amplification and Sequencing of Positive Library cDNAs	38
14.	Domain Organization of the Six GAL4-BD-LOX Bait Proteins	42
15.	Representative Scans from the Direct Interaction Verification Assays	43
16.	Domain Organization of the 5 GAL4-BD-LOXL and -LOXL2 Bait Proteins	44
17.	Yeast Spotted in Direct Interaction Assays – pGADT7 and Placental Lactogen	45
18.	Yeast Spotted in Direct Interaction Assays – Fibronectin and Fibulin-1	46
19.	Streaks of Yeast in Direct Interaction Assays with Fibronectin and Fibulin-1	48
20.	3 Dimensional Structures of Placental Lactogen and Growth Hormone	51
21.	Domain Organization of the Human Fibulin Family of Proteins	53

22. Domain Organization of Human Fibronectin and Isolated Fragments 55

23. Diagram of Potential Alternative Splicing of Three Fibronectin Domains 56

Chapter 3.

24. The pGEX-4T-1 Bacterial Expression Vector 78

25. Domain Organization of the Six GST-LOX Fusion Proteins 80

26. Coomassie-stained SDS-PAGE of GST-LOX Fusion Protein Extractions 81

27. Western Blots of GST-LOX Fusion Protein Extractions 82

28. Coomassie-stained SDS-PAGE of GST-LOX Fusion Protein Purifications 85

29. Diagram of the GST Pull-down Assays 86

30. Western Blots of GST-LOX Pull-downs with Fibronectin 87

31. Far-Western Blots of GST-LOX Fusion Proteins with Fibronectin 89

32. Diagram of the Co-immunoprecipitations 90

33. Western Blot of the Co-immunoprecipitation of Fibronectin with LOX 91

34. Solid Phase Binding Assay of ECM Proteins with Immobilized GST-LOX 92

35. Solid Phase Binding Assay of GST-LOX Proteins with Immobilized Fibronectin 93

36. ELISA Verification of Anti-LOX Antibody Binding to GST-LOX 95

37. Solid Phase Binding Assay between LOX and Fibronectin with Antibody 96

38. Histidine-tagged LOX was Designed and Expressed in Low Levels 98

Chapter 4.

39. The Principle of the Fluorescent Lysyl Oxidase Activity Assay 114

40. LOX Activity Assay with Equal Molar Amounts of Various Substrates 118

41. LOX Activity Assay in the Presence of Fibronectin 119

42. LOX Activity Assay of LOX bound to Solid Phase Fibronectin 120

43. Immunofluorescent Co-staining of LOX and Fibronectin in Cultured Fibroblasts 121

44. Immunofluorescent Co-staining of LOX and Fibronectin in Human Tissues #1 124

45. Immunofluorescent Co-staining of LOX and Fibronectin in Human Tissues #2 126

46. Immunofluorescent Co-staining of LOX and Fibronectin in Human Muscle 128

47. Cultured Embryonic Fibroblasts from the Fibronectin Knockout Mouse 129

48. LOX Protein Analysis in Fibronectin-null Embryonic Fibroblast Media 131

49. Western Blot of BMP-1 in Fibronectin-null Embryonic Fibroblast Media 132

Chapter 5.

50. Far-Western Blotting Data of GST-LOX Fusion Proteins with Placental Lactogen 144

51. Solid Phase Binding Assays of GST-LOX with Immobilized Placental Lactogen 145

52. Western Blot of Placental Lactogen in Breast Cancer Cell Lines 146

53. Western Blot of the Co-immunoprecipitation of Fibulin-1 with LOX 148

54. Western Blots of LOXL and LOXL2 in Fibronectin-null Embryonic Fibroblasts Media 151

55. Model of the Current Working Hypothesis of the LOX and Fibronectin Interaction 159

LIST OF ABBREVIATIONS

aa	amino acid
A, ala	alanine
C, cys	cysteine
D, asp	aspartic acid
E, glu	glutamic acid
F, phe	phenylalanine
G, gly	glycine
H, his	histidine
I, ile	isoleucine
K, lys	lysine
L, leu	leucine
N, asn	asparagine
P, pro	Proline
Q, gln	Glutamine
R, arg	Arginine
S, ser	Serine
T, thr	Threonine
V, val	Valine
W, trp	Tryptophan
Y, tyr	Tyrosine
AD	active domain
amp^r	ampicillin resistance
ATP	adenosine triphosphate
BAPN	β-aminopropionitrile
BD	binding domain
bFGF	basic fibroblast growth factor
bLOX	bovine lysyl oxidase
BMP-1	bone morphogenic protein-1
bp	base pair
BSA	bovine serum albumin
CCM	conditioned cell media
cDNA	complementary DNA
cFN	cellular fibronectin
cfu	colony-forming unit
cm	centimeter
CMV	cytomegalovirus
Co-IP	co-immunoprecipitation
CRL	cytokine receptor-like
Cu	copper
CuAO	Copper-binding amine oxidase
D	Dalton
DAO	diamine oxidase
DEAE	diethylaminoethyl
DMEM	Dulbecco's modified Eagle medium
DNA	deoxyribonucleic acid
dNTP	deoxynucleoside triphosphate
DTT	dithiothreitol
ECM	extracellular matrix
EDTA	ethylenediamine tetracetic acid
EK	enterokinase
EK-CS	enterokinase cleavage site
ELISA	enzyme-linked immunosorbent assay
EMT	epithelial-mesenchymal transition
EtOH	ethanol
FBLN1	fibulin-1
FBLN5	fibulin-5
FBS	fetal bovine serum
FN	fibronectin
g	gram
GH	growth hormone
GHR	growth hormone receptor
GST	glutathione S-transferase
His	6x Histidine epitope tag
hr	hour
HRP	horseradish peroxidase
I	induced
IB	inclusion bodies
IF	immunofluorescent
IP	immunoprecipitation
IPTG	isopropyl-1-thio-β-D-galactopyranoside
IVTnT	*in vitro* transcription and translation
Kan^r	kanamycin resistance
kb	kilobase pair
kD	kiloDalton
K_d	equilibrium disassociation constant
Lam	lamin C

LB	Luria-Bertani
LDL	low density lipoproteins
LOX	lysyl oxidase
LOXL	LOX-like
LOXL2	LOX-like 2
LOXL3	LOX-like 3
LOXL4	LOX-like 4
LTQ	lysyl-tyrosylquinone
LS	lysozyme soluble
M	Molar (mole/liter)
mA	milliamp
MCS	multiple cloning site
MEF	mouse embryonic fibroblast
mg	milligram
µg	microgram
ml	milliliter
µl	microliter
mm	millimeter
µm	micrometer
mM	millimolar
µM	micromolar
MAO	monoamine oxidase
min	minute
mRNA	messenger RNA
mTLD	mammalian tolloid
mTLL	mammalian tolloid-like
MW	molecular weight
MWCO	molecular weight cut off
ng	nanogram
NI	non-induced
nm	nanometer
nmol	nanomole
nM	nanomolar
OD	optical density
onfFN	oncofetal fibronectin
OMIM	Online Mendelian Inheritance in Man
ORF	open reading frame
PAGE	polyacrylamide gel electrophoresis
PAO	polyamine oxidase
PBS	phosphate buffered saline
PBST	PBS with 0.1% Tween-20
PCR	polymerase chain reaction
PEG	polyethylene glycol
pFN	plasma fibronectin
pI	isoelectric point
PL	placental lactogen
pmol	picomole
pM	picomolar
PRL	prolactin
PRLR	prolactin receptor
proLOX	full-length LOX proenzyme
PVDF	polyvinylidene fluoride
RNA	ribonucleic acid
rpm	revolutions per minute
Rrg	*ras* recision gene
RT	room temperature
SDS	sodium dodecyl sulfate
SEM	standard error measurement
SPBA	solid phase binding assay
SRCR	scavenger receptor cysteine rich
SS	signal sequence
SSAO	semicarbizide-sensitive amine oxidase
TAE	Tris-acetate-EDTA
TE	Tris-EDTA
TGF-β	transforming growth factor-β
ThCS	thrombin cleavage site
TPQ	topaquinone
U	unit
UAS	upstream activating sequence
UTR	untranslated region
UV	ultraviolet
V	volts
VAP-1	vascular adhesion protein-1
VSMC	vascular smooth muscle cells
x g	times gravitational force
Zn	zinc

CHAPTER 1. INTRODUCTION

No cell is an island. Throughout decades of cell biology research, increasing attention has been focused on a cell's extracellular environment as a determinant of cellular function and fate. Cells receive signals to grow, divide, differentiate, migrate, commit suicide, or secrete their own signaling molecules, all from extracellular environmental signals. The extracellular matrix (ECM), a complex network of fibrous proteins and polysaccharides, is the supporting structure that gives human tissues strength and elasticity. In many human diseases, an imbalance of ECM deposition, assembly, or degradation, either as a primary or secondary determinant, contributes greatly to the pathology. This dissertation research is focused on a critical enzyme, lysyl oxidase, that is involved in ECM assembly, and that has a wide range of influence over cellular functions.

LYSYL OXIDASE (LOX)

The discovery of LOX was due to the convergence of two areas of scientific research in the 1960s. The first was the study of lathyrism, a disease condition known to cause increased fragility of connective tissues and increased solubility of collagen from most tissues. It was known that chronic ingestion of the sweet pea *Lathyrys odoratus* resulted in lathyrism [1], and the main causative agent of the symptoms was found to be β-(γ-glutamyl)aminopropionitrile which gets metabolized *in vivo* to β-aminopropionitrile (BAPN) [2, 3]. In lathyrism, it was found that newly synthesized collagen failed to become insoluble, and not that the already insoluble collagen was degraded [4-6]. In further research, it was discovered that lathyritic collagen had reduced levels of covalent crosslinks, with corresponding increases in lysine residues [7-10]. It was also

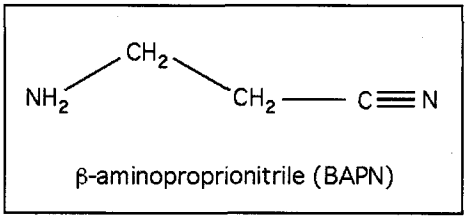

β-aminoproprionitrile (BAPN)

discovered that lathyritic elastin in the aorta contained decreased covalent crosslinks and increased lysine residues [11-13].

The second major area of research was focused on dietary copper deficiency. Since dietary copper was found to be nutritionally essential in a landmark study in 1928 [14], research has continued to investigate the consequences of copper deficiency on mammalian growth and development. What was discovered was that animal models with a limited copper intake displayed phenotypes similar to lathyritic animals, with premature death due to ruptures of large blood vessels [15-21]. The animals also displayed an increased proportion of soluble collagen and elastin, with a decreased number of covalent crosslinks in both collagen and elastin [11, 15, 22]. Protein extracts from kidneys of normal animals could increase elastin crosslinking in cultures from copper-deficient animals, but boiling of the extracts inhibited this affect [23]. From the theoretical conversion of a peptidyl lysine to δ-aminoadipic-β-semialdehyde (or allysine), an amine oxidase enzyme was theorized to carry out such a reaction, and several isolated amine oxidases had been shown to contain copper [24-26].

Results from the two areas of research suggested the existence of a copper-dependent enzyme which converts peptidyl lysines to the allysines that form the intermolecular covalent crosslinks in collagen and elastin, and which is inhibited by lathyrogens. In the first paper to establish a method for measuring catalytic crosslinking activity, Pinnell and Martin demonstrated that BAPN was an irreversible inhibitor of an extracellular enzyme with substrate specificity for peptidyl lysine residues [27]. This enzyme would be named lysyl oxidase (LOX) [28-31].

The LOX enzyme belongs to the amine oxidase enzyme family, which includes monoamine oxidases A and B (MAO A and MAO B), polyamine oxidase (PAO), semicarbizide-sensitive amine oxidase (SSAO) or vascular adhesion protein-1 (VAP-1), and diamine oxidase (DAO) [32, 33]. This enzyme family is subdivided based on their cofactors, which is either a flavin-adenine dinucleotide (FAD) cofactor or a copper atom and a quinone cofactor (Table 1). The FAD-containing enzymes can oxidize primary, secondary, or tertiary amines [34, 35], but the quinone-containing copper-binding amine oxidases (CuAO) only oxidize primary amines in which

the amino group is linked to an unsubstituted -CH_2 [36-40]. LOX, and the four mammalian LOX-like enzymes, contain a copper atom and a unique lysyl-tyrosylquinone (LTQ), which is critical for its catalytic activity [38, 39, 41](Table 1). The peptidyl lysine substrates of the lysyl oxidase family also make it unique among the amine oxidases, which primarily act on small soluble polyamines.

Table 1. Members of the mammalian amine oxidase family are categorized by their cofactors. MAO and PAO have a FAD cofactor, and DAO, SSAO/VAP-1, and LOX have copper and quinone cofactors.

Amine Oxidase	Enzyme Classification	Co-factors	Substrates
MAO A & B	EC 1.4.3.4	FAD	Arylalkyl amines (dopamine, serotonin, benzylamine, phenethylamine)
PAO	EC 1.5.3.11	FAD	Di and Polyamines (spermine, spermidine)
DAO	EC 1.4.3.6	Copper + Quinone (TPQ)	Diamines (histamines, cadaverine, putrescine, spermine, etc.)
SSAO /VAP-1	EC 1.4.3.6	Copper + Quinone (TPQ)	Monoamines (dopamine, methylamine, aminoacetone, tyramine)
LOX and LOX-like	EC 1.4.3.13	Copper + Quinone (LTQ)	Peptidyl lysines (collagen, elastin, novel), cadaverine, benzylamine

Lysyl oxidase enzyme family

When LOX was first purified from such tissues as chick cartilage, aorta, and lung, it separated based on DEAE chromatography into multiple isoforms [42-48]. This result led to the hypothesis that the multiple forms were LOX isozymes. However, it wasn't until the 1990's that the first lysyl oxidase-like enzyme (LOXL) was identified and characterized [49, 50]. In the past decade, with the emergence of human genome sequencing, the complete lysyl oxidase enzyme family has been identified [51-58]. There are four LOX-like amine oxidases in mammals (LOXL, LOXL2, LOXL3, and LOXL4) that share several homologous domains [41].

The genes for these five lysyl oxidase enzymes are spread throughout the genome, each on a different chromosome (Figure 1). Based on the human genome data at Ensembl (http://www.ensembl.org): LOX spans 11.9 kb on chromosome 5 with 7 exons; LOXL spans 25.7

kb on chromosome 15 with 7 exons; LOXL2 spans 106.9 kb on chromosome 8 with 14 exons; LOXL3 spans 21.1 kb on chromosome 2 with 14 exons; LOXL4 spans 20.6 kb on chromosome 10 with 15 exons. Based on the organization of the exons and the length of the genes' open reading frames (ORF), the lysyl oxidase genes can be subdivided into two groups; LOX and LOXL are most similar to each other, and LOXL2, LOXL3, and LOXL4 are most similar to each other. The exons containing the conserved sequence that is highly homologous between all the lysyl oxidase genes are in shown red in Figure 1. This shared homologous sequence defines this enzyme family, and encodes the catalytic site and a C-terminal cytokine receptor-like domain [41].

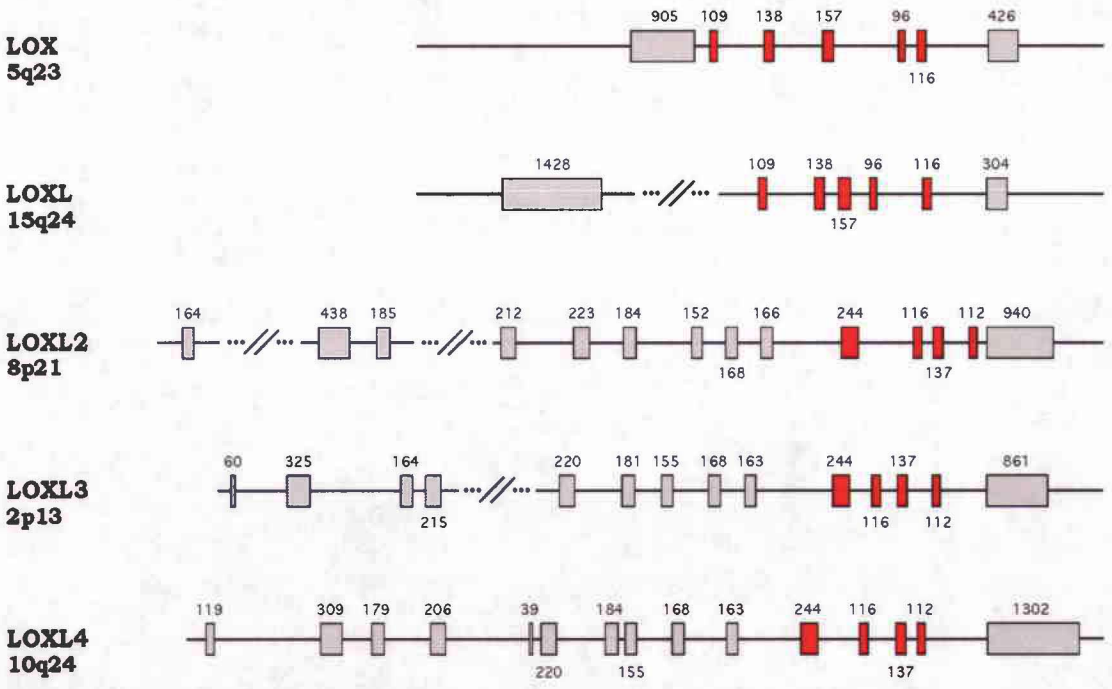

Figure 1. The genomic organization of the human lysyl oxidase gene family. The chromosomal locations are indicated, as are the number of basepairs in each exon. The exons in red include the highly homologous sequence that encodes the catalytic site and defines the lysyl oxidase gene family. Data from Ensembl database (http://www.ensembl.org/).

Multiple species of LOX mRNA have been detected (5.5, 4.3, 2.4, and 2.0 kb) by Northern blot analysis, due to alternative polyadenylation and transcription initiation sites [59-61]. However, the open reading frame of the human LOX gene is 1251 kb, resulting in a translated protein of 417 amino acids (Genbank Accession #NM_002317). The LOX amino acid sequence is annotated in Figure 2.

```
1    MRFAWTVLLL GPLQLCALVH CAPPAAGQQQ PPREPPAAPG AWRQQIQWEN NGQVFSLLSL
61   GSQYQPQRRR DPGAAVPGAA NASAQQPRTP ILLIRDNRTA AARTRTAGSS GVTAGRPRPT
121  ARHWFQAGYS TSRAREAGAS RAENQTAPGE VPALSNLRPP SRVDGMVGDD PYNPYKYSDD
181  NPYYNYYDTY ERPRPGGRYR PGYGTGYFQY GLPDLVADPY YIQASTYVQK MSMYNLRCAA
241  EENCLASTAY RADVRDYDHR VLLRFPQRVK NQGTSDFLPS RPRYSWEWHS CHQHYHSMDE
301  FSHYDLLDAN TQRRVAEGHK ASFCLEDTSC DYGYHRRFAC TAHTQGLSPG CYDTYGADID
361  CQWIDITDVK PGNYILKVSV NPSYLVPESD YTNNVVRCDI RYTGHHAYAS GCTISPY
```

Figure 2. Annotated amino acid sequence of human LOX. The propeptide region, which is cleaved between G168 and D169 by BMP-1, is underlined. The signal sequence to designate LOX for secretion is in blue. The copper-binding motif is in red. The CRL domain is in green. The lysyl residue (K314) and the tyrosyl residue (Y349) that together form the LTQ cofactor are boxed.

Analysis of the protein domain organization of the lysyl oxidase family shows a high degree of homology in the C-terminal domains, but diversity in the N-terminal domains (Figure 3). Each protein has a signal sequence on the N-terminal end that designates it for secretion. The copper-binding site is well-conserved, as is the cytokine-receptor like (CRL) domain on the C-terminus. The N-terminal regions of these proteins show more variation; LOXL2, LOXL3, and LOXL4 contain four scavenger receptor cysteine-rich (SRCR) domains [62], and LOXL contains a proline-rich domain [41, 57, 58].

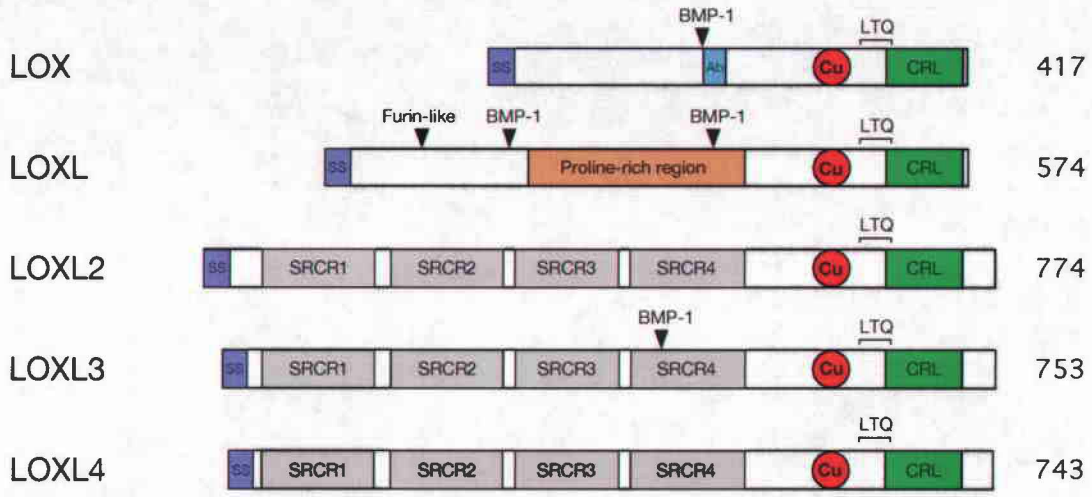

Figure 3. Domain organization of the five members of the mammalian lysyl oxidase family. Each protein contains a signal sequence (purple), a copper-binding domain (red), and a cytokine receptor-like (CRL) domain (green). In addition, LOXL2, LOXL3, and LOXL4 also contain four N-terminal scavenger-receptor cysteine-rich (SRCR) domains (grey), and LOXL has a proline-rich region (orange). The 22-mer peptide used as an epitope to generate a polyclonal anti-LOX antibody is marked in blue. The known proteolytic processing sites are marked by arrowheads, and the number of amino acids of each protein is listed on the right.

The copper-binding motif of each enzyme consists of 11 residues, with 4 histidines that coordinate the binding of the copper molecule (Figure 4). As in all CuAO whose molecular structure has been described, three of the four histidines bind to the copper atom via their nitrogen atoms, with help from a nearby carboxylate oxygen contributed by a nearby residue [63-68]. The copper molecule gets incorporated into the lysyl oxidase enzymes during transport through the Golgi apparatus [69]. The presence of copper has been shown to be essential for catalytic function [67], and it was theorized that this was the result of the copper participating in the formation and stablization of the LTQ co-factor [70], but it is unclear if the copper atom itself contributes to the amine oxidase reaction directly. In one study, LOX molecules that were stripped of their copper atoms, but were able to maintain their LTQ, retained only 50-60% of their catalytic activity [71]. This suggests that the copper atom may actually participate in the oxidation reaction or may be involved in interacting with the substrate molecule.

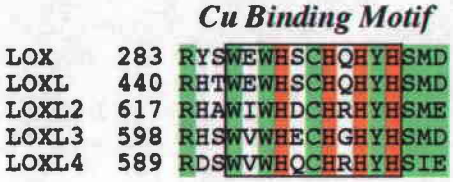

Figure 4. Sequence alignment of the copper-binding motifs for the human lysyl oxidase enzymes. The 11-residue binding site is boxed. Conserved residues are highlighted in green, and the four histidine residues thought to contribute to binding the copper atom are highlighted in orange.

LOX was first theorized to contain a carbonyl cofactor by observations that lathyrogenic compounds formed complexes with carbonyl groups [72]. The presence of a covalently-bound carbonyl cofactor was confirmed in LOX purified from bovine aorta [73, 74]. The type of carbonyl was eventually discovered to be a lysyl-tyrosylquinone (LTQ) formed from a covalent bond between lysine 314 (K314) and tyrosine 349 (Y349) [70, 75]. The LTQ cofactor is unique to the lysyl oxidase family of enzymes, and the residues involved are highly conserved (Figure 5). It is theorized that the LTQ's formation results from the oxidation of Y349 in the close presence of the copper atom while the protein is traveling through the Golgi apparatus. The NH_2 group of K314 would then attack the quinone ring to form the final LTQ (Figure 5) [38, 70, 76]. Mutagenesis studies have demonstrated that the LTQ cofactor is essential for catalytic activity of lysyl oxidase [70, 75]. The LTQ is theorized to participate directly in the oxidation reaction: the primary amine of the substrate attacks the LTQ to form a quinone ketimine, and a Schiff's base reaction generates a quinolaldimine, which is then hydrolyzed to release the peptidyl allysine and form an aminophenol. To reset the cofactor for the next reaction, the aminophenol is oxidized by the copper atom generating quinoneimine and a H_2O_2 molecule. Hydrolysis of the quinoneimine results in the release of NH_3, and the restoration of the LTQ [77].

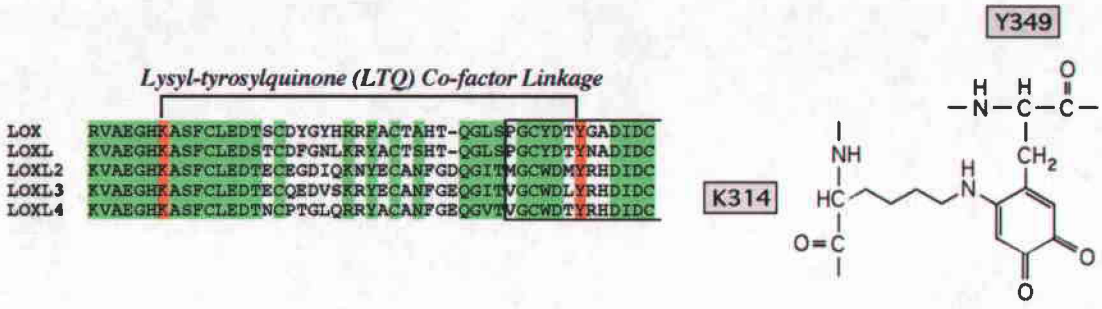

Figure 5. The LTQ cofactor is unique to the lysyl oxidase family of amine oxidases. *Left*: Sequence alignment of the LTQ-forming regions of the human lysyl oxidase enzymes. The lysine and tyrosine residues that form the LTQ are highlighted in orange. Conserved residues are highlighted in green. *Right*: Chemical structure of the LTQ cofactor, with the lysine and tyrosine residues of human LOX numbered.

The CRL domains of the human lysyl oxidase enzymes are highly conserved (Figure 6), each with homology to the N-terminal half of the class I superfamily of cytokine receptors [78]. The N-terminal half of these receptors have consensus residues that are critical in forming the barrel-shaped structure of the domain, and each lysyl oxidase family member shares these particular residues (Figure 6) [41, 57]. It is uncertain if only one half of the cytokine receptors could be functional by binding to cytokines and small signaling molecules. Theoretically, if the LOX proteins form dimers or multimers (which is discussed further below), then it's possible that multiple CRL domains could be brought close enough together to form a complete receptor-like domain. However, as of yet, no function for the CRL domain in the lysyl oxidase enzyme family has been demonstrated.

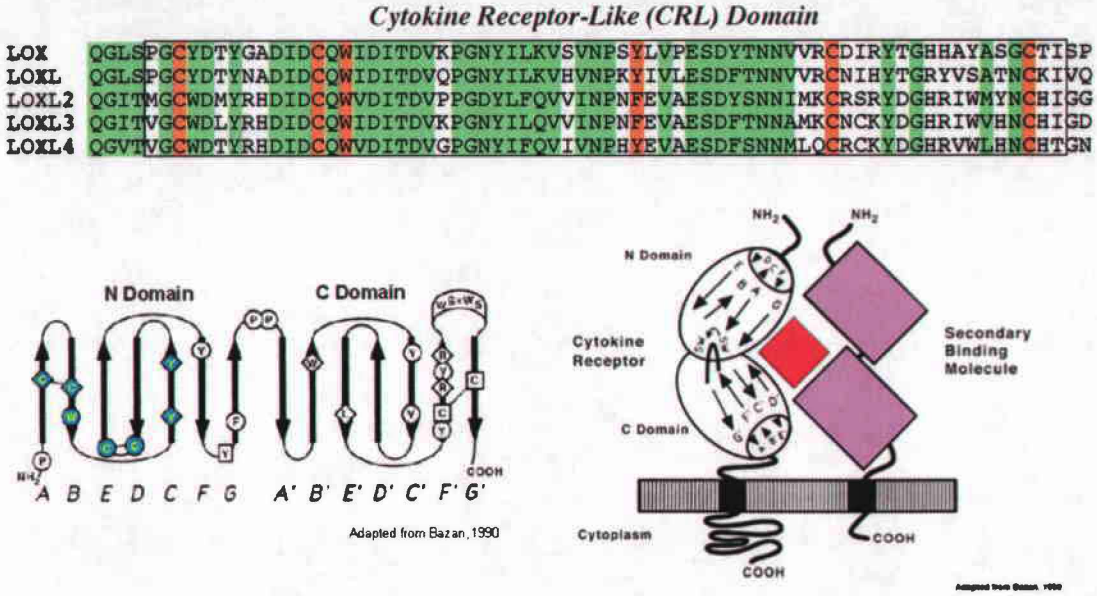

Figure 6. The CRL domain is highly conserved among the lysyl oxidase enzymes, and is named for its sequence homology to the N domain of the class I cytokine receptor. *Top*: Sequence alignment of the CRL domains of the human lysyl oxidase enzymes. Conserved residues are highlighted in green, and residues that match the consensus sequence of the cytokine receptor are highlighted in orange. *Bottom left*: Diagram of the β sheet structures forming the N domain and C domain of the class I cytokine receptors, with consensus residues identified. Residues matching the CRL domain of the lysyl oxidases are in blue. *Bottom right*: Diagram of the cytokine receptor as it dimerizes to bind a cytokine molecule. Diagrams are adapted from Bazan, 1990 [78].

The 3D structure of the LOX enzyme remains unsolved as X-ray crystallography has proved difficult with purified LOX due to its insolubility and tendency to form protein aggregates. The cloning and crystallization of a *Pichia pastoris* LOX (PPLO) has been reported [79-81], and the data suggests PPLO forms a homodimer in solution. In fact, every CuAO whose 3D structure has been solved forms a dimer, but no mammalian CuAO's 3D structure has been solved yet [40].

However, there remain doubts about the classification of this PPLO as a lysyl oxidase enzyme even though it is able to oxidize tropoelastin *in vitro* [79]. First, it has no sequence similarity to the mammalian or drosophila lysyl oxidases, only sequence similarity with members of the TPQ cofactor-containing CuAOs [79]. Indeed, PPLO contains a TPQ instead of a LTQ

[79], so it is doubtful that the 3D structure of PPLO's active site can be applied to mammalian LOX enzymes. Therefore, it remains an important goal of LOX researchers to generate enough stable mammalian LOX protein to crystallize for structural analysis.

Protein biosynthesis of LOX

The human LOX protein is translated as a 48-kD preproenzyme of 417 amino acids with an N-terminal signal sequence. During protein trafficking through the endoplasmic reticulum and Golgi, the signal peptide is cleaved off and the LOX protein acquires N-linked oligosaccharides on the N-terminal region [82]. The molecular weight increases due to this glycosylation to ~50 kD [82]. A copper molecule is incorporated at the copper-binding site (amino acids 286-296) [67, 69, 83], which allows the formation of the LTQ cofactor derived from K314 and Y349 residues [70]. The LOX protein is then secreted into the extracellular space as an inactive proenzyme (designated here as proLOX).

In the extracellular environment, the activation of LOX is a result of proteolytic cleavage between amino acids G168 and D169, which removes the N-terminal propeptide yielding an active enzyme of 30 kD (Figure 2 and 3) [82, 84-86]. This activation is accomplished by the same protease that cleaves the C-terminal propeptide ends of procollagen triple helical molecules, which is a necessary event for subsequent collagen fiber assembly. Although both the procollagen C-proteinases bone morphogenic protein-1 (BMP-1) and mammalian Tolloid-like 1 protein (mTLL-1) are able to activate LOX *in vitro*, BMP-1 has a much greater catalytic rate for LOX processing than mTLL-1 [87, 88]. In addition, LOXL has been shown to be processed by BMP-1 at more than one site, and additional processing by a furin-like enzyme has been reported (Figure 3) [89]. However, very little is known about the conditions surrounding the *in vivo* proteolytic activation of LOX or the LOX-like enzymes.

Biological functions of LOX

Collagen and Elastin Crosslinking

Collagen is a structural component of the ECM and is the most abundant protein in the human body. There have been at least 35 collagen genes identified to form a large protein family organized into 9 classes, one of which is collagens that form fibers (including type I, II, and III collagens). The formation of mature collagen fibers is highly dependent on covalent crosslinks between secreted and aligned tropocollagen molecules. Only after being crosslinked can collagen fibers provide the tensile strength necessary for the structural integrity of tissues.

Two distinct pathways of fibrillar collagen crosslinking have been characterized, and both require lysyl oxidase activity. The oxidation of lysine and hydroxylysine residues (which are formed from lysine residues by the lysyl hydroxylase enzyme) is performed by members of the lysyl oxidase enzyme family (Figure 7), and can only occur at specific residues in the N- and C-terminal telopeptides [47, 90-92]. The two pathways result in either an allysine or hydroxyallysine residue, which can then spontaneously condense with lysines, allysines, or hydroxylysines to form bi-, tri- or tetrafunctional crosslinks [93]. However, this oxidation is regulated so that fibrillar tropocollagen molecules first have to be properly aligned so that the N-terminal end of one is adjacent to the C-terminal end of another [93-95]. In this way, the collagen fiber is elongated and organized into larger diameter bundles providing increased tensile strength.

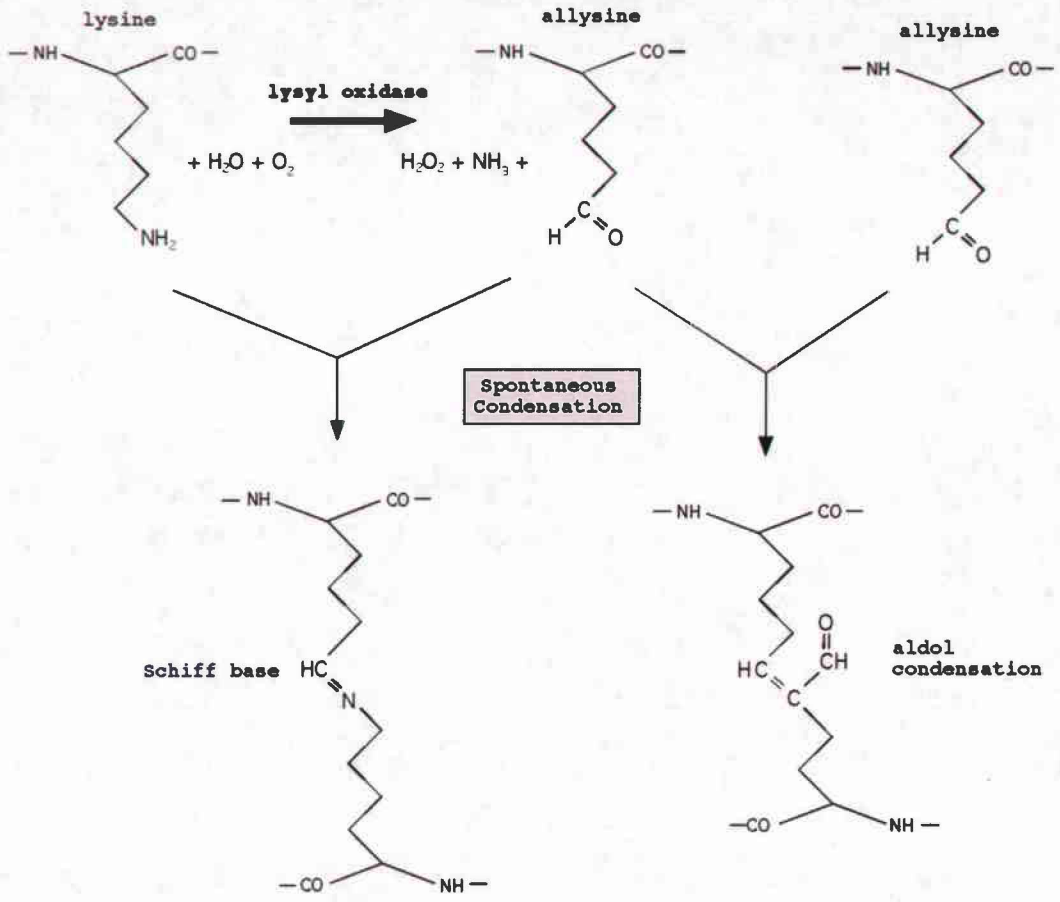

Figure 7. The catalytic activity of the lysyl oxidase amine oxidase. Peptidyl lysine residues are deaminatedly oxidized to form peptidyl allysines. The reactive aldehyde of the allysine is then able to spontaneous condense with other peptidyl lysines or allysines to form covalent cross-links between proteins. Adapted from Kagan and Cai (1995) [96].

The elasticity necessary for resilient tissues such as the skin and arteries is a result of mature elastic fibers. The process of elastic fiber assembly is complex and has been shown to be dependent on a large number of proteins. Cells secrete tropoelastin molecules, which get deposited onto microfibrils, which are comprised by a large variety of ECM proteins including fibrillins, fibulins, and various glycoproteins and proteoglycans [97-99]. The elastin is stretched along the microfibrils and crosslinked by lysyl oxidases into mature insoluble fibers [30, 94, 100-102]. In contrast to collagen, elastin contains many more lysine residues per molecule that are oxidized by lysyl oxidase enzymes, and elastin does not contain hydroxylysines. It has been

reported that 30 of the 40 lysine residues in tropoelastin are oxidized into allysines, which can then condense with lysines or allysines to form covalent crosslinks [30, 102-104]. The mature elastic fiber is a highly crosslinked mesh of elastin molecules in compacted conformations, which can expand and retract with little or no permanent deformation.

Novel Functions of LOX

In addition to its well-studied function of oxidizing the lysine residues of collagen and elastin, LOX has recently been reported to have novel biological functions. First, evidence has been accumulating for a nuclear function of LOX [105, 106]. In pre-confluent smooth muscle cell culture studies, the active LOX enzyme is able to enter the cell from the extracellular space and travel to the nucleus [107, 108]. There is also histological evidence of the LOX protein presence in the nuclei of several types of cells [109, 110]. A possible explanation for a nuclear role is given by *in vitro* biochemical experiments showing LOX oxidation of several lysine-containing basic nuclear proteins, such as histone H1 [111, 112]. This enzyme activity mirrors that of histone deacetylase complex, which results in chromatin structure modulation. There is some recent evidence to support chromatin modulation by LOX [106, 113]. The details about LOX activity in the nucleus need much more investigation, but this radical role of the LOX enzyme is challenging the dogma of LOX as only an ECM crosslinking enzyme.

LOX's influence on cell growth and cell senescence has been demonstrated, and LOX has been classified as a tumor suppressor, which will be discussed further below. It seems unlikely that LOX's control of cell growth and senescence is due entirely to its crosslinking of collagen and elastin substrates. There is also evidence for a chemotactic affect of LOX activity, which has been shown to promote the migration of various cell types, such as monocytes [114], vascular smooth muscle cells (VSMC) [115], fibroblasts [116], and breast cancer cell lines [117]. It is unclear how LOX influences this migration, but the studies demonstrated that the enzyme activity is a required component.

Another novel function of LOX that may not be explained by the collagen or elastin crosslinking is the direct transcriptional regulation of genes. An increase in LOX activity has been shown to upregulate the mRNA expression of type III collagen [118], which would be an interesting example of an enzyme regulating its substrate's expression. The proposed mechanism for this activity is LOX binding to the Ku antigen, a transcription factor that shuttles between the cytoplasm and the nucleus [118]. Studies have also shown LOX prevents *ras*'s activation of the transcription factor NF-kB [119]. However, the molecular mechanisms by which LOX regulates transcription of these genes are still unclear.

Perhaps some of LOX's diverse novel functions can be attributed to novel non-fibrillar substrates. In one study, Li et al showed that LOX oxidized basic fibroblast growth factor (bFGF) *in vitro* and in cell cultures [120]. The bFGF subsequently formed crosslinked multimers, which dramatically altered its biological functions. In this way, LOX was able to inactivate bFGF's mitogenic potential and thus regulate cell proliferation. With the reports of histone oxidation by LOX, it is becoming more likely that novel substrates for the lysyl oxidase enzymes remain to be discovered.

LOX in Mammalian Development

Many past studies have detailed the mammalian expression of LOX, and have shown that LOX is expressed in many cell types and tissues throughout the body [41, 109]. In tissues requiring mechanical strength and resiliency, like skin, heart, arteries, lungs, bone, placenta, stomach, intestine, and general connective tissue, LOX is highly expressed. LOX is also expressed in certain areas of the brain, kidney, and retina. Many clues to the importance of LOX for mammalian development have been provided by studies of lathyrism and copper deficiencies. However, due to possible overlapping expression of the LOX-like enzymes, which also are inhibited by BAPN and require a copper cofactor, these areas of research could not clearly indicate the individual contribution of LOX to mammalian development.

Recently, LOX knockout mice were created by two different research groups and individually characterized [121, 122]. These mice allowed the evaluation of LOX's contribution to normal mouse development, which had proved difficult with BAPN studies due to the overlapping expression and activity of the lysyl oxidase-like enzymes. These knockout mice did not necessarily reveal all the developmental functions of LOX, but only the ones that could not be compensated for by the LOX-like family members.

The mice homozygous deleted for the LOX gene developed to full term but died at birth due to aortic aneurysms with general cardiovascular dysfunction. There were no observable structural defects in the heart, but abnormalities were seen in the aortic walls. The elastic fibers looked fragmented with disorganized VSMC, and the vessel walls were thicker than normal in the LOX-/- mice. In addition, the diaphragm was often ruptured, likely due to a collagen defect in the central tendon, and the descending aorta was tortuous [121]. In the LOX-/- mice, detectable differences were observed in the fetal Doppler ultrasonography, indicating increased pulsatility index values for arteries and for veins, and pulmonary valve regurgitation [122]. By biochemical analysis of elastin crosslinks from aorta and lung extracts, the LOX-/- mice showed a decrease to 39% and 45%, respectively, of what was measured in wild type mice. Similar analysis of collagen crosslinks from whole body extracts showed a decrease to about 60% of that measured in wild type mice [121].

The initial two papers characterizing the LOX knockout phenotype focused on the most obvious abnormalities. In the future, more studies of these mice will certainly more clearly elucidate the specific functions of the LOX enzyme during development.

LOX IN HUMAN PATHOLOGIES

In many human pathologies, LOX expression and activity has been demonstrated to be altered compared to normal conditions. There is accumulating evidence that this misregulation of LOX contributes to the pathogenesis of these diseases.

Disease of Copper Metabolism

As discussed above, LOX is a member of the copper-dependent amine oxidase family. The proper biological functioning of these amine oxidases, and several other critical copper-binding enzymes, is dependent on the availability of copper molecules during protein biosynthesis (Table 2). Several conditions have been identified where abnormally low levels of cellular copper result in severe human pathologies. Copper was found to be nutritionally essential in 1928 [14], and since then, many studies have been done to examine the effects of nutritional copper deficiency [123-128]. Dietary deficiencies of trace elements, like copper and zinc, is a widespread problem in underdeveloped countries, but can also affect people in developed countries, including pregnant and nursing women. In contrast, too much dietary copper leads to copper toxicity due to its ability to participate in reactions that generate highly reactive oxygen species [129-131].

Table 2. Various mammalian copper-dependent enzymes [132].

Enzyme	Function
Cu, Zn-superoxide dismutase	Antioxidant
Cytochrome c oxidase	Mitochondrial respiration
Tyrosinase	Melanin production
Lysyl oxidase	Collagen and elastin crosslinking
Ceruloplasmin	Ferroxidase
Hephaestin	Intestinal iron efflux
Dopamine b-hydroxylase	Catecholamine production
Peptidylglycine a-amidating mono-oxygenase	Neuropeptide/peptide hormone processing

During fetal development, copper deficiency results in severe abnormalities of the vascular and skeletal system, dilation of the terminal airways in the lungs, and fragility of skin [133, 134]. For growing animals, a copper deficiency can also result in growth retardation, anemia, bone defects, and general weakening of connective tissues [134, 135]. There is also a strong link between cardiovascular disease and dietary copper deficiency, which can present as vascular lesions (including atherosclerosis), aneurysms, or myocardial hypertrophy [124, 136-140]. Even a mild copper deficiency may result in vascular lesions affecting elastic lamina and the vascular endothelium [138, 141, 142].

Due to the importance of LOX enzyme activity during development and homeostasis of tissues such as the heart, vasculature, bones, lungs, and connective tissues, decreased LOX activity is a main contributor to the disease symptoms in copper deficiency. Although the decreased crosslinked collagen and elastic fibers in the tissues was identified as the major causative factor for the copper-deficient phenotypes [138, 143], this does not exclude the possibility that novel functions of LOX may also be inhibited in cases of copper deficiency.

Recessive genetic syndromes involving abnormal copper metabolism have been identified, including Menkes disease (OMIM 309400), Occipital horn syndrome (OMIM 304150), and Wilson disease (OMIM 277900) [127, 132]. In normal copper metabolism, copper is ingested, absorbed in the small intestine, and stored in the liver. Excess copper is normally pumped into the bile and excreted from the body [127, 128]. Copper is imported into hepatocytes by the copper membrane transporter Ctr1, and disruption of this critical transporter leads to embryonic lethality [144, 145].

Menkes and Wilson diseases are due to mutations in the ATP7A and ATP7B genes, respectively, which encode ATP-dependent copper transporters [146-149]. Occipital horn syndrome also is caused by mutations in the ATP7A gene [150]. ATP7B is expressed in the liver and functions to excrete excess copper into the bile, and when it is defective in Wilson disease, copper accumulates to toxic levels causing progressive damage to the liver and the brain [127, 132]. ATP7A is more ubiquitously expressed, and in Menkes disease the primary symptoms

derive from defective ATP7A in intestinal cells, which prevent copper transport into the blood and leads to a general copper deficiency [127, 132]. ATP7A has been localized to the trans-Golgi network [151, 152], so cells with defective ATP7A proteins cannot transport copper from the cytosol into the Golgi apparatus for secretion. In addition, the defective ATP7A is expressed at the blood-brain barrier, which probably prevents the already low level of copper from getting into the brain [153, 154]. The resultant phenotype of Menkes disease includes brain damage, mental retardation, kinky hair, fragile bones, and aortic aneurysms [125, 127, 132]. It has been theorized that the problems of fragile bones, vascular defects, and connective tissues are largely due to the dramatically decreased lysyl oxidase activity [138, 155-158].

Cardiovascular Disease

The abnormal deposition, degradation, and repair of the ECM is a critical pathogenic factor in the development of vascular diseases [159-165]. In occlusive cardiovascular diseases, degradation of the subendothelial basement membrane results in increased permeability and migration of VSMC from the tunica media to the tunica intima [160, 166-169]. In late stage atherosclerosis, ECM proteins may be upregulated to form a fibrous lesion that when ruptured, leads to thrombus formation [160, 170]. This fibrous cap of highly crosslinked collagen and elastin may be responsible for the irreversibility of atherosclerotic lesions. Aortic and cerebral aneurysms result from degradation of the vascular ECM leading to the failure of the vessel's mechanical strength [171-174].

LOX expression has been demonstrated in almost all cardiovascular tissue and cell types, including VSMC, fibroblasts, and vascular endothelial cells [175-178]. Alterations in LOX expression and enzyme activity has been observed in a large number of cardiovascular diseases, including atherosclerosis, restenosis, hypertension, and aortic aneurysms, as well as inherited vascular and copper deficiency diseases [41, 138, 143, 179]. LOX induces chemotaxis for VSMC, which is an important event early in atherosclerosis. It was shown that the H_2O_2 product of LOX enzyme activity was the principle mediator of LOX-dependent VSMC migration

by abolishing the chemotactic effect with BAPN [115]. In addition, VSMC were shown to increase expression of stress fibers and focal adhesions in response to LOX-induced chemotaxis. In vascular endothelial cells, LOX expression is downregulated by atherogenic amounts of LDL [178] and high levels of homocysteine [180], two risk factors for atherosclerosis. This altered cellular behavior may help explain the increased permeability of the endothelium in response to high levels of LDL, as BAPN treatment caused increased permeability in endothelial cell models [178]. In hypertensive rat models with overt coronary artery disease (CAD) characterized by atherosclerotic plaque destabilization and myocardial injury, increased expression of LOX was measured in right ventricles compared to hypertensive rats with quiescent CAD [181]. When BAPN was given to rabbits after angioplasty, the inhibition of LOX resulted in lessening of restenosis [182], and in a rat model, arterial LOX mRNA expression was increased 212% by day 3 after balloon angioplasty [183].

Cancer

ECM proteins are fundamental regulators of cell growth, motility, differentiation, apoptosis, and signaling. In the cancer research field, increasing attention is being focused on the role of the ECM surrounding solid cancers as determinants of tumor growth rate, tumor invasiveness and metastatic potential, and angiogenesis [184-191]. Changes in the ECM, through degradation or a imbalance in homeostasis, are commonly associated with the appearance and spread of tumors. LOX, as a key enzyme in determining the composition of the ECM, has been implicated in a large variety of human cancers.

In one of the first papers to link LOX and cancer, LOX enzyme activity was found to be dramatically decreased in a panel of sarcoma cell lines compared with a panel of normal fibroblast lines [192]. An additional link was made when Contente et al. cloned a gene, termed *ras*-recision gene (*rrg*), that reversed the oncogenic phenotype associated with *ras* transformation of fibroblasts [193]. This *rrg* was subsequently identified as LOX [194]. In addition, when phenotypic revertants of *ras*-transformed NIH3T3 cells are transfected with

antisense LOX, they returned to a transformed phenotype [193, 194]. Transfection of normal rat kidney fibroblasts with antisense LOX also causes oncogenic transformation [195]. In 2003, Jeay et al demonstrated that LOX inhibited *ras*-mediated transformation by preventing *ras*'s activation of NF-kB [119]. LOX accomplished this by partially inhibiting the Raf/MEK signaling pathway and potently inhibiting the PI3K/Akt signaling pathway. Since then, LOX has been shown to be downregulated in various cancer cell lines, and many studies have shown a link between decreased LOX expression and tumor formation [196-201]. This extensive evidence has led to the classification of LOX as a tumor suppressor gene.

However, evidence has also emerged suggesting that LOX activity can contribute to the invasive properties of breast carcinoma cells [117, 202]. LOX and LOXL2 were identified by a differential expression study as genes upregulated in invasive breast cancer cells compared with non-invasive cells [202]. Further studies demonstrated non-invasive breast cancer cells (MCF-7) transfected with LOX became more invasive. Conversely, invasive breast cancer cells (Hs578T and MDA-MB-231) transfected with antisense LOX, or treated with BAPN, became much less invasive [117]. More recently, LOX upregulation has been shown to be concomitant with the epithelial-mesenchymal transition (EMT) that occurs when *in situ* breast cancer cells penetrate their basement membrane in local invasion (unpublished data). Microarray studies have also shown upregulation of LOX in mesenchymal-like breast cancer cell lines [198].

This apparent paradox of LOX as a tumor-suppressing and a pro-invasion protein can be reconciled. There is strong evidence for both roles. Evidence of epigenetic silencing of LOX early in carcinogenesis [199, 203] could allow the re-expression of LOX later when the cell starts to invade and form metastases. Another possibility is that tumors of mesenchymal origin and those of epithelial origin display very different genomic patterns and LOX expression may have different affects. All the studies showing *ras*-recision by LOX were done in transformed fibroblasts, and most cancer cell lines with down-regulated LOX have been sarcomas, which are tumors of mesodermal origin. The studies showing upregulated LOX and pro-invasive LOX have been mostly of carcinomas, tumors of ectodermal origin. It may be that upregulation of LOX

occurs in epithelial cancer cells during EMT as they are acquiring phenotypic traits of mesenchymal cells.

Finally, there has been a recent report that the *ras*-recision activity of LOX is due to its N-terminal propeptide region and not the active enzyme [204]. Palamakumbura et al repeated the original studies using *ras*-transformed NIH3T3 cells and determined that with BAPN, *ras*-transformation was not reversed. However, they could get phenotypic reversion with expression of antisense LOX, and they found that they could duplicate the phenotypic reversion using only the 18-kD recombinant LOX propeptide added to the culture. This would suggest a specific role for the LOX propeptide, perhaps in a similar way as endostatin after it is cleaved from the C-terminal end of type XVIII collagen [205].

These studies overwhelmingly show that LOX has a role in carcinogenesis, but the exact nature of this role needs much more investigation.

Cutis Laxa

Cutis laxa is a heterogenous collection of connective tissue disorders that can result from mutations in genes involved in elastic fiber synthesis [171, 206]. Cutis laxa is characterized by loose, sagging skin and can be subdivided into three classifications: the autosomal dominant form (OMIM 123700) is mild without systemic symptoms; the Type I recessive form (OMIM 219100) has the poorest prognosis and is characterized by pulmonary emphysema, inguinal and umbilical hernias, and diverticuli in organs of the gastrointestinal and urinary systems; the Type II recessive form (OMIM 219200) shows joint laxity and developmental delay, and is more common than Type I. Relatively little is known about the genetic causes of the different forms of cutis laxa. Some cases of the dominant form of cutis laxa have been demonstrated to be results of mutations in the elastin gene [207-209], and very recently mutations in the fibulin-5 (FBLN5) have been shown to cause severe recessive forms of the disease [210-212]. However, there are many cases of cutis laxa with no known mutations and efforts are still under way to screen other candidate genes for mutations, including the lysyl oxidase family of enzymes. As FBLN5 has

also been shown to interact with LOXL [213], and given the role in the lysyl oxidase enzymes in crosslinking elastin, it remains possible that genetic alterations affecting a lysyl oxidase enzyme's activity, expression, or regulation may be identified to play a causative role in cutis laxa. Indeed, there has been at least one report of decreased lysyl oxidase levels in a recessive cutis laxa patient [214].

Fibrosis

The medical definition of fibrosis is "formation of fibrous tissue as a reparative or reactive process, as opposed to formation of fibrous tissue as a normal constituent of an organ or tissue." Simply phrased, fibrosis is an abnormal accumulation of ECM in tissues, which in many cases is a chronic condition that can be triggered by injury, inflammation, or infection. Progressive fibrosis of liver, lungs, kidneys, heart, and blood vessels are major causes of human morbidity and mortality. In addition, skin fibrosis can also be a serious medical problem, presenting as keloids, dermal scars, and scleroderma.

Many causes of fibrosis have been identified, but some causes are more likely to affect specific organs. Hepatitis infection and chronic alcohol consumption are the main causes of liver fibrosis [215, 216]. Glomerular nephritis, diabetes, and hypertension are the primary causes of kidney fibrosis [217, 218], and hypertension can also cause diffuse cardiac fibrosis [219]. Pulmonary fibrosis is most often caused by infections or inhalation of toxic vapors or inorganic dusts [220-222]. Relatively little is known about the causes of skin fibrosis, but both environmental and genetic factors have been identified [223-225].

Despite the variety of causes of fibrosis, the pathology remains very similar on the cellular and molecular level. Inflammation is induced in the tissue, and cytokines are released at high levels, including TGF-β [226, 227]. These signals stimulate the proliferation of fibroblasts and the increased synthesis of ECM components, of which collagen is the predominant component. This large increase in synthesis of collagen fibers cannot be accomplished without

the corresponding increase in lysyl oxidase enzyme activity. The upregulation of LOX has become a biological marker of fibrosis in various organs [228-234], and has been examined as a valid therapeutic target [235, 236]. Treatment of fibrotic diseases with BAPN has shown some promise, but has proved problematic because of the toxicity [236].

DISSERTATION HYPOTHESIS AND SPECIFIC AIMS

LOX is a copper-dependent amine oxidase secreted into the extracellular space as a glycosylated proenzyme, where it is proteolytically cleaved into an active enzyme. LOX catalyzes the oxidative deamination of peptidyl lysine residues in collagen and elastin molecules to allysine residues, which can then spontaneously condense with a neighboring protein's lysine or allysine residues to form covalent cross-links in fibrillar collagens and elastin. This covalent crosslinking is essential to the formation of mature collagen and elastic fibers, and LOX has been shown to be essential to normal mammalian development. There are four LOX-like amine oxidases in mammals (LOXL, LOXL2, LOXL3, and LOXL4) that form the 5-member lysyl oxidase enzyme family.

A key factor during development, tissue repair, and in the progression of many diseases is the remodeling of the ECM that surrounds almost every cell type in the human body. Understanding the body's regulation of the balance between ECM deposition and degradation is critical for understanding the pathogenesis of diseases such as cardiovascular disease, fibrosis, arthritis, pathogenic infection, and cancer. It has been repeatedly demonstrated that altered expression and activity of LOX contributes to the ECM alterations and pathogenesis of these diseases.

Despite previous research, fundamental questions about LOX and the lysyl oxidase family of enzymes remain unanswered. These include the following questions about the molecular mechanisms governing LOX's biological activity: What are the functional roles of the various protein domains? Are the individual lysyl oxidase enzymes tissue-specific or substrate-specific? How do the lysyl oxidase proteins regulate cell growth? How does LOX transcriptionally regulate other genes? How is the post-transcriptional proteolytic activation of LOX regulated? How does LOX find its substrates in the extracellular environment?

The **overall goal** of this dissertation research was to characterize unexplored mechanisms of ECM assembly and regulation, and to determine novel roles of the LOX enzyme, by identifying proteins that interact with LOX. Once identified, these interactions would be

studied to determine their biological significance. *Our hypothesis is that there are unidentified protein interactions of the LOX enzyme that contribute to the regulation of its enzyme activity and to its newly recognized biological functions.*

To accomplish this goal, the following specific aims were proposed:

Specific Aim 1. Identify potential LOX-binding proteins by screening a yeast two-hybrid library.

a) Prepare the yeast two-hybrid cDNA library for screening by performing a large-scale plasmid DNA amplification.

b) Design and clone the LOX bait constructs and verify that the GAL4-BD-LOX fusion protein is correctly expressed in yeast.

c) Screen the yeast two-hybrid cDNA library with LOX, isolate the positive clones that express all three reporter genes, and identify the contained library cDNA by sequencing.

d) Determine if the binding in yeast is specific between the positive library protein and LOX by directly co-transforming various combinations of bait and target plasmids into yeast and assaying for reporter gene activation.

Specific Aim 2. Confirm and characterize LOX's interactions with high priority yeast two-hybrid positive proteins.

a) Generate expression constructs for LOX and LOX deletion fragments.

b) Express and purify recombinant LOX proteins in quantities required for *in vitro* biochemical experiments.

c) Perform *in vitro* binding analysis using pull-down and far-Western assays.

d) Co-immunoprecipitate LOX and interacting proteins from cultured cells.

e) Use solid phase binding assays to measure the equilibrium disassociation constant (K_d) of each protein interaction in order to quantitatively compare binding affinities.

Specific Aim 3. Investigate the effects of the identified protein interactions on LOX's enzymatic activity.

a) Determine if the LOX interacting proteins are novel substrates for the LOX enzyme.

b) Determine if the interaction inhibits or enhances LOX enzyme function towards known substrates.

Specific Aim 4. Explore the biological significance of the protein-protein interactions.

a) Perform immunofluorescent co-staining using human tissue arrays to identify cells and tissues where LOX and interacting proteins may interact *in vivo*.

b) Evaluate if LOX's activity is regulated by this interaction *in vivo* by downregulating the interacting proteins in cell cultures and subsequently analyzing LOX's activation.

c) Explore downstream molecular events to develop a working hypothesis to explain the purpose of these interactions in human health and disease.

CHAPTER 2. YEAST TWO-HYBRID SCREENING WITH LOX

INTRODUCTION

The overall goal of this research was to discover novel molecular mechanisms of LOX's regulation and function. *Since a protein's biological functions are determined by its molecular interactions, our approach was to screen for novel proteins that interact with LOX.* Several molecular biology techniques have been developed to identify and characterize protein-protein interactions. However, the most direct methods require some knowledge about the potential interacting protein, and there was no information to suggest any novel proteins as LOX-binding candidates. After evaluating the potential methodologies, we decided to perform a yeast two-hybrid screen with the LOX protein.

The yeast two-hybrid system is a well-established method in which the protein of interest, termed the "bait," is co-expressed with a random "target" protein in a yeast cell [237-241]. The target proteins are encoded by a plasmid library, which is cloned from mRNA extracted from a specific tissue or cell line. The two-hybrid principle is based on the observation that certain transcriptional factors, such as GAL4, can be divided into separate functional domains: the DNA-binding domain (BD) and the activation domain (AD). When these domains are brought close enough together in the nucleus, they can functional as a complete transcription factor and activate transcription of responsive genes. For screening, the bait and target proteins are cloned as fusion proteins to the GAL4-BD and the GAL4-AD, respectively (Figure 8). Therefore, when the bait and target proteins bind in the yeast nucleus, the GAL4 domains can activate transcription of reporter genes with GAL4 upstream activating sequences (UAS). These reporter genes are used to identify which yeast cells contain interacting proteins, enabling the identification of the library target protein.

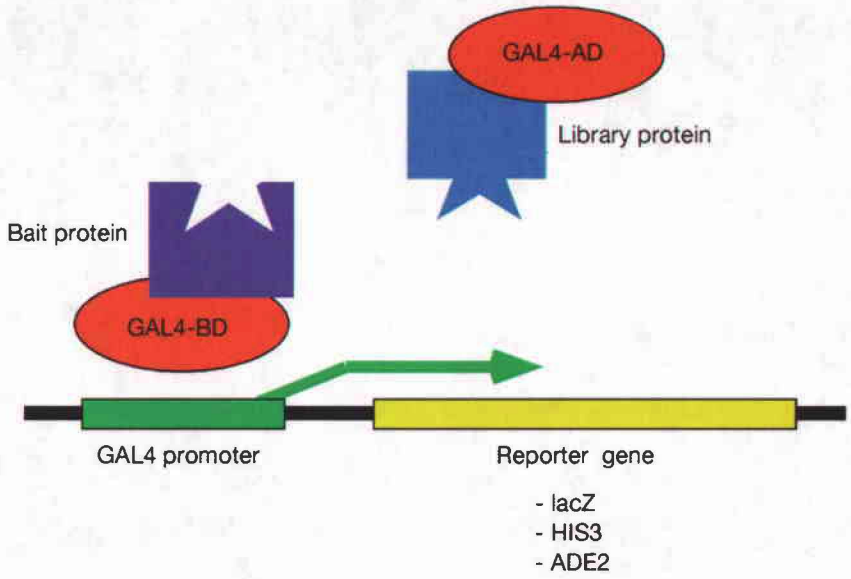

Figure 8. The principle of the yeast two-hybrid screening method for identifying novel protein-protein interactions. Transcription factors such as GAL4 can be split into 2 domains, the DNA-binding domain (BD) and the activation domain (AD). When the two halves are brought into close proximity, they can function together to activate the transcription of reporter genes. The bait protein is cloned as a fusion protein to the GAL4-BD, and a library of proteins is cloned as fusion proteins to GAL4-AD. The library is then screened for proteins that interact with the bait, as positive interactions bring the GAL4 domains together to activate transcription of the reporter genes (lacZ, HIS3, and ADE2).

The yeast two-hybrid system had several advantages over other molecular methods for identifying potential protein-protein interactions. Specifically, the yeast two-hybrid system: i) is a well established method, unlike the new variations of bacterial and mammalian two-hybrid [242, 243]; ii) identifies large fragments of the target proteins, unlike phage display which identifies short protein-binding peptides [244]; iii) does not require a purified protein-of-interest or a specific antibody against the protein-of-interest; iv) screens millions of potential target proteins from user-chosen tissue libraries; v) can be used to narrow down the binding domains once a potential interaction has been identified; and vi) is a comparably low cost method of screening.

The yeast two-hybrid system we used for this study was Clontech's MATCHMAKER System 3, which included frozen stocks of the yeast strain AH109 [245], the bait and target expression vectors, a pair of positive control bait and target plasmids (pGBKT7-p53 and

pGADT7-Lam), the single stranded carrier DNA used for yeast transformations, and an extensive set of protocols. The AH109 strain already contained the three reporter genes, so only the bait and target plasmids needed to be transformed into the cells. The included empty target vector was only used for post-screening verification assays, as the two-hybrid plasmid library was purchased separately.

We chose to screen a human placental library on the basis of the high expression of the LOX and LOX-like genes in placenta [176, 246-248]. We believed this would give us the maximum chance of discovering potential interacting proteins. This particular library was constructed from cDNA reverse transcribed using oligo-dT primers, which hybridize to the polyA tails of mRNA molecules. The common alternative to this method is to use random hexamers, which hybridize at random points in the mRNA molecules. The advantage of the oligo-dT primers is that a higher proportion of complete cDNAs are synthesized, but the disadvantage is that for long mRNA molecules, the reverse transcription may fail to get the entire 5' sequence. This placental plasmid library, which was purchased from Clontech, required amplification prior to the two-hybrid screening.

The bait for the two-hybrid screen was the active, 30-kD form of the LOX enzyme, which we chose for several reasons. The 30-kD LOX is the predominant form found in the extracellular environment, which increases the probability of detecting biologically relevant extracellular proteins. The 30-kD LOX is also the form shown to be transported from the ECM into the nucleus [107, 108], which increases the probability of detecting biologically relevant nuclear proteins and plasma membrane receptors. In addition, numerous studies have demonstrated that the N-terminal propeptide inhibits LOX's catalytic activity, and it has been proposed that this is due to an electrostatic interaction of the propeptide region with the C-terminal active site [105]. We were fearful that the propeptide domain may have likewise prevented the interaction of target proteins in the two-hybrid screen. Therefore, we believed that using the active, 30-kD LOX as bait would result in a greater number of potential interacting proteins, as well as a higher percentage of biologically relevant proteins, than screening with the full-length proLOX.

Here in Chapter 2, data from our yeast two-hybrid screen with LOX is presented. The cloning of various LOX bait proteins is described, and the amplification of the placental library prior to screening is also detailed. The isolation of the positive clones from the screen and the identification of the contained library cDNAs are also described. Furthermore, the results of direct co-transformations of various bait and library plasmids indicated the specificity of the detected interactions in yeast.

RESULTS

Generation of the LOX yeast bait plasmid constructs

The MATCHMAKER System 3 (Clontech) included the bait vector used in the yeast two-hybrid screen, pGBKT7 (Figure 9). This vector has a multiple cloning site (MCS) that allows the insertion of the bait cDNA in-frame with the GAL4-BD and a c-myc epitope tag in-between. This epitope tag allows for easier detection by Western blotting using a commercial anti-c-myc antibody, so an antibody against the bait protein is not needed. The pGBKT7 vector also contains two selection genes, *TRP1* for yeast selection, and a kanamycin resistance gene (*Kan*^{r}) for bacterial selection.

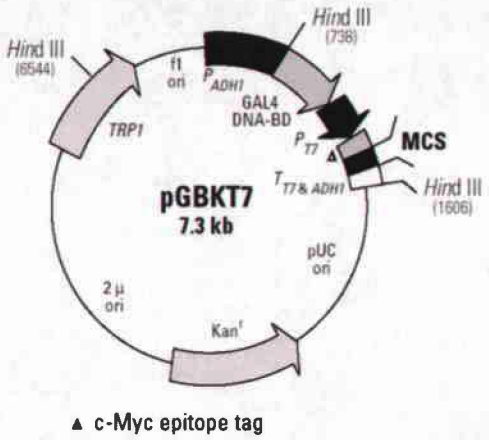

Figure 9. Diagram of pGBKT7 bait vector used to screen the human placental Y2H library in this study. The bait vector contains both the DNA-binding domain of GAL4 transcription factor (GAL4-BD) and a c-myc epitope tag in-frame with the MCS, where the bait cDNA fragment is inserted. LOX, proLOX, and various LOX deletion fragments were ligated into pGBKT7. Figure was taken from Clontech's MATCHMAKER System 3 manual.

Previously, our lab had cloned the complete human LOX cDNA into a plasmid construct [61], which has been completely sequence verified. This plasmid was used as a PCR template to clone all the LOX expression constructs used in this project. Six pairs of primers were designed to amplify six different LOX cDNA fragments for cloning. These primers were designed to introduce restriction sites on each end of the amplicon to allow subcloning of the LOX fragments. Restriction analysis was performed on the LOX cDNA sequence to map all restriction sites that could potentially be used to clone LOX into pGBKT7. It was found that the LOX ORF sequence lacks *EcoR*I and *BamH*I restriction sites, and so the forward primers were designed to introduce an *EcoR*I site 5' to the LOX sequence, and the reverse primers were designed to introduce a *BamH*I site 3' to the LOX sequence. For the LOX cDNA fragments that stopped prior to LOX's natural STOP codon (TAG), the corresponding reverse primers were designed to introduce a STOP codon (TAG).

In addition to the LOX cDNA encoding the mature 30-kD LOX, we cloned five other LOX cDNA fragments into the pGBKT7 vector. These LOX constructs were used for the post-

screening direct co-transformation assays in order to help determine the LOX domains responsible for the interaction. These additional LOX cDNA fragments were: full-length proLOX, LOX propeptide, proLOX minus the CRL, LOX minus the CRL, and the LOX CRL domain alone (Table 3).

Table 3. pGBKT7-LOX bait constructs for yeast two-hybrid studies. pGBKT7-LOX, in bold, was the bait used to screen the human placental yeast two-hybrid library.

Name of Construct	LOX nucleotides	LOX Amino Acids	Cloning Restriction Sites	Brief Description
pGBKT7-proLOX	1-1254	1-417	*EcoR*I & *BamH*I	Full-length proLOX
pGBKT7-LOX	**505-1254**	**169-417**	***EcoR*I & *BamH*I**	**Processed active LOX**
pGBKT7-LOX_{1-168}	1-504	1-168	*EcoR*I & *BamH*I	Propeptide domain
pGBKT7-LOX_{1-348}	1-1044	1-348	*EcoR*I & *BamH*I	Full-length minus CRL
pGBKT7-$LOX_{169-348}$	505-1044	169-348	*EcoR*I & *BamH*I	Active LOX minus CRL
pGBKT7-$LOX_{349-417}$	1045-1254	349-417	*EcoR*I & *BamH*I	CRL domain

After PCR was performed, the amplified LOX fragments were agarose gel purified and restriction digested with *EcoR*I and *BamH*I enzymes. The pGBKT7 plasmid was also digested with the same restriction enzymes to prepare it for ligation. The digested DNA was agarose gel purified, and then ligation reactions were set up with the pGBKT7 vector and the LOX DNA fragments. Aliquots of these ligation reactions were transformed into *E. coli* to select for successful ligations. Plasmid DNA was extracted from the colonies that grew on the LB-kanamycin plates, and plasmids containing the correct-sized LOX insert were screened for using restriction digests with *EcoR*I and *BamH*I followed by agarose gel electrophoresis. Finally, the LOX bait constructs were sequenced to verify that the cloning was successful (Figure 10).

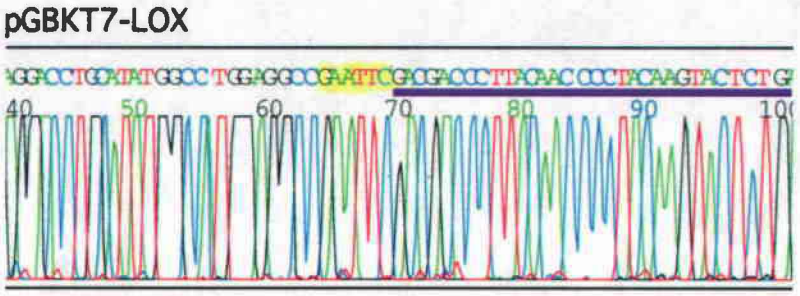

Figure 10. Representative DNA sequence verifying the correct cloning of the yeast expression construct pGBKT7-LOX. Each cloned bait construct was verified by DNA sequencing. The *EcoR*I restriction site is highlighted, and the beginning of the LOX sequence is underlined in purple.

The bait we chose for yeast two-hybrid screening was the human 30-kD LOX enzyme for reasons discussed in the Introduction. The pGBKT7-LOX bait plasmid was transformed into yeast strain AH109, and its presence was selected for with Trp^- (W^-) nutritional dropout plates. Before screening, it was necessary to confirm that the bait protein was being expressed at the correct molecular weight, and at a sufficient level. For this, we grew the cells in liquid culture (W^- media) and performed a crude protein extraction. We analyzed the yeast proteins by Western blot analysis using an antibody against the c-myc epitope. The expression of pGBKT7-LOX, and the other LOX baits, were compared with the control baits (pGBKT7 vector only and pGBKT7-Lam). The GAL4-BD-LOX was detected at the expected size (50 kD), and was present in a high quantity, comparable to the controls and rest of the bait clones (Figure 11).

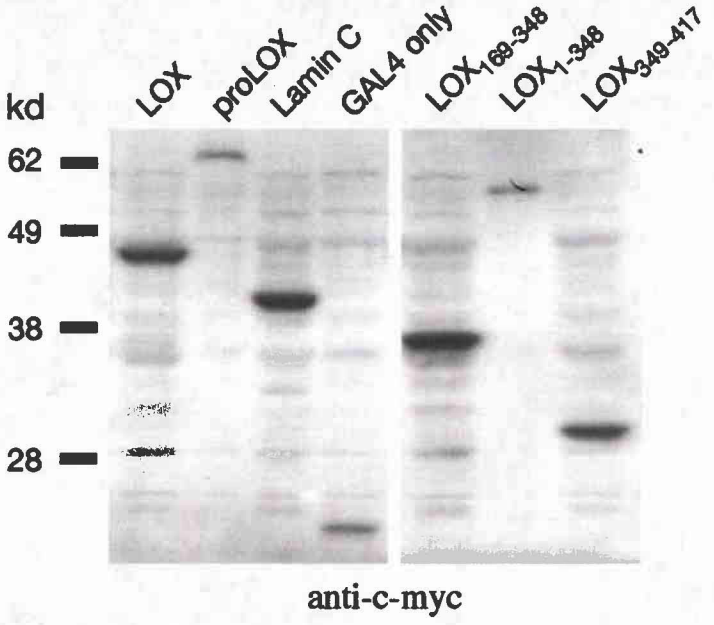

Figure 11. Western blot of yeast protein extracts confirming expression of pGBKT7-LOX fusion bait proteins. The Western blot was done using protein extracts of log growth-phase yeast cells containing the indicated bait plasmids. Also included was the vector only, yielding the GAL4-BD only, and the negative control bait, pGBKT7-Lamin C. Blotting was performed using an anti-c-myc antibody.

In addition, it was necessary to determine if LOX alone could activate transcription of the reporter genes ADE2, HIS3, and lacZ. This could happen if the LOX bait protein had any autonomous transcriptional activity, and testing this gave an indication of the level of non-specific background we might observe from the two-hybrid screen. Yeast containing the pGBKT7-LOX plasmid were streaked onto $Ade^-/His^-/Trp^-$ (AHW$^-$) dropout plates and W$^-$/X-Gal plates. The yeast on AHW- plates failed to grow, and the yeast on W$^-$/X-Gal plates grew without any trace of blue color. Therefore, none of the reporter genes were activated with expression of GAL4-BD-LOX alone, so we proceeded with the yeast two-hybrid screen using pGBKT7-LOX as bait.

Amplification of the yeast two-hybrid library

The human placental cDNA plasmid library was purchased from Clontech and consisted of the library cDNA inserts ligated into the pACT2 vector (Figure 12), which arrived packaged in bacteria frozen stocks. To perform the screen, it was necessary to amplify the two-hybrid library and purify the plasmid DNA on a large scale, and it was crucial to amplify the library in a way that maintained the proportional representation of each gene. For this reason, the bacteria containing the library plasmids were diluted and grown on a large number of agar plates instead of in liquid culture. In a liquid culture, each bacterium's relative growth is only limited by its rate of division, therefore if a library cDNA is somewhat toxic to the bacteria, this cell will grow slower than the rest, and that plasmid will be under-represented in the amplified library. Likewise, if a cDNA gives a growth advantage, even slight, that plasmid will be over-represented in the subsequent two-hybrid screening. Bacteria plated on solid substrates, like LB agar, are nutritionally limited by their immediate surrounding area. So cells with slower growth rates will catch up in number with the faster growing colonies.

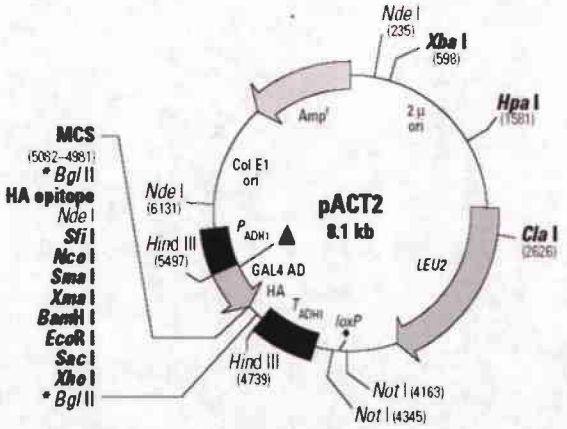

Figure 12. Diagram of pACT2 vector used to construct the human placental yeast 2-hybrid library screened in this study. The pACT2 vector contains both the GAL4 active domain (GAL4-AD) and a HA epitope tag in-frame with the multiple cloning site (MCS), where the placental library cDNA fragments are inserted. pACT2 also contains an Ampicillin resistance gene for selection in bacteria, and a LEU2 nutritional gene for selection in yeast. Figure was taken from Clontech's MATCHMAKER System 3 manual.

The library arrived as a glycerol stock of bacteria frozen at -70°C. To estimate the concentration of bacteria cells in the suspension, 1 µl was diluted into 1 mL of LB media (dilution A = 1:1000), and then diluted further by adding 1 µl of dilution A into 1 mL of LB media (dilution B = $1:10^6$). Three LB agar plates, containing ampicillin, were spread with 1 µl of dilution A (diluted in 50 µl LB), 50 µl of dilution B, and 100 µl of dilution B. After incubation overnight at 37°C, the resultant number of colonies allowed the calculation of the concentration of bacteria in the glycerol frozen stock at ~3.2×10^6 colony-forming units (cfu)/µl.

The placental yeast two-hybrid library specifications indicated that there were 3.5×10^6 independent clones, and the Clontech amplification protocol recommended plating 3 colonies per individual library plasmid to ensure a good representation. Therefore, my goal was to have 10.5×10^6 independently growing colonies on the LB agar plates. To plate this number of bacteria, we diluted 3.27 µl of the glycerol frozen stock into a LB volume large enough to plate on a large number of plates (45 mL). From previous estimations of colony spacing on large plates, we estimated that 250,000 colonies could grow on the large square plates (500 cm^2). Therefore, we spread the 10.5×10^6 bacteria onto 43 large square LB-agar plates using sterile glass beads for even dispersion. We incubated the plates at 37°C for 30 hours, and then harvested the bacteria. This was accomplished using cell scrapers to gather all the colonies and then pooling the cells and washing them with a LB-glycerol solution. Aliquots of the well-mixed bacteria were resuspended in LB-glycerol and frozen at -70°C until the plasmid DNA extraction could be performed. Qiagen's MEGA plasmid isolation and purification kit was used to extract the library plasmid DNA, which resulted in 3 mg of purified plasmid library DNA. This amplified plasmid library was then used for yeast two-hybrid screening.

Screening the yeast two-hybrid library with LOX

To screen the placental yeast two-hybrid library, we performed a large scale transformation of the plasmid library into the AH109 yeast, which already contained the pGBKT7-LOX bait plasmid. The transformed yeast cells were spread onto $Ade^-/His^-/Trp^-/Leu^-/X$-

Gal (AHWL⁻/X-Gal) dropout plates to select for expression of the three reporter genes, ADE2, HIS3, and lacZ, as well as to keep selective pressure for the bait and library plasmids (TRP1 and LEU2). From plated dilution controls, the library transformation efficiency was calculated to be over 5 x 10^5 cfu/µg, which was high enough to ensure a well-representative screen. With 200 µg of the library DNA transformed, the screen theoretically covered 100 x 10^6 clones from the library of 3.5 x 10^6 independent clones, meaning the screen had 28X coverage. We spread the cells on ~50 petri dishes (150 mm) and incubated them at 30°C for 3 days. By the end of 3 days, there were a great number of colonies that grew, and only the largest blue colonies were selected from each plate and restreaked on fresh AHWL- plates until single colonies were obtained. From the clones positive for the expression of all three reporter genes (Ade, His, lacZ), plasmid DNA was extracted from the yeast cells using Zymolase digestions. From this mix of bait and target plasmid DNA, the library cDNA insert was amplified by PCR with primers specific for pACT2 vector sequence (Figure 13). The PCR products were agarose gel purified and sequenced using an ABI 310 capillary sequencer (Figure 13).

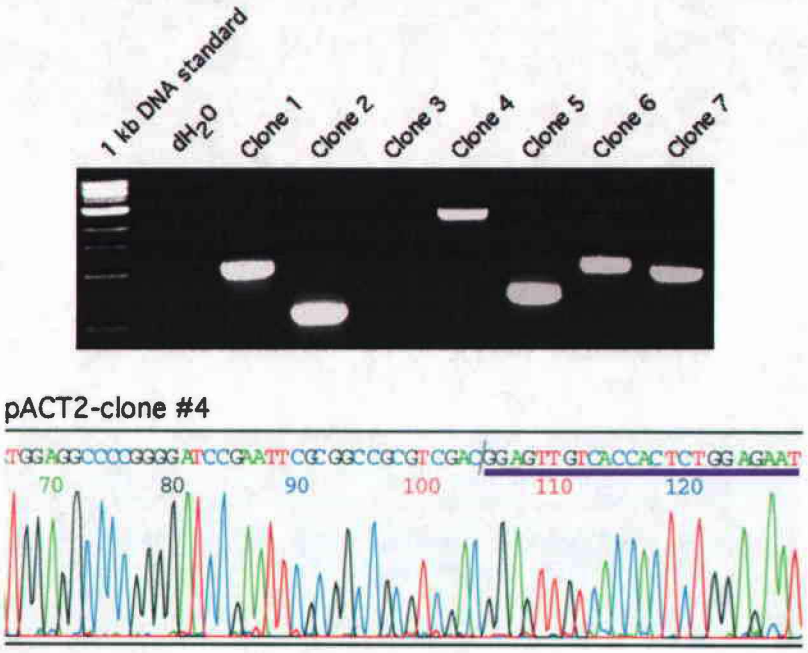

Figure 13. Library cDNAs isolated in the two-hybrid sequence were PCR amplified and sequenced. *Above*: Representative agarose gel analysis of PCR-amplified cDNA inserts from positive clones isolated in the two-hybrid screen. Primers used to amplify these inserts matched flanking sequence from the pACT2 library vector. *Below*: Representative sequence results from a positive cDNA. The end of the pACT2 vector sequence is marked with a slash, and the beginning of the library cDNA is underlined in purple.

From this yeast two-hybrid screen, 81 positive clones were isolated. Of these, 58 clones had their library plasmid cDNA inserts successfully amplified and sequenced. From the resulting nucleotide sequence, BLASTN (http://www.ncbi.nlm.nih.gov/blast) was used to identify the genes transcribed by these library cDNAs. Of the 58 sequenced cDNA clones, 13 were out of frame with the gene's known ORF, and 6 contained only a gene's 3'UTR. These clones were disregarded. Of the remaining 39 positive clones, there were 5 genes represented by multiple overlapping clones, and all 5 encoded extracellular proteins (Table 4). The cDNA found in the highest proportion (9 clones) encoded the hormone **placental lactogen (PL)**. Four cDNAs encoded **fibulin-1 (FBLN1)**, and 3 encoded **fibronectin (FN)** - both extracellular matrix proteins. Three cDNAs encoded pregnancy-associated plasma protein A and 2 encoded pregnancy specific beta-glycoprotein e. The rest of the cDNAs were only represented by a single plasmid.

These included nuclear proteins, extracellular proteins, cytoplasmic proteins, and one plasma membrane receptor (Table 4).

Table 4. Identified positive cDNAs from a Y2H screen of a human placental library using pGBKT7-LOX as bait. The insert size was determined by agarose gel analysis of PCR products using vector primers. The genes are color-coded to designated the cellular localization of the encoded proteins: blue = extracellular; red = nuclear; purple = cytoplasmic; green = transmembrane; black = unknown.

LOX pos. clone #	Insert Size (kb)	Identified Gene
1	1	Placental lactogen (chorionic somatomammotropin hormone 1)
4	2.4	Fibronectin (FN) – splice variant V4
11	1.4	Ring finger protein 10 (RNF10)
12	3	Pregnancy-associated plasma protein A (PAPPA)
13	1.25	Placental lactogen (chorionic somatomammotropin hormone 1)
15	1	Tissue factor pathway inhibitor 2 (TFPI2)
17	0.8	CGI-39 protein; cell death-regulatory protein (GRIM19)
20	1.2	P2ECSL protein (LIECG2)
21	0.85	Placental lactogen (chorionic somatomammotropin hormone 1)
23	0.9	Placental lactogen (chorionic somatomammotropin hormone 1)
24	2.2	Fibronectin (FN) – splice variant V2
28	1.2	Cell division cycle 2-like 1 (PITSLRE protein); CDC2L2
30	2.4	Pregnancy-associated plasma protein A (PAPPA)
31	1.9	Fibronectin (FN) – splice variant V2
36	0.65	Placental lactogen (chorionic somatomammotropin hormone 1)
37	1.65	Mago-nashi (Drosophila) homolog, proliferation-associated (MAGOH)
43	1.3	Putative small GTP-binding protein (rab1b)
45	2	Pregnancy-associated plasma protein A (PAPPA)
47	1.4	MyoD family inhibitor (MDFI), myogenic repressor I-mf (MDFI)
48	0.85	Fibulin 1 (FBLN1) – splice variant C
49	1.35	Fibulin 1 (FBLN1) – splice variant C
50	1.15	Pregnancy-specific beta-glycoprotein e mRNA
52	1	Placental lactogen (chorionic somatomammotropin hormone 1)
54	1.1	Pregnancy-specific beta-glycoprotein e mRNA
55	1	Proto-oncogene Wnt-7a
56	0.9	Angiotensin receptor-like 1 (AGTRL1), HG11 orphan receptor, G protein-
57	1.3	Fibulin 1 (FBLN1) – splice variant C
61	1	Placental lactogen (chorionic somatomammotropin hormone 1)
62	1.6	MafK - v-maf musculoaponeurotic fibrosarcoma (avian), protein K
63	1.6	cDNA DKFZp586I0324
66	1.5	Single strand DNA-binding protein
68	1.1	IgG Fc binding protein (FC(GAMMA)BP) mRNA
70	0.9	Placental lactogen (chorionic somatomammotropin hormone 1)
71	1.6	Glycogen synthase kinase 3 alpha (GSK3A)
75	0.65	Splicing factor, arginine/serine-rich 5 (SFRS5)
78	1.05	Fibulin 1 (FBLN1) – splice variant C
79	1	Placental lactogen (chorionic somatomammotropin hormone 1)

It is important to note that the FN and FBLN-1 cDNAs from the library encoded only partial fragments from these two proteins. These are large proteins - FBLN1 is 556-703 amino acids and FN can be as large as 2477 amino acids (both genes have multiple alternative splicing patterns). Therefore it is not surprising that the clones isolated in the yeast two-hybrid screen are only C-terminal fragments, as the placental mRNA was reverse transcribed with oligo-dT primers. In contrast, PL is a relative small hormone of 256 amino acids, and most of the positive cDNAs included the full ORF. Table 5 lists the FBLN1 and FN positive cDNAs and the nucleotide and amino acid at which each clone started. Table 5 also lists the splice variants of each clone, which could be determined for the FBLN1 clones after the initial sequencing, but required a few extra sequencing reactions for the FN clones.

Table 5. The FN and FBLN1 cDNA fragments isolated in the yeast two-hybrid screen with LOX. Listed for each clone is the starting nucleotide and amino acid of the sequenced cDNA fragment, as well as the splice variant of the transcript. The reference sequences are the transcript variant C of FBLN1 (Genbank Accession # NM_001996), and the transcript variant 1 of FN (Genbank Accession # NM_212482).

Positive cDNA clone	Starting Nucleotide	Starting Amino Acid	Splice Variant
Fibulin-1 (FBLN1)			
Clone 48	1394 (cagtgt...)	462 (QCYC...)	C
Clone 49	977 (cataca...)	323 (HTCI...)	C
Clone 57	1133 (aactct...)	375 (NSPG...)	C
Clone 78	1328 (gaagac...)	440 (EDIN...)	C
Fibronectin (FN)			
Clone 4	5958 (gttgtc...)	1871 (GVVT...)	V64
Clone 24	6286 (cccaat...)	1981 (PNSL...)	V95
Clone 31	6435 (ggaacc...)	2031 (GTEY...)	V95

Verifying the interactions in yeast

To further verify that the binding of the detected positives were specific to LOX, yeast direct interaction assays were performed. The two-hybrid systems can be prone to false positives due to either autonomous transcriptional activation by the bait protein or a non-specific "stickiness" of certain library proteins. Since we demonstrated the LOX bait had no autonomous

transcriptional activity prior to the screen, the post-screen verifications focused on demonstrating the detected interactions were absolutely specific between the LOX protein and the library protein. For the actual screen, the MATCHMAKER System 3 relied on three separate reporter genes to help eliminate false positives. After the screen, these direct co-transformations of combinations of bait and target plasmids were used to rule out false positives. Instead of re-screening the two-hybrid library with every individual LOX fragment or domain, the direct co-transformations also allowed us to individually test if these various LOX baits interacted with our detected positive clones. As described above, in addition to pGBKT7-LOX, five other LOX protein fragments were cloned into the pGBKT7 bait vector. Figure 14 shows a schematic of these LOX bait proteins and their included domain organization.

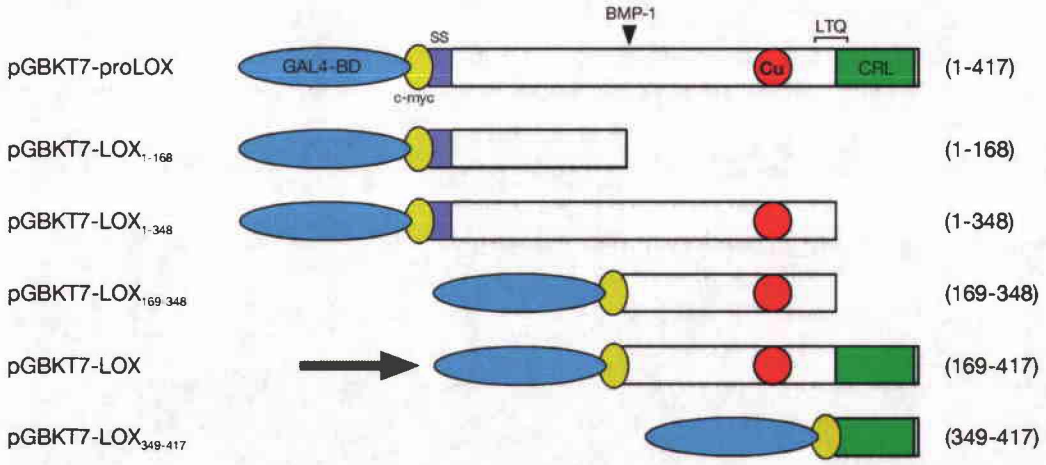

Figure 14. Protein domain organization of the GAL4-BD-LOX two-hybrid baits used in this study. The bait used for the initial yeast two-hybrid screen (GAL4-BD-LOX) is indicated with an arrow. Numbers refer to the included LOX amino acids. The individual domains are indicated: GAL4 DNA-binding domain (blue); c-myc epitope tag (yellow); signal sequence (purple); BMP-1 proteolytic cleavage site (arrowhead); copper-binding site (red); LTQ co-factor; CRL domain (green).

Combinations of bait constructs and the library plasmids that were isolated from the two-hybrid screen were directly co-transformed into AH109 yeast. The empty vector negative controls (pGBKT7 and pGADT7) were included, as well as pGBKT7-Lamin C as an additional

negative control bait protein (which was included with the Clontech's MATCHMAKER System 3). The pGADT7 vector is the updated replacement to pACT2, which had been discontinued. pGADT7 contains the exact same genes and coding sequences as pACT2, so was used as the library vector negative control. To preliminarily access the specificity of these protein interactions, I also tested the homologous region C-terminal region of LOXL2 as bait.

After co-transformation, the yeast were assayed for expression of the nutritional reporter genes by streaking on AHWL$^-$ plates. The yeast were also assayed for lacZ expression by lifting the cells onto a nylon filter, freezing them with liquid nitrogen, and then exposing the lysed cells to X-Gal. The plates and filters were scanned on a flatbed scanner. Figure 15 shows representative examples from three of the positive library clones.

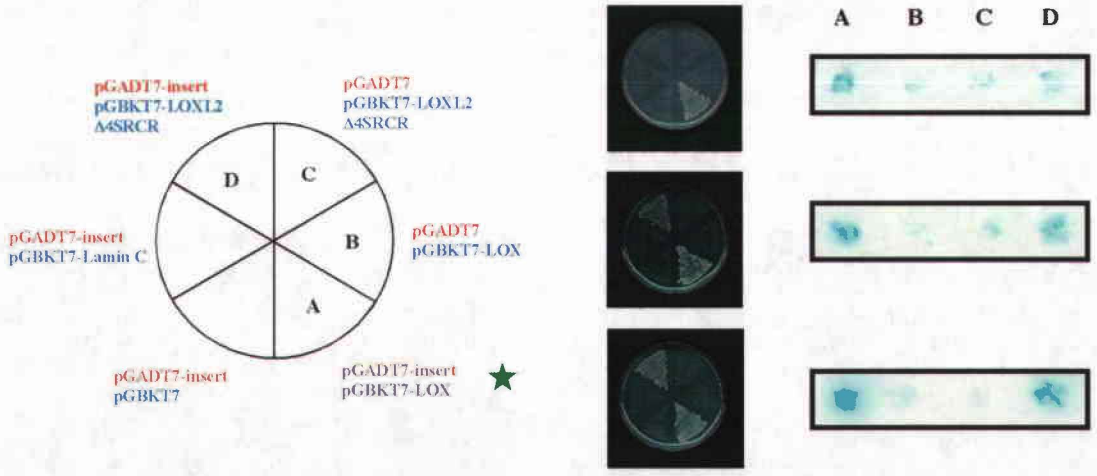

Figure 15. Representative scans from direct interaction verifications of isolated positive LOX-interacting proteins. Plates selective for reporter gene expression (AHWL$^-$) were streaked with yeast cells containing combinations of the pGADT7-positive cDNA, pGBKT7-LOX bait, empty cloning vector pGBKT7, empty library vector pGADT7, and negative control pGBKT7-Lamin C. In addition, the interaction with the conserved C-terminal domain of LOXL2 of each positive clone was tested, with appropriate negative control (pGADT7 and pGBKT7-LOXL2-4SRCR). Shown in the middle are AHWL$^-$ plates that demonstrate the interactions between three representative positive proteins and the LOX bait are specific. On the right are yeast cells, containing the indicated combinations of baits, spotted on nylon membranes and exposed to X-Gal. Blue color indicates lacZ activity in the yeast.

For a few selected positives (PL, FN, and FBLN1) further direct interaction assays were performed in attempts to narrow down the binding domains of LOX. Overall, six LOX bait constructs were tested, but we also tested LOXL and LOXL2 bait constructs that other members of the lab had cloned (Figure 16). Yeast were co-transformed with combinations of bait and library plasmids and spotted on AHWL- selective plates. After incubation at 30°C for 3 days, the growth of the yeast colonies were recorded by scanning the plates on a flatbed scanner. The results are shown in Figure 17 and Figure 18. The pGBKT7 bait constructs are listed down the rows, and the pGADT7/pACT2 library constructs are listed across the columns.

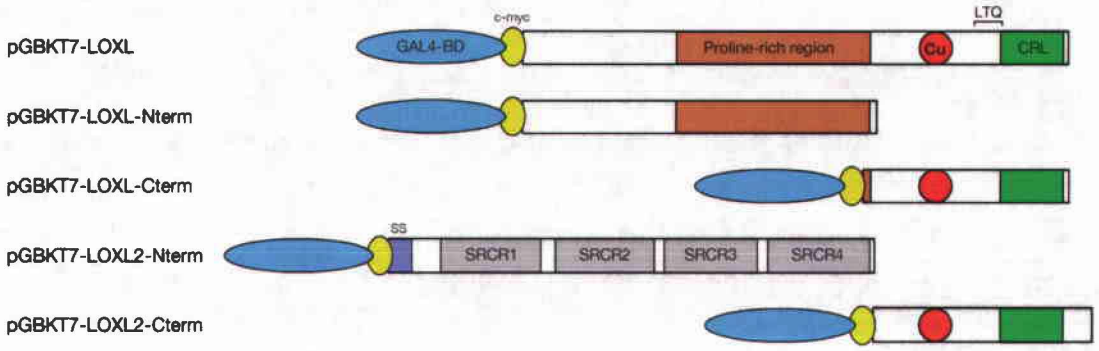

Figure 16. Protein domain organization of the GAL4-BD-LOXL and GAL4-BD-LOXL2 two-hybrid baits used for direct interaction assays. The individual domains are indicated: GAL4 DNA-binding domain (blue); c-myc epitope tag (yellow); signal sequence (purple); SRCR domains (gray); proline-rich region (orange); copper-binding site (red); LTQ co-factor; CRL domain (green).

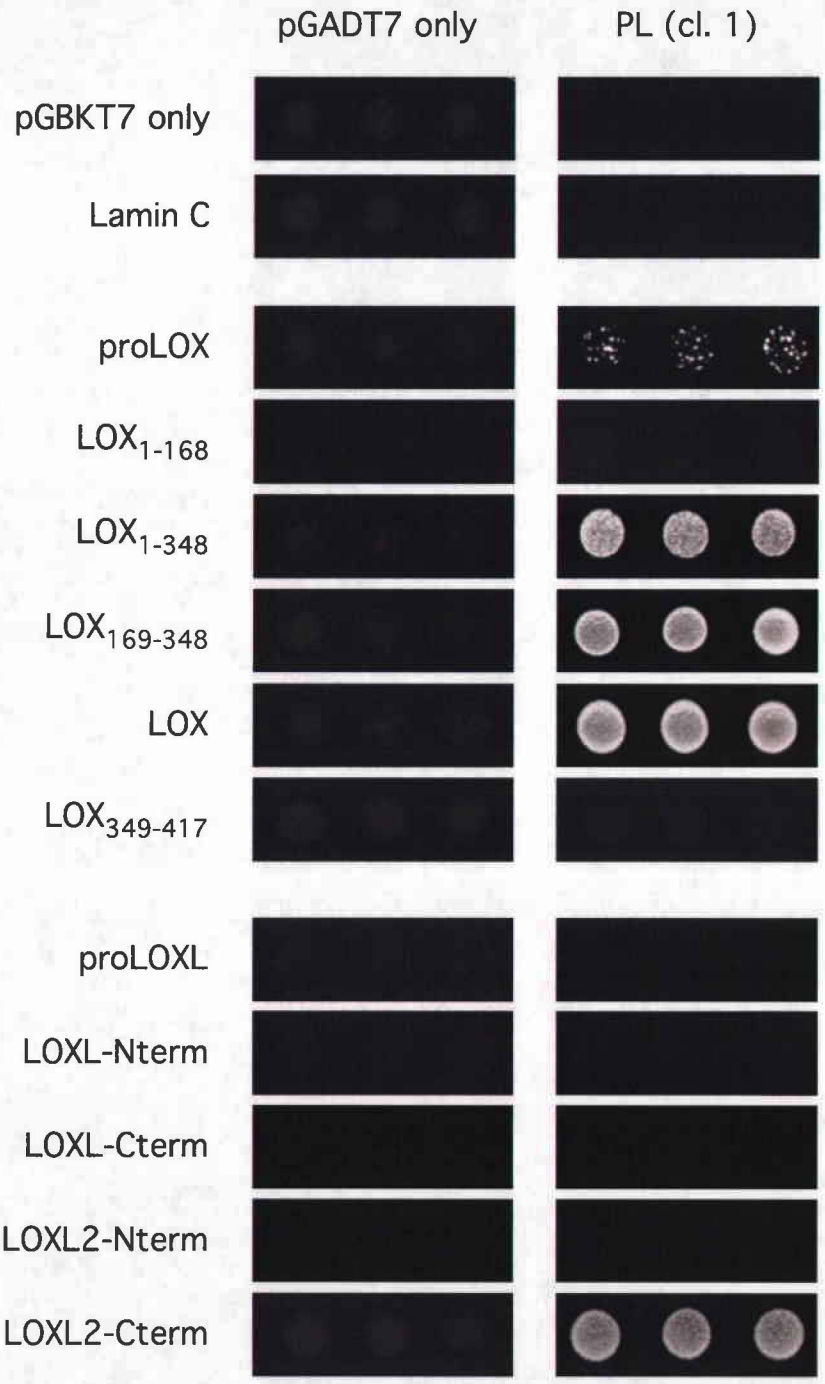

Figure 17: Spots of yeast grown for 3 days on AHWL$^-$ selective plates in direct interaction experiments. Each square shows triplicate spots of yeast cells containing both the bait plasmid (listed down the rows) and the library plasmid (listed across the columns). The empty vector controls, pGBKT7 and pGADT7, are shown in the first row and first column and demonstrate that the interactions are not due to binding with a GAL4 BD or AD domain. Lamin C is a non-interacting negative control bait included with the MATCHMAKER System 3.

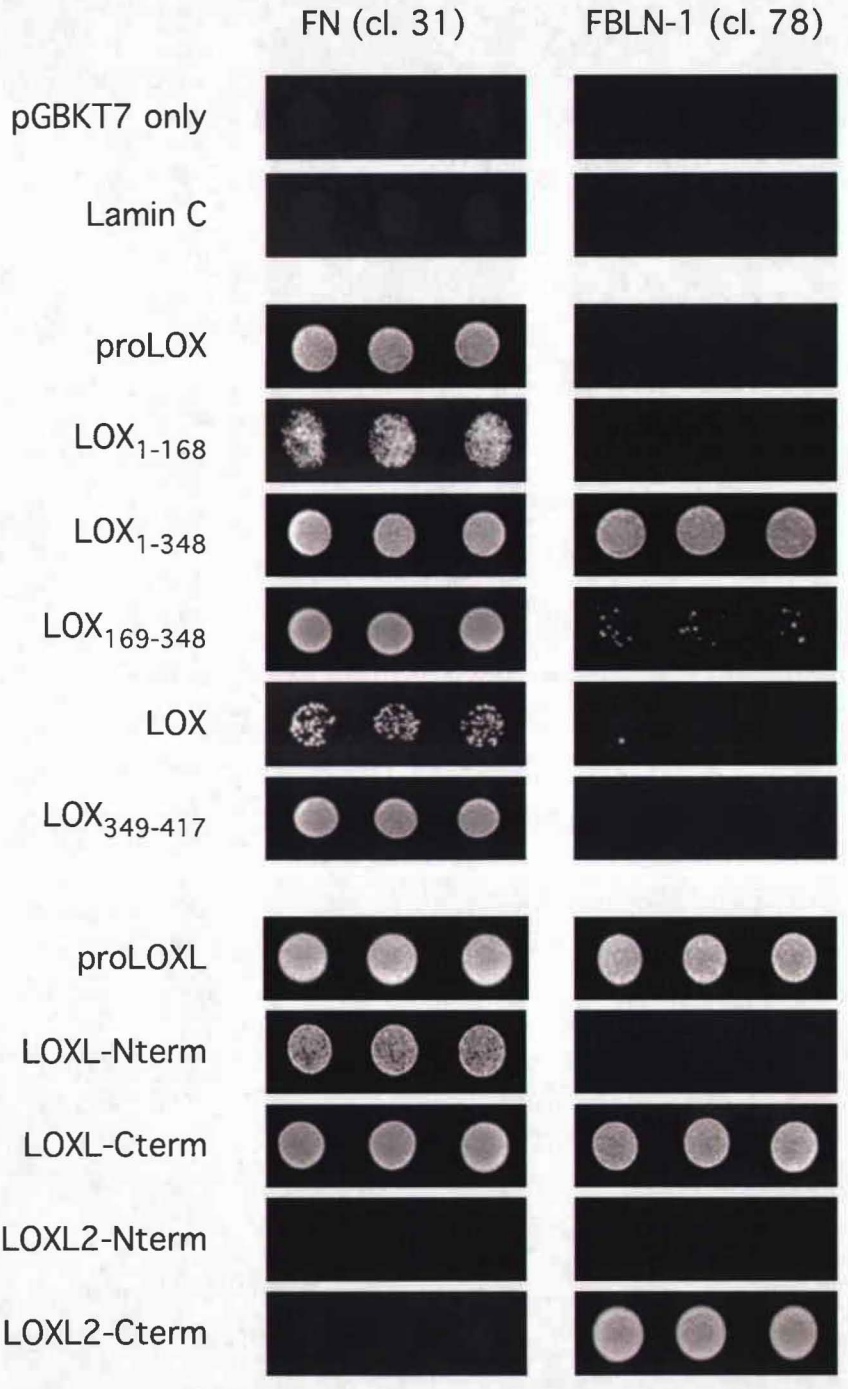

Figure 18: Spots of yeast grown for 3 days on AHWL$^-$ selective plates in direct interaction experiments. Each square shows triplicate spots of yeast cells containing both the bait plasmid (listed down the rows) and the library plasmid (listed across the columns). The empty vector controls, pGBKT7 and pGADT7, are shown in the first row and first column and demonstrate that the interactions are not due to binding with a GAL4 BD or AD domain. Lamin C is a non-interacting negative control bait included with the MATCHMAKER System 3.

These direct interaction data showed that none of the combinations with the negative control plasmids allowed yeast growth on the selective AHWL$^-$ plates. This was good evidence that the detected protein interactions were not due to binding to GAL4, or just general "stickiness" of a protein to any bait.

For FN (clone 31), some binding to every domain of LOX was demonstrated. Surprisingly, the weakest binding seemed to be with the yeast two-hybrid screening bait, LOX. Although with the variations in bait expression levels, and other uncontrollable variables, it may not be appropriate to make conclusions about relative binding affinities from this assay. The results also show FN binding to LOXL (both the N-terminal and C-terminal fragments), but no binding to LOXL2 was detected. These results with the FN and LOX interaction are not necessarily consistent with later data using the human proteins in direct biochemical experiments (presented in Chapter 3). One reason may be that the conformation of the FN molecule is a critical factor in determining its protein interactions, and these direct interactions use only a partial fragment FN.

For PL, which was the only cDNA to encode the entire protein, the results were very consistent - suggesting the PL binding site in LOX was between amino acids 169-348 (Figure 17). It also suggested there was some binding of PL to the proLOX protein. No PL binding was detected for LOXL, but there was a detected interaction with the C-terminal region of LOXL2. For FBLN-1, the data showed interactions with LOX_{1-348}, but with a little interaction with $LOX_{169-348}$, and a very little with the screening bait, LOX. However, in earlier preliminary direct interaction experiments, FBLN-1 showed strong interactions with both proLOX and LOX (Figure 19). FBLN-1 also seemed to interact with proLOXL, the C-terminal of LOXL, and the C-terminal of LOXL2.

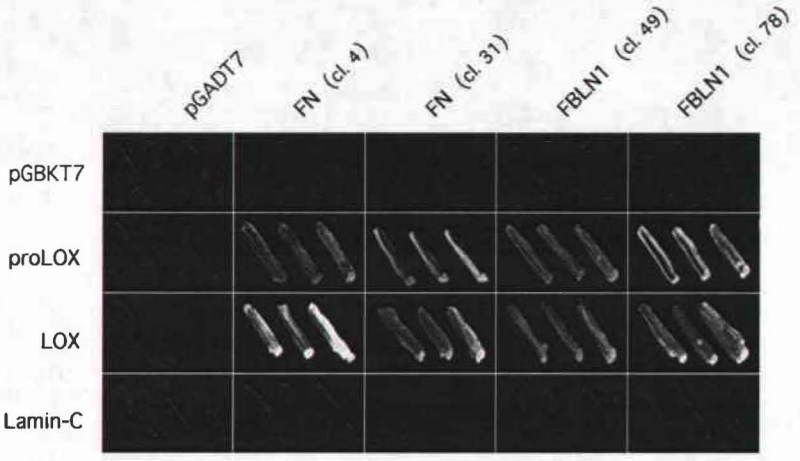

Figure 19. Streaks of yeast containing combinations of bait and target proteins on AHWL$^-$ plates. The bait protein is listed on left and the positive target proteins are listed along the top. These are earlier direct interaction assays confirming FN and FBLN1 interaction with both LOX and proLOX.

DISCUSSION

The yeast two-hybrid screening of the human placental library with LOX was successful, which completed Specific Aim #1 of this dissertation. The cloning of LOX bait cDNAs produced sequence-verified LOX plasmid constructs, and the bait proteins were expressed in yeast at the correct molecular weight. The baits did not have autonomous transcriptional activity, which allowed the screen to proceed. The screening of the placental library with the 30-kD LOX generated a substantial, but manageable, list of positives. Finally, the direct interaction assays verified that the interactions were real, and that they were specifically between LOX (or LOXL and LOXL2) and the positive library proteins.

There are limitations of the yeast two-hybrid screen, and we addressed them as best as possible. The Clontech two-hybrid plasmid libraries require amplification prior to screening. This must be done with a reliable method that maintains proportional representation of each cDNA. We accomplished this by amplifying the library (packaged in *E. coli*) on a large surface

area of LB-agar plates, rather than liquid culture. Also, if the bait protein has any intrinsic transcriptional activity, then the screen cannot be performed, as the number of false positives would be too high. Therefore, we tested our bait for autonomous transcriptional activity prior to screening, and we detected none. Another potential problem with the bait is the possible toxicity to the yeast cell. As these proteins are being expressed in the yeast nucleus, some proteins can disrupt the normal growth of the cells and reduce the growth rate (or kill the cells) [241]. This indeed has a dramatic impact on the success of the screen. To address this, we closely monitored growth rates of the yeast cultures containing our bait plasmid. The yeast two-hybrid screening method has demonstrated the potential for yielding false positives [249]. We addressed this by performing direct co-transformations of the baits and library positives, along with various negative controls to ensure the specificity of the interactions. As a consequence of how our library was constructed (using oligo-dT's), the cDNAs encoding large proteins tend to be only C-terminal fragments of the entire protein. The only way to address this is to confirm that the interaction also occurs with the full-length protein using additional assays, which are detailed in Chapter 3. However, it is worth noting that library cDNAs encoding small proteins, like PL, mostly contained the entire ORF.

Another limitation was evident in analyzing the percentage of positive cDNAs identified from the number of yeast positive clones isolated. We picked and restreaked 81 positive yeast clones, but we were successful in sequencing the library inserts from only 58 of these clones. The reasons for this include inefficient lysis of yeast, despite Zymolase treatment, due to its tough cell wall. Also, the plasmid DNAs may be of lower copy number in yeast than would normally be in bacteria, resulting in a small yield of DNA. For a few samples, despite isolating plasmid DNA, the PCR did not amplify a library insert. However, because the sequencing of the 58 clones was very successful in generating a long list of positives, extreme attempts were not made to sequence more of these clones.

From the sequencing of the 58 positive clones, 13 of these cDNAs were out of frame with the gene's known ORF, and 6 contained only a gene's 3' UTR sequence. It is not clear why

these clones were isolated in the two-hybrid screen, but perhaps because they contain some short peptide motifs that may interact with our bait protein. However, as these are not biological relevant proteins, these clones were disregarded as false positives and no further efforts were spent on analyzing them. It would be expected from the library's construction (with oligo-dTs) that only 1/3 of the library clones actually encode the gene in-frame with its ORF. The high percentage of in-frame positive clones (39/52 = 75%) was another reassuring sign of a successful screen.

A yeast two-hybrid screen can sometimes yield an enormous amount of data - a very long list of potential positives that looks exciting but can drown the scientist in never-ending follow-up experiments. After the screen, it was absolutely essential to carefully evaluate the list of positives and set priorities for follow-up experiments. The number of times a particular cDNA was identified is highly relevant for setting further research priorities, as a higher number of identified cDNAs usually suggests stronger evidence for a true interaction. The amount of work and time required to verify and further characterize these protein-protein interactions is great, so it was very important to carefully analyze the results of the yeast two-hybrid screen to look for true positives. The fact that all of the positive proteins that were encoded by more than one plasmid are located in the extracellular environment was another reassuring sign that the screen was successful.

Here is a brief review of three of the more interesting multiple-clone positives: PL, FBLN1, FN.

PLACENTAL LACTOGEN (PL)

PL is a growth hormone and signaling molecule produced by placental tissues during pregnancy [250-252]. It is a member of a hormone family that includes growth hormone (GH) and prolactin (PRL), both produced in the pituitary gland [253-256]. This family of hormones regulates an extensive variety of physiological functions, and acts by binding to two receptors termed growth hormone receptor (GHR) and prolactin receptor (PRLR). All three hormones are

20-22 kD and able to bind and dimerize both receptors to act through the JAK/STAT and MAPK signaling pathway [257-260]. The "PL gene cluster" is at 17q22~24, and contains 2 identical genes encoding PL [251]. Immediately upstream is the "GH gene cluster," which contains 3 identical genes encoding GH, which are 95% homologous to PL [261-263]. The 3D structural comparison of human GH and ovine PL demonstrated that receptor binding sites #1 and #2 are remarkably similar in both hormones (Figure 20) [264].

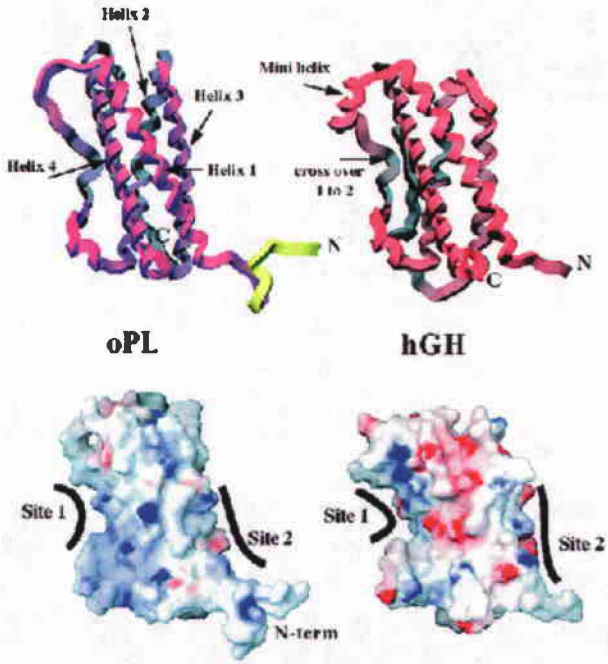

Figure 20. 3D structure analysis of ovine PL and human GH proteins shows the similarity of the two hormones. The PL cDNAs identified in the Y2H screen encode the entire peptide sequence. Figure taken from Elkins et al, 2000 [264].

PL, like GH and PRL, is classified as an oncogene due to its pro-growth signaling, autocrine activation in cancer cells, downstream transcriptionally-activated genes, and pro-angiogenesis activity [255, 256, 265]. PL is not normally expressed in adult tissues except in cases of breast tumors, where it is dramatically overexpressed by the cancer cells. Similarly, GH, PRL, GHR, and PRLR have all been shown to be overexpressed in breast tumors. The

chromosomal region of the PL and GH genes is commonly amplified in breast cancers; one study showed 22% of adenocarcinomas had DNA amplification of the PL and GH genes [266]. Given LOX's emerging roles in cell growth regulation, carcinogenesis, and metastasis, it will be important to investigate any potential interaction with the PL hormone.

FIBULIN-1 (FBLN1)

The FBLN1 protein is member of the fibulin family of calcium-binding extracellular matrix proteins, which all contain binding sites for several other ECM proteins, including fibronectin, tropoelastin, fibrillin, proteoglycans, and the basement membrane proteins nidogen, laminin, perlecan, and collagen IV [267-269]. This family has been only recently described, and their biological roles are still being characterized (Figure 21). The first discovered [267], FBLN1 is also the most evolutionarily conserved, as orthologues have been identified in zebrafish [270], *Caenorhabditis elegans* [271], chickens [271], and *Drosophila melanogaster* [268]. FBLN1 is expressed in the ECM of many organs and is associated with fibrillar matrix proteins, most basement membranes, and deposits of elastin [272-276]. FBLN1 also circulates in human serum at high concentrations (10-50 μg/ml) [277, 278].

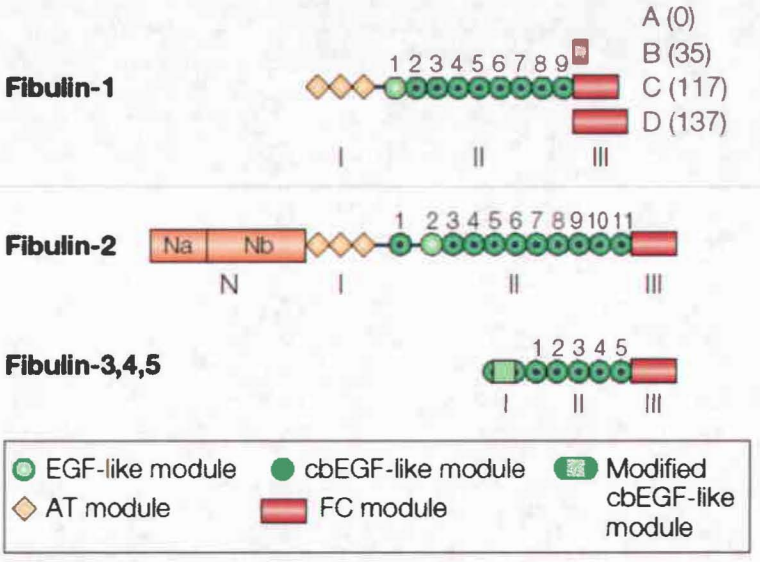

Figure 21. Domain organization of the human Fibulin family of extracellular proteins. The four FBLN1 cDNAs identified in the LOX yeast two-hybrid screen were the C splice variant. Figure taken from Timpl et al., 2003 [268].

In mammalian development, FBLN1 expression starts early during embryogenesis and is located throughout the body in basement membranes and the ECM of the heart (endocardium, myocardium, and epicardium), blood vessels, lung, intestine, brain, kidney, liver, and various connective tissues [274, 276]. The FBLN1 knockout mice die immediately after birth due to massive hemorrhaging in skin, muscle, and perineural tissue, which actually starts midgestation [279]. In addition, kidney glomeruli and lung alveoli were malformed. Despite the high expression in the developing heart and vasculature, gross abnormalities of the heart, large blood vessels were not observed, and basement membranes normally containing FBLN1 were intact [279]. It was hypothesized that overlapping expression of the other fibulin family members compensated for the loss of FBLN1 in unaffected tissues.

Much recent attention has been paid to the role of fibulins in elastic fiber assembly. In immunolocalizations, fibulin proteins have co-localized with elastin and microfibrils [275, 280], and molecular interaction studies have demonstrated high affinity binding to tropoelastin [281]. FBLN5 has been shown to bind to LOXL, which has been shown to be critical for elastin

homeostasis [213]; also mutations in FBLN5 have been shown to give rise to severe cases of cutis laxa (see Chapter 1 for more details). A potential FBLN1 interaction with LOX is interesting to explore their contribution towards elastin synthesis. Although it will be important to resolve the details about which lysyl oxidase enzymes can bind to which fibulin proteins, as the specificity of these interactions may influence how elastic fiber synthesis is regulated.

The splicing of FBLN1 can be altered on the 3' end of the gene to result in four different isoforms (Figure 21) [277, 282]. Mice only express FBLN1 variants C and D [283], and variant A and B have only been detected in very low amounts in the human placenta [277]. Splice variants C and D seem equally abundant in most tissues and cells, but the C domain is homologous to the C-terminal domains of the other fibulin proteins. This, and biochemical and genetic evidence, has suggested distinct functions for the two splice variants. Nidogen has shown a higher binding affinity for FBLN1-C than FBLN1-D [284], and decreased expression of FBLN1-D has been associated with limb malformation [285] and a giant platelet syndrome [286]. From the yeast two-hybrid screening data (Table 5), it can not be concluded that LOX preferentially binds to the C variant of FBLN1, but it remains a possibility to be investigated.

FIBRONECTIN (FN)

FN has been well characterized as an extracellular matrix glycoprotein that can regulate many cellular functions such as proliferation, differentiation, migration, adhesion, and apoptosis [287-291]. FN accomplishes this diverse array of functions through interactions with a large variety of extracellular proteins including collagens, fibrin, thrombospondin, cell surface integrins, heparin sulfate proteoglycans, and tenascin-C. FN is expressed by most cell types and is secreted as a 450 kD dimer held together by C-terminal disulfide bonds, although the two subunits can vary due to alternative splicing. The FN fiberous molecule is mostly comprised of three types of repeating globular domains (Type I, II, and III) that stretch along the fiber (Figure 22).

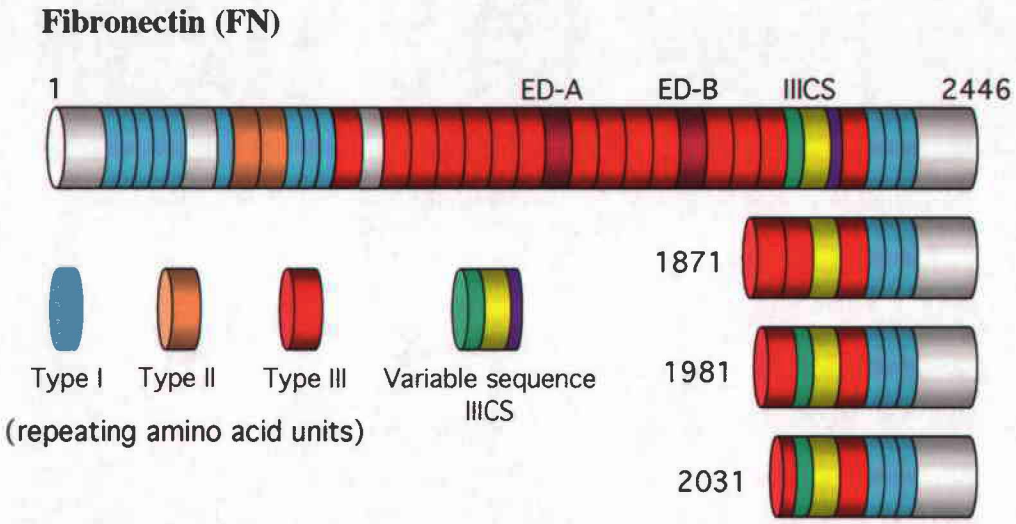

Figure 22: Schematic of the FN protein and the three FN fragments isolated in the Y2H screen with LOX. The fibronectin protein has three types of repeated motifs and can be alternatively spliced at the ED-A, ED-B, or the IIICS domain. The three C-terminal FN fragments all contain the central part of the IIICS segment, which is often spliced out in FN molecules expressed by hepatocytes (pFN). The numbers designate amino acids.

The FN dimer is secreted as a soluble molecule folded into a closed conformation, unable to form fibrils [292-295]. Activation of soluble FN induces a conformational change resulting in an insoluble molecule that is highly self-adhesive through revealed binding domains. This activation of FN is a tightly regulated process, occurring at specific areas of the cell surface [289, 291]. In tissues, activated FN is deposited and organized into a polymeric matrix attached to cell surface integrins. This matrix is critical to proper embryonic development, as demonstrated by the early embryonic lethality of the FN knockout mouse due to a failure to develop a cardiovascular system [296, 297].

When purified, FN has been traditionally categorized as either plasma FN (pFN) or cellular FN (cFN). pFN is very soluble, is synthesized by heptocytes, and circulates in the plasma at a high concentration (300 µg/mL) in a closed, non-active form. After tissue damage, pFN is an integral part of the clotting response, as it gets covalently crosslinked to fibrin by

Factor VIIIa (or transglutaminase). pFN is not efficiently assembled into a polymeric matrix due to its conformation, but it can be activated by cell-surface integrins [289, 291]. cFN is synthesized in tissues by various cell types (epithelial, fibroblasts, muscle cells, etc.) and exhibits a more complex pattern of alternative splicing than pFN [290, 298, 299]. In addition, cFN usually exists in an open, activated conformation when purified. Due to this conformation, and included domains not produced in pFN, cFN has been found to interact with more molecules and have more widespread cellular effects than pFN [300-304].

There is an extensive degree of tissue-specific alternative splicing of the human FN gene, which results in at least 20 possible splice variants [298]. The main alternatively spliced domains are individual type III repeats called the ED-A, ED-B, and IIICS (or variable) domains. In the human FN protein, the ED-A and ED-B can be included or excluded due to exon skipping, but the IIICS or V domain can be present in 5 possible conformations (Figure 23). It has been estimated that less than 1% of pFN molecules contain ED-A and ED-B domains, but a majority of the cFN contain these domains [305, 306]. In other species, the level of alternative splicing of the IIICS domain varies [298].

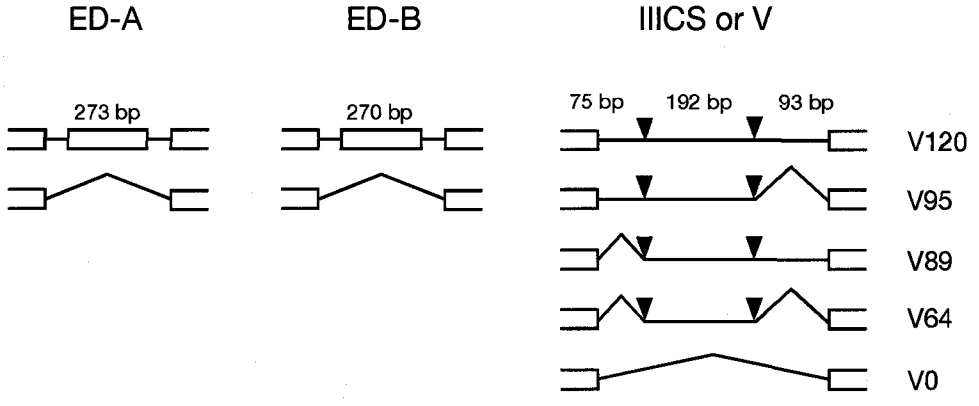

Figure 23. Fibronectin contains 3 major alternatively spliced domains. ED-A and ED-B are type III repeats that can be present or not in the protein. The type III connecting sequence or variable domain (IIICS or V domain) can exist in 5 alternatively spliced conformations. Figure modified from Matsui et al, 1997 [307].

There is increasing evidence that the FN splice variants can have differing functional roles. There is evidence that the inclusion of the alternatively spliced domains, as seen in cFN, promotes FN activation [308-310]. This may be due to at least two additional integrin binding sites (LDV and REDV) located in the IIICS domain [311, 312], which may specifically bind to $\alpha_4\beta_1$ and $\alpha_4\beta_7$ integrins instead of the $\alpha_5\beta_1$ which binds to the RGD sequence [313, 314]. In addition, novel protein binding sites in the IIICS domain have been identified, including sites for heparin [315]. There is also an oncofetal FN (onfFN) that is a unique splice variant expressed in fetal tissues and in solid tumors, but not in normal adult tissues [316-320]. In onfFN, the ED-B domain is included, as well as the IIICS which contains a glycosylation pattern unique to onfFN [321, 322].

Another very important function of FN has been recently discovered, one which makes the link to LOX of greater interest. The formation of the FN matrix has been recently shown to be critical for the subsequent assembly of Collagen I and III fibrils [323, 324]. The binding between collagen and FN was first published in 1977 [325] and has since been well characterized, and extensive co-distribution in tissues is observed [287, 288]. It has also been demonstrated that cFN is required for collagen gel contraction in wound healing models [300, 326, 327]. Lysyl oxidase enzyme activity has also been shown to be a critical factor in similar collagen gel contraction models [328, 329]. It has been previously suggested that the FN matrix acts as a scaffolding to regulate the deposition and assembly of type I and III collagens [323, 324, 330, 331], but the molecular mechanisms by which the FN matrix may accomplish this have not been explored.

The data from the direct interaction assays in yeast raise some questions about the domains responsible for binding and the specificity. The FN fragment seemed to bind to perhaps multiple sites along both LOX and LOXL, but did not bind to LOXL2. The PL protein

was consistent in its binding to LOX between amino acids 169-348, and PL bound to the Cterm of LOXL2 but not LOXL. The FBLN1 fragment bound to LOX, LOXL, and LOXL2. Are these interactions with the other LOX-like proteins real? What might the significance be of multiple interactions? Do the conserved lysyl oxidase domains have the same function in each family member? Will the results for LOXL and LOXL2 be confirmed in a mammalian system and *in vivo*? These questions should be investigated further, but unfortunately were beyond the scope of this dissertation. We continued to focus our attention on LOX, and perhaps these studies will also shed light on potential commonalities. In the future, what we discover with the LOX interactions will surely be tested for the other LOX-like family members.

The yeast two-hybrid screening is a powerful tool to discover potential interacting proteins and our results seemed very plausible, but screening is only the beginning of characterizing a novel protein-protein interaction. The bits of inconsistency from the direct interactions demonstrated why it is important to verify these protein-protein interactions in mammalian systems. We also kept in mind that the FN and FBLN1 cDNAs did not encode full-length proteins, and the extra domains not evaluated in this yeast system could very possibly interfere with interactions with LOX. In addition, although the screen uses human gene cDNA, the interactions occur in the nucleus of the yeast cell, which is a very different environment than where the proteins may encounter each other *in vivo*. Indeed, the proteins may never be co-localized *in vivo*, meaning they never have the potential to interact, despite the yeast two-hybrid results. The yeast two-hybrid screening also gives no estimation of the binding affinity of the two proteins, and the possibility of interaction does not indicate the biological significance of the interaction - of *why* these two particular proteins bind together. Therefore, a more detailed characterization of the protein-protein interaction is described in Chapter 3, and the investigation of the biological significance is described in Chapter 4.

MATERIALS AND METHODS

POLYMERASE CHAIN REACTION (PCR)

As a template for cloning the LOX cDNAs used as yeast two-hybrid baits, we used a plasmid expression construct previously cloned in our lab, pcDNA3.1-LOX, which was cloned and sequence-verified to include the complete LOX open reading frame (nucleotides 1-1254). PCR primers were designed to introduce restriction sites 5' and 3' to the amplified LOX cDNAs in order to clone the various inserts into Clontech's pGBKT7 vector downstream and in-frame with the GAL4 DNA-binding domain (GAL4-DB). Six pGBKT7-LOX bait plasmids were designed and cloned with the primers detailed in Table 6. Using a previously cloned and sequenced LOX cDNA as template, DNA fragments were amplified in a total volume of 50 μl containing 10 mM KCl, 20 mM Tris-HCl (pH 8.8), 10 mM $(NH_4)_2SO_4$, 2 mM $MgSO_4$, 0.1% Triton X-100, 125 μM of each dNTP, 0.5 μM of each primer, 1 U of Vent DNA polymerase (New England Biolabs), and 100 ng of template DNA. The PCR conditions were as follows: initial denaturation at 95°C for 5 min; 30 cycles of 95°C for 30 sec, 60-64°C for 30 sec, and 72°C for 1 min; and a final extension at 72°C for 7 min.

Table 6. PCR Primers for cloning pGBKT7-LOX baits.

Primer Name	Primer Sequence	Restriction Site
pGBKT7-proLOX F	5'-ACA TGC CAT GGT GAT GCG CTT CGC CTG GAC CG-3'	*EcoR*I
pGBKT7-proLOX R	5'-CGC GGA TCC CTA ATA CGG TGA AAT TGT GCA GC-3'	*BamH*I
pGBKT7-LOX F	5'-CCG GAA TTC GAC GAC CCT TAC AAC CCC TA-3'	*EcoR*I
pGBKT7-LOX R	5'-CGC GGA TCC CTA ATA CGG TGA AAT TGT GCA GC-3'	*BamH*I
pGBKT7-LOX_{1-168} F	5'-ACA TGC CAT GGT GAT GCG CTT CGC CTG GAC CG-3'	*EcoR*I
pGBKT7-LOX_{1-168} R	5'-TAT GGA TCC TTA GCC CAC CAT GCC GTC CAC-3'	*BamH*I
pGBKT7-LOX_{1-348} F	5'-ACA TGC CAT GGT GAT GCG CTT CGC CTG GAC CG-3'	*EcoR*I
pGBKT7-LOX_{1-348} R	5'-GC GGA TCC CTA ACT CAA TCC CTG TGT GTG TG-3'	*BamH*I
pGBKT7-$LOX_{169-348}$ F	5'-CCG GAA TTC GAC GAC CCT TAC AAC CCC TA-3'	*EcoR*I
pGBKT7-$LOX_{169-348}$ R	5'-GC GGA TCC CTA ACT CAA TCC CTG TGT GTG TG-3'	*BamH*I
pGBKT7-$LOX_{349-417}$ F	5'-CCG GAA TTC CCT GGC TGT TAT GAT ACC TA-3'	*EcoR*I
pGBKT7-$LOX_{349-417}$ F	5'-CGC GGA TCC CTA ATA CGG TGA AAT TGT GCA GC-3'	*BamH*I

After the yeast two-hybrid screen, isolated positive interacting clones contained two plasmids, the bait plasmid (pGBKT7) and the library plasmid (pACT2). To identify the library cDNA insert, PCR was performed with primers designed to flank the cDNA insert of the pACT2 library plasmid. The primers used were: F: 5'-CTA TTC GAT GAT GAA GAT ACC CCA CCA AAC CC-3' and R: 5'-AAG TGA ACT TGC GGG GTT TTT CAG TAT CTA CG-3'. DNA fragments were amplified in a total volume of 50 µl containing 10 mM KCl, 20 mM Tris-HCl (pH 8.8), 10 mM $(NH_4)_2SO_4$, 2 mM $MgSO_4$, 0.1% Triton X-100, 125 µM of each dNTP, 0.5 µM of each primer, 1 U of Vent DNA polymerase, and 100 ng of template plasmid DNA. The PCR conditions were as follows: initial denaturation at 95°C for 5 min; 30 cycles of 95°C for 30 sec, 60°C for 30 sec, and 72°C for 1 min; and a final extension at 72°C for 7 min.

AGAROSE GEL ELECTROPHORESIS

PCR products and DNA restriction digests were analyzed by agarose gel electrophoresis. Agarose (USB) was added to 1 x TAE buffer (40 mM Tris-acetate, 1 mM EDTA) to a final concentration of 1.2% and heated to near-boiling to dissolve the agarose. After cooling, ethidium bromide was added to a final concentration of 0.5 µg/mL, and the liquid agarose was poured into the gel casting kit of the HE 33 Mini Submarine Electrophoresis Unit (Amersham). Either a 16-well comb for a sample volume of 12 µl or an 8-well comb for a sample volume of 60 µl was used to create wells for sample loading. The gel was allowed to cool to room temperature, and was transferred to the resolving chamber and 1 x TAE buffer was added until it covered the gel. 2 µl of loading dye (0.25% bromophenol blue, 0.25% xylene cyanol, 15% ficoll) was added to each 10 µl of DNA sample, and samples were then loaded in the wells of the agarose gel. Molecular weight DNA markers (New England Biolabs) were used to determine the sizes of the separated DNA fragments. Electrophoresis was performed at 100 V

for 50-80 minutes, and the gel was analyzed on a UV transilluminator with a Kodak EDAS 290 imaging system.

DNA Purification from Agarose

To recover DNA fragments separated by agarose gel electorphoresis for cloning or sequencing, we used buffers and columns from a Qiagen Gel Extraction kit (Qiagen). Under UV light, the DNA fragments were excised using a scapel, and transferred to microcentrifuge tubes. The tubes were weighed before and after to estimate the mass of the gel slice. We dissolved the agarose gel by adding 3 volumes of Buffer QG to 1 volume gel (100 mg ~ 100 µl) and incubating for 10 min at 50°C. Once dissolved, 1 volume of isopropanol was added and the mixture was applied to a QIAquick DNA binding column. After centrifuging out the liquid, the DNA bound in the column was washed with Buffer PE, and eluted in dH_2O. An aliquot of this purified DNA was analyzed again by agarose gel to determine the DNA concentration and verify the quality of purification.

Measurement of DNA concentration.

To determine the concentration of plasmid DNA and amplified fragments of DNA in solution, we used agarose electrophoresis to compare aliquots of our samples with known quantities of DNA. The agarose gel electrophoresis was performed and imaged as previously described, and lambda DNA digested with the *HindIII* restriction enzyme (New England Biolabs) was used as a molecular weight marker. Serial dilutions of the DNA sample to be quantified were resolved in adjacent lanes and visually compared to those bands of the marker. From these comparisons, the quantity of DNA in these known volumes could be calculated.

Restriction Enzyme Digestion

The PCR-amplified LOX fragments, and the plasmid vector pGBKT7 (Clontech), were double digested with either *EcoRI* and *BamHI*, or *NcoI* and *BamHI* (all from New England

Biolabs), in preparation for cloning. The double digestions were performed using *EcoRI* digestion buffer (50 mM NaCl, 100 mM Tris-HCl, 10 mM MgCl, 0.025% Triton X-100, pH 7.5) with 100 µg/ml BSA as recommended by the manufacturer. After incubation at 37°C for 120 min, the digested DNA was analyzed by agarose gel electrophoresis and gel purified as described above.

DNA Ligations

The digested LOX fragments and plasmid vector, pGBKT7, were ligated together in a 20 µl reaction containing 1 x Ligation Buffer (50 mM Tris-HCl (pH 7.6), 10 mM $MgCl_2$, 1 mM ATP, 1 mM DTT, 5% PEG-8000), 60 fmol of the digested LOX DNA, 20 fmol of the digested vector DNA, and 0.1 U of T4 DNA Ligase (Invitrogen). This mixture was incubated at room temperature for 75 min and then transformed into *E. coli* to isolate successful ligations. Parallel ligations were performed with digested vector only as a negative control to indicate the rate of self-ligation.

Bacteria Media and Plates

E. coli were grown with Luria-Bertani (LB) media and agar plates. The LB media was made by mixing 10 g of Tryptone (Difco), 5 g of yeast extract (Difco), and 10 g of NaCl (Fisher Scientific), and then adjusting the pH to 7.0 with NaOH. The media was then autoclaved and kept in airtight bottles until use. If needed, antibiotics were added immediately before use. For LB-agar plates, 15 g of agar (Difco) was added after the pH was adjusted, then the mixture was autoclaved. After cooling to ~50°C, antibiotics were added, and the liquid was poured in sterile 10 cm Petri dishes (Fisher). For selectively growing *E. coli* resistant to antibiotics, ampicillin and kanamycin were both used at 50 µg/ml.

Bacterial Transformations

Plasmid DNA was transformed into XL-1 Blue *E. coli* bacteria (Stratagene) using a heat-shock method. Frozen competent XL-1 Blue cells were thawed and 50 µl were transferred to a

sterile round bottom polypropylene tube on ice (Falcon). 1.7 µl of β-mercaptoethanol was added and the mix was incubated on ice for 10 min. The plasmid DNA to be transformed was added, either 50 ng of a known plasmid or 2 µl of the ligation reaction, and the mix was incubated for 30 min on ice. The cells were heat-shocked at 42°C for 45 sec and then put back on ice for 1 min. To allow expression of the antibiotic resistance gene on the plasmids, 950 µl of LB media was added to the cells, and they were incubated at 37°C with shaking at 250 rpm for 1 hr. 100 µl of the cells were then spread on LB-agar plates containing the appropriate antibiotic, and the plates were incubated overnight at 37°C. Colonies were then picked up with a sterile wire loop and streaked on fresh LB-agar plates to obtain single colonies.

PLASMID PURIFICATIONS FROM BACTERIA

To extract and purify plasmid DNA from bacteria, we used the buffers and columns included in the Qiagen Plasmid Midiprep kit (Qiagen) according to the manufacturer's protocol. The bacteria containing the plasmid was inoculated in 100 ml of LB media with the appropriate antibiotic, and the cells were grown overnight at 37°C with shaking at 250 rpm. The cells were harvested from the culture by centrifugation at 3300 x g for 15 min, and the cell pellet was resuspended in 4 ml of Buffer P1 (50 mM Tris-HCl (pH 8.0), 10 mM EDTA, 100 µg/ml RNase A). 4 ml of Buffer P2 (200 mM NaOH, 1% SDS) was added and the mixture was incubated at room temperature for 5 min. 4 ml of ice-cold Buffer P3 (3 M KAc, pH 5.5) was added, and the mixture was incubated on ice for 15 min to precipitate the bacterial proteins. The samples were centrifuged for 45 min at 3300 x g, and the supernatant containing the plasmid DNA was then filtered with sterile nylon filters to remove the residual precipitated protein. After equilibrating a Qiagen-tip 100 column with 4 ml of Buffer QBT (750 mM NaCl, 50 mM MOPS (pH 7.0), 15% isopropanol), the filtered supernatant containing the plasmid DNA was passed through the column. We subsequently washed the column twice with Buffer QC (1.0 mM NaCl, 50 mM MOPS (pH 7.0), 15% isopropanol), and then eluted the plasmid DNA with 5 ml of Buffer QF (1.0

mM NaCl, 50 mM Tris-HCl (pH 8.5), 15% isopropanol). The plasmid DNA was precipitated by adding 3.5 ml of isopropanol to the elutant, mixing well, and centrifuging at 3300 x g for 60 min. The supernatant was aspirated, and the DNA pellet was washed twice with 70% ethanol, and allowed to air-dry. The purified plasmid DNA was dissolved in 500 µl of TE buffer (10 mM Tris-HCl (pH 8.0), 1 mM EDTA).

DNA SEQUENCING

Purified plasmids and purified PCR products were amplified in a cycle-sequencing PCR reaction containing 80 mM Tris-HCl (pH 9.0), 2 mM $MgCl_2$, 0.16 µM of the sequencing primer, 200 ng of template DNA, 2 µl of ABI Prism BigDye Terminator Mix (Perkin Elmer-Applied Biosystems, Inc.), and 1 U of Amplitaq (Perkin Elmer – Applied Biosystems, Inc.). For sequencing the pGBKT7-LOX bait constructs, the T7 vector primer was used: F: 5'-TAA TAC GAC TCA CTA TAG GG-3'. For sequencing the cDNA fragments that were PCR amplified from the positive library plasmids isolated in the two-hybrid screen, both forward and reverse primers were used: F: 5'-CTA TTC GAT GAT GAA GAT ACC CCA CCA AAC CC-3' and R: 5'-AAG TGA ACT TGC GGG GTT TTT CAG TAT CTA CG-3'. After the cycle-sequencing reaction, the DNA in each sample was precipitated by adding 2 µl of 3 M sodium acetate (pH 4.6) and 50 µl of 100% EtOH, and incubating at room temperature for 15 min. The samples were centrifuged at 3300 x g for 30 min and the DNA pellets were washed with 70% EtOH and allowed to air-dry. After drying, the DNA was dissolved in 20 µl of Template Suppression Reagent (TSR) buffer (Perkin Elmer – Applied Biosystems, Inc.). Before loading on the ABI 310 capillary sequencer, the samples were denatured at 95°C for 2 min and quickly put on ice.

YEAST MEDIA AND PLATES

Yeast cells not containing plasmids were grown with YPD media and agar plates. The YPD media was made by mixing 10 g of yeast extract (Difco) and 20 g of peptone (Difco) into 0.9 liter (total volume) of dH_2O, and then adjusting the pH to 5.8 with NaOH. The media was then

autoclaved, allowed to cool, and 100 mL of a sterile 20% dextrose solution (Fisher Scientific) was added. The YPD media was kept in airtight bottles until used. For YPD-agar plates, 15 g of agar (Difco) was added after the pH was adjusted, then the mixture was autoclaved. After cooling to ~50°C, the dextrose was mixed in, and the liquid was poured in sterile Petri dishes (Fisher). For selectively growing yeast with plasmids encoding, we used nutritional dropout media and plates. This dropout media lacks particular amino acids, and was made by mixing 6.7 g of yeast minimal media (Difco) and 0.6-0.7 g of dropout supplement (Clontech). The pH of this media was adjusted to 5.8, and the media was autoclaved. After cooling, 100 mL of a sterile 20% dextrose solution was added, and the media was kept in airtight bottles until use. For dropout plates, 15 g of agar was added to the media after adjusting the pH. After autoclaving, the liquid was cooled, the dextrose mixed in, and the solution was poured into sterile Petri dishes (Fisher).

YEAST TRANSFORMATIONS

Plasmid DNA was inserted into AH109 yeast cells (Clontech) using a heat-shock method. Frozen yeast cells were streaked onto YPD plates and grown for 2 days at 30°C. From these plates, single colonies were inoculated in 50 ml of YPD media and grown overnight at 30°C with shaking at 270 rpm. The next morning, 90 ml of fresh YPD media was added to the overnight culture and incubated for another 4 hr at 30°C with shaking at 270 rpm to achieve logarithmic growth. The cells were pooled by centrifugation at 3300 x g for 5 min and then were washed once with sterile dH_2O. After removing the supernatant, the cell pellet was resuspended in 1.5 ml of sterile TE/LiAc (lithium acetate) solution (10 mM Tris-HCl (pH 7.5), 1 mM EDTA, 100 mM LiAc). For each transformation, 100 µl of this cell suspension was aliquoted into a fresh microcentrifuge tube, and to this was added 0.1 µg of each plasmid to be transformed, 100 µg of Herring testes carrier DNA (Clontech), and 600 µl of freshly made sterile PEG/LiAc solution (TE/LiAc with 40% polyethylene glycol 4000). After vortexing, the cells were incubated for 30

min at 30°C with shaking at 200 rpm. 70 µl of DMSO was then added and the cells were heat-shocked in a 42°C water bath for 15 min. The cells were chilled on ice for 2 min and then centrifuged at 14,000 x g for 5 sec. The pelleted yeast cells were resuspended in 150 µl of sterile TE buffer and spread on the appropriate selective dropout agar plates. These plates were incubated at 30°C for 3 days, and positive colonies were picked with a sterile loop and streaked on fresh dropout plates to obtain single colonies.

Polyacrylamide Gel Electrophoresis (PAGE) of Proteins

Protein samples were separated by electrophoresis through SDS-polyacrylamide gels prior to Western blotting. For analyzing recombinant proteins expressed in yeast, cells were grown in overnight cultures at 30°C with shaking at 270 rpm. For each sample, 1.5 mL of the yeast cultures was aliquoted into a microcentrifuge tube and centrifuged at 14,000 x g, and the supernatant was aspirated. The yeast pellet was resuspended in 40 µl of 2X Laemmli buffer (125 mM Tris–HCl (pH 6.8), 4% SDS, 20% glycerol, 100 mM DTT), boiled for 5 minutes, and then chilled on ice for 2 min. After mixing the SDS-acrylamide gel mixture for the resolving gel (10% acrylamide, 375 mM Tris-HCl (ph 8.8), 0.1% SDS), ammonium persulfate (APS) and TEMED were added to initalize polymerization. This mixture was poured between glass plates separated by 1 mm spacers. After the resolving gel polymerized (~45 min), the overlaying dH_2O was poured off, and the stacking gel mixture (5% acrylamide, 130 mM Tris-HCl (pH 6.8), 0.1% SDS, with APS and TEMED) was pipetted onto the top. The comb was inserted and the stacking gel was allowed to polymerize for ~45 min. 5 µl of each protein sample was then loaded into the wells, as was 12 µl of SeeBlue+2 protein molecular weight marker (Invitrogen), and the gels were resolved on a Hoeffer miniVE protein gel apparatus (Amersham) for 2 hr at a constant 16 mA per gel.

WESTERN BLOT ANALYSIS

After protein samples were resolved by SDS-PAGE, they were transferred onto a pre-treated Immobilion-P membrane (Millipore P-15552, Fisher). The membrane was activated by soaking in methanol for 1 min, washed in dH_2O twice for 1 min each, and then soaked in transfer buffer (48 mM Tris, 39 mM glycine). The gel was layered next to the membrane between two pieces of filter paper (presoaked in transfer buffer) and placed in a Trans-blot semi-dry apparatus (Biorad). A constant electrical current was applied (2 mA/cm^2) for 60 min to promote an efficient protein transfer. After the blotting, the top right corner of the membrane was cut to mark orientation, and the blot was blocked with 5% Carnation non-fat dry milk in PBST (13.7 mM NaCl, 10 mM Na_2HPO_4, 0.27 KCl, 0.17 mM KH_2PO_4, 0.1% Tween-20 for overnight at 4°C. The next morning, the blot was rinsed 5 times with dH_2O, and washed once with PBST for 5 min with orbital rotation. The blot was then incubated with the appropriate primary antibody, diluted in PBST, for 1 h at room temperature with slow orbital rotation. To detect the presence of the bait GAL4-BD-fusion proteins in yeast cells, a mouse monoclonal anti-c-Myc antibody was used (Clontech) at 2 µg/ml concentration. After incubation with the primary antibody, the blot was rinsed again 5 times with dH_2O and washed once with PBST for 5 min with orbital rotation. The blot was then incubated with the appropriate secondary antibody conjugated to horseradish peroxidase (HRP), diluted in PBST, for 1 h at room temperature. To detect the anti-c-Myc antibody, the anti-mouse secondary antibody conjugated to HRP from Amersham was used at 1:5000 dilution in PBST. The blots were again washed as described above, with three final washes with PBS for 1 min each. To detect the presence of bound HRP, the ECL kit (Amersham) was used for chemiluminescent detection. Equal volumes of ECL reagent #1 and #2 were mixed, and the blots were incubated in this mix for 1 min. After briefly draining, the blots were then inserted into clear plastic envelopes and exposed to autoradiograph film for various amounts of time, depending on the strength of the signal. The exposed film was soaked in developer solution (Sigma) for 1 min, rinsed in dH_2O, soaked in fixer solution (Sigma) for 2 min,

and then rinsed well in dH_2O. The film was air-dried and then aligned with the blot in order to mark the molecular weight marker bands.

AMPLIFICATION OF TWO-HYBRID LIBRARY

The human yeast two-hybrid plasmid library to be screened was purchased from Clontech (Cat # HL4025AH). This library was constructed from cDNA reverse-transcribed from placental mRNA using oligo-dT primers with an introduced XhoI restriction site. A short adapter sequence was blunt-end ligated to the 5' end of the cDNAs, and they were cloned into the pACT2 plasmid vector. From the manufacturer's specifications: 95% of the colonies were estimated to have inserts; the number of independent clones was 3.5×10^6; and the average cDNA size was 2.0 kb. The plasmid library arrived packaged in *E. coli* as frozen glycerol stocks and required an amplification step before being used for yeast two-hybrid screening. The titer of viable bacteria was determined by plating dilutions of the frozen stock, incubating the plates at 37°C overnight, and then counting the colonies. The number of colony-forming units (cfu) per microliter was calculated to be 3.2×10^6 cfu/µl. Since there was 3.5×10^6 independent clones in the library, in order to amplify with a 3X coverage, we needed to plate 10.5×10^6 bacteria in enough surface area to ensure each could grow into a independent colony. Therefore, 3.27 µl of the bacteria frozen stock was diluted into 42 mL of LB media and equally spread on 42 large square LB-agar plates (500 cm^2). The cells were plated by pipetting 1 ml of the cell suspension onto the LB-agar, adding ~30 sterile glass beads (diameter ~5 mm) (Sigma), and shaking the plate randomly until the liquid was evenly distributed (~2 min). The plates were then incubated at 30°C for 30 hours, and the bacterial colonies were collected with a sterile cell scraper and pooled in LB media with 25% glycerol. Once all the bacterial colonies were collected, the cells were washed twice with the LB-glycerol media, and centrifuged at 3300 x g for 5 min. The library plasmid DNA was extracted and purified using a Qiagen MegaPrep Kit (Qiagen) in the same manner as described above in "*Plasmid Purifications from Bacteria.*"

SCREENING OF TWO-HYBRID LIBRARY

We performed the yeast two-hybrid screening according to the protocol described by Clontech's MATCHMAKER GAL4 Two-Hybrid System 3. Once the pGBKT7-LOX bait construct was transformed into AH109 yeast cells, the expression was verified, and the autonomous activation of the reporter genes was verified negative, the two-hybrid plasmid library was transformed into the AH109 yeast that contained pGBKT7-LOX. For the library-scale transformation, freshly-grown yeast colonies were inoculated into 150 ml of Trp^- dropout media and grown at 30°C overnight with shaking at 270 rpm. The next morning, 850 ml of fresh Trp^- dropout media was added to the culture, and this was grown at 30°C with shaking at 270 rpm until the OD @ 600 nm = 0.5. The cells were divided into 50 ml conical tubes and centrifuged at 3300 x g for 10 min. The cells were pooled, washed with sterile dH_2O, and resuspended in 8 ml of TE/LiAc solution. In a 500 ml flask, 20 mg of Herring testes carrier DNA, 200 µg of the yeast two-hybrid, the 8 ml of yeast cells, and 60 ml of sterile PEG/LiAc solution were all mixed and incubated at 30°C for 30 min with shaking at 200 rpm. 7 ml of DMSO was then added, and the cells were heat shocked in a 42°C water bath for 15 min with occasional swirling. After chilling the cells on ice for 2 mins, they were centrifuged at 3300 x g for 5 min. The cell pellet was resuspended in 10 ml of sterile TE buffer. Clones containing interacting proteins were selected by growth on a dropout plates lacking leucine, tryptophan, histidine, and adenine and by activation of the *lacZ* gene. The cells were evenly spread on ~50 $Ade^-/His^-/Trp^-/Leu^-$ ($AHWL^-$) selective dropout agar plates (150 mm). These plates were incubated at 30°C for 3 days, and positive colonies were picked with a sterile loop and streaked on fresh $AHWL^-$ dropout plates to obtain single colonies.

ASSAY FOR LACZ ACTIVITY IN YEAST

To assay for lacZ activity, colonies isolated from the AHWL- plates were spotted onto nylon membrane (Amersham). The filters were then frozen in liquid nitrogen, and then thawed at room temperature, in order to lyse the cells. Under a fume hood, the filters were then laid on

Whatman paper pre-soaked in Z buffer/X-Gal solution (0.1 M Na phosphate (pH 7.2), 10 mM KCl, 2 mM $MgSO_4$, 50 mM b-mercaptoethanol, 0.334 mg/ml X-gal). The filters were incubated in the this solution, and the appearance of blue color was closely monitored. After ~4 hours, the images of the filters were recorded using a flatbed scanner.

PLASMID PURIFICATIONS FROM YEAST

Purifying plasmids from yeast cells is similar to bacteria, and several of the same reagents used are detailed above in *"Plasmid Purifications from Bacteria."* Yeast colonies isolated as positives from the two-hybrid screen were inoculated in 3 ml of WL^- dropout media and incubated at 30°C overnight with shaking at 270 rpm. The next morning, 1.5 ml of the cultured cells were transferred to a microcentrifuge tube and centrifuged at 14,000 x g for 5 min to pellet the cells. The media supernatant was aspirated, and the cells were resuspended in 150 µl of Buffer P1. To digest the yeast cell wall, 2 µl of Zymolase enzyme was added to the cell suspension and the sample was incubated at 37°C for 60 min. 150 µl of Buffer P2 was added, then 150 µl of Buffer P3, and the sample was incubated on ice for 5 min. The sample was centrifuged at 14,000 x g for 20 min at 4°C to spin down the yeast proteins. The supernatant containing the DNA was then transferred to a fresh microcentrifuge tube. The plasmid DNA was precipitated by adding $1/10^{th}$ of the total volume of 3 M sodium acetate (pH 5.2), and twice the total volume of ice-cold 100% EtOH. The sample was mixed well, and frozen at -80°C for 60 min. The sample was centrifuged at 14,000 x g for 20 min at 4°C to pellet the DNA, and then the supernatant was aspirated. The DNA pellet was washed once with 70% EtOH, and air-dried. Finally the plasmid DNA was dissolved in 20 µl of TE buffer.

CHAPTER 3. CHARACTERIZATION OF LOX'S INTERACTION WITH FN

INTRODUCTION

The yeast two-hybrid screening with LOX was successful in identifying several potential protein-protein interactions. However, to continue further we needed to prioritize the positives because of the large quantity of work required to verify and characterize the interactions. Twenty-three positive proteins were too many to pursue each putative interaction individually. In evaluating priorities, we had three main qualifications for choosing high priority positives – plausibility, relevance, and feasibility.

Plausibility: With the interaction between LOX and these positive proteins requiring verification in a mammalian system, we had to evaluate which interactions were most likely to be real. Only plausible interactions were considered for follow-up experiments. Immediately, this suggested that we limit the positives under consideration to ones represented by multiple clones. There were some very interesting single-clone positives detected in the two-hybrid screen, but the investment in time was too much to try and work with each protein.

Relevance: The multi-clone positives included two proteins that were strictly pregnancy-specific: pregnancy-associated plasma protein A and pregnancy-specific beta-glycoprotein e. We wanted to focus on protein interactions that might have a wide-ranging impact on normal biological processing as well as pathological conditions such as cardiovascular disease and cancer, so we did not pursue LOX's potential interaction with these two proteins.

The PL protein is also pregnancy associated, however there are a couple of points that make PL more interesting. The first is the expression in a high percentage of breast tumors, and thus the classification of PL as an oncogene. The second is the high homology of PL with its hormone family members GH and PRL, which suggested that LOX might also interact with these two hormones. For these two reasons, we did not rule out PL for follow-up experiments.

The ECM proteins FN and FBLN1 both have a wide range of functions, and both have been implicated in several human pathologies in a similar way as LOX. Knockout mice for both FN and FBLN1 died due to cardiovascular defects, as did the LOX knockout mouse. In addition, recent evidence for FN's regulation of collagen matrix assembly strongly suggested that this would be an important interaction to characterize. For these reasons, we considered FN and FBLN1.

Feasibilty: To perform the follow-up experiments to characterize these interactions, we determined whether critical reagents were available for these proteins. For the *in vitro* binding analysis proposed in Specific Aim 2 and 3, purified PL and FN proteins were commercially available, but FBLN1 protein was not. This was a serious limitation for any further research to investigate the interaction between FBLN1 and LOX, as an extra investment of time and resources would be necessary to produce sufficient quantities of FBLN1 protein. For this reason, FBLN1 was considered a lower priority than PL and FN.

From the considerations discussed above, and from extensive literature research and analysis, we decided to focus our efforts on characterizing LOX's interaction with the extracellular matrix protein ***fibronectin (FN).*** This is not to say that no further studies concerning PL and FBLN1 are being undertaken. The possibilities are exciting, and some of the results will be discussed in Chapter 5 under "Future Directions."

FN is a very exciting molecule because it has a wide range of functions and regulates many aspects of cell phenotype, including proliferation, differentiation, migration, adhesion, and apoptosis [287-291]. This range of cellular functions mirrors some of what has been reported for LOX (discussed in Chapter 1) and there seemed to be some connections in the biological roles of the two proteins. Characterizing this interaction could have wide ranging implications for basic scientific knowledge and implications for understanding the progression of human pathology, making it clinically relevant.

There also is overwhelming data suggesting FN has a role in regulating the assembly of other ECM components, including collagen fiber assembly. However, no molecular mechanism on how FN might function this way have been described. In two recent studies of FN-null cultured cells, the polymerization of type I and III collagen was dependent on the preceding polymerization of the FN matrix [323, 324]. It is not known how this FN matrix directs the deposition or assembly of the collagen matrix, but the binding of FN to a number of ECM molecules is well characterized. This includes type I collagen [332], type III collagen [332], tenascin-C [333], FBLN-1 [267], fibrin [332], thrombospondin [334], latent TGF-β binding protein-1 [335], and heparin sulfate proteoglycans [336]. If FN binds to LOX in this complex extracellular environment, it is possible that FN could bring together enzyme and substrate to direct local areas of catalytic crosslinking of ECM molecules.

Another open question about LOX that the FN interaction had the potential to address was how the proteolytic activation of LOX is regulated. It has been assumed that LOX is immediately processed following secretion into the extracellular space. However, experimental evidence suggests that the proteolytic activation LOX is more regulated than automatic, that the secreted proLOX might be held in the ECM until needed. The induction of LOX mRNA expression in response to dermal injury has been demonstrated to be rapid (peaking after 3 days) and to precede Collagen III deposition [337]. However, LOX enzyme activity has been shown to peak later (8-10 days post-wound) [338], which suggests that the LOX pro-enzyme may be held in the extracellular space for a period of time before activation. Many studies have described alterations of LOX expression, or of LOX enzyme activity, in response to biological stimuli, but in many of these studies the level of alteration between LOX mRNA and LOX activity were not consistent [339-345]. This suggests that the regulation of LOX's post-transcriptional activation is an important factor in the overall regulation of LOX activity, but this process remains poorly understood.

Another important reason to investigate a potential LOX-FN interaction was to more clearly illustrate the role of these proteins in certain human pathologies. The misbalance of ECM

deposition, homeostasis, and degradation often results in diseases such as cancer, cardiovascular disease, and fibrosis. Like LOX, FN has been implicated in cardiovascular diseases such as atherosclerosis, hypertension, restenosis, and aneurysms [289, 346, 347]. In the atherosclerosis vascular intima, FN upregulation is associated with the VSMC migratiory phenotype [348-350]. The upregulation in atherosclerotic lesions is also co-localized with an upregulation of type III collagen, mimicking the wound healing process [351]. The re-expression of the fetal form of FN (discussed more below) after vascular injury, and in dialated cardiomyopathies, has also been demonstrated [352, 353]. Inhibition of FN expression also inhibits the overall thickening of the intima [354]. The summary of the data indicates that increased levels of both FN and LOX are associated with the worsening of atherosclerosis, and that FN and LOX are also upregulated after vascular injury or angioplasty, which contributes to the restenosis of the vessel.

In human carcinogenesis, FN has been traditionally characterized as a tumor suppressor, due to the consistent loss of pericellular FN upon malignant transformation [288, 355]. Transformed cells revert to a normal phenotype when cellular FN is added [356, 357], or when the cells are seeded on pericellular matrix isolated from normal cells [358]. Interestingly, an increased production of the FN matrix often surrounds a non-invasive tumor as part of the dense stromal ECM accumulation [359]. Additionally, certain FN splice variants and proteolytic fragments can actually promote tumorigenesis [360-364]. There is an oncofetal splice variant of FN, which includes the ED-A, ED-B, and IIICS domains with a special glycosylation pattern [316, 322]. This oncofetal FN is expressed in fetal tissues and not normally in adult tissues, but gets activated in tumor cells and surrounding stroma [317, 318], and has been associated with increasing staging of colorectal and breast cancers [319, 365].

The multiple functions and complex molecular mechanisms of FN in cardiovascular disease and cancer is still being explored, but an interaction with LOX may contribute to these pathologies and may be a valid therapeutic target. For all the reasons presented above, we decided to focus most of our efforts on studying the FN-LOX interaction.

The main challenge for this section was generating enough purified LOX protein to biochemically study the protein interactions. The purified human FN was commercially available, either purified from plasma (pFN) or from tissues (cFN). Purified LOX protein is not commercially available, so we were required to develop a method for producing sufficient quantities of purified LOX protein. We decided on the approach of expressing and purifying recombinant LOX, and towards this goal, we tested several expression systems. This included rabbit reticulolysate *in vitro* transcription and translation (IVTnT) reactions, mammalian cell transfections, and a bacterial expression system.

In our evaluation of these systems, it was quickly apparent that although the IVTnT and mammalian cell systems successfully produced LOX, it was not in quantities sufficient for our experiments. Therefore, after our initial evaluation of these three systems, we decided to use the bacterial expression system to generate LOX and various LOX deletion fragments as glutathione S-transferase (GST)-tagged recombinant proteins. The expression level was very high with this system, and the GST tag allowed for the rapid purification through the well-characterized binding of GST to glutathione [366]. In addition, the GST tag is large (26 kD) and very soluble, which was beneficial when trying to express insoluble proteins such as LOX. Only after we were able to generate purified GST-LOX protein were we able to perform further experiments to accomplish our specific aims.

Our experimental approach to characterizing this interaction of LOX with FN was to use a combination of *in vitro* and *in vivo* binding assays. The first priority was to demonstrate that the native biological forms of the mammalian proteins would confirm what was detected in yeast. Towards this, we performed pull-down assays and far-Western blots. In addition, we tested if LOX and FN interacted in a cell culture model where both proteins were expressed and secreted. A major goal of this characterization was to quantify the binding affinity of LOX and FN by measuring the equilibrium disassociation constant (K_d). This K_d value is commonly used

to objectively compare the strength of molecular interactions. For this, we used solid phase binding assays (SPBA), which are classic experiments for measuring binding affinities of extracellular matrix proteins, as well as receptor-ligand interactions [367]. We also used these assays to test FN's affinity for the various LOX deletion fragments, and to test if the LOX antibody could be used to inhibit these interactions.

RESULTS

Generation of expression constructs for recombinant LOX

To express LOX as a GST fusion protein in *E. coli*, the plasmid vector pGEX-4T-1 was obtained from Amersham. The GST-encoding sequence is 5' of the MCS, and the sequence between the GST sequence and the MCS encodes a thrombin cleavage site (Figure 24). The thrombin site allows for directed proteolytic cleavage to remove the GST tag from the purified fusion protein. The expression of the GST fusion gene is under transcriptional control of the IPTG-inducible *Ptac* promoter (Figure 24). The pGEX-4T-1 vector also contains an ampicillin resistance gene (Amp^r) for bacterial selection.

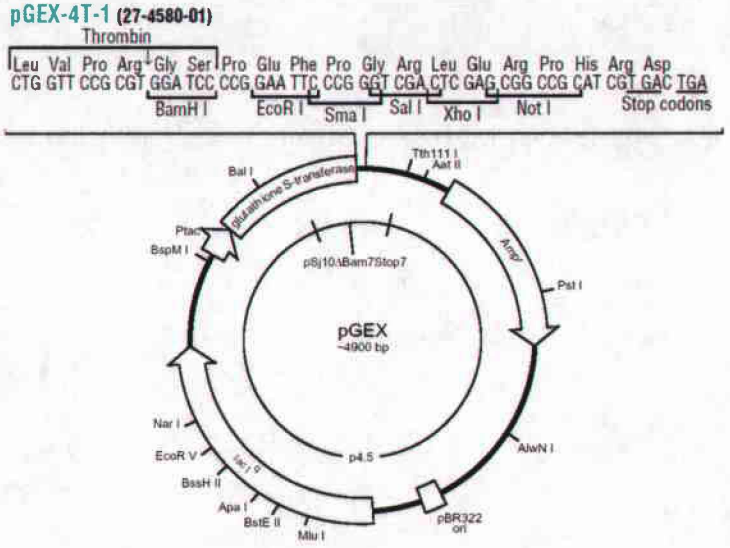

Figure 24. Diagram of pGEX-4T-1 vector used to express GST-fusion proteins in *E coli*. The pGEX-4T-1 vector contains both the GST protein and a thrombin cleavage site 5' of the MCS, where the cDNA fragment of interest is inserted in frame. The expression of the GST-fusion protein is under the control of the inducible promoter *Ptac*. pGEX-4T-1 also contains an Ampicillin resistance gene for selection. Figure taken from Amersham's technical literature.

Based on the six pGBKT7-LOX constructs described in Chapter 2, six LOX expression constructs were designed and successfully cloned to produce GST-LOX fusion proteins in *E. coli*. The LOX cDNA inserts of the pGBKT7-LOX plasmid constructs were cloned into the pGEX-4T-1 vector. To remove the LOX inserts, pGBKT7-LOX and all the LOX constructs shown in Figure 14 were digested with *EcoR*I and *Sal*I restriction enzymes. The digested plasmids were analyzed by agarose gel electrophoresis and the band corresponding to the LOX cDNA insert was agarose gel purified. The pGEX-4T-1 plasmid was also digested with *EcoR*I and *Sal*I and agarose gel purified. The inserts were ligated into the pGEX-4T-1 vector in-frame with the N-terminal GST and thrombin cleavage site (ThCS). Aliquots of the ligation reactions were transformed into *E. coli* to select for successful ligations. Plasmid DNA was extracted from the colonies that grew on the LB-amp plates, and plasmids containing the correct-sized LOX insert were screened for using restriction digests with *EcoR*I and *Sal*I followed by agarose gel

electrophoresis. Finally, the pGEX-LOX plasmids were sequenced to verify that the cloning was successful. Table 7 lists the six pGEX-LOX plasmid constructs generated by this cloning.

Table 7. Generated pGEX-LOX constructs for bacterial expression of recombinant GST-LOX fusion proteins.

Name of Construct	LOX nucleotides	LOX Amino Acids	Cloning Restriction Sites	Brief Description
pGEX-proLOX	1-1254	1-417	*EcoR*I & *Sal*I	Full-length proLOX
pGEX-LOX	505-1254	169-417	*EcoR*I & *Sal*I	Processed active LOX
pGEX-LOX_{1-168}	1-504	1-168	*EcoR*I & *Sal*I	Propeptide domain
pGEX-LOX_{1-348}	1-1044	1-348	*EcoR*I & *Sal*I	Full-length minus CRL
pGEX-$LOX_{169-348}$	505-1044	169-348	*EcoR*I & *Sal*I	Active LOX minus CRL
pGEX-$LOX_{349-417}$	1045-1254	349-417	*EcoR*I & *Sal*I	CRL domain

Expression and purification of recombinant GST-LOX fusion proteins

The pGEX-LOX constructs were transformed into the BL21 strain of *E. coli*, which is a low-protease strain developed for recombinant protein expression. We also transformed the pGEX-4T-1 vector to express just the GST protein alone as a negative control for the binding experiments. To express GST and the GST-LOX fusion proteins (shown as a diagram in Figure 25) the cells were grown in LB-amp cultures overnight at 37°C. The next morning, the cells were diluted 10-fold with fresh LB media and allowed to grow for 2 more hours at 37°C. To induce the expression of the recombinant fusion proteins, IPTG was added to the culture and the cells were grown at 30°C for 2 more hours. The lower induction temperature slowed the rate of bacterial growth in order to decrease the formation of inclusion bodies. The cells were centrifuged down to a pellet, and the proteins were extracted and analyzed.

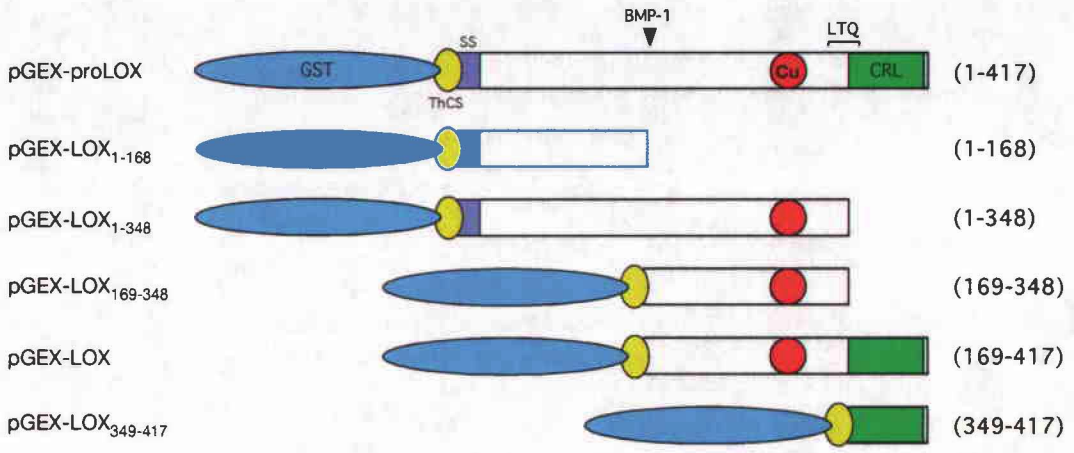

Figure 25. Protein domain organization of the GST-LOX fusion proteins. The bait used for the initial yeast two-hybrid screen (GAL4-BD-LOX) is indicated with an arrow. Numbers refer to the included LOX amino acids. The individual domains are indicated: GST (blue); thrombin cleavage site (yellow); signal sequence (purple); BMP-1 proteolytic cleavage site (arrowhead); copper-binding site (red); LTQ co-factor; CRL domain (green).

Based on the Amersham protocols of GST expression in *E. coli*, we extracted the proteins into 3 fractions based on solubility. The first fraction was the "soluble" fraction, which was extracted using a commercial bacterial lysis buffer. We centrifuged the non-solubilized cell debris down to a pellet and collected the supernatant containing the soluble proteins. From the debris pellet, we then extracted the "lysozyme soluble" fraction with a lysozyme digestion in lysis buffer. After three sequential repetitions of lysozyme treatment (resulting in three lysozyme soluble fractions), the remaining insoluble cell debris was pelleted by centrifugation and was termed the "inclusion body" fraction.

For each GST-LOX fusion protein, as well as the GST only control, the protein fractions were extracted and analyzed. We asked the following questions: In which fraction is the majority of the fusion protein? Is the fusion protein present at the correct molecular weight? Is the correct-sized fusion protein expressed in sufficient quantities for further binding studies? If these results were unsatisfactory for any fusion protein, numerous optimization strategies were attempted and the protein extractions and analysis were repeated.

The protein fractions were analyzed by SDS-PAGE and either stained for total proteins with Coomassie Brilliant Blue, or immunoblotted (Western blotting) with an anti-GST antibody. Figure 26 shows representative Coomassie-stained SDS-PAGE gels of extracted proteins of the soluble and lysozyme soluble fractions. In these two gels, GST-LOX and GST-$LOX_{169-348}$ can be observed at the predicted molecular weights in the lysozyme soluble fractions (indicated by the arrows in Figure 26). The increase in the quantity of the fusion proteins was clear in the samples induced with IPTG, although even when not induced the fusion proteins were still expressed at a lower level.

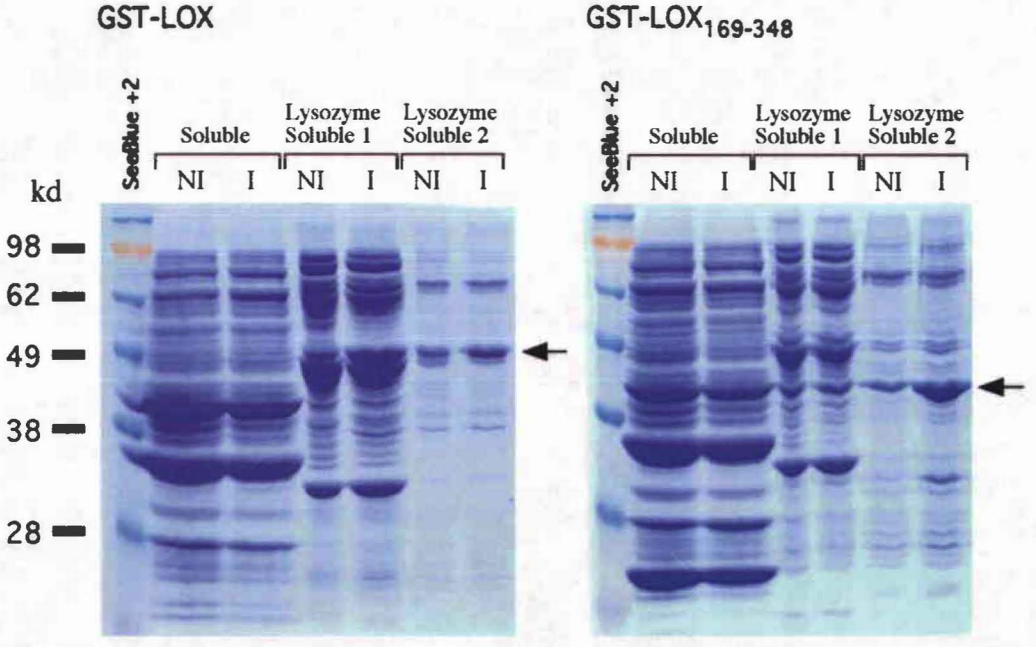

Figure 26. Representative coomassie-stained SDS-PAGE of extracted bacterial proteins expressing GST-LOX fusion proteins. The recombinant GST-LOX and GST-$LOX_{169-348}$ protein bands are indicated with arrows. NI = non-induced, I = IPTG induced. These two fusion proteins were expressed at the correct molecular weight and were found mostly in the lysozyme soluble fractions and inclusion bodies.

All fusion proteins detected by Coomassie-stained SDS-PAGE were confirmed by Western blots with an anti-GST antibody. Figure 27 shows representative Western blots of GST-LOX and GST-LOX_{1-348} expression in soluble, lysozyme soluble, and inclusion body

fractions for both non-induced and induced cultures. The vast majority of the GST-LOX fusion protein was extracted as inclusion bodies. The full-length 56-kD GST-LOX fusion protein was seen in the lysozyme soluble fractions and the inclusion bodies. However, some degradation or proteolysis of the GST-LOX fusion proteins was detected, as smaller GST products are visible. GST-LOX_{1-348} was present in very low amounts in the soluble and lysozyme soluble fractions, where proteolytic cleavage at the ThCS may have resulted in the detected 26-kD GST without any attached LOX fragment. As the fusion proteins degraded, and contained proportionally more GST and less LOX, the more soluble they appeared.

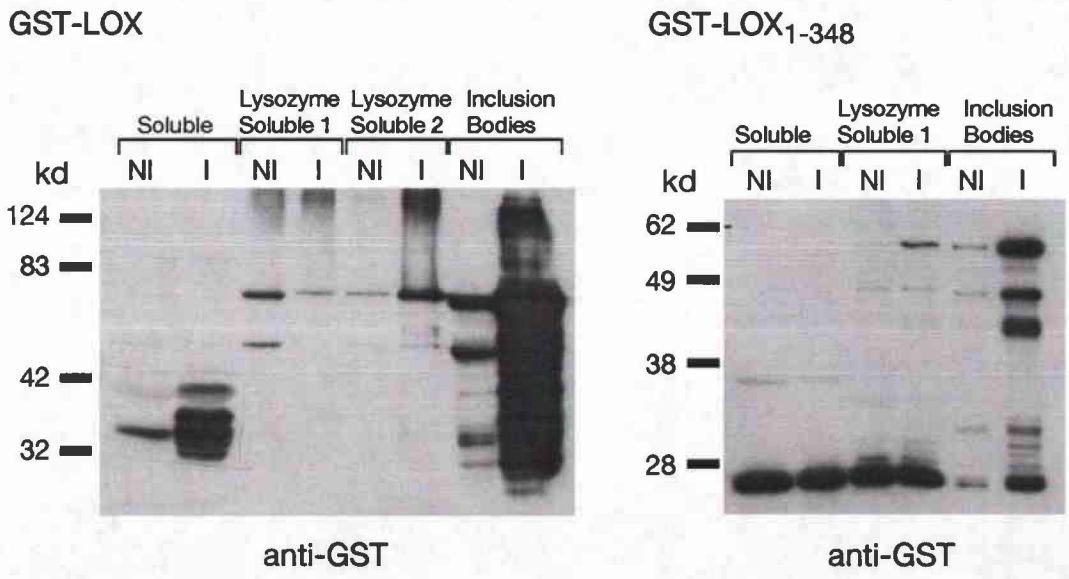

Figure 27. Representative Western blots of extracted protein fractions from *E. coli* expressing GST-LOX and GST-LOX_{1-348} fusion proteins. Immunoblots were performed with anti-GST antibody. NI = non-induced, I = IPTG induced. Proteolytic degradation is observed for both proteins, which is demonstrated by the lower molecular weight bands. For GST-LOX_{1-348}, the fusion protein was cleaved at the ThCS, resulting in the presence of 26-kD GST in the soluble and lysozyme soluble fractions. Despite optimization, this proteolysis proved problematic.

The initial attempts at generating of the GST-LOX fusion proteins was partially successful. All but one of the proteins expressed at the correct molecular weight, although there was some degradation. Table 8 summarizes the expression data for the GST-LOX fusion

proteins. The fractions where the proteins were primarily found correlated with the predicted solubility of the fusion protein. In the last column of Table 8 is the predicted isoelectric point (pI) of each protein, and it was found that the proteins only found in the inclusion bodies also had the highest pI. Unfortunately, despite attempts to optimize the growing conditions, GST-proLOX never expressed at the correct molecular weight, so it could not be used for further experiments.

Table 8. Summary of recombinant GST fusion protein extraction and fraction analysis.

GST Fusion Protein	Predicted MW (kD)	Expressed MW (kD)	Protein Fraction Containing Highest %	pI (without GST tag)
GST	26	26	Soluble / IB	6.1
GST-proLOX	72	45	IB	7.5 (8.4)
GST-LOX	52	52	LS / IB	5.9 (5.8)
GST-LOX_{1-168}	45	45	IB	9.1 (11.7)
GST-LOX_{1-348}	65	65	IB	8.4 (9.0)
GST-$LOX_{169-348}$	46	46	LS / IB	6.2 (6.3)
GST-$LOX_{349-417}$	33	33	Soluble / IB	5.7 (4.6)

Initially, we tried to utilize the GST-LOX fusion proteins that we were able to extract in the soluble and lysozyme soluble fractions, and we were able to successfully purify these proteins with glutathione affinity resin. This approach of trying to work with just the soluble GST fusion proteins had several limitations. The first was the proteolytic degradation of the GST-fusion proteins that resulted in large quantities of the cleaved GST fragment in the soluble and lysozyme soluble fractions (Figure 27). We attempted to eliminate this contaminating GST fragment based on molecular weight separation, and we also attempted to prevent this proteolysis with various mixtures of protease inhibitors, but these methods were not successful. Another limitation was that only GST-LOX, GST-$LOX_{349-417}$, and GST-$LOX_{169-348}$ were present in the soluble or lysozyme soluble fractions in any significant amount. GST-LOX_{1-348} and GST-LOX_{1-168} were present almost exclusively in the inclusion body fractions. In addition, the quantities of GST-LOX fusion proteins that did present in the soluble fractions were much lower

than found in the inclusion bodies, which showed incredibly high amounts of recombinant protein.

Despite many attempts to optimize protein induction and extraction conditions, these problems persisted. Because of these difficulties, and a recently published protocol for inclusion body extraction and protein refolding of a His-tagged recombinant LOX [368], we decided to change our approach and attempt to purify the GST-LOX fusion proteins from the bacterial inclusion bodies. This method required using a buffer with 8 M urea for the protein extraction, with a subsequent protein refolding prior to purification.

Using a modified method of protein refolding based on that of Jung et al. [368], we were successfully able to purify large amounts of GST and four GST-LOX fusion proteins from the bacteria inclusion bodies: GST-LOX, GST-LOX_{1-168}, GST-$LOX_{169-348}$, and GST-$LOX_{349-417}$. Expression of the GST fusion proteins was performed as outlined above, but with the IPTG induction at 37°C for 4 hours to encourage inclusion body formation and maximize expression of the recombinant fusion proteins. The soluble proteins were first extracted with lysis buffer, lysozyme digestion, and sonication. The inclusion bodies were recovered by centrifugation and solubilized with 8 M urea in a potassium phosphate buffer overnight. The refolding was performed by rapidly diluting the inclusion body proteins into a potassium phosphate buffer to a final urea concentration of 2 M. The GST fusion proteins were then purified using glutathione resin. Figure 28 shows representative coomassie-stained SDS-PAGE gels of the inclusion body protein fractions, both before purification (left) and after purification (right). Using this protocol, the relative quantity of the GST-LOX fusion proteins was very high, and there was very little proteolytic degradation. With this method of protein production, we were able to generate milligram quantities of purified GST, GST-LOX, GST-LOX_{1-168}, GST-$LOX_{169-348}$, and GST-$LOX_{349-417}$ fusion proteins to use in subsequent *in vitro* binding assays.

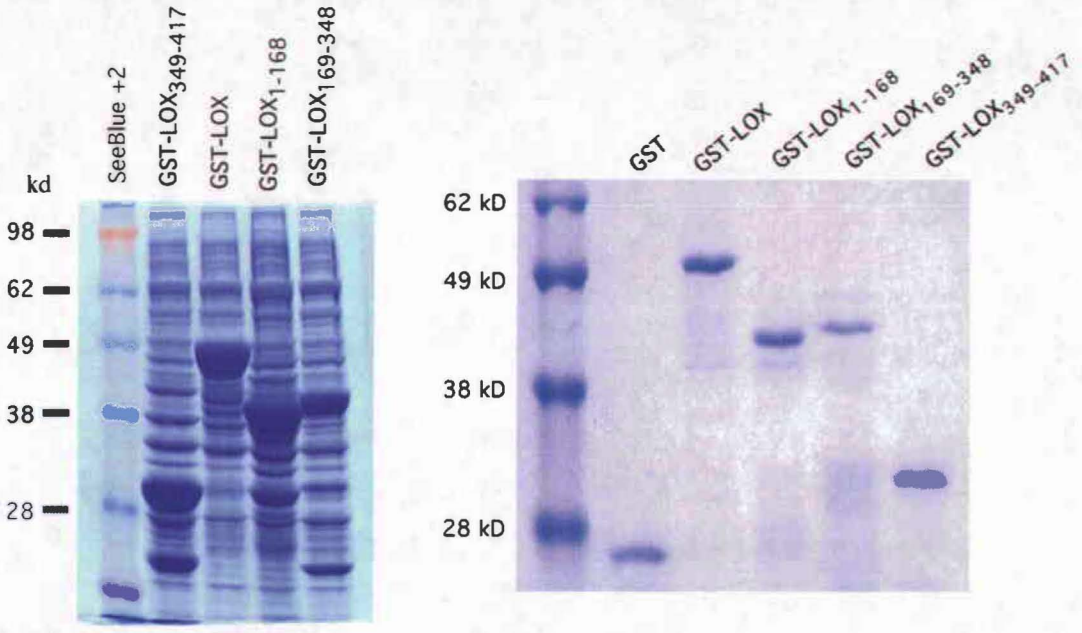

Figure 28. Coomassie-stained SDS-PAGE analysis showing GST fusion proteins extracted and purified from bacterial inclusion bodies. *Left*: Unpurified proteins extracted from inclusion bodies. The recombinant GST-LOX fusion proteins can be seen as the most intense bands in each lane. 20 µg of total protein was loaded into each lane. *Right*: GST fusion proteins purified from inclusion bodies using glutathione resin. 5 µg of each purified protein was loaded into each lane. Very little degradation is observed using this purification method.

In vitro binding analysis using pull-down and far-Western assays.

GST pull-down assays

The pull-down assay using GST fusion proteins was developed for determining if two proteins could bind together in a solution [369]. In this experiment, the input (a solution containing the target protein) is mixed with a purified GST fusion protein in the presence of glutathione resin, and incubated to allow protein binding to occur (Figure 29). Since the GST tag binds to the resin, the fusion proteins and any bound proteins can be pelleted by centrifugation. Washes then remove any non-specific binding proteins, and the complex is analyzed by Western blot analysis to detect the presence of the target protein. To control for the possible binding of the target to the GST tag alone, parallel pull-down assays are done with GST only.

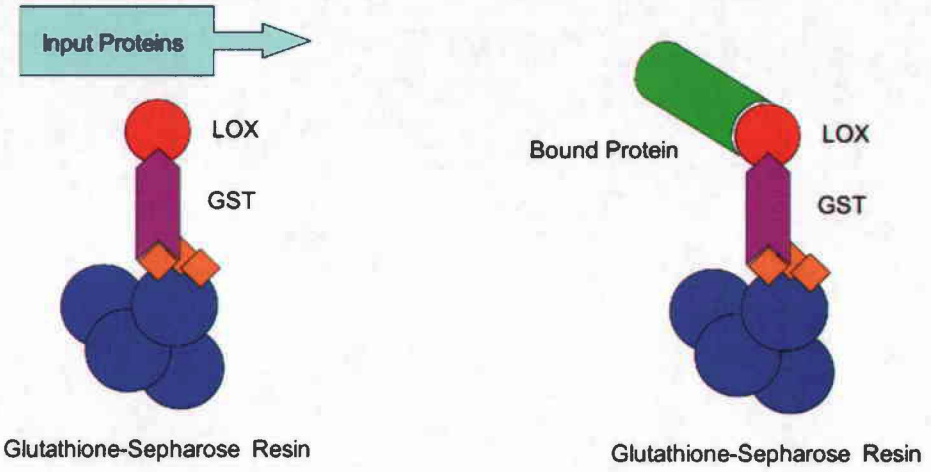

Figure 29. Summary of the GST pull-down assay. The GST fusion protein is attached to glutathione resin and incubated with an input sample containing the target protein. The resin is centrifuged and washed, and the presence of the bound target protein is determined by Western blotting.

For the pull-down experiments, equal amounts of GST-LOX or GST alone was attached to glutathione resin and incubated for 1 hr at 4°C with purified pFN, purified cFN, or conditioned cell media (CCM) from cultured human dermal fibroblasts. After centrifugation, the resin was washed with PBST several times and then resuspended in 2X Laemmli buffer and boiled. Equal amounts were resolved by SDS-PAGE, and bound FN was detected by Western blot analysis using an anti-FN antibody (IST-4). As a positive control for the Western blots, aliquots of the input solution (either pFN, cFN, or the fibroblast CCM) were resolved in adjacent lanes.

Using purified FN as input, we were able to successfully pull-down both plasma and cellular forms of FN with GST-LOX but not with GST alone (Figure 30). In addition, using CCM from human dermal fibroblasts as input, we were able to pull-down secreted FN with GST-LOX but not with GST alone (Figure 30). This was the first experimental evidence that demonstrated the LOX protein could bind to the full-length human FN protein from various sources, including the complex protein mixture of CCM.

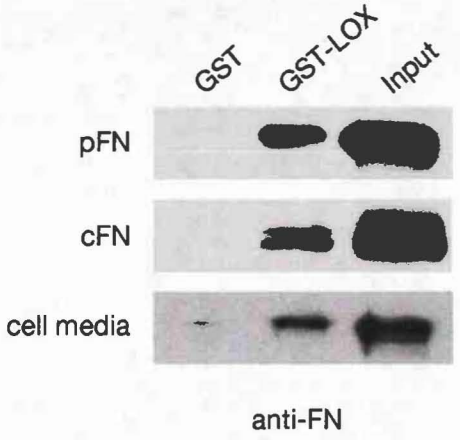

Figure 30. Western blots of GST pull-down assays showing FN can bind to GST-LOX. Purified human plasma FN (pFN) and cellular FN (cFN) were used as input, as well as the conditioned medium from human cultured skin fibroblasts. Bound FN was detected using an anti-FN antibody. Low binding of FN to GST alone shows the interaction is not due to the GST tag.

Far-Western assays

Another method to verify that the mammalian FN protein can bind to LOX is far-Western blotting [369]. In this experiment, the purified GST-LOX fusion proteins are analyzed by SDS-PAGE, electroblotted, refolded, and incubated with a solution of the target protein. After washing away the unbound protein, the quantity of bound target is detected using specific antibodies against the target protein. In addition, we can use far-Western analysis to begin to narrow down the position of the binding site in LOX, and to attempt to more quantitatively compare binding affinities of the LOX domains. We resolved equal microgram amounts of purified GST-LOX fusion proteins by SDS-PAGE and electroblotted the proteins onto a PVDF membrane. Then the denatured proteins were refolded by soaking the membrane in decreasing concentrations of guanidinium hydrochloride in PBS, and the PVDF membrane was blocked with milk. After incubating the refolded GST fusion proteins in a solution of purified cFN for 1 hr at

4°C, we washed the far-Western blot several times and detected bound cFN with an anti-FN antibody (IST-4).

As negative controls, we performed parallel far-Western blots that were exactly the same except without the cFN incubation step. This controlled for the non-specific binding of the primary and secondary antibodies to the GST fusion proteins. Running GST alone controlled for any binding of cFN to the GST tag. After the ECL detection, we scanned the autoradiograph film and quantified the intensity of the protein bands using the Kodak EDAS 290 software. The net band intensities for the no-target negative control blot were subtracted from the corresponding net band intensities of the far-Western blot. We also normalized the quantity of bound target for equal molar amounts of the GST-LOX fusion proteins (since equal microgram amounts were loaded), and finally, the binding data was normalized against the amount of cFN bound to GST alone. The data for the cFN far-Western is shown in Figure 31, with the scanned autoradiographs above, and the quantified, normalized data graphed below.

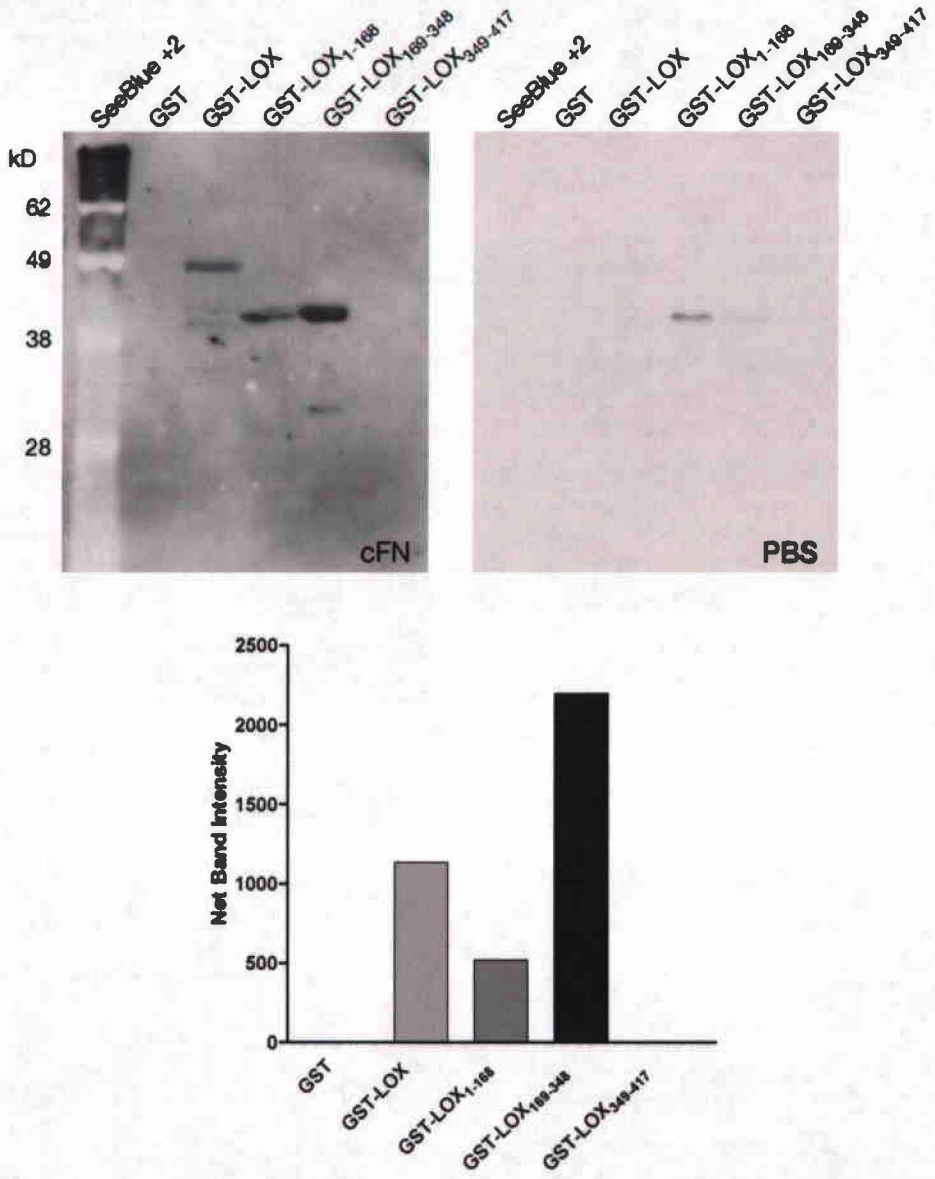

Figure 31. Far Western blots show binding of cFN to GST-LOX fusion proteins. *Above*: SDS-PAGE gels were resolved with equal amounts of purified GST and GST-LOX fusion proteins and electroblotted onto PVDF membranes. After protein refolding and membrane blocking, the blots were incubated with either cFN (left) or just PBS (right) as a negative control. An anti-FN antibody was used to detect bound cFN, and the Western blots were scanned and the band intensities were measured. The two blots were exposed to autoradiograph film for equal times, and the far-Western blot with cFN demonstrated more background. *Below*: Quantified net band intensities for the cFN far-Western blot. Relative band intensities were quantified with Kodak 1D software and the background intensity was subtracted. There was no significant binding to the GST alone or GST-$LOX_{349-417}$.

Co-immunoprecipitation of LOX and FN from cultured cells

To detect proteins bound together *in vivo*, the co-immunoprecipitation (Co-IP) assay has been used for decades [370]. The principle of the method is that antibodies against a protein-of-interest can be added to protein extracts, and the antigen-antibody complex can then be bound by protein A or protein G, two *Staphylococcus aureus* surface proteins shown to bind to the constant domain of the IgG. The protein A/G can be covalently attached to agarose resin, which allows separation by centrifugation. The resin is washed to remove unbound proteins, and the immunoprecipitated proteins are detected by Western blotting. Using an antibody specific for a target protein that may bind to the protein-of-interest determines if that target protein was co-immunoprecipitated (Figure 32).

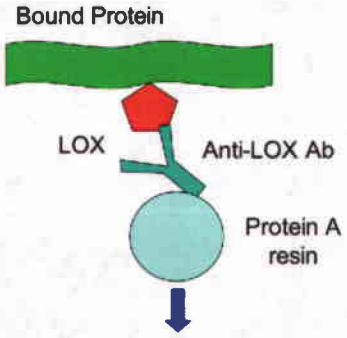

Figure 32. Diagram of the theoretical Co-IP of a target protein with LOX. Anti-LOX antibody is added to cultured cell media to bind to LOX. Using protein A resin, which binds to antibodies, the LOX and bound proteins are centrifuged to a pellet and washed. The identity of the bound protein is determined by Western blotting.

We performed Co-IPs from human fibroblast CCM to determine if endogenous LOX and FN proteins were interacting in this environment. We collected CCM from these cells and added the anti-LOX antibody to complex with the LOX proteins. We used protein A-agarose resin to capture the anti-LOX antibody, and washed the complex several times. Using Western blot analysis, we assayed for the presence of the FN protein. As a positive control, we performed a parallel IP with an anti-FN antibody. As a negative control, we performed a parallel IP with an

anti-His antibody used to detect 6xHistidine epitope tags, which would demonstrate if FN bound to unrelated antibodies, protein A, or the agarose resin.

The data showed that when LOX was immunoprecipitated with our polyclonal anti-LOX antibody, FN was also precipitated and was detectable by Western blotting (Figure 33). The bands are strongly visible in the two positive control lanes (the CCM input and the FN IP) and absent in the negative control lane (the IP with anti-His antibody). This was the first experimental evidence that showed the LOX enzyme can be bound to FN molecules in the medium of cultured human fibroblasts.

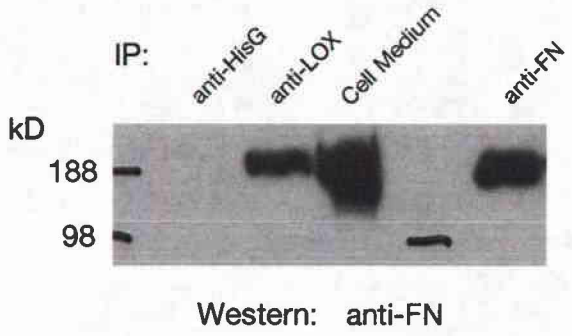

Figure 33. Western blot showing a co-immunoprecipitation of FN with LOX from cultured fibroblast cell media. 5 µg of anti-LOX antibody, anti-FN, or anti-HisG antibody (as a negative control) were incubated with 5 mL of fibroblast CCM. Proteins were precipitated with protein A-agarose, and the presence of bound FN was detected by Western blotting with an anti-FN antibody.

Solid phase binding assays to measure the equilibrium disassociation constant (K_d)

To further characterize the binding of LOX to FN, and to estimate an equilibrium disassociation constant (K_d) for this interaction, we performed solid phase binding assays [367]. These are classic assays used for studying extracellular matrix proteins, as well as ligand-receptor binding, which allowed us to compare the strength of LOX's binding to FN with LOX's binding to type I collagen and tropoelastin. The K_d value is calculated as the ligand concentration at which half the ligand quantity at saturation point is bound to the immobilized

protein. Data points are generated, and then statistical software is used to perform a non-linear regression to curve fit the data. The K_d value is then calculated along the curve at half the plateau fluorescence value.

In the first experiment, microplate wells were coated with purified pFN, cFN, type I collagen, tropoelastin, or BSA as a negative control. Purified GST-LOX, in a concentration range of 0 – 100 nM, was incubated with the immobilized proteins overnight at 4°C. After washing, bound GST-LOX was detected using antibodies and a fluorescent substrate for HRP, which was measured using a fluorescent microplate reader. The GST-LOX protein bound to cFN, type I collagen, and tropoelastin with high affinity, as the K_d was calculated at 2.5, 5.2, and 1.9 nM, respectively (Figure 34). No binding to BSA was detected. The binding of GST-LOX to pFN was much lower than to cFN in these assays, but still above that of the BSA negative control, showing that there may be a weak interaction with the plasma form of FN.

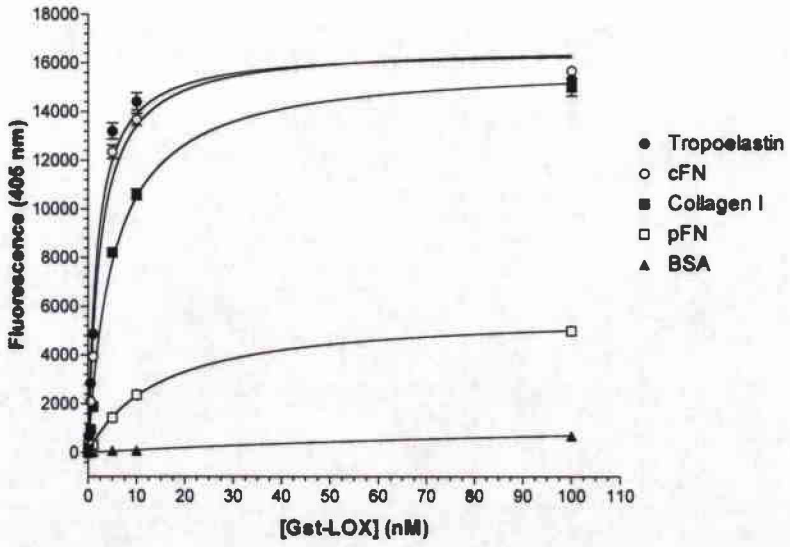

Figure 34. Solid phase binding assays demonstrated high affinity binding of LOX to cFN, type I collagen, and tropoelastin. Various concentrations of GST-LOX were incubated in microplate wells coated with cFN (O), pFN (□), type I collagen (■), tropoelastin (●), or BSA (▲). After washing, bound GST-LOX was detected using an anti-GST antibody in an ELISA assay. Each sample was done in triplicate, and the error bars for each data point represent the SEM. To estimate the affinity constants, we used non-linear regressions to curve fit the experimental data, which are shown by the continuous lines.

To test the binding of cFN to solid phase GST-LOX and the individual LOX domains, we coated microplate wells with purified GST-LOX, GST-LOX_{1-168}, GST-$LOX_{169-348}$, GST-$LOX_{349-417}$, or GST alone. Purified cFN, in a concentration range of 0 – 100 nM, was incubated with the immobilized proteins as described. We observed that cFN bound to solid phase GST-LOX with a calculated K_d of 3.8 nM (Figure 35), consistent with the high affinity detected in the previous solid phase binding assay. We also detected cFN binding to the GST-$LOX_{169-348}$ protein, although not at an equal affinity as the 30-kD form of LOX, which includes the CRL domain (aa 349-417). cFN demonstrated much less binding to the other LOX fragments and no binding to GST alone was detected.

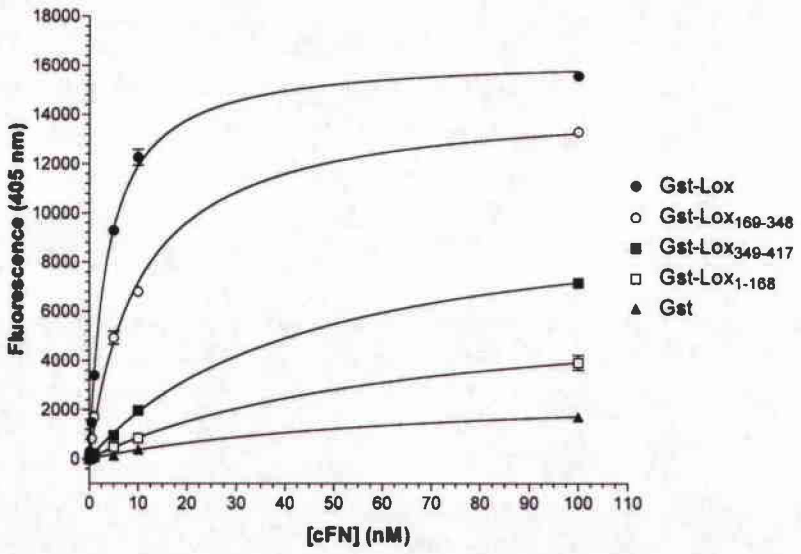

Figure 35. Solid phase binding assays demonstrate high affinity binding of cFN to the mature form of LOX. Various concentrations of cFN were incubated in microplate wells coated with GST-LOX (●), GST-LOX_{1-168} (□), GST-$LOX_{169-348}$ (○), GST-$LOX_{349-417}$ (■), or GST alone (▲). After washing, the bound cFN was detected using an anti-FN antibody in an ELISA assay. Each sample was done in triplicate, and the error bars for each data point represent the SEM. To estimate the affinity constants, we used non-linear regressions to curve fit the experimental data, which are shown by the continuous lines.

We also used these SPBAs to determine if the FN-LOX interaction could be inhibited by our antibody against LOX. Our hypothesis was that if the epitope site is close enough to the FN-binding site, then the physical bulk of the antibody could potentially inhibit the FN-LOX interaction. To test this, we bound the GST-LOX fusion proteins to microplate wells, and then pre-incubated them with or without our polyclonal anti-LOX antibody. We verified that the LOX antibody remained bound to only the LOX fragments containing the epitope site. Since this LOX antibody was designed against LOX amino acids 176-197, only GST-LOX and GST-$LOX_{169-348}$ should have bound the antibody. The experimental results confirmed this, showing retention of the antibody by only GST-LOX and GST-$LOX_{169-348}$ proteins (Figure 36). The low levels detected with the other three fusion proteins confirmed the specificity of this antibody. The other important result of this experiment was the confirmation that the anti-LOX antibody was able to bind to the LOX protein when it was in a non-denatured conformation. The negative controls, which were the GST-LOX fusion proteins incubated without primary antibodies (PBST only), showed that the secondary antibodies did not bind directly to the fusion proteins.

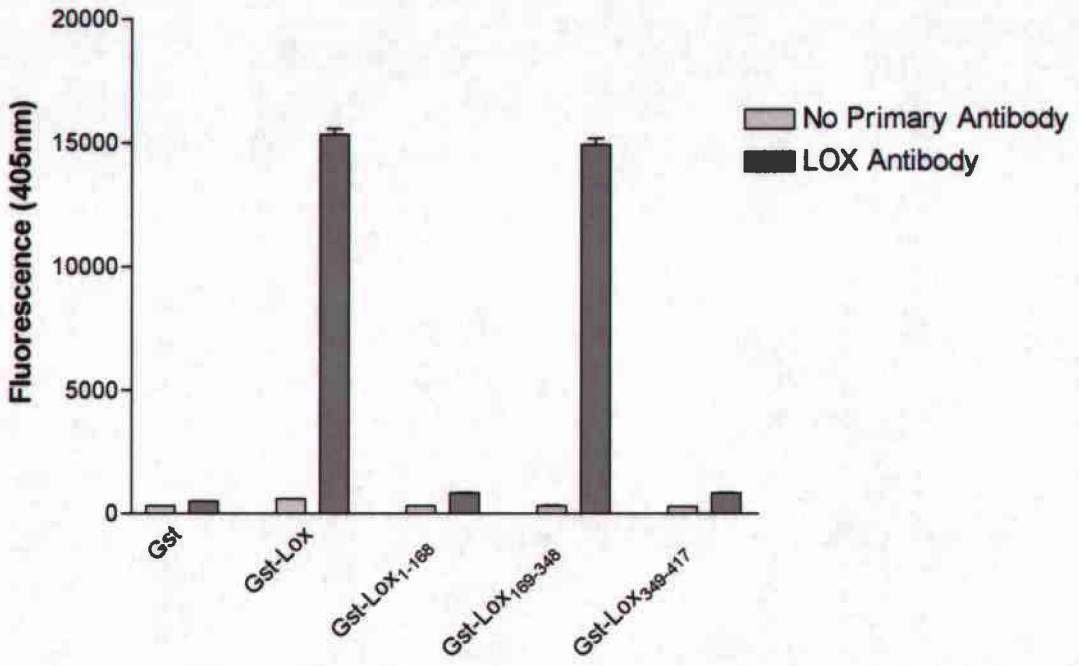

Figure 36. An ELISA assay verified specificity of our polyclonal LOX antibody designed against LOX residues 176-197. Microplate wells were coated with GST fusion proteins, and the antibody or PBS alone was incubated in the wells. After washing, the bound antibody was quantified with an HRP-conjuged secondary antibody and fluorescent HRP substrate. All samples were performed in triplicate, and error bars represent SEM.

After confirming that the antibody bound to the intended LOX epitope, we repeated the SPBA using immobilized GST-LOX proteins preincubated with or without the LOX antibody. After incubating with the cFN ligand at 100 nM concentration, we detected the levels of bound cFN with a monoclonal FN antibody (IST-4) and followed the previously described SPBA protocol. The data showed that relatively little cFN binding was inhibited by the LOX antibody (Figure 37). Although this decrease in cFN binding was statistically significant, it was not the complete inhibition that would have resulted in cFN levels similar to what was detected bound to GST alone. The data from this experiment indicated that the FN-binding site is located more towards the C-terminus of the active LOX enzyme, away from the LOX antibody epitope site.

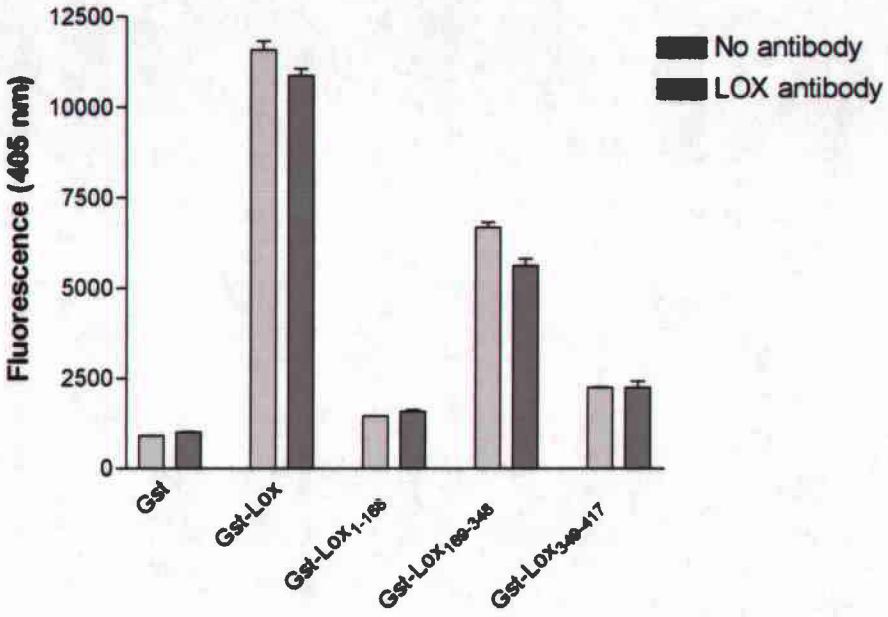

Figure 37. Solid phase binding assay showed the LOX antibody cannot block the LOX-cFN interaction. Microplate wells were coated with GST-LOX fusion proteins and the LOX antibody or PBS was added to the wells. After incubation, the wells were washed and the SPBA was performed using cFN at 100 nM. All samples were performed in triplicate, and the error bars are SEM.

DISCUSSION

The experiments described in this Chapter were designed to verify the interaction between LOX and FN proteins, which was previously detected by a yeast two-hybrid screen. The FN protein isolated in the screen was only a partial fragment and provided no guarantee that LOX could interact with the full-length FN found *in vivo*. In addition, these experiments were designed to characterize the specificity and strength of this molecular interaction. The generated data allowed us to speculate on the nature of the FN-LOX interaction and how it compares with other similar interactions.

To perform the *in vitro* binding experiments outlined in Specific Aim 2, our biggest limitation was the lack of available purified LOX enzyme. Traditionally, active LOX is purified

from tissues such as bovine aorta or placenta using a urea buffer [93]. This classic method was used to purify the bovine aorta LOX used for activity assays in Chapter 4. However, these tissue extractions often does not yield in enough quantities of enzyme to perform the *in vitro* binding studies that are necessary to characterize a protein interaction. For reasons discussed in the Introduction (Chapter 3), we decided to generate recombinant LOX to use for the binding experiments.

After several preliminary trials, we decided to use *E. coli* to generate GST-tagged LOX, as detailed above in the *Results*. However, we had also used mammalian expression systems to generate a recombinant 6xHistidine-tagged LOX. We cloned both LOX and proLOX expression constructs using the pcDNA3.1/His vector and expressed LOX proteins in mammalian cells with transfections and with *in vitro* transcription and translation (IVTnT) reactions (Figure 38). From these preliminary experiments, the His-tagged LOX and proLOX were generated at the correct molecular weights, as detected by Western blotting using anti-His antibody (Figure 38). Unfortunately, neither the transformations nor the IVTnT reactions resulted in large enough quantities of recombinant LOX proteins to perform the planned experiments.

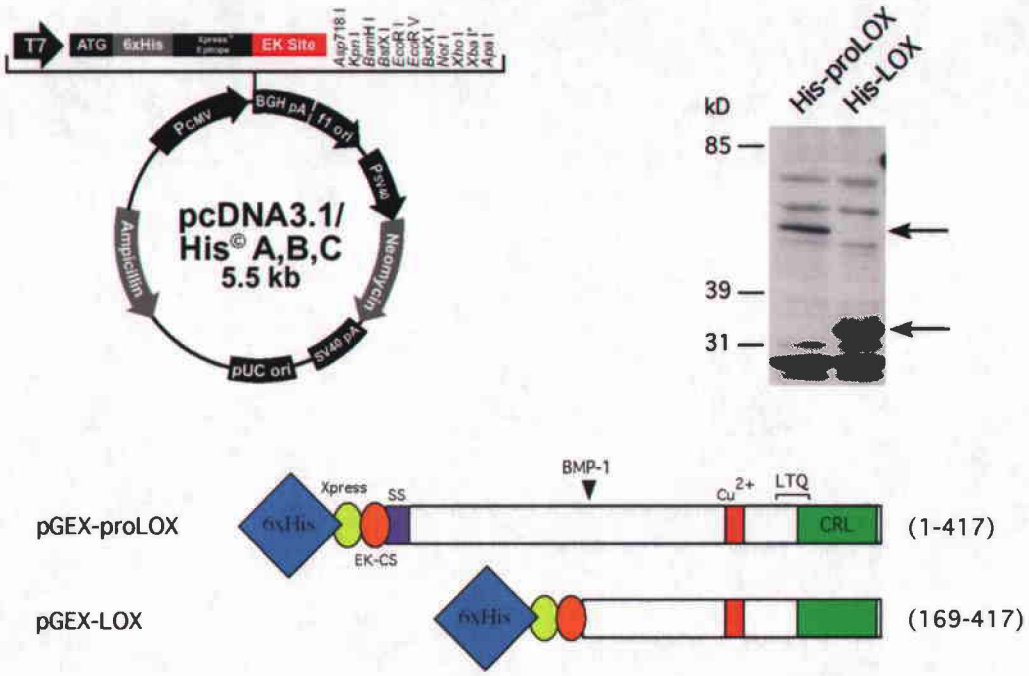

Figure 38: The pcDNA3.1/His vector was used to express His-tagged proLOX and LOX proteins in mammalian cell systems. *Above Left*: The pcDNA3.1/His vector contains a 6xHistidine tag, an Xpress epitope tag, and an enterokinase (EK) cleavage site 5' to the MCS, where the cDNA fragment of interest is inserted in-frame. The expression of the protein is under the control of the cytomegalovirus (CMV) promoter. *Above Right:* Western blot showing expression of recombinant His-proLOX and His-LOX proteins from *in vitro* transcription and translation (IVTnT) reactions using an anti-His antibody. *Below*: Schematic diagram of His-tagged proLOX and LOX proteins. The N-terminal His tag (blue) is followed by an Xpress tag (yellow) and an EK cleavage site (EK-CS, orange).

Another potential problem with Histidine tags arose when a collaborator recommended caution about working with LOX and His epitope tags. As LOX is a copper binding protein, and the His tag has a high affinity for metals such as nickel and copper, he reported that the His tag could compete for copper atoms, which may result in misfolded LOX. Because of this advice, and because of the relatively small quantities of recombinant His-LOX, we decided to focus on the bacterial expression system.

Using the bacterial system resulted in the successful production of large quantities of recombinant GST-LOX fusion proteins, which were easy to purify and refold. Unfortunately, with this method the catalytic activity of the recombinant LOX was not recovered by our refolding

protocol. This may be due to several reasons, but has been consistent with communications from other LOX researchers. Despite two separate publications reporting successful refolding of bacterial expressed LOX achieving catalytic activity [368, 371], we could not duplicate those results with identical conditions, nor could several other groups (personal communications by Phil Trackman, Ian Hornstra, John Bollinger, and David Hulmes). Even David Hulmes, who was the senior author on the Ouzzine et al, 1996 paper [371] told us that he could not repeat their experiment to generate active LOX. The Jung et al, 2004 refolding protocol, which we duplicated, did not yield an active LOX enzyme. Talking with Dr. Youngho Kim, the senior author on that study, revealed that their catalytic activity was extremely low and even undetectable by the standard Amplex Red methodolgy. There could be several explanations why the refolded GST-LOX did not acquire amine oxidase activity. Usually when a copper-binding enzyme is expressed in *E. coli*, copper is dialyzed into the refolding protein. This is a critical step because if the copper is not incorporated correctly, catalytic activity will not be achieved despite proper refolding. It is entirely possible that we never found the optimal dialysis conditions for copper incorporation. Despite this, we were confident that our refolded LOX had similar molecular properties as the native LOX because our refolded protein specifically bound to tropoelastin and type I collagen.

By using several different *in vitro* assays to demonstrate that LOX could bind to FN, we aimed to eliminate any doubt about whether the interaction was real. This was very necessary because of the conception of FN as a "sticky" protein. Many ECM proteins bind to numerous other proteins, and we wanted to show FN's interaction with LOX was not a non-specific interaction due to our experimental technique. The GST pull-down assay is a well-established method to test interactions between a GST fusion protein and a potential interactor in solution [369]. The far-Western blot was originally established to screen protein libraries with ^{32}P-labeled GST fusion proteins [372, 373], but has developed into a sensitive method for showing binding between two known proteins [369]. The data from these two methods consistently

demonstrated binding between LOX and FN, and also showed that FN did not bind to the GST protein domain alone.

The *in vivo* method of Co-IP demonstrated that LOX and FN can circulate bound together in cultured cell medium, although the technique could not distinguish if other proteins are bound with them. Despite the clear results of the Co-IP experiment detailed above, we are hesitant to rely on the Co-IP technique, especially when working with FN. The "stickyness" of FN was evident when FN would sometimes bind to the protein A and G resin without any antibodies. Despite preclearing the CCM, this was sometimes a problem. Although we could control for this binding by using the negative control of anti-His antibody, we were very critical of the data because of the inconsistency.

There were also problems encountered for the reverse Co-IP experiment, which is the IP of FN and detection of bound LOX. The major problem was the size of the LOX enzyme (~30 kD), which is in the vicinity of the immunoglobulin light chain (~25 kD), which gave a very strong signal on Western blots of the IPs. The Ig light chain band would eclipse the area where the LOX protein would resolve. Another limitation of this reverse Co-IP was the relative levels of FN versus LOX. The relative number of FN molecules in the cell media is much, much greater than the relative number of LOX molecules. Therefore, when FN is immunoprecipitated from the media, a very small percentage of the precipitated FN molecules could potentially be binding LOX. This means a very small relative amount of LOX to detect by Western blot. We believe that for these reasons, we could not successfully show co-immunoprecipitated LOX using FN antibodies. Fortunately, the accumulation of data from other techniques is sufficiently convincing to verify the LOX-FN interaction, which was enforced by the strongest experimental evidence for a direct interaction: the solid phase binding assays.

These *in vitro* assays measured the binding affinity directly between the two ECM molecules in a direct and rapid methodology. This experiment has been used before to study FN interactions [288, 374], and is well-accepted to give reliable results. The caveat is that the quantity of purified proteins is sufficient, which was achieved by purifying the recombinant GST-

LOX fusion proteins. In addition, the SPBAs allowed us to measure LOX's binding affinity to type I collagen and tropoelastin, which has not been done before with this method. The data indicated that LOX bound to cFN with a K_d of 2.5 nM, which was in the range as the K_d measured for type I collagen (5.2 nM) and tropoelastin (1.9 nM). The non-binding of LOX to BSA was very reassuring that the interactions with the ECM proteins were specific.

What was interesting from these assays was the difference in measured affinity for cFN and pFN. This lower affinity for pFN may be due to the closed conformation of pFN, which may obscure certain binding sites [292-295]. It is also possible that the alternative splicing of cFN versus pFN was the reason, as extra domains are typically found in cFN (reviewed in Chapter 2: *Discussion*). This difference in LOX's binding affinity is perhaps one of the body's ways to regulate LOX activity - to make sure active LOX remains in tissues rather than circulating in the plasma. Further experiments will be necessary to determine what causes this large difference in binding affinity, and what is the biological significance of this difference.

The SPBAs with the immobilized GST-LOX fusion proteins and soluble cFN ligand indicated that the primary cFN-binding site was between LOX residues 169-348. This seemed to be consistant with the data from the far-Western experiment. However, without the CRL domain, the LOX protein loses some of it's ability to bind cFN. This suggests that the CRL domain may add some stability to LOX's protein interactions and perhaps is critical for its activity *in vivo*. We will continue to pursue experiments to determine the function of the CRL domain. All the LOX fragments bound higher than the GST alone, to which cFN binding was negligible. These data may help explain some of the inconsistency of the yeast two-hybrid direct interaction assays, which showed that multiple LOX fragments had some ability to bind to the FN fragment. However, from the SPBA data, it became clear that the active 30-kD form of LOX (amino acids 169-417) has the highest binding affinity for cFN.

An important future goal is the determination of the exact binding sites on the LOX and FN molecules. This information will enable the design of short peptides to specifically disrupt the interaction without totally disrupting all of the protein's other functions. Unlike

downregulating the gene expression, which can have wide ranging ramifications, or inhibiting the catalytic activity of LOX, which can be toxic to the human body, disrupting peptides can be specific for the protein-protein interaction. Alternatively, chemical compound libraries can be screened for efficient inhibitors of the LOX-FN interaction. Inhibiting the interaction is a useful experimental approach to evaluate the specific biological significance of the LOX-FN interaction. In addition, disrupting peptides or chemical inhibitors can be viable clinical therapeutics, and may be a step towards developing a therapy based on the targeting of LOX or FN interaction. However, the narrowing down of the binding site to a few specific residues takes a huge amount of work, and was not in the scope of this dissertation. We have designated these experiments as high priorities for future projects.

For this study, we wanted to develop a plausible working hypothesis to explain the biological significance of the LOX-FN interaction. This required performing experiments to gather some basic data about the LOX and FN interaction. Our approach was to evaluate FN's influence on LOX's amine oxidase activity, and whether FN could be a substrate for the LOX enzyme. We also wanted to survey various human tissues to find areas where FN and LOX can be co-localized. Finally, we wanted to analyze the LOX enzyme in FN-null conditions *in vivo* to determine if FN could contribute to the regulation of LOX activity. The results from these experiments are presented in Chapter 4.

MATERIALS AND METHODS

Cloning of GST-LOX Expression Constructs

The vector pGEX-4T-1 (Amersham) was used to generate bacterial expression constructs for LOX, proLOX, and various LOX cDNA fragments. These plasmid constructs were designed to produce recombinant LOX proteins containing an N-terminal glutathione S-

transferase (GST) tag. The pGBKT7-LOX plasmid constructs used for yeast expression were used as templates for the creation of pGEX-LOX plasmid constructs. The six pGBKT7-LOX plasmids (pGBKT7-proLOX, pGBKT7-LOX, pGBKT7-LOX_{1-168}, pGBKT7-LOX_{1-348}, pGBKT7-$LOX_{169-348}$, and pGBKT7-$LOX_{349-417}$), as well as the pGEX-4T-1 vector, were each restriction digested with *EcoRI* and *SalI* enzymes. The digested DNA fragments were purified from the agarose gel, and the vector and insert DNAs were ligated together and transformed into XL-1 Blue *E. coli* (methods detailed in Chapter 2). The transformed cells were plated on LB-amp plates to select for successfully ligated plasmids, and growing colonies were picked with a sterile loop and streaked on fresh LB-amp plates to obtain single colonies. Each pGEX-LOX plasmid construct was verified by DNA sequencing using the T7 vector primer (methods detailed in Chapter 2).

Bacterial Expression of GST-LOX Fusion Proteins

The pGEX-LOX plasmid expression constructs were transformed into the BL21 strain of *E. coli* (Stratagene) using the heat shock method (detailed in Chapter 1). After the transformation, the cells were plated on LB-amp plates to select for cells containing the pGEX-LOX constructs. After incubating the plates at 37°C overnight, the growing colonies were picked by a sterile loop and streaked on fresh LB-amp plates to obtain single colonies. To express the recombinant GST-LOX proteins, the bacteria containing the constructs were inoculated in 10 ml of LB media with ampicillin and grown overnight at 37°C with shaking at 250 rpm. The next morning, 90 ml of fresh LB media with ampicillin was added to the culture, which was incubated for another 2 hours at 37°C with shaking at 250 rpm. To induce GST fusion protein expression, 0.1 mM isopropyl-1-thio-β-D-galactopyranoside (IPTG) was added to the growing culture, which was then incubated for another 4 hours at 37°C with shaking at 250 rpm.

Attempts to optimize the expression of the GST-LOX fusion proteins were made in order to increase the solubility of the fusion proteins, prevent degradation of the fusion proteins, and prevent the formation of inclusion bodies. All alterations of the expression protocol were

suggested by Amersham's *troubleshooting* guide to GST protein expression. The induction temperature was reduced to 20°C-30°C, and induction time was shortened. The concentration of IPTG was varied. Titrations of protease inhibitors were added to the culture media including Pefabloc (Roche) and Halt protease inhibitor cocktail (Pierce Biotechnology, Inc.).

EXTRACTION AND PURIFICATION OF GST-LOX FUSION PROTEINS

Micro-scale extractions of protein fractions – After induction of the GST fusion protein, 1.5 ml of the bacteria culture was transferred to an microcentrifuge tube and centrifuged at 14,000 x g. The media was aspirated and the pelleted cells were resuspended in 200 µl of CellLytic BII lysis solution (Sigma) containing Pefablock protease inhibitor (Roche). The sample was vortexed for 2 min at room temperature, and then centrifuged at 14,000 x g for 5 min. The supernatant was collected and termed the "soluble fraction." The pellet was resuspended in 200 µl of CellLytic BII containing protease inhibitor and also 100 U of DNase I (Roche) and 200 µg of lysozyme (Sigma). The sample was incubated for 10 min at room temperature with intermittent vortexing, and then centrifuged at 14,000 x g. The supernatant was collected and termed the "lysozyme soluble fraction #1." This lysozyme treatment was repeated twice more to obtain lysozyme fractions 2 and 3. The final pellet of insoluble protein was termed the "inclusion body fraction."

Micro-scale purification of soluble GST fusion proteins - The purification of the GST fusion proteins was based on Amersham's protocols. 50 µl aliquots of Glutathione Sepharose 4B resin (Amersham) was pipeted into a microcentrifuge tube and 950 µl of PBS was added to remove any trace of the EtOH used for resin storage. The resin was centrifuged at 14,000 x g for 15 sec, and the supernatant was aspirated. The soluble or lysozyme soluble protein fraction was incubated with glutathione resin for 1 hr at 4°C with gentle mixing. The sample was then centrifuged at 14,000 x g for 15 sec, and the supernatant collected for analysis (termed the "flow-through"). The resin was washed with CellLytic BII lysis buffer 3 times to remove any unbound proteins. The bound proteins were prepared for analysis by SDS-PAGE and Western

blotting by adding 50 µl of 2 x Laemmli Buffer and boiling for 5 min. To elute the bound GST fusion proteins, 50 µl of glutathione elution buffer (10 mM reduced glutathione, 50 mM Tris-HCl (pH 8.0)) was incubated with the resin for 10 min at room temperature. The sample was centrifuged at 14,000 x g for 15 sec, and the eluted protein (supernatant) was transferred to a fresh tube.

Large-scale extraction of GST fusion proteins from inclusion bodies - The protein expression in inclusion bodies was carried out using the modified protocol of Jung et al. 2003 [368]. After induction of the GST fusion proteins, the 100 ml culture was transferred to conical tubes and centrifuged at 3300 x g for 10 min at 4°C. The media was aspirated and the pelleted cells were resuspended in 6 ml of ice-cold Buffer A (50 mM Tris-HCl (pH 8.0), 1 mM EDTA, 100 mM NaCl, 1% Triton X-100, 1 mg/ml lysozyme). This mixture was mixed for 1 hr at 4°C, and then 0.1 mg/ml of DNase I was added and the sample was mixed for another 1 hr at 4°C. The sample was then sonicated three times for 30 sec each at 70% strength with a Sonic Dismembrator Model 100 (Fisher Scientific). The insoluble proteins were then pelleted by centrifugation at 3300 x g for 20 min at 4°C, washed with 6 ml of Buffer B (10 mM K_2HPO_4 (pH 8.2), 2 M urea). The inclusion bodies were solubilized overnight at 4°C with 6 ml of Buffer C (10 mM K_2HPO_4 (pH 8.2), 8 M urea, 2 mM β-mercaptoethanol, 5 mM DTT). The next morning, the solubilized inclusion body proteins were passed through a 0.45 µm syringe filter and stored at 4°C.

Large-scale purification of GST fusion proteins from inclusion bodies - After the solubilized inclusion bodies were filtered, 18 ml of Buffer D (10 mM K_2HPO_4 (pH 7.0)) was added. 1.5 ml aliquots of Glutathione Sepharose 4B resin (Amersham) was pipeted into a 50-ml concial tube and 40 ml of PBS was added to remove any trace of the EtOH used for resin storage. The resin was centrifuged at 3300 x g for 5 min, and the supernatant was aspirated. The inclusion body protein fraction was incubated with glutathione resin for 2 hr at 4°C with gentle mixing. The sample was then centrifuged at 3300 x g for 5 min, and the resin was washed with 40 ml of

Buffer B 3 times to remove any unbound proteins. The bound proteins were eluted with 4 ml of Buffer C, incubated overnight at 4°C. The next morning, the sample was centrifuged at 3300 x g for 5 min, and the eluted protein (supernatant) was transferred to a fresh tube.

MEASUREMENT OF PROTEIN CONCENTRATION

The Bradford reagent (Biorad) was used to measure the concentration of proteins in solution. We performed these assays in 96-well microplates (Corning) according to the manufacturer's protocol. First, concentration standards were made: 0, 5, 10, 15, 20, and 25 µg/ml BSA in PBS (2 mg/ml BSA stock from Pierce). In triplicate microplate wells, 160 µl of each standard was mixed with 40 µl of Bradford reagent. For the protein samples, 40 µl of Bradford reagent was mixed with X µl of protein samples and 160-X µl of PBS, where X was determined by visual estimation to result in the sample being within the linear range of the protein standards (0-25 µg/ml). Each sample was mixed thoroughly and the absorbance at a wavelength of 600 nm was measured using a POLARstar Optima microplate reader (BMG Labtech). A linear regression was performed with the measured absorbance values of the BSA standards in order to calculate a protein concentration standard curve. The measured absorbance values of the protein samples were then plotted along this standard curve, allowing the calculation of the protein concentration in each sample. This statistical analysis was performed using Graphpad Prism 3.0 statistical software package (Graphpad Software, Inc.).

PROTEIN-STAINING OF SDS-PAGE GELS

To visualize the total proteins after SDS-PAGE electrophoresis of protein samples, we stained the gels with Coomassie Brilliant Blue. After the electrophoresis was complete, which was judged by the migration of the prestained protein molecular weight marker (SeeBlue +2), the gel apparatus was disassembled. The gel was transferred to a plastic tray containing the

Coomassie solution (0.25% Coomassie Brilliant Blue in 35% methanol and 10% acetic acid). The gel was stained overnight at room temperature, rotating gently. The next morning, the gel was destained with consecutive washes of destaining solution (35% EtOH and 10% acetic acid) for 30 min each until the protein bands were clearly visible. The gel was then rehydrated by soaking in a 2% glycerol solution overnight. The gel was then imaged using the Kodak EDAS 290 imaging system, and subsequently dried on Whatman paper at 60°C for 90 min using a Biorad gel dryer with a Biorad vacuum pump.

WESTERN BLOT ANALYSIS

Western blots were performed as described in Chapter 2 under "Materials and Methods: *Western Blot Analysis*," but using the following additional antibodies. The mouse monoclonal anti-GST antibody (Upstate Biotechnology) was used at 0.2 µg/ml to detect GST fusion proteins. Two mouse monoclonal anti-FN antibodies were used for Western blots: FN8-12 (Takara Bio, Inc.) was used at 2 µg/ml, and IST-4 (Sigma) was used at 5 µg/ml. The rabbit polyclonal anti-LOX antibody was designed by our lab in collaboration with Drs. Dawn Kirschmann and Mary Hendrix, and the production and purification of this antibody was done by Zymed Laboratories, Inc. The antibody was designed against LOX amino acids 176-197, and recognizes both the full length proLOX and the mature, active form of LOX (Figure 3). This antibody has previously been described (Li et al, 2004). For Western blotting, the LOX antibody was used at 3 µg/ml.

GST PULL-DOWN ASSAYS

To determine if LOX could pull-down FN from solution, pull-down assays were performed. In a microcentrifuge tube, 5 µg of purified GST-LOX or GST alone was mixed with enough CellLytic BII to result in a final volume of 500 µl. For these pull-down assays, the GST was purified from the soluble fraction, and GST-LOX was purified from the lysozyme soluble fractions. To the protein solutions, 50 µl of pre-washed Glutathione Sepharose 4B resin was added, and the tubes were rotated for 1 hr at 4°C. The samples were then centrifuged at 14,000

x g for 15 sec, and the supernatant was aspirated. The resin was washed three times with PBS, and then incubated for 1 hr at 4°C with either 10 µg of purified pFN (Sigma), 10 µg of purified cFN (Sigma), or 1 mL of conditioned cell media (CCM) from human neonatal skin fibroblasts. The resin was then washed three times with PBST and resuspended in 30 µl of 2X Laemmli buffer for SDS-PAGE and Western blot analysis.

FAR-WESTERN BLOTTING ANALYSIS

Five micrograms of purified GST-LOX fusion proteins (purified from inclusion bodies) were separated by electrophoresis using SDS-PAGE, and electroblotted as described in Chapter 2. Two identical blots were made in this way, one to serve as a parallel negative control. After blotting, the proteins were refolded by soaking the membranes in Refolding Buffer R6 (20 mM Hepes (pH 7.7), 25 mM NaCl, 5 mM MgCl, 1 mM DTT, 6 M guanidinium hydrochloride) for 30 min at room temperature. This incubation was repeated once with fresh buffer, and then the blots were soaked in Refolding Buffer R4 (20 mM Hepes (pH 7.7), 25 mM NaCl, 5 mM MgCl, 1 mM DTT, 4 M guanidinium hydrochloride) for 15 min at room temperature. The blots were then soaked in Refolding Buffer R2 (20 mM Hepes (pH 7.7), 25 mM NaCl, 5 mM MgCl, 1 mM DTT, 2 M guanidinium hydrochloride) for 15 min at room temperature, and finally soaked in Refolding Buffer R1 (20 mM Hepes (pH 7.7), 25 mM NaCl, 5 mM MgCl, 1 mM DTT, 0.187 M guanidinium hydrochloride) for 15 min at room temperature. The Refolding Buffer R1 wash was repeated once more, and then the blots were incubated in Refolding Buffer R1 overnight at 4°C with gentle agitation. The next morning, the blots were blocked with 5% Carnation non-fat dry milk in PBST for 1 hr at room temperature. To lessen non-specific binding to the GST tag, the blots were incubated with 3 µM reduced glutathione and 2.5% Carnation non-fat dry milk in PBST for 1 hr at room temperature. The blots were washed 3 times in PBST for 10 min, 5 min, and 5 min at room temperature. One of the blots was then incubated in a 5 µg/ml solution of purified human cFN in PBST for 1 hr at 4°C, but the other parallel blot was instead incubated in PBST for

1 hr at 4 °C. Both blots were washed again 3 times in PBST as above, and incubated with the monoclonal anti-FN antibody (IST-4) at 0.5 µg/ml for 1 hr at room temperature with gentle shaking. The blots were then washed again as above, and incubated with the HRP-conjugated anti-mouse secondary antibody for 1 hr at room temperature with gentle shaking. The blots were washed again as above, and after three final washes with PBS for 1 min each, the blot was treated with ECL and exposed to film as described in Chapter 2. The developed film was scanned on a flatbed digital scanner, and the relative intensities of the bands were calculated by the Kodak 1D software.

CELL CULTURING OF HUMAN DERMAL FIBROBLASTS

Human neonatal foreskin fibroblasts were obtained from Clonetics, Inc. and grown using Dulbecco's modified Eagle medium (DMEM) supplemented with 10% fetal bovine serum (FBS) (Serologicals Corporation), penicillin, streptomycin, and amphotericin. The cells were kept cultured in T75 flasks under sterile conditions. Only human fibroblasts less than passage 10 were used for protein analysis. For experiments using conditioned cell medium (CCM), cells were grown to 2 days post-confluent, washed with PBS, and incubated with serum-free, phenol-red free DMEM. After an additional 48 hr in culture, the CCM was collected and transferred to conical tubes. The CCM was centrifuged at 3300 x g for 10 min to pellet any remaining cells. The CCM was transferred to a fresh tube and kept on ice until used. To concentrate total proteins from the CCM for Western blotting, 10 µl of Strataclean Resin (Stratagene) was added to the appropriate volume of CCM in microcentrifuge tubes. The samples were then vortexed, and mixed for 30 min at 4°C. After centrifugation at 14,000 x g for 1 min, the supernatant was aspirated, and 10 µl of 2X Laemmli buffer was added to the resin. The sample was boiled for 5 min and then frozen until analyzed by Western blotting.

CO-IMMUNOPRECIPITATIONS (CO-IPS)

Human fibroblasts were grown and CCM was collected as described above. For Co-IPs, we used the polyclonal anti-LOX antibody described in Chapter 2, the monoclonal anti-FN antibody described in Chapter 2, and the monoclonal anti-His tag antibody used as a negative control. First the collected CCM was pooled and pre-cleared with 20 µl of Protein A Agarose resin (Roche) for 30 min at 4°C. The CCM was centrifuged at 3300 x g to pellet the resin, and the CCM was aliquoted into fresh tubes. 14 µg of each primary antibody was added to 5 ml of CCM in 15-ml conical tubes, and the samples were incubated for 2 hr at 4°C. Next, 15 µl of Protein A-agarose resin was added and the samples were mixed for 1 hr at 4°C. The samples were then centrifuged at 3300 x g for 5 min to pellet the resin, and the resin was washed three times with PBST. 20 µl of 2X Laemmli buffer was added and the samples were boiled for 5 min and then frozen until analyzed by Western blotting.

SOLID PHASE BINDING ASSAYS

Wells of high protein-binding EIA/RIA microplates (#3590; Corning) were coated with 50 µl of purified "receptor" protein at 200 nM in PBS or in 10 mM K_2HPO_4 (pH 8.2) overnight at 4°C. The next morning, the fluid was removed from the wells, which were then blocked with 200 µl of 1% BSA in PBS for 3 hr at 37°C. After removing the blocking solution, wells were washed three times with 200 µl of 0.1% BSA in PBS. Then, 50 µl of purified soluble "ligand" protein was then added to the wells at various concentrations (0 - 100 nM) in PBS or in 10 mM K_2HPO_4 (pH 8.2) and the plate was incubated overnight at 4°C. The next morning, the wells were washed three times with PBST and 50 µl of a monoclonal anti-GST antibody (diluted to 0.5 µg/ml in PBST) (Upstate Biotechnology) or the IST-4 anti-FN antibody (diluted 1:500 in PBST) was added to each well. The plate was incubated at room temperature for 1 hr, the fluid was removed, and the wells were washed three times with PBST. 50 µl of HRP-labeled anti-mouse antibody (diluted 1:1000 in PBST)(Amersham) was added to each well, and the plate was incubated at room temperature for 1 hr. The fluid was removed, and the wells were washed three times with

PBST and once with PBS. The HRP activity in each well was measured by adding 50 µl of the QuantaBlu Fluorogenic Peroxidase Substrate (Pierce Biotechnology). After the plate was incubated for 60 min at 37°C, 50 µl of the QuantaBlu Stop Solution was added, and the fluorescence was measured at 405 nm using a POLARstar Optima microplate reader. All samples were performed in triplicate to minimize experimental error. The dissociation constants were calculated using non-linear regression analysis performed by Graphpad Prism 3.0 statistical software.

CHAPTER 4. INVESTIGATION OF THE BIOLOGICAL ROLE OF THE LOX-FN INTERACTION

INTRODUCTION

The overall goal of this research was to identify protein interactions of LOX in order to discover novel mechanisms of LOX activity regulation and novel mechanisms of LOX activity. Proteins may interact with each other for many different purposes: to be a substrate for an enzyme, to function together as subunits of a larger protein complex, to change the subcellular localizations of the proteins, to inhibit the function of one, or to change other interactions by altering the physical conformation of the proteins. *In the scope of this dissertation, we are aiming for experimental evidence to develop a working hypothesis about why LOX and FN may be interacting in the extracellular environment.*

An obvious and relevant question was how FN influences LOX's catalytic activity, and to investigate this possibility, we designed experiments to address the following questions. Can the FN protein act as a novel substrate of the LOX enzyme? Does binding to FN inhibit or promote LOX catalytic activity towards known substrates? These questions needed to be answered before we could formulate any hypothesis about the biological role of this interaction.

From the SPBA data, LOX demonstrated a binding affinity to cFN in the same range as type I collagen and tropoelastin, two known substrates of LOX. However, the FN matrix does not seem to be covalently crosslinked, except in situations of blood clotting [287, 288]. This process requires circulating pFN to be crosslinked to fibrin by factor VIIIa (a transglutaminase), which is among the first responses to wounding. It has also been shown *in vitro* that factor VIIIa can crosslink FN to collagen and itself [375], and that soluble polyamines (such as spermidine and cadaverine) can inhibit the crosslinking of FN to fibrin, itself, and collagens [376]. Because of crosslinking of FN by factor VIIIa, and because of the presence of 78 lysine residues in the longest variant of the FN protein, one of the first questions to answer about this LOX-FN

interaction was if FN could be a potential substrate for LOX oxidation. Therefore, we felt it important to experimentally determine with *in vitro* activity assays if LOX could directly oxidize FN.

Since the active, 30-kD form of LOX bound tightly to cFN, it was possible that LOX's conformation would be altered by this interaction, or that the catalytic site would be blocked to substrate molecules. In addition, it was possible that the presence of cFN could accelerate the catalytic reaction of LOX towards known substrates. To test this, we performed *in vitro* lysyl oxidase activity assays after pre-incubating the LOX enzyme with or without equal amounts of FN.

Historically, lysyl oxidase activity had been measured using a radioactively-labeled collagen/tropoelastin substrate, which would be prepared by growing cultured cells with ^{14}C-lysine or ^{3}H-lysine in the presence of BAPN and purifying the ECM proteins [27, 30]. The catalytic activity of LOX was measured either by measuring the final quantities of ^{14}C-labeled allysine products [27] or by measuring the release of labeled hydrogen atoms (as ^{3}HHO) into the supernatant [30]. Once it was discovered that LOX could oxidize nonpeptidyl alkyl amines and diamines [377], it became possible to use these soluble substrates for real-time activity assays which used peroxidase to generate fluorescent homovanillic acid products as the H_2O_2 molecules were generated by the LOX oxidation reactions [378]. In 2002, Palamakumbura et al published a more sensitive method based on detecting the H_2O_2 generated from each oxidation reaction using Amplex Red (10-acetyl-3,7-dihydroxyphenoxazine), which forms the fluorescent molecule resorufin when oxidized by HRP with available H_2O_2 (Figure 39) [379]. When multiple assays are done in parallel with a BAPN control, this protocol allows for the rapid detection of lysyl oxidase enzyme activity from complex biological samples.

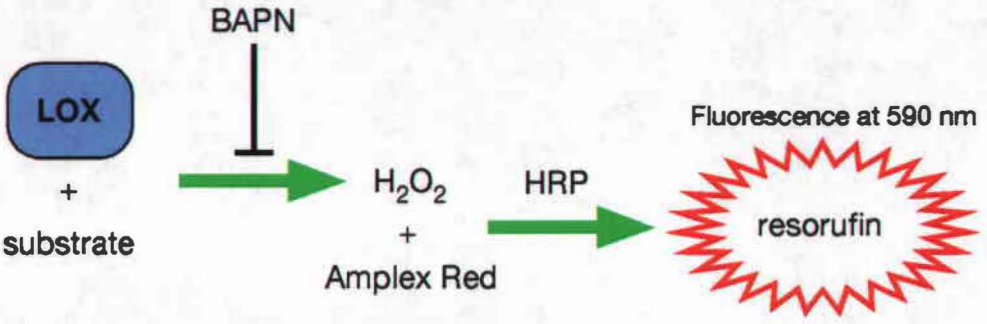

Figure 39. The principle of the lysyl oxidase enzyme activity assay is the detection of generated H_2O_2 by Amplex Red and HRP. Since BAPN is a specific inhibitor of the lysyl oxidase family of enzymes, it is added to parallel reactions to determine the quantity of H_2O_2 released specifically due to lysyl oxidase activity. A microplate reader measures the resorufin fluorescence by exciting at 560 nm and reading at 590 nm. This protocol is based on Palamakumbura et al (2002) [379].

For the lysyl oxidase activity assays, the typical substrate is 1,5-diaminopentane, or cadaverine, which is a naturally occurring diamine (H_2N-CH_2-CH_2-CH_2-CH_2-NH_2) that is produced from the decomposition of lysine amino acids. Cadaverine has long been identified, along with putrescine, to be partly responsible for the odors of rotting organic material as well as bad breath and urine [380]. This molecule is commercially available, is very soluble, and can be used at a very high concentration in order to detect small amounts of lysyl oxidase activity. Since the recombinant GST-LOX fusion protein was not catalytically active, LOX enzyme purified from bovine aorta (bLOX) was generously provided by Dr. Herbert Kagan, a collaborator from Boston University, to use in these activity assays [381].

The next step of our approach was to screen for environments *in vivo* where FN and LOX co-localize. This was necessary because it is possible for two proteins to have the potential to interact, but never actually encounter each other *in vivo*. It was also important in order to help form a working hypothesis about the biological function of the LOX-FN interaction. The expression of FN has been widely studied; it is expressed by many cell types in almost every tissue, as well as secreted into the plasma by hepatocytes [287, 288]. LOX is expressed in many tissues, including skin (dermis and epidermis), aorta, heart, lung, kidney, liver, cartilage,

stomach, and general connective tissues [41, 109]. Based on the reported expression patterns, LOX and FN seemed likely to be in the same tissues. However, this is the first time the specific co-localization of FN and LOX has been performed examining the various cellular structures of each tissue.

We used human fibroblasts cultured on glass coverslips and fixed with formaldehyde to optimize conditions for immunofluorescent (IF) co-staining with FN and LOX antibodies. For the co-localization studies, we used commercial arrays of formaldehyde-fixed normal human tissues, which included major organs such as heart, kidney, lung, liver, adipose tissue, placenta, intestine, colon, and skeletal muscle. We also used a cardiovascular-specific tissue array, which included large arteries and veins, mitral and tricuspid valves, epicardium, and ventricle and atrial walls. These arrays included eight different tissue sections per slide, and allowed a rapid screening for LOX and FN co-localization. In addition, because these were commercially available arrays, there was no need for Internal Review Board approval to use human tissues.

The use of a Zeiss LSM 5 Pascal V5 confocal laser microscope allowed imaging at a high resolution, which is critical to attempt to show two proteins are close enough together to interact. Based on electron microscopy, the length of a FN dimer (with monomer FN subunits bound together at the C-terminal end) has been estimated at 160 nm, with a width of 2-3 nm [382]. The theoretical diameter of a 30-kD globular protein like LOX can be estimated based on the assumption of a constant protein density. Since globular proteins tend to fold in a conformation to minimize water molecules in the interior, the proteins tend to have very similar densities, about 1.37 g/cm^3 [383]. This equates to a specific volume of about 0.73 cm^3/g, and so we can calculate the volume based on the protein's mass in Daltons. For a globular protein the size of LOX (30,000 Daltons), the volume is calculated to be 35.8 nm^3. The diameter is estimated from this volume with the assumption of a spherical shape, where D (nm) = 2 x $(3V/4\pi)^{1/3}$ and V = volume in nm^3. This estimates the diameter of the LOX molecule at 4.1 nm. We did not expect to achieve the resolution of the individual protein sizes, but we aimed to at least achieve a

resolution of 0.1 μm using the laser confocal microscope in order to conclude that the two proteins have the potential to interact *in vivo*.

Next, we tested if FN is a molecular regulator of LOX activity by analyzing LOX in the absence of FN using a cell culture model. For this analysis, we were able to use a mouse embryonic fibroblast (MEF) line derived from the FN knockout mouse (FN-/-), which was generously provided by Dr. Deane Mosher of the University of Wisconsin-Madison. He also provided a MEF cell line from the FN heterozygous sibling (FN+/-) to use as a control. Typically, MEFs are isolated and cultured by homogenizing E12.5-E14.5 mouse embryos and disassociating the cells with a brief trypsin digestion. The cells that grow in culture after this process are the embryonic fibroblasts. The FN-null embryos did not continue to develop after the 10^{th} day, and by then acquired many severe abnormalities [296]. Therefore these MEF lines were established by generating FN-/- and FN+/- embryonic stem (ES) cell lines from isolated blastocysts, and then differentiating the ES cells into fibroblasts [384]. By analyzing the LOX protein in these FN-/- and FN+/- cells, we aimed to find further experimental evidence suggesting a biological role of the LOX-FN interaction.

This combined approach of *in vitro* activity assays, *in vivo* co-localizations, and cell culture studies seemed the best way to begin to investigate the biological significance of the LOX interaction with FN.

RESULTS

Effects of FN on LOX's catalytic activity

Since cFN bound to LOX with approximately the same affinity as tropoelastin and type I collagen, two known LOX substrates, we tested if LOX could directly oxidize cFN *in vitro*. Purified bLOX was incubated with purified cFN, tropoelastin, type I collagen, or 1,5-diaminopentane (all substrates in equal molar amounts), and the quantity of H_2O_2 generated was measured using Amplex Red and HRP [379]. As a negative control, BAPN was added to parallel reactions to inhibit bLOX activity. LOX enzyme activity was calculated as the increase in fluorescent units over time (120 min) above BAPN controls.

The results show that cFN is not oxidized at statistically significant levels *in vitro* compared to type I collagen, tropoelastin, or 1,5-diaminopentane (Figure 40). Tropoelastin had the highest rate of oxidation, which was 7.9 fold higher than 1,5-diaminopentane, and 2.2 fold over type I collagen. This was expected as tropoelastin contains more lysine residues than type I collagen, and elastin molecules have been shown to have crosslinks at 37 of its 40 peptidyl residues, while each molecule of type I collagen has only two. Although when using equal molar amounts of these substrates, tropoelastin and type I collagen appear to be better suited than 1,5-diaminopentane for detecting LOX activity, we prefer to use 1,5-diaminopentane because it is possible to use much higher substrate concentrations in the reactions. The small soluble molecule allows us to use high molar quantities in each enzyme reaction, which allows us to perform very sensitive assays for detection of low levels of LOX activity.

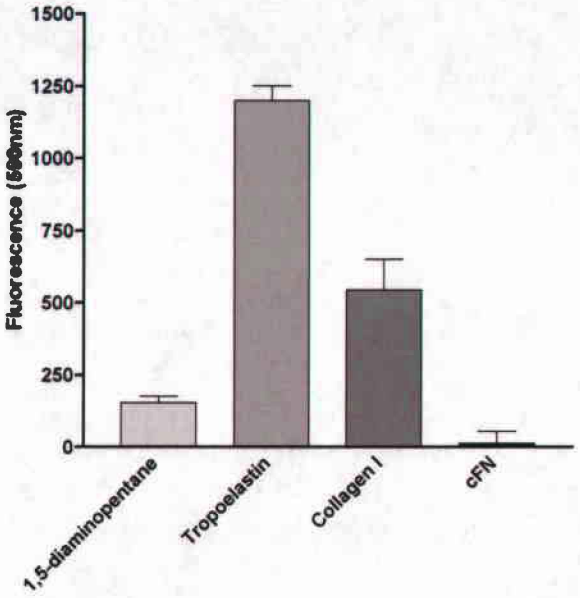

Figure 40. LOX enzyme activity was measured using equal molar amounts of either cFN, tropoelastin, type I collagen, or 1,5-diaminopentane as substrate. With cFN, the measured LOX activity was not significantly above zero (calculated by t-test). Tropoelastin had the highest levels of released H_2O_2 per mole of substrate, followed by type I collagen. Each assay was performed with parallel control reactions containing 500 μM BAPN, which allow the calculation of the oxidation specifically due to the LOX enzyme.

As the data suggested that LOX does not directly oxidize FN, we next investigated if the presence of FN inhibited or enhanced LOX amine oxidase activity towards a known substrate (1,5-diaminopentane). To determine this, we performed an activity assay with bLOX that had been pre-incubated with an equal amount of pFN, cFN, or BSA as a negative control. We also included parallel reactions with BAPN, and as before, we measured the increase in fluorescence over a 120 min period. No significant change in LOX activity was detected due to FN binding, as indicated by comparisons to reactions with bLOX alone and bLOX pre-incubated with BSA (Figure 41). This suggested that FN does not inhibit LOX catalytic activity in solution.

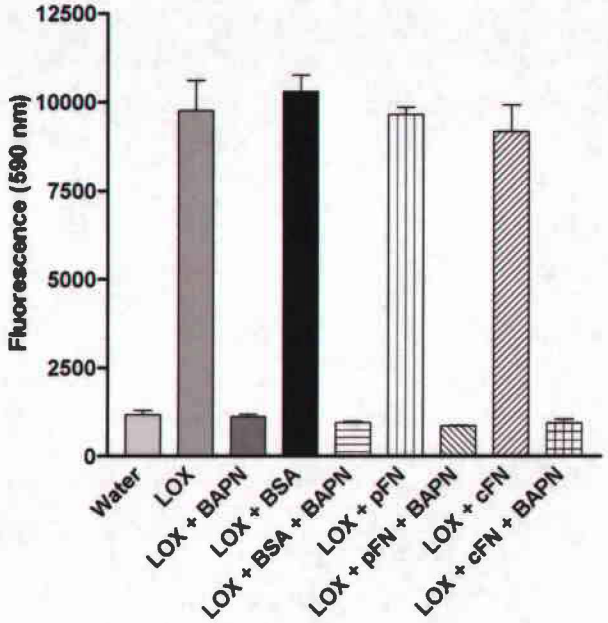

Figure 41. LOX activity assays showing FN does not inhibit LOX amine oxidase activity in solution. Purified bLOX was pre-incubated with equal amounts of cFN, pFN, or BSA, and then a LOX activity assay was performed with 1,5-diaminopentane as substrate. Control reactions with 500 μM BAPN were performed in parallel. By t-test analysis, there was no significant change in activity due to cFN, pFN or BSA.

In further experiments, we used a combination of solid phase binding assay and lysyl oxidase activity assay to determine if LOX, when bound to solid phase cFN, would remain active against other substrates. First, we incubated 0, 10, or 100 nM of purified bLOX with immobilized cFN (prepared as described in Chapter 3), allowing the proteins to bind overnight. Then we washed away the unbound bLOX protein and performed a lysyl oxidase activity assay in the same microplate wells by adding the Amplex Red reaction mixture and 1,5-diaminopentane substrate, with BAPN controls in parallel. We calculated the increase in fluorescence over 60 min, minus the BAPN controls (Figure 42). We also performed a parallel assay that confirmed the bLOX was bound to the cFN matrix (Figure 42). The results of this assay showed that LOX, when bound to immobilized cFN, remained enzymatically active towards other substrates *in vitro*.

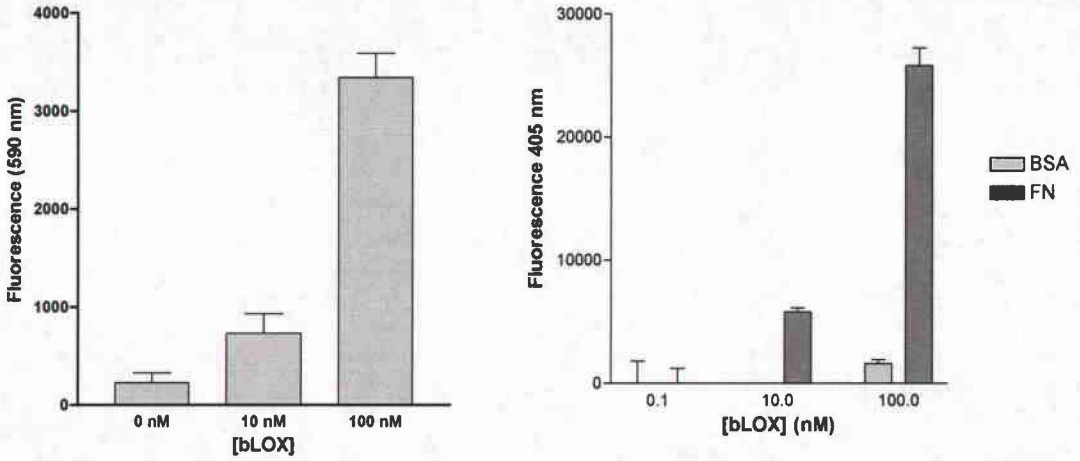

Figure 42. cFN-bound LOX remains active towards other substrates. *Left*: LOX activity assay of cFN-bound LOX. 0, 10, or 100 nM of bLOX was incubated with solid phase cFN overnight, the unbound LOX removed, and an activity assay performed with 1,5-diaminopentane as substrate. Parallel control wells contained 500 μM BAPN to determine H_2O_2 generation specifically due to LOX catalytic activity. Activity was detected in a dose-dependent manner. *Right*: A parallel SPBA was performed to verify that the bLOX was bound to the immobilized cFN (versus BSA control). Anti-LOX antibody detection verified that bLOX remained in the microplate wells in dose-dependent amounts that paralleled the results of the LOX activity assay.

Immunofluorescent co-staining of human cells and tissues

Before performing IF staining on fixed human tissue sections with FN and LOX antibodies, we first optimized the procedure using fixed cultured human skin fibroblasts. The cells were grown on glass coverslips until 6 days post-confluent, and then fixed with formaldehyde. The cells were washed and incubated with anti-LOX and anti-FN antibodies in a titration of concentrations. Secondary antibodies conjugated to red and green fluorescent dyes were incubated with the cells, and finally the coverslips were mounted on slides. Confocal microscopy was used to capture images of the co-staining at high resolution. Since this was the first time this particular LOX antibody was used for IF staining, parallel stainings were performed with purified Rabbit IgG isotype control at the same concentrations as anti-LOX. This negative

control allowed the optimization of the laser confocal exposure settings to ensure that the captured signal was due to specific LOX staining.

The results show a continuous FN matrix (red) that is consistent with the many published studies of FN in cultured fibroblasts (Figure 43). The LOX staining (green) appeared in a very punctate pattern situated along and between the FN fibrils. We know that the length of a single FN molecule is ~160 nm (with a thickness of 2-3 nm) [382], and the theoretical diameter of a globular protein the molecular weight of LOX (30 kD) is 4.1 nm. At many locations in the ECM, we observed FN and LOX co-localization at a resolution of < 500 nm. This supports the theory that FN and LOX are in the same ECM microenvironments of these cultured fibroblasts.

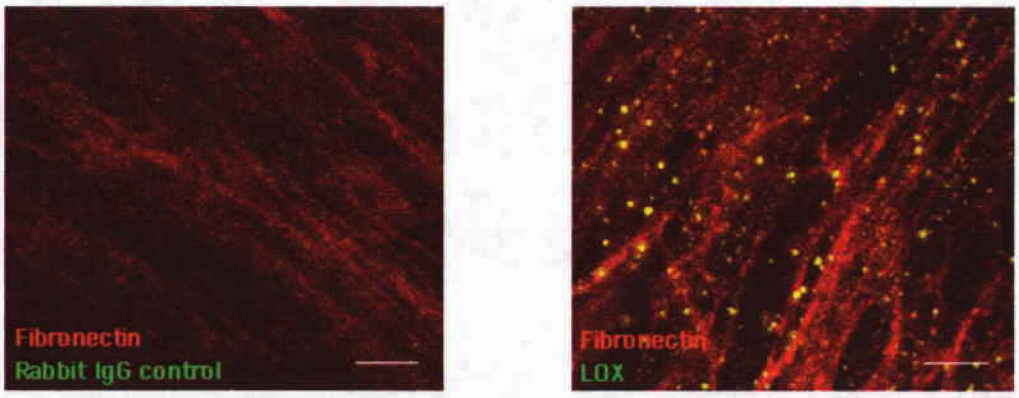

Figure 43. Confocal images of post-confluent neonatal skin fibroblasts co-stained for FN and LOX (or rabbit isotype control). Cells were grown and fixed on glass coverslips. FN (red) stained as a continuous polymerized matrix while LOX (green) stained in a punctate pattern, which was consistent in examined tissues. At this close magnification, the LOX staining appears yellow, as LOX is co-localized with the polymerized FN. Scale bars = 5 μm.

To discover areas in human tissues where LOX and FN co-localize, we acquired 3 sets of normal human tissue macroarrays from Novagen. Each set included 5 slides, and each slide contained sections of 8 different tissues, which are listed in Table 9. Additional information about the sources of the tissues was limited to patient sex and age. Each section was a few square millimeters of tissue, but was simply detailed, such as "brain." Despite this limited

information, most of the cellular structures were identifiable using histology references and consultations with laboratory members experienced with histology.

Table 9. Novagen tissue macroarrays that were co-stained for LOX and FN and analyzed by IF confocal microscopy. Each macroarray slide contained 8 tissues, and each set contained multiple slides with serial tissue sections. The age and sex of the patients who were the sources of the tissues are listed to the right.

Novagen Slide	Catalog #	Included Tissues	Age	Sex
Human Macroarray 1	70312	Brain	70	M
		Heart	72	F
		Kidney	19	M
		Liver	19	M
		Lung	82	M
		Skeletal muscle	19	M
		Pancreas	70	M
		Spleen	14	F
Human Macroarray 2	70313	Adipose tissue	26	M
		Bladder	29	M
		Colon	37	F
		Esophagus	83	F
		Placenta	28	F
		Small intestine	64	M
		Stomach	24	M
		Uterus	40	F
Human Cardiovascular Tissue Set	70316	Artery	91	F
		Atrium	91	F
		Epicardium	91	F
		Interventricular septum	91	F
		Mitral valve	91	F
		Tricuspid valve	91	F
		Vein	91	F
		Ventricle	91	F

As done with the cultured fibroblasts, these tissues were either co-stained with FN and LOX antibodies or with the FN antibody and purified Rabbit IgG as a negative control. The slides were also analyzed by laser confocal microscopy, with the negative control slides used to optimize the exposure settings for each tissue. This ensured that the green fluorescence

detected on the LOX-stained slides was specific to the anti-LOX antibody and not background fluorescence. In the co-stained images, the overlap in green and red fluorescent signal results in a yellow color, demonstrating areas of co-localization.

As characterized by previous studies, FN was localized in an almost ubiquitous pattern, with intense areas of staining in areas of connective tissue and epithelial cells. LOX was also expressed in almost every tissue studied, with very high staining in epithelial cells of the gastrointestinal tissues (stomach, colon, esophagus), connective tissue, smooth muscle cell layers of blood vessels and tissues such as the bladder and uterus, and also in both cardiac and skeletal muscle.

Co-staining in normal human tissue arrays demonstrated many areas of co-localization supporting the possibility of an *in vivo* biological interaction between FN and LOX. The punctate staining pattern of LOX, observed in cultured fibroblasts, was consistent with that seen in distinct microenvironments of fixed tissues. In the heart, FN and LOX staining were both intense, with many areas of co-localization surrounding the cardiac myocytes (Figure 44A). The intense yellow staining likely represents the strong ECM skeleton of the heart, to which the cardiac myocytes attach. More details of LOX and FN in muscle are presented below. In the lung bronchial epithelium and the underlying lamina propria, comprised of smooth muscle and connective tissue, LOX and FN co-localization was detected (Figure 44B). FN and LOX were also co-localized in the smooth muscle cell layers of large and small blood vessels (Figure 44C and 44D). In liver hepatocytes, LOX staining was present, but did not appear to be co-localized with the intense FN staining that presumably represents pockets of pFN to be secreted (Figure 44E). In the kidney, both proximal and distal tubules show strong LOX staining that overlaps with the FN staining around the tubule epithelial cells, particularly the basal side of the epithelium (Figure 44H). Intense red FN staining can also be observed in the connective tissue between the kidney tubules. No LOX staining within the renal corpuscles were detected.

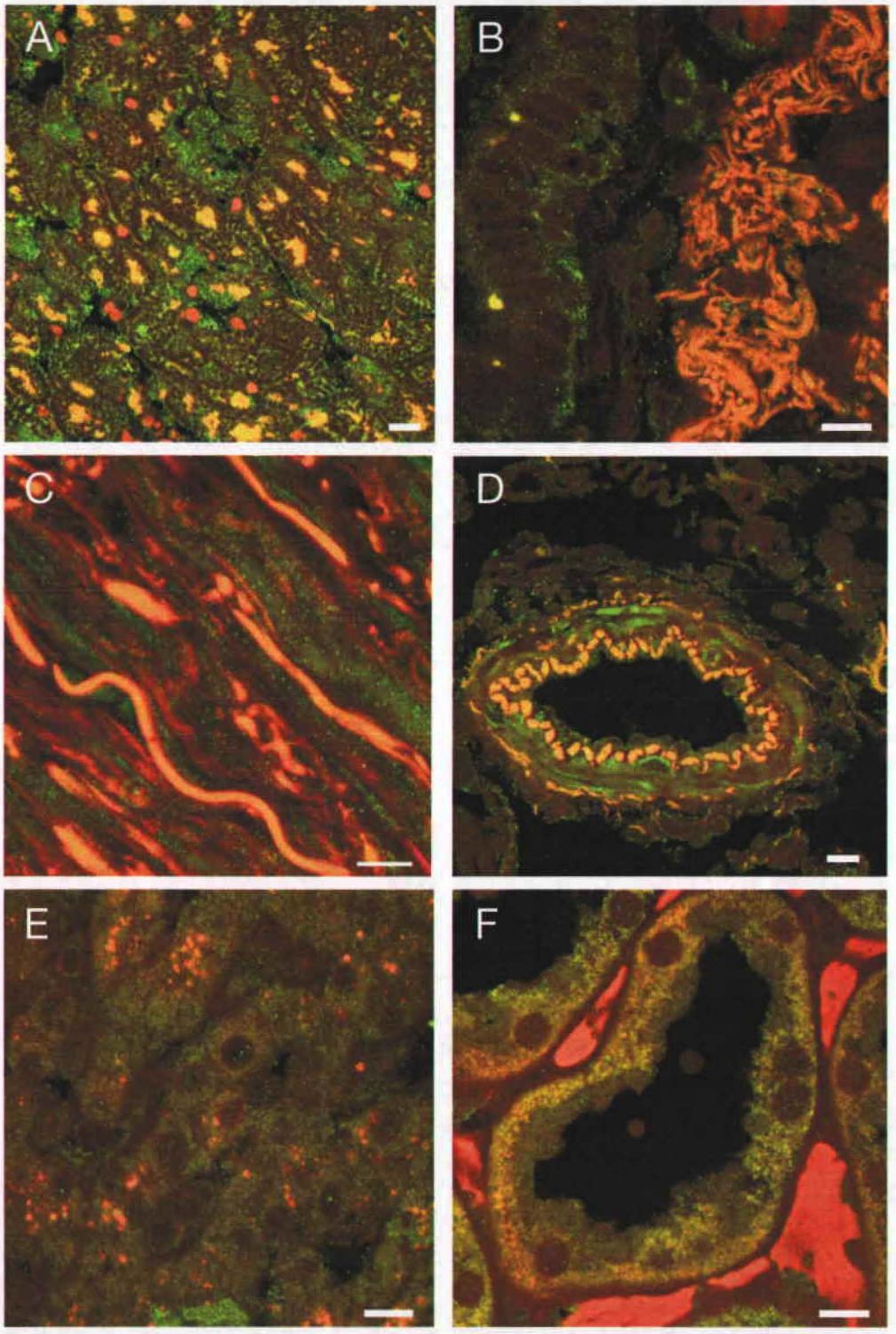

Figure 44. Immunofluorescent co-staining of FN and LOX in fixed human tissues detected by confocal microscopy. LOX staining is shown in green, FN staining is shown in red, and areas of overlapping signal show as yellow. A: Heart: Cardiac muscle. B: Lung: Bronchial epithelium with underlying lamina propria. C: Media of large vein. D: Small blood vessel. E: Liver heptocytes. F: Proximal convoluted tubules of the kidney. All scale bars = 10 μm.

Staining in placental tissue demonstrated intense FN and LOX staining surrounding the epithelial cells of the chorionic, floating, and stem villi (Figure 45A and 45B). LOX was also located to the stroma and along the basement membrane beneath the epithelium. Adipocytes have individual basement membranes surrounding each cell, and adipose tissues showed LOX and FN co-localization closely bordering each cell (Figure 45C). In the esophagus, LOX co-stained strongly with FN along the basal layer beneath the stratified squamous epithelium (Figure 45D). Strong co-staining was also observed throughout the esophagus epithelium. In the stomach and other gastrointestinal tissues, LOX was present at very high levels in the epithelium and the underlying basement membrane (Figure 45E and 45F), but FN was present at mostly at lower levels. In the connective tissue and muscle layers beneath the epithelium, LOX and FN were also present. In Figure 45E, a gastric pit of the stomach is shown in transverse, and the LOX staining is very intense along the basement membrane that lies under the large mucus-secreting cells and throughout the connective tissue that surrounds the stomach glands. In Figure 45F, the epithelial layer of the colon is shown, and LOX staining is prominent throughout the epithelium, as well as underlying this cell layer along the basement membrane.

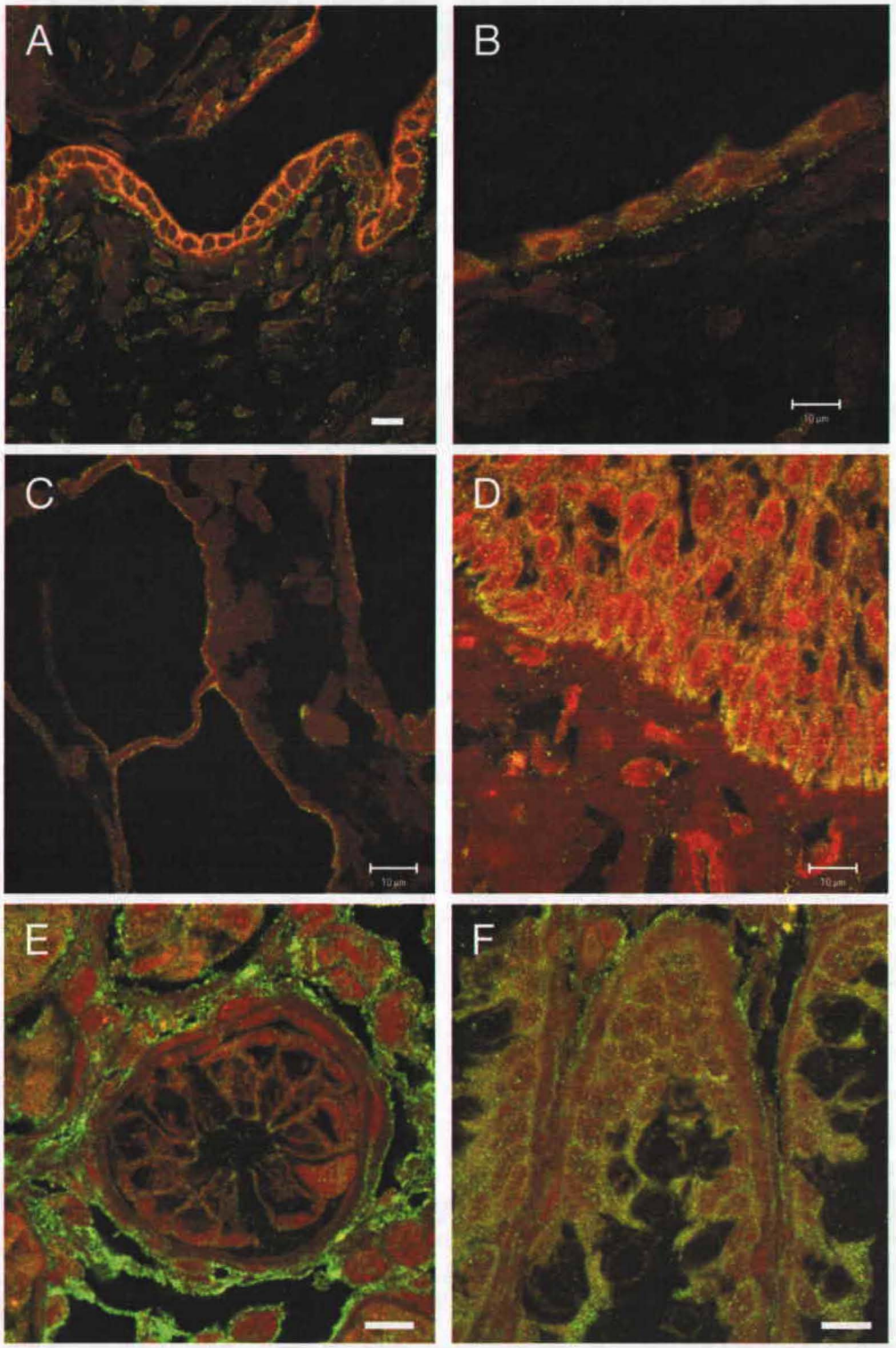

Figure 45. Immunofluorescent co-staining of FN and LOX in human cells and tissues detected by confocal microscopy. LOX staining is shown in green, FN staining is shown in red, and areas of overlapping signal show as yellow. A & B: Placenta: chorionic villi. C: Adipose tissue. D: Esophagus: Stratified squamous epithelium (upper) and lamina propria (lower). E: Stomach: transverse section of gastric pit and surrounding lamina propria. F: Colon: Mucosal epithelium. All scale bars = 10 μm.

An interesting finding was that LOX was clearly detected in a striated pattern in both skeletal muscle and cardiac muscle sections (Figure 46A, 46B, and 46C). This has never been described before and was surprising as LOX is primarily an extracellular enzyme. Typically, proteins appearing in this striation pattern are located to specific sections of the muscle sarcomere. However, FN was also seen localized in a somewhat striated pattern, although the staining was not as intense as LOX. By observing cross-sections of the cardiac myocytes, we see a pattern of staining coming in toward the center of the fiber (Figure 46A and Figure 46D, 46E, and 46F). Based on previous descriptions of FN localization in cardiac myocytes [385], we believe that LOX and FN are located within the transverse tubules (T tubules) that stretch inwards perpendicular to the muscle fibers. The T tubules are aligned with the Z disks of the cardiac muscle sarcomeres, and the A-I boundary in skeletal muscle sarcomeres. These T tubules have been shown to contain such ECM proteins as FN, laminin, and collagens [385], so it would seem plausible that LOX could also localize there as well. This could result in the striated pattern for LOX observed in cardiac and skeletal muscle fibers.

Another point to note was that in the transverse sections of cardiac muscle, prominent LOX staining (but not FN) was visible along the intercalated discs (Figure 46C). These special cell-cell junctions have been shown to occur only in cardiac muscle tissues, and are not known to contain collagen or elastic fibers. However, some non-fibrillar collagens, such as type XIII collagen, has been shown to localize to the intercalated discs [386]. This staining was consistently visible for LOX, and needs to be further researched.

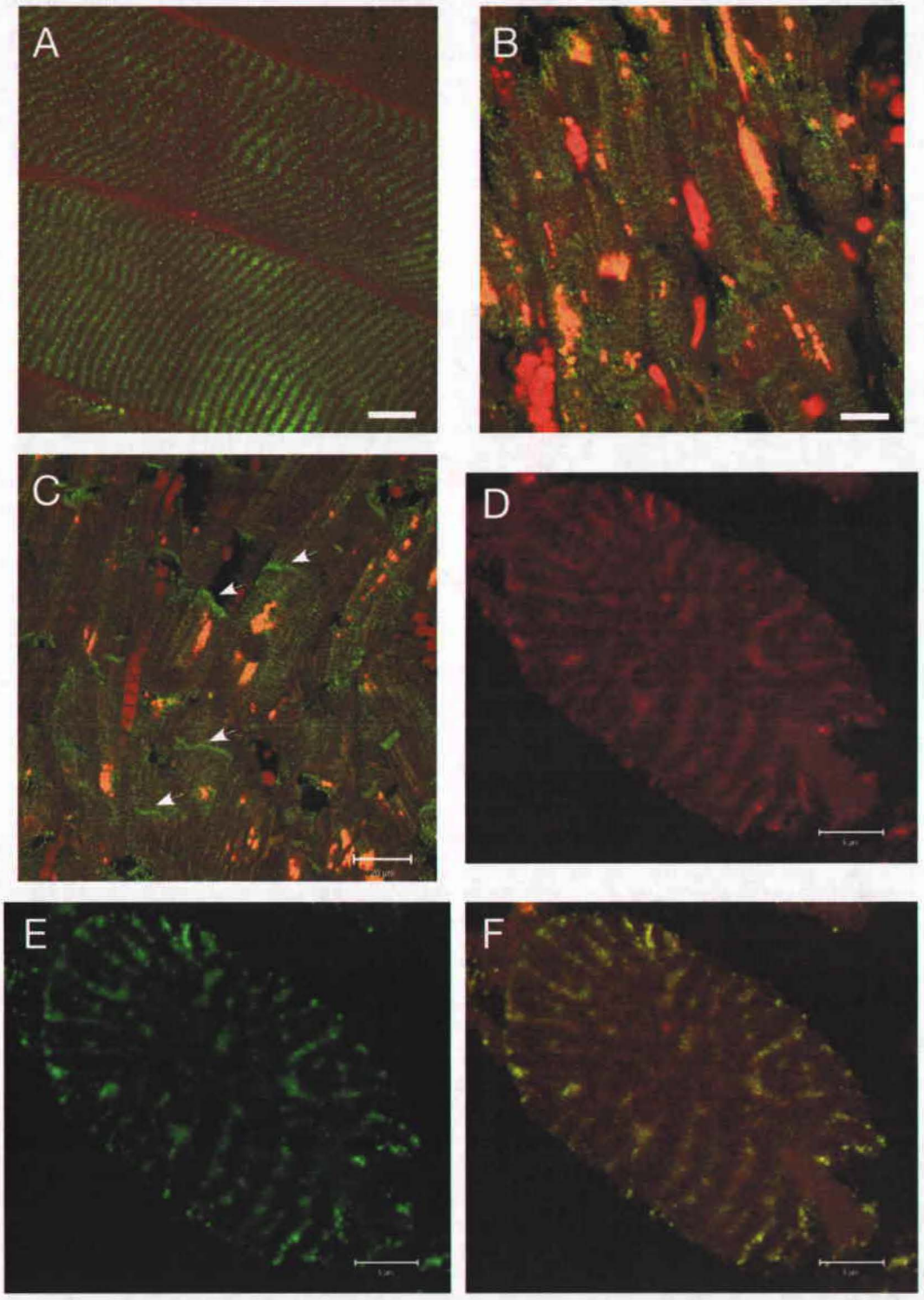

Figure 46. Immunofluorescent co-staining of FN and LOX in human muscle cells detected by confocal microscopy. LOX staining is shown in green, FN staining is shown in red, and areas of overlapping signal show as yellow. A: Skeletal muscle: longitudinal section. B & C: Cardiac muscle in longitudinal section. Intercalated discs are indicated with arrows. D, E, & F: Single cardiac myocyte in transverse section: imaged with separate red and green channels and then with both merged. Scale bars in A, B, & C = 10 µm. Scale bars in D, E, & F = 5 µm.

Analysis of LOX in FN-null conditions

As mentioned in the Introduction, we were able to correspond with Dr. Deane Mosher from the University of Wisconsin-Madison, who generously provided cultured mouse embryonic fibroblasts (MEFs) derived from a FN-null embryo (FN-/-) and a heterozygous sibling (FN+/-) (Figure 47) [384]. The FN knockout mice fail to develop past embryonic day 10.5, and exhibit a wide range of morphological and physiological defects. Mutant embryos display shortened anterior-posterior axis, deformed neural tubes, and severe defects of mesodermally-derived tissues, including the heart and vasculature [296].

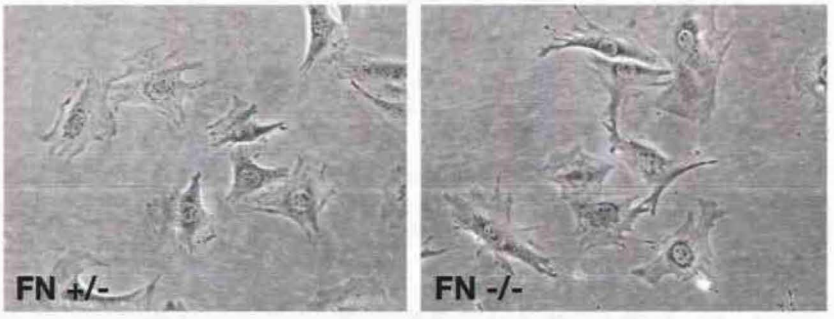

Figure 47. Cultured embryonic fibroblasts from the FN knockout mouse (FN-/-) and heterozygous sibling (FN+/-). Both cultures are grown in DMEM supplemented with FN-depleted fetal bovine serum. The two cell lines have not demonstrated any obvious morphological differences.

To investigate the possible regulation of LOX by FN *in vivo*, we analyzed the LOX protein in the MEF cultures from the FN+/- and FN-/- mice. To maintain FN-null conditions, the cells were cultured in DMEM with FN-depleted FBS. To remove the FN from the FBS, we incubated the FBS with gelatin-sepharose at 4°C overnight and used centrifugation to separate the sepharose from the FN-depleted FBS. This method has been established for removing FN from solutions based on the very high affinity of FN for gelatin [332, 387]. Like many ECM proteins, LOX protein levels dramatically increased when the MEFs were grown past confluency, as

detected by timepoint Western blots (data not shown). Therefore, further LOX protein analysis was performed with cells grown to 2 days post-confluency and then incubated with serum-free medium for another 2 days. This conditioned cell medium (CCM) was collected for protein analysis.

Western blots were performed with 15 μg of total proteins from the CCM of these cells using a LOX-specific antibody. The results showed dramatically decreased levels of the 30-kD LOX in the media of FN-/- cells (Figure 48A). In addition, an increased amount of 46-kD proLOX is clearly observed in the FN-/- medium compared to the FN+/- medium. A novel 40-kD band was observed in the FN-/- samples, but also was present in FN+/- samples as seen by longer autoradiograph exposures. This 40-kD protein remains unidentified, but it may represent an intermediate processed form of LOX or perhaps a novel embryonic-specific LOX variant. By analyzing 3 replicates and quantifying the relative amounts of LOX in the media, the amount of 30-kD LOX is decreased by ~90% in the FN-/- medium compared with the FN+/- medium. However, the total sum of detected LOX protein, both processed and unprocessed, was quantified using Kodak imaging software and was found to be approximately equal in both FN-/- and FN+/- samples. No difference was detected in the cell lysate protein fraction, which contained only low levels of proLOX in both cell lines.

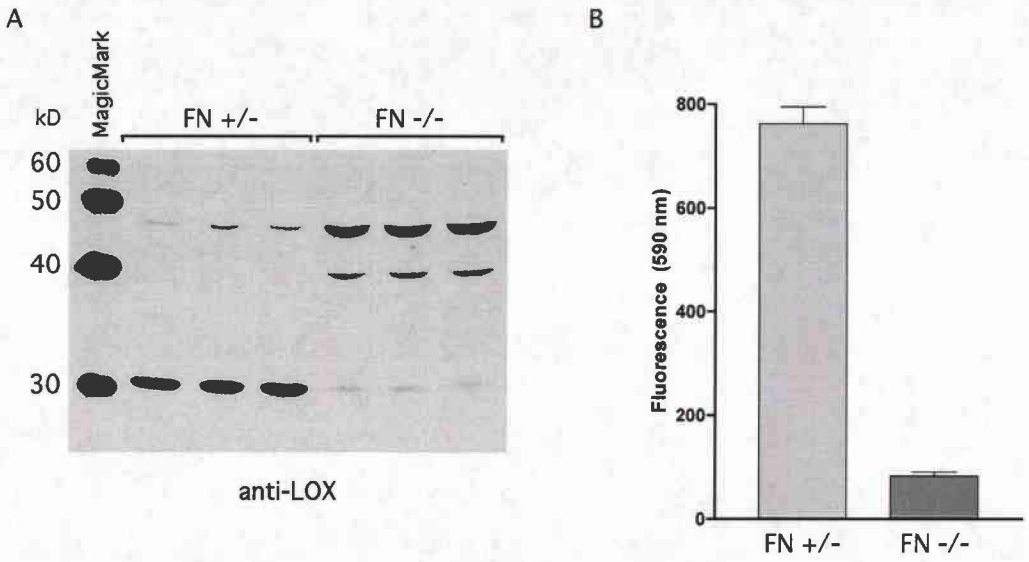

Figure 48. Decreased activation of LOX in FN-/- cell medium compared to in FN+/- medium. *A*: Using anti-LOX antibody, Western blots of CCM from FN+/- and FN-/- showed dramatically decreased levels of the mature form of LOX in FN-null conditions, as well as corresponding increased amounts of full length proLOX. 15 µg of CCM proteins were loaded into each lane of these blots, and the samples were run in triplicate. *B*: In FN-/- media, lysyl oxidase activity was decreased to approximately 10% of the activity measured in FN+/- media ($p<0.0001$). Activity was calculated as increase of fluorescent units over time (120 min) above that measured in parallel BAPN controls.

To determine if the changes in LOX proteolytic processing observed by immunoblotting corresponded to changes in LOX enzyme activity, lysyl oxidase activity assays were performed from the CCM collected from FN+/- and FN-/- cells. Proteins in the CCM were concentrated with Amicon centrifugation filter units with a 10 kD molecular weight cutoff. The LOX activity was measured in equal microgram amounts of total proteins from both FN+/- and FN-/- CCM. As described previously, the activity was calculated as increase in fluorescent units over time (120 min) minus the increase of the BAPN controls. The data showed that LOX catalytic activity was decreased by 89.2% in the FN-/- cell media compared with the FN+/- cell media, with $p<0.0001$ (Figure 48B). *The decrease in 30-kD LOX protein levels and the corresponding decrease in LOX catalytic activity in FN-/- media were verified in 3 independent experiments.*

To confirm that these decrease in LOX proteolytic activation is not due to a general downregulation of BMP-1, we also performed Western blot analysis of the CCM samples using a

anti-BMP-1 antibody. As above, 15 µg of total proteins from FN-/- and FN+/- CCM samples were loaded in each lane, and done in triplicate. As BMP-1 is processed by the furin protease prior to secretion into the extracellular space [388], the active form of BMP-1 is 628 aa and predicted to be 70 kD [389]. The results of the Western analysis showed that the levels of BMP-1 are not decreased in FN-/- cultures (Figure 49).

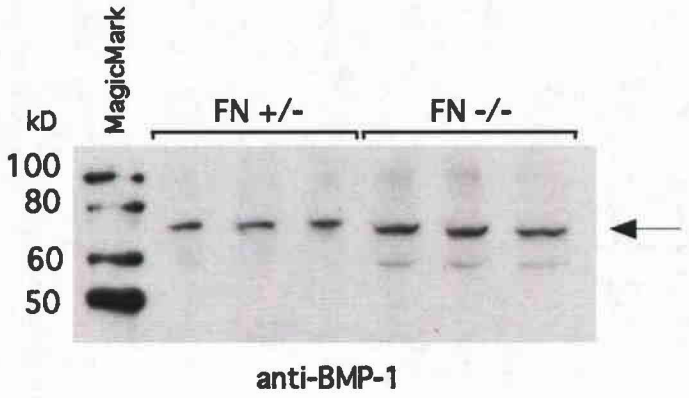

Figure 49. Western blot with the same CCM samples as in Figure 48 using anti-BMP-1 antibody. The CCM of FN+/- and FN-/- cell lines showed similar levels of the BMP-1 protease, suggesting that the decrease in LOX activity was not due to downregulation of BMP-1. 15 µg of CCM proteins were loaded into each lane of these blots, and the samples were run in triplicate. The arrow indicates the 70-kD mature BMP-1 protease.

DISCUSSION

The measurement of LOX enzyme activity has historically been a difficult procedure. The first assays to be developed used radioactively-labeled ECM proteins and measured the radioactivity released into the supernatant using centrifugation or ultrafiltration [27, 30]. With the development of a fluorescent assay based on the detection of H_2O_2 with Amplex Red and HRP [379], we have much more flexibility and sensitivity for these assays. Since 2002, we established and optimized this fluorescent assay in our laboratory, and can now accurately measure the lysyl oxidase activity in cell culture media and lysates, tissue extracts, and purified

protein solutions. These assays depend on parallel controls using BAPN to provide a H_2O_2 baseline value to subtract from the experimental sample. This makes the assay specific for lysyl oxidase activity, and excludes any measurement of activity from other amine oxidases.

From the activity assay data, it appears that FN is not a substrate for LOX's amine oxidase activity. This is in agreement with data from previous studies of the FN matrix, which has been shown to be incredibly dynamic. In cell cultures, this matrix undergoes constant reorganization and is able to be broken and reformed rapidly [291]. It has also been shown that the integrity of the FN matrix depends on the high concentration of soluble FN molecules, which constantly exchange places with the matrix-bound FN molecules [324]. Covalent crosslinks in the FN matrix would hypothetically prevent this dynamic exchange, and also prevent the rearrangement of the FN matrix without the use of proteases. However, this does not exclude the possibility that FN may get oxidized by LOX under special circumstances *in vivo*. During wound healing, FN can get covalently crosslinked to fibrin by factor VIIIa, and FN does contain many lysine residues in the C-terminal portion of the protein where LOX bound in the yeast two-hybrid assays. Perhaps there are some circumstances *in vivo* when LOX may oxidize peptidyl lysines of FN, but we think this LOX-FN interaction most likely has a different biological role.

In the course of testing LOX activity towards cFN, we noticed that tropoelastin and type I collagen were much more efficient LOX substrates than 1,5-diaminopentane. Using equal molar amounts of these substrates demonstrated a 9-fold higher oxidation rate of tropoelastin over 1,5-diaminopentane, and a 4-fold higher oxidation rate of type I collagen. This perhaps raises the question: why did we continue to use 1,5-diaminopentane for all the subsequent LOX activity assays? The answer is that because of the small molecular weight, much more of the 1,5 diaminopentane molecules can be used in each reaction. Higher molar amounts of the substrate make the reactions more sensitive to detect smaller quantities of lysyl oxidase activity. In addition, the cost of using tissue-purified tropoelastin or type I collagen for all of the future activity assays was prohibitively greater than 1,5-diaminopentane.

The data indicates that cFN binding does not inhibit LOX's catalytic activity. This was shown by two different methods – one with LOX-cFN binding in solution, and the other with LOX bound to a solid phase FN matrix. In solution, the measured LOX activity was statistically equal when alone or with added cFN, pFN, or BSA. With solid phase cFN, the bound LOX was washed several times, so the measured LOX activity must have come from the LOX bound to the FN matrix. To be fully confident that the bovine LOX bound to the cFN matrix and the activity was due to this bound enzyme, we performed a parallel SPBA measuring the presence of bound LOX with our anti-LOX antibodies. Indeed, the results from this assay demonstrated the presence of bound LOX in same relative proportion as the measured enzyme activity. Together, these results supported the hypothesis that LOX circulating with soluble FN molecules can retain it's activity, and that the FN matrix can provide a scaffold for LOX activity.

This is the first study to perform co-staining of LOX and FN and the first to specifically demonstrate FN and LOX co-localization in tissues and cultured fibroblasts. Based on each gene's expression profile, it was not a surprise to see that in many of the same tissues, both proteins were present. However, although many of the same cell types express both LOX and FN, this did not guarantee that these proteins would co-localize after they are secreted into the extracellular environment.

The importance of co-localizing these two proteins in tissues is that if we want to ascribe a biological function to their interaction, we first must be confident that they have the opportunity to interact *in vivo*. In addition, the specific areas where LOX and FN may co-localize may provide clues as to how they may function together. The laser confocal microscopy used in this study, while not as powerful as electron microscopy or atomic force microscopy, can achieve a resolution of less than 0.5 μm. The higher the resolution of our images, the higher our confidence that when we observed overlapping red and green fluorescence (yellow), the LOX and FN proteins were close together.

When optimizing the antibodies for immunostaining, we performed LOX and FN co-staining on human cultured fibroblasts. These cells were grown on coverslips and formalin-fixed, and from previous Western blots, we knew to grow the cells with conditions so both LOX and FN were expressed. The FN stained as expected, with a strong red meshwork of fibrils covering the cell layer surface. The LOX stained quite differently, but consistent with a globular enzyme, rather than a structural ECM protein. The LOX stained in a punctate pattern, with bright dots of green fluorescence scattered throughout the cell layer and ECM. The signal was clearly specific for LOX, as the rabbit isotype control staining was negative for this punctate green pattern. In previous reports showing LOX immunofluorescent stainings, this punctate pattern was not as prominent. This may be because the previous immunostainings either used chromogenic detection methods [109, 183, 248] or did not use as high a resolution when imaging the fluorescent stainings [213]. However, electron microscope studies of LOX have demonstrated uneven concentrations of LOX throughout the ECM [175, 176, 390], which supports our punctate localization data.

The human tissue macroarrays from Novagen proved very efficient in screening many different tissues for LOX and FN co-localization. The details about the tissues were not always clear, nor was it possible to know the exact location within the organs that the section derived from, but they still yielded valuable data. For most of the tissues, the cellular structure was clearly identifiable.

Many tissues showed LOX and FN co-localization, including heart, blood vessels (arteries and veins), placenta, adipose tissue, lung, kidney, and GI organs like the esophagus, stomach, and intestines. In addition to areas of connective tissue, polarized epithelial cells displayed LOX and FN co-localization, like in the placenta, kidney, esophagus, and lung. There was evidence that many epithelial cells secrete LOX and FN onto the basal surface, but there was also evidence that certain epithelial cells secrete FN and LOX together onto the apical surface. In staining of the lung bronchial epithelium, intense FN and LOX staining was co-localized in globs at intermittent points along the epithelial layer (Figure 44B). Our best

explanation for this staining is that these large globs of protein are actually secretetory vesicles in Goblet cells, which secrete surfactant into the lung. This would be very interesting if LOX is present in lung surfactant, as this would indicate a complete novel function of this enzyme. The FN protein is secreted into the lung as high levels are measured in bronchoalveolar lavage fluid [391], but this has never been shown before for LOX. Further research should be done to confirm this data.

The localization of LOX to the basolateral surfaces of epithelium, and to several basement membrane structures, is important to note, as this has not been shown before. There are a couple of reports demonstrating LOX functioning in basement membrane barrier maintenance [178, 180], but no proposed mechanism or function. The localizations presented here give some support for this idea. We saw clear basement membrane staining of LOX in the placenta, gastrointestinal tissues, kidney, adipocytes, blood vessel endothelium, and epicardium. Given the observation in the LOX knockout mouse of a disrupted aortic endothelium [121, 122], it will be critical to determine what LOX's role is in forming and maintaining basement membranes.

Does the FN and LOX co-localization data suggest any possible function of their interaction? It is possible that LOX and FN have a basement membrane or epithelial cell layer maintenance function, as several tissues showed basement membrane and epithelial co-localizations. Also, it seems like LOX and FN co-localize in areas of heavy ECM deposition, as in the lung, heart, and aorta. This suggests that the interaction may be involved in ECM maintenance, since these were adult tissues. It would be interesting to co-stain for LOX and FN in developing tissues or areas of wound healing, where ECM synthesis would generally be more active. This may better show if the LOX-FN interaction is specifically associated with areas of ECM assembly, which would be expected if FN acts as scaffolding for LOX activity.

Most importantly to this study, the immunofluorescent co-staining of FN and LOX demonstrated that there were numerous tissues and environments where these two proteins can potentially interact with each other *in vivo*.

The next aim of this project was to determine if FN participates in regulating LOX activity *in vivo* by downregulating FN in a cell culture model. The establishment of embryonic fibroblast cultures from the FN knockout mouse allowed us to analyze the LOX protein in FN-null conditions without any dramatic manipulation of the cells. The two MEF cultures, FN-/- and FN+/-, grew without any obvious morphological differences in the conditions used in this study. We were able to successfully culture these cells according to Dr. Mosher's recommendations using DMEM media supplemented with FN-depleted FBS.

The absence of active LOX in the FN-/- cultures was quite surprising. There have been no reports of any functional link between FN and any of the tolloid family of proteases such as BMP-1. This is also the first indication that the proteolytic processing of LOX is regulated in the extracellular environment. This regulation may be a key factor in explaining the reported temporal differences in LOX mRNA expression and LOX activity. Many studies have described up- or down-regulation of LOX in response to biological stimuli, but in many of these studies, the level of alteration between LOX mRNA and LOX activity were not consistent [340-345]. In addition, the production of LOX mRNA in response to dermal injury has been demonstrated to be rapid (peaking after 3 days) [337]. However, LOX enzyme activity has been shown to peak later (8-10 days post-wound) [338], which suggests that the LOX pro-enzyme may be held in the ECM for a significant period of time before activation.

These results give strong evidence for the direct regulation of LOX's proteolytic activation by FN. It seems unlikely that this is due to altered LOX transcription levels, as by Western blot analysis, we observed approximately equal total amounts of LOX protein (processed and full length) in FN+/- and FN-/- cultures. Also from Western blots, we observed approximately equal amounts of BMP-1 in the media of the two cultures, which shows that the decreased LOX processing is not due to an absence of BMP-1.

We made attempts to induce an increase in LOX activation by adding exogenous cFN and pFN to FN-/- cultures, but these experiments were not successful in increasing the

processing of LOX. There are a couple of possibilities why increased levels of 30-kD were not detected in these experiments. The first may be a limitation of how efficiently these FN-/- MEFs incorporate exogenous FN into matrices. Recently, Bae et al. demonstrated that the protein adhesive substrate determined if the FN-/- MEFs could incorporate exogenous pFN into the ECM [392]. In our MEF cultures, it is unclear which were the main adhesive proteins supplied by the FN-depleted DMEM for attachment to the polystyrene flasks. We are currently trying to use culture flasks pre-coated with FN protein to stimulate the assembly of added cFN and pFN into the ECM [392]. The other possibility is that the activation of LOX cannot be recovered solely by adding exogenous FN. If this is the case, we will have the complex task of diagnosing what molecular components for LOX activation could not be recovered by adding purified FN protein alone.

Clearly, proLOX and BMP-1 are both present in the extracellular environment of the FN-/- cells, so why is LOX not processed as seen in the FN+/- cells? One possible explanation is that LOX binding to FN causes a conformational change in LOX that allows cleavage by BMP-1. There are many examples of this principle in protein biology, where a protein is proteolytically processed only after binding to other proteins, as with apoptosome binding allowing the proteolytic activation of initiator caspase proteases [393, 394]. Another possible explanation is that BMP-1 may be brought into the close proximity of LOX more efficiently when FN is present. Since FN is known to bind collagen, which also gets processed by BMP-1, it is possible that FN acts to bring together tropocollagen, proLOX, and BMP-1. The BMP-1 could cleave both tropocollagen and proLOX, and the active LOX could go on and oxidize the collagen molecule. More research needs to be done to determine if these molecules interact in a larger protein complex with various subunits. Given the number of different molecular interactions of FN, it is doubtful that the bound LOX remains uninfluenced by these other FN-binding proteins.

In summary, we discovered that FN and LOX co-localize at high resolutions in many extracellular microenvironments of various human tissues. We experimentally demonstrated that when the LOX enzyme is bound to FN, it remains catalytically active against third party

molecules. We also showed that the presence of FN is critical for the proteolytic activation of the LOX enzyme. These discoveries have wide-ranging implications for human biology and disease, which will be further discussed in Chapter 5.

MATERIALS AND METHODS

LYSYL OXIDASE ACTIVITY ASSAYS

Purified active bovine LOX (bLOX) was generously provided by Dr. Hebert Kagan [381]. The LOX enzyme activity was measured using the Amplex Red fluorescence assay [Palamakumbura, 2002 #490], which we adapted for use in microplate format. The assay reaction mixture consisted of 50 mM NaBorate (pH 8.2), 1.2 M Urea, 50 µM Amplex Red (Molecular Probes, Inc.), 0.1 U/ml HRP (Sigma), and 10 mM 1,5-diaminopentane substrate (Sigma). The protein samples were added to the reaction mix, in the presence or absence of 500 µM BAPN (Sigma), and the reactions were then incubated in a POLARstar Optima microplate reader prewarmed to 37°C. The fluorescent product was excited at 560 nm and the emission was read at 590 nm every 5 min for 2 hours. All samples were assayed in triplicate to minimize experimental error. Statistical analysis was performed using Graphpad Prism 3.0 statistical software.

To measure if cFN could be a substrate for LOX in vitro, 10 pmol of bLOX was used in each activity assay with 100 pmol of each substrate: 1,5-diaminopentane, type I collagen, tropoelastin, and cFN - with parallel BAPN negative controls for each. To measure if LOX activity is affected by binding to FN, 10 pmol of purified bLOX was incubated with 10 pmol of purified cFN or BSA for 1 hr at 4°C. Purified pFN, cFN, bovine serum albumin (BSA), and chick tropoelastin proteins were purchased from Sigma. Purified rat tail collagen type I was purchased from BD Biosciences.

To determine if LOX retains amine oxidase activity when bound to a solid phase FN matrix, we performed an experiment similar to the solid phase binding assays. We coated wells of an EIA/RIA microplate with 50 µl of purified cFN at 200 nM in PBS overnight at 4°C. The next morning, the fluid was removed and the wells were blocked with 200 µl of 1% BSA in PBS. Then 50 µl of purified bLOX was added to the wells at a concentration range of 0 to 100 nM and incubated overnight at 4°C. The fluid was removed and the unbound bLOX was washed away 3 times with PBST and once with PBS. To measure the activity of the bound bLOX, 200 µl of the

above Amplex Red reaction mix was added (without urea, and using 1,5-diaminopentane as substrate). The reactions were incubated for 60 min at 37°C, and the fluorescence was measured as described above.

To measure lysyl oxidase activity in CCM, 10,000 MWCO Amicon Ultra centrifugal filter units (Millipore) were used to concentrate proteins in the CCM. The collected CCM was transferred to the column, which was centrifuged at 3300 x g until the CCM was concentrated at least 20-fold. The concentration of protein in the sample was measured using a Bradford assay as described previously. An equal microgram amount of concentrated CCM proteins were added to microplate wells, and the volume was brought up to 100 µl with serum-free, phenol red-free DMEM. To these samples was added 100 µl of the Amplex Red reaction mix listed above, using 1,5-diaminopentane as a substrate. Parallel samples were incubated with 500 µM BAPN as a negative control. The reactions were incubated at 37°C, and the fluorescence was measured every 5 min as described above. Replicate samples were used to minimize experimental error.

MEASUREMENT OF PROTEIN CONCENTRATION

Determining the protein concentration of a given solution was performed as previously described in Chapter 3 under "Material and Methods: *Measurement of Protein Concentration.*"

IMMUNOFLUORESCENT STAINING

Cultured human fibroblasts were grown, as described in Chapter 3, on glass coverslips until 6 days post-confluent, then washed with PBS three times and fixed with 10% formalin for 10 min at room temperature. After fixation, the cells were treated with 0.1% Triton X-100, washed again in PBS, and blocked with 0.1% BSA in PBS for 30 min at room temperature. The fixed cells were incubated with primary antibodies diluted in 1% BSA in PBS for 1 hr at room temperature, then washed in PBS with 0.1% BSA three times for 5 min each. The bound primary antibodies were reacted with fluorescently-labeled secondary antibodies diluted in 1%

BSA in PBS for 1 hr at room temperature, and then the coverslips were washed three times in PBS with 0.1% BSA for 5 min each. After a final wash in PBS for 5 min, the coverslips were mounted using Vectashield Mounting Medium (Vector Laboratories).

Immunofluorescent staining on fixed human tissues was performed using human tissue macroarrays (Cat # 70312-3 and 70313-3, Novagen). The tissue sections were deparaffinized by heating at 60°C for 30 min and washing three times in xylene for 15 min. Tissue sections were then rehydrated in 100%, 95%, 80%, and 70% ethanol, followed by immersion in PBS. When needed, antigen retrieval was performed by microwaving the sections in 0.01 M citric acid on high, medium, and then low power for 5 min each. The sections were washed in PBS three times for 5 min, then blocked with 5% normal goat serum (Pierce) at room temperature for 30 min. The sections were reacted with primary antibodies for 2 hr at room temperature, washed three times in PBST, and then incubated with fluorescently-labeled secondary antibodies for 45 min at room temperature. After three final washes in PBS, Vectashield was used to mount coverslips. All slides were analyzed with a Zeiss LSM Pascal confocal microscope.

For the immunostaining, monoclonal anti-FN antibody (FN8-12), which recognizes all isoforms of FN, was purchased from Takara Bio Inc. The polyclonal rabbit anti-LOX antibody was previously described in Chapter 3 Materials and Methods. Purified rabbit IgG, used as an isotype negative control for immunofluorescent staining, was purchased from Zymed Laboratories, Inc. Secondary antibodies for immunofluorescent staining, which included anti-mouse antibody conjugated to Alexa 546 (red) to visualize the anti-FN antibody and anti-rabbit antibody conjugated to Alexa 488 (green) to visualize the anti-LOX antibody and the purified rabbit IgG negative control, were purchased from Molecular Probes, Inc.

Cell Culturing of Mouse Embryonic Fibroblasts

Cultures of embryonic fibroblasts isolated from a FN knockout mouse (FN-/-) and a heterozygous sibling (FN+/-) were generously provided by Dr. Deane Mosher (University of Wisconsin-Madison). These cells were grown using Dulbecco's modified Eagle medium (DMEM)

supplemented with FN-depleted 10% FBS (Serologicals Corporation), penicillin, streptomycin, and amphotericin. To remove the FN from the FBS, 8 ml of gelatin-Sepharose resin (Amersham) was mixed with 50 ml of the FBS overnight at 4°C. The next morning, the resin was pelleted by centrifugation at 3300 x g for 10 min, and the FN-depleted FBS was removed and sterile-filtered through a 0.22 μm filter (Millipore) before added to the DMEM. The cells were kept cultured in T75 flasks under sterile conditions. Only MEFs less than passage 10 were used for protein analysis. For experiments using CCM, cells were grown to 2 days post-confluent, washed with PBS, and incubated with serum-free, phenol-red free DMEM. After an additional 48 hr in culture, the CCM was collected as described in Chapter 3 under "Material and Methods: *Cell Culturing of Human Dermal Fibroblasts.*"

WESTERN BLOT ANALYSIS

Western blots were performed as previously described in Chapter 2 under "Materials and Methods: *Western Blot Analysis*." The rabbit polyclonal anti-LOX antibody was described in Chapter 3 under "Materials and Methods: *Western Blot Analysis*," and the polyclonal anti-BMP-1 antibody, which recognizes the CUB2 domain shared by all splice variants, was purchased from Affinity Bioreagents. The BMP-1 antibody was used at 1:1000 for Western blots. To quantify band intensities on Western blots, the Kodak 1D software was used as described in Chapter 3 under "Materials and Methods: Far-*Western Blotting Analysis*."

CHAPTER 5. FUTURE DIRECTIONS AND FINAL DISCUSSION

FUTURE DIRECTIONS

Other candidate interactions identified in the LOX yeast two-hybrid screen

Placental lactogen (PL)

To begin to verify the LOX-PL interaction detected in the yeast two-hybrid screen, we have used far-Western blotting with the GST-LOX fusion proteins as described in Chapter 3 for FN. The results demonstrated that the PL hormone preferentially bound to LOX residues 169-348, which was consistent with the data from the yeast direct interaction assays (Figure 50). Currently, we are using GST pull-downs, co-immunoprecipitations (Co-IP), and solid phase binding assays to further characterize this the LOX-PL interaction. In addition, we have obtained purified human growth hormone (GH) and prolactin (PRL) to determine if LOX can bind to the other members of this important hormone family.

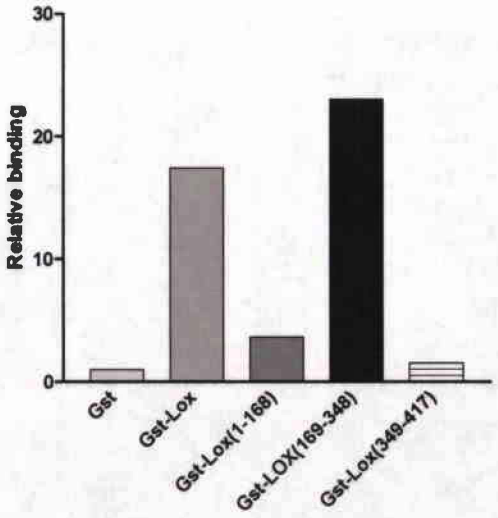

Figure 50: Data from far-Western blotting analysis that demonstrated the binding of PL to LOX residues 169-348. As described in Chapter 3, the net band intensities due to PL binding to each GST-fusion protein were each normalized against the results for GST alone.

We have performed preliminary solid phase binding assays using purified PL and GH as ligands for immobilized GST-LOX protein fragments, and the reverse with GST-LOX ligand and immobilized hormones. For these first experiments, the background was high, but binding of PL and GH to GST-LOX was significantly above GST alone, and the binding of GST-LOX to PL and GH was significantly above binding to the BSA negative control (Figure 51). These experiments were the first to show any evidence that LOX may also be able to interact with GH, which we had theorized to be possible based on the high homology between PL and GH. These solid phase binding assays are currently being repeated with a wider range of ligand concentrations and with more stringent washing conditions.

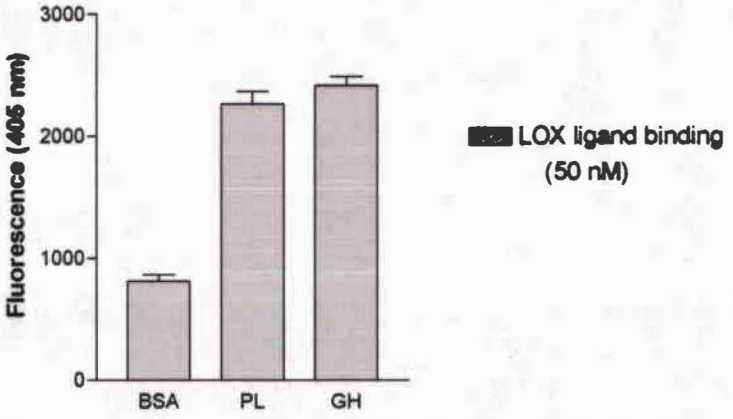

Figure 51. Solid phase binding assay data measuring the amount of bound GST-LOX ligand in wells coated with equal amounts of PL, GH, or BSA. The GST-LOX was incubated in the microplate wells at a 50 nM concentration. The assay was performed with the same protocol as described in Chapter 3.

The only human tissue that expresses PL under normal conditions is the placenta, but high expression of PL seen in human breast, testicular, and ovarian tumors [255, 258, 265]. Given the results of previous studies on LOX's role in breast cancers, we will investigate coincident expression of PL and LOX in various breast cancer cell lines and primary tumors. Initially, we performed Western blot analysis to characterize the expression of PL from a panel of breast cancer cells lines, with a chorioncarcinoma cell line (JAR) as a positive control for PL

expression (Figure 52). Higher levels of secreted PL was detected in the two highly-invasive cell lines, Hs578T and MD-MB231, which coincidently are the cell lines that express high levels of LOX [117]. We are currently attempting to perform Co-IP experiments with PL and LOX from the cell media of MD-MB231.

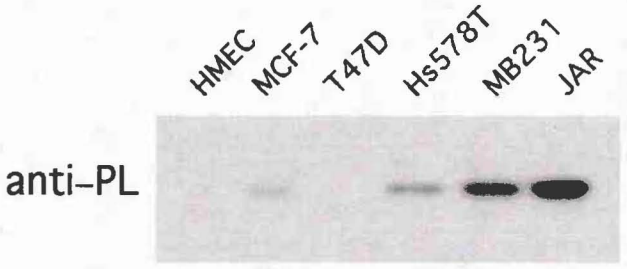

Figure 52. Western blot measuring PL protein levels in the media of various breast cancer cell lines. Equal amounts of total media protein from post-confluent CCM were loaded in each lane. The two invasive breast cancer lines, Hs578T and MB231, secrete the most PL. Normal human mammary epithelial cells (HMEC) had no detected PL. The chorioncarcinoma JAR cell line served as the positive control for PL expression.

There has been a report of *in vitro* LOX inactivation of basic fibroblast growth factor (bFGF), where LOX oxidizes bFGF to cause the formation of cross-linked bFGF aggregates. We wanted to determine if LOX could oxidize PL in a similar way. In conditions identical to H. Kagan's experiment with bFGF [120], we measured the activity of purified bovine LOX with purified human PL as a substrate. The activity assays were performed as described above for FN, with Amplex Red, horseradish peroxidase, and parallel 500 μM BAPN controls. The results showed that PL was not oxidized by LOX in statistically significant quantities (data not shown).

We plan to perform IF co-localization of LOX and PL in breast cancer tissue sections. Commercial tissue arrays containing multiple breast tumor sections will be acquired and immunofluorescent co-staining will be performed. We plan to look for specific tumor microenvironments with co-localized PL and LOX, and statistically evaluate the percentage of tumors that have co-expressed PL and LOX. In addition, we will evaluate the stages of these

cancers, examining any correlation of LOX and PL expression, localization, and tumor aggressiveness.

The relationship between LOX and PL is less developed than for LOX and FN. We need to finish the experiments detailed above for PL, and evaluate all the data to develop a working hypothesis about the significance of PL binding to LOX. We also need to expand the previous studies to further confirm GH and PRL interactions with LOX. Once we characterize these interactions, we plan to look at LOX's affects on PL/GH/PRL cell signaling through their membrane receptors and cytoplasmic signaling pathways. Additionally, it would be interesting to look at how PL, GH, and PRL function in the LOX knockout mouse model. We will also examine the role of these interactions in breast carcinogenesis using the breast cancer cell line panel. Much work still needs to be done to confirm and characterize the LOX-PL interaction, but it has a high potential for yielding valuable novel information about the biological roles of these proteins in normal development and human disease.

Fibulin-1 (FBLN1)

The characterization of a possible LOX-FBLN1 interaction is relatively incomplete, as much more work needs to be done. However, some preliminary data has been generated, and we have taken steps to advance this research project. We obtained an antibody for FBLN1, and performed Western blot analysis of human dermal fibroblasts, that detected FBLN1 secretion into the cell media. Since this result showed the presence of both LOX and FBLN1 in the same cell media, we performed preliminary Co-IPs of LOX and FBLN1 from the cultured fibroblast CCM (Figure 53). FBLN1 was co-immunoprecipitated with both anti-LOX and anti-FN antibody, but not with the negative control antibody. FBLN1's binding affinity for FN has been well characterized [395-397], and it was not surprising to detect this interaction. We will repeat these experiments with additional controls, as well attempt to Co-IP LOX with the anti-FBLN1 antibody. In addition, we have initiated a collaboration with the investigators responsible for characterizing the FBLN1 knockout mouse, Dr. Mon-li Chu and Dr. Gunter Kostka. They have

provided us with the full-length FBLN1 cDNA, from which we will clone mammalian expression constructs. We can use these to produce a recombinant FBLN1 protein in order to characterize it's binding to LOX with more quantitative methods.

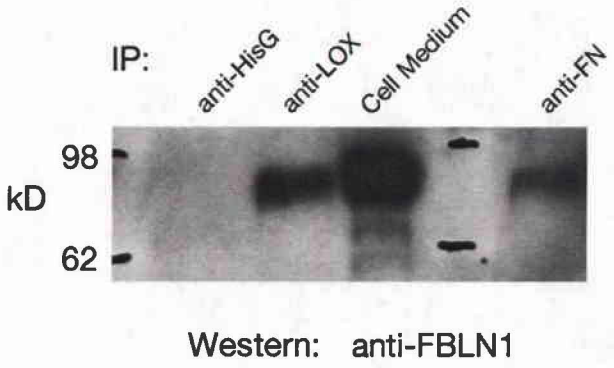

Figure 53. Western blot showing a Co-IP of FBLN1 with LOX from cultured fibroblast cell media. 5 µg of anti-LOX antibody, anti-FN, or anti-HisG antibody (as a negative control) were incubated with 5 mL of fibroblast CCM. Proteins were precipitated with protein A-agarose resin, and the presence of bound FBLN1 was detected by Western blotting with an anti-FBLN1 antibody.

Despite the fact that little is known about the role of FBLN1and we have not followed-up this detected interaction, we believe it remains important to characterize LOX's association with FBLN1. Recently, FBLN5 has been shown to bind to LOXL, possibly to direct the LOXL enzyme to areas of elastic fiber synthesis [213]. Given the detection of LOX in proximity with multiple basement membranes (described in Chapter 4), and since FBLN1 has been associated with various basement membranes [272, 278, 283], we could hypothesize that FBLN1 may be the structural protein that holds LOX in these extracellular structures. To test this, we will obtain tissues from the FBLN1 knockout mouse in order to perform immunostaining with our anti-LOX antibody. If LOX fails to localize to the same basement membranes in these FBLN1-null tissues, it will provide evidence that the FBLN1-LOX interaction may function in basement membrane synthesis or maintenance.

LOX-like enzymes and FN

As discussed in Chapter 1, the lysyl oxidase enzymes share several homologous domains, including the copper binding site, the active site where the LTQ is formed, and the CRL domain at the C-terminus. From this study, the interaction between LOX and FN seems to be located to one of these homologous regions, which raises the question: is the FN interaction specific to LOX only, or does FN also interact with any other lysyl oxidase family members? These family members have overlapping expression in many tissues and have been shown to have the capability to oxidize some of the same ECM substrates, but there is strong evidence suggesting they have individual biological functions. The lysyl oxidase family members differ in their N-terminal protein domain structure, and LOX is the only member to have been detected as an active enzyme inside the cell. The LOX and LOXL knockout mice show a very different phenotype: the LOX knockout mice die quickly after birth due to cardiovascular aneurysms [121, 122], but the LOXL knockout mice were viable, but showed elastic fiber disruption in the skin and lung, and in the pelvic organs of pregnant females [213]. Not as much is known about the LOXL2, LOXL3, and LOXL4 proteins, but LOXL2 has been the only LOX-like enzyme to be implicated in carcinogenesis [117, 398, 399]. By experimentally determining whether FN interacts with any of the LOX-like enzymes, we aim to identify additional functional similarities and differences among this enzyme family.

From preliminary studies of yeast direct co-transformations after the two-hybrid screen, it appeared that the FN C-terminal fragment could interact with LOXL but not LOXL2. However, the interaction results from the yeast cells have not always been consistent, and we must use caution when interpreting them. Since we have generated LOXL and LOXL2 antibodies, but have not yet purified significant amounts of recombinant LOXL or LOXL2, it would be worthwhile to perform some Co-IP assays from cultured cells. The purification of LOXL and LOXL2 proteins are projects currently being pursued in our laboratory, and when successful, solid phase binding assays will be used to quantitatively measure the binding affinities.

To analyze the FN-null MEFs for alterations in either LOXL or LOXL2, we ran Western blots with equal amounts of CCM and cell lysate proteins from the FN+/- and FN-/- cultures. From the Western using our anti-LOXL antibody, we did not detect the active form in either FN+/- or FN-/-, but only the 60-kD full-length proLOXL in the CCM and in larger quantities in the cell lysate fractions (Figure 54). In FN-null conditions, there was a significant decrease in the amount of proLOXL in the CCM and a corresponding increase of proLOXL in the cell lysates. From the Western blot using our anti-LOXL2 antibody, we observed a novel 40-kD LOXL2 band in the CCM of FN-/- cells but not in FN+/- cells, even with longer exposures (Figure 54). In the cell lysates, equal amounts of full-length LOXL2 was observed. Not much is known regarding proteolytic processing and activation of LOXL2, but in at least one study, LOXL2 has been shown to be processed into a smaller form of approximately 70 kD [398]. We have detected this 40-kD LOXL2 band only once before in MDCK canine kidney epithelial cells (unpublished observations), but we have no evidence to say if it is an alternative spliced form of LOXL2 or a proteolytic fragment of the full-length LOXL2. If the removal of FN from these MEF cultures results in the processing of LOXL2, it would be the opposite affect as the decreased processing of LOX shown in Chapter 4. In addition, because the level of BMP-1 remains constant in the FN-/- cells, it may be possible that BMP-1 is either not responsible for LOXL2 processing or that FN inhibits the BMP-1 processing of LOXL2. A more detailed analysis should be performed to investigate these hypotheses.

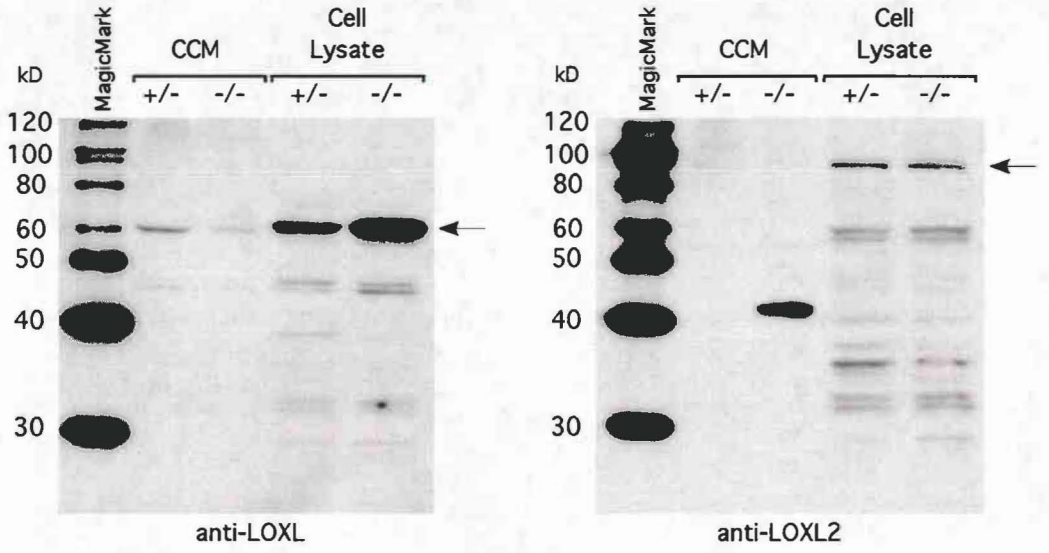

Figure 54. Western blots for LOXL and LOXL2 with protein sample extracted from the FN+/- and FN-/- MEFs. 15 µg of proteins from either CCM or cell lysate were loaded into each lane. The arrows designate the full-length LOXL and LOXL2 proteins, based on their predicted molecular weights. Many bands are observed in the cell lysate lanes due to a non-specific binding of the secondary antibodies.

Downstream of the FN-LOX interaction

Our current experiments are focused on identifying downstream effects of the FN-LOX interaction *in vivo*. The best method to determine these effects is by specifically disrupting the FN-LOX interaction without inhibiting the other functions of either protein. One approach to accomplish this requires using our protein binding assays to narrow down the FN-binding site on the LOX protein. However, this may prove difficult, as some of our experimental evidence suggested multiple binding sites. In the yeast direct interactions, FN bound to non-overlapping LOX fragments, and in the solid phase binding assays we observed that FN bound to several LOX domains at a greater-than-zero affinity. From the data, it appears the primary binding site for FN is between LOX amino acids 169-348, but the CRL domain seemed to contribute to the stability of the interaction. It is possible that the 3 dimensional folding of LOX allows multiple

sites of interaction with FN, and together they result in the high-affinity binding represented by the ~3 nM affinity constant. Primarily, we should be able to accomplish this using site-directed mutagenesis of the bacterial-expressed GST-LOX, and then screen for decreases in binding affinity using the solid phase binding assays. Our main reason for determining the primary FN-binding site on LOX is to design small disruptor peptides that could specifically compete for the binding sites, thus specifically inhibiting the FN-LOX interaction in cell based assays to address the functional significance.

The other option for disrupting the FN-LOX interaction is to use pharmacological methods to screen large compound libraries to discover small chemical inhibitors of this interaction. We would first need to develop a reliable high-throughput FN-LOX binding assay to use to screen thousands of chemicals, but the chemical libraries are already available for use. This screening for small chemical inhibitors can be more effective than searching for disrupting peptides, as FN may have a complicated binding site that relies on several stretches of amino acids or on the 3 dimensional conformation that a single peptide cannot duplicate. Screening for chemical inhibitors also does not require any additional information about the protein interaction, and the resultant inhibitors can be rapidly tested for therapeutic value (as discussed below in "*Implications for human disease*").

By specifically inhibiting the FN-LOX interaction, rather than inhibiting LOX's catalytic activity or removing the entire proteins, we can more clearly determine the biological role of the interaction. Using disrupting peptides or chemical inhibitors, we could determine if the interaction directly allows the proteolytic activation of LOX *in vivo*. They would also allow us to measure any change in cell phenotype, such as cell proliferation, migration, or differentiation, which may be a downstream consequence of the FN-LOX interaction. Changes in cellular phenotype and ECM assembly would allow us to make more accurate assessments of the *in vivo* biological functions of the FN-LOX interaction.

Previous studies have shown that types I and III collagens fail to form fibrils in the absence of FN, but the reasons for this failure were not explored in depth. Our data suggests that this is at least partially due to a dramatically decreased activation of the LOX enzyme, and in order to test this, we plan to examine the extent of collagen intermolecular crosslinking in the FN-/- cultures. Since we have shown a putative relationship between BMP-1 protease and FN, we will also examine whether tropocollagen molecules are processed on the C-terminus in FN-/- cultures, since this is also accomplished by BMP-1. We will also determine if by adding exogenous FN, or exogenous LOX enzyme, collagen assembly can be rescued. In addition, we will examine the extent of the elastin crosslinking and assembly in these MEF cultures to determine if there is a relationship between the FN matrix and elastic fiber assembly.

We have shown with *in vitro* activity assays that when the LOX enzyme is bound to the FN matrix, it remains in an active conformation. This was demonstrated with a 1,5-diaminopentane substrate, which is a very small molecule used at high concentrations. The accessibility of the active site of FN-bound LOX by larger substrate molecules like type I collagen and tropoelastin still needs to be determined. By mutating the residues surrounding peptidyl lysines, it has been demonstrated that the electrostatic charge of the substrate highly influenced the efficiency of oxidation by LOX [105]. This suggests a more complex interaction between LOX and its peptidyl lysine substrates than with 1,5-diaminopentane.

We plan to perform *in vitro* LOX activity assays with tropoelastin and collagen substrates in the presence of FN. Thus far, we have been unsuccessful with these experiments due to very limited amounts of tissue-purified LOX, since higher concentrations of the substrates need to be used to compensate for the low LOX concentrations. Unfortunately, there have been technical limitations to using higher concentrations of collagen and tropoelastin substrates. Purified type I collagen is solubilized with 0.02 N acetic acid, and increasing amounts of this substrate in the LOX activity assay reaction buffer leads to a sharp decrease in pH, which seems to lead to a decrease in LOX activity. In contrast, using increasing amounts of tissue-purified tropoelastin is prohibitively expensive. However, we recently acquired a bacterial strain containing a

tropoelastin expression construct [103], and after purifying recombinant tropoelastin from these bacteria, we will repeat the LOX activity assays with much higher substrate concentrations to determine if FN-bound LOX can oxidize tropoelastin.

FINAL DISCUSSION

The overall goals of this dissertation were to characterize unexplored mechanisms of ECM assembly and regulation by identifying novel LOX-interacting proteins and determining the biological significance of these interactions. LOX is a copper-dependent amine oxidase essential to mammalian development, and misregulation of its expression and activity has been implicated in many human pathologies. By elucidating new molecular mechanisms of how LOX functions and how it is regulated, we aimed to better understand how LOX contributes to human development and how abnormal LOX contributes to the progression of human diseases.

To accomplish our goals, we designed a series of Specific Aims, which were presented in Chapter 1 under "Dissertation Hypothesis and Specific Aims." By using a powerful screening technique like yeast two-hybrid, we planned to identify several potential LOX-interacting proteins. After verifying and characterizing these interactions with various molecular biology methods, we aimed to explore their biological roles *in vitro* and *in vivo*. These were ambitious aims, and when the LOX yeast two-hybrid screen yielded a long list of positive proteins, we chose to focus on our highest priority LOX-interacting protein, FN.

The results of this study demonstrate that FN binds the LOX protein, and provide evidence suggesting this as a novel mechanism by which FN may regulate the proteolytic activation of LOX and contribute to the assembly of the collagen matrix. Co-distribution of FN and collagen matrices have long been noted [287, 288], and recent studies have shown that the assembly of types I and III collagen into fibers is dependent on the preceding polymerization of

FN [323, 324]. FN has been also shown to directly bind to several collagen molecules [332, 400, 401], but this binding does not fully explain the role of FN in the regulation of the collagen matrix assembly. LOX initiates the covalent cross-linking of fibrillar collagen molecules, which is the final enzymatic step in the formation of mature collagen fibers. Therefore, the discovery that FN can directly bind LOX and regulates LOX's activation provides an attractive explanation about how FN can guide the formation of mature collagen fibrils.

From the solid phase binding assays, we demonstrated that LOX's binding affinity for cFN was much greater than its affinity for pFN. While the categorization of plasma versus cellular FN may have been originally based on solubility, another discovered difference is that pFN circulates in a compact, inactive conformation with concealed binding sites. In contrast, cFN is usually present in an activated, open conformation [290, 291]. LOX's higher affinity for cFN may be due to this open conformation through a revealed LOX-binding site. The other main difference between pFN and cFN, which arise from the same gene, is alternative splicing. It is also possible that the alternative spliced domain IIICS, which is found more prevalently in cFN molecules [290, 298], contains the LOX-binding site. Each FN cDNA fragment isolated in the yeast two-hybrid screen contained the middle 192 bp IIICS segment, and two also contained the 75 bp IIICS segment.

The FN-binding domain within the LOX protein appears to be located between residues 169 and 348, but the C-terminal CRL domain may play a role in stabilizing the interaction. In the solid phase binding assays, we detected binding of cFN to GST-$LOX_{169\text{-}348}$, but at a significantly lower affinity than GST-LOX, which contains the CRL domain. By sequence, the CRL domain is homologous to the N-terminal extracellular domain of the Class 1 cytokine receptor superfamily [50, 78]. However, no function for LOX's CRL domain has previously been shown. Our results suggest this C-terminal domain may add stability to the protein interactions of LOX. In a separate experiment, we tested if our polyclonal anti-LOX antibody, which was designed against amino acid residues 176-197, could be used to block the interaction with cFN. No significant

decrease in cFN binding was measured when GST-LOX was preincubated with excess amounts of antibody, which is consistent with the site of interaction being closer to LOX's CRL domain.

Confocal microscopy of FN and LOX immunofluorescent co-staining in fibroblast cultures showed a pattern of continuous FN matrix with overlapping punctated LOX. At this high resolution, the distribution of LOX seen in the fibroblast extracellular matrix appeared non-random and co-localized with the FN meshwork at many points. Co-expression of LOX and FN was also observed in a wide range of normal human tissues. Primarily, we observed high-resolution co-localization around areas of heavy ECM deposition, such as in blood vessels and connective tissue, but we also noted co-localization at the basal surface of epithelial cells in the esophagus and kidney. In the placenta, stomach, colon, and adipose tissues, LOX staining was observed in a pattern suggesting localization to basement membranes. There have been no previous reports of LOX being associated with basement membranes, although FN localization to basement membranes has been well characterized [287, 288, 347]. Since type I, II, and III collagens and elastin are not typical components of the basal lamina, this localization of LOX suggests that LOX may have yet unidentified functions or substrates. The striated pattern of staining of LOX in cardiac and skeletal muscle was surprising, but may possibly result from LOX's presence in the extracellular T tubules, which invaginate into the muscle cell. Also intriguing was the LOX staining at the intercalated discs of the cardiac myocytes, as these are cell-cell junctions that do not contain fibrillar collagens or elastin. The localization of LOX in these muscles needs to be investigated in more detail.

The results of *in vitro* activity assays suggest that cFN is probably not a substrate for the LOX enzyme. These results do not exclude the possibility that lysyl residues within FN are oxidized by LOX under specific conditions *in vivo*. Covalent cross-links in the FN matrix have not been commonly reported, except in conditions of wound healing and clotting when FN is cross-linked to fibrin by factor VIIIa (transglutaminase) [402-404]. The data showed that cFN-bound LOX retains its enzyme activity towards 1,5-diaminopentane, which indicates LOX remains in an active conformation. This ability to bind an active LOX enzyme at specific

domains may allow the FN matrix to provide specific microenvironments to guide the cross-linking of ECM molecules. A detailed characterization of how these complex molecular interactions influence collagen and elastic fiber assembly remains to be determined.

To analyze LOX in the absence of FN *in vivo*, we obtained embryonic fibroblasts generated from FN-null mice and their heterozygous siblings. As detected by Western analysis, the quantity of 30-kD LOX in the cell culture media was decreased by approximately 90% in FN-null conditions. We also observed a corresponding increase of the 45-kD unprocessed proLOX in the cell media of the FN-/- cells, and an increase of a 40-kD band, which does appear in the FN+/- lanes in longer exposures. This 40-kD protein remains unidentified, but it may represent an intermediate processed form of LOX or perhaps a novel embryonic-specific LOX variant. Consistent with the dramatic decrease in 30-kD LOX seen by Western analysis, LOX amine oxidase activity assays demonstrated that LOX activity in FN-/- cell media was approximately 10% of what was measured in FN+/- media. The relatively equal amounts of active BMP-1 protease in FN+/- and FN-/- culture media indicated that the decrease in LOX activation was not due to an absence of BMP-1 protease levels. These data suggest that the presence of FN is critical for LOX activation *in vivo*.

Proteolytic activation of LOX has been shown to be primarily performed by BMP-1/procollagen C-proteinase, which is also responsible for cleaving the C-terminal end of type I, II, and III procollagens [86, 88, 405]. No evidence for a relationship between FN and BMP-1 has previously been shown, however our results suggest that there may be some connection. Perhaps FN facilitates LOX processing by bringing BMP-1 into close proximity, or by altering the conformation of proLOX to make the cleavage site more accessible. FN may even act as a guiding scaffold to bring LOX, BMP-1, and procollagen molecules together in areas of collagen fiber assembly. The FN-binding site on the type I collagen molecule is about 250 residues N-terminal from the lysyl substrate of LOX, which is 10 residues N-terminal to the BMP-1 cleavage site [406]. Further studies may elucidate the molecular mechanism by which FN regulates LOX

processing, and how the FN-LOX interaction affects the assembly of the extracellular matrix in various tissues.

Current working hypothesis

Based upon the findings of this research, and upon the current understanding of ECM biology, our working hypothesis is: *the FN matrix acts as a scaffold for the proteolytic activation of the LOX enzyme, and guides LOX's activity to microenvironments of ECM assembly.* Figure 55 illustrates the proposed functional relationship between LOX, FN, BMP-1, and collagen.

Because of the high affinity of cFN for LOX, and based on the Co-IP assays showing that LOX and FN can circulate bound together in cell media, it is possible that a high portion of extracellular LOX remains bound to soluble FN molecules. When these soluble FN molecules are incorporated into the FN matrix, LOX may remain bound and therefore be directed to specific areas in the extracellular space. Given the evidence for FN's necessity for collagen assembly, we believe that FN specifically binds LOX to guide its catalytic activity towards the ends of collagen molecules, where the intermolecular crosslinks are located. In addition, there are indications that the processing of LOX by BMP-1 might not occur immediately after secretion. We believe FN regulates this activation process - proLOX may be held in the ECM by FN until LOX enzyme activity is required. Our approaches to test these working hypotheses involve exploring collagen and LOX synthesis in the absence of FN, testing the relationship between BMP-1 and FN, and screening for inhibitors of the FN-LOX interaction.

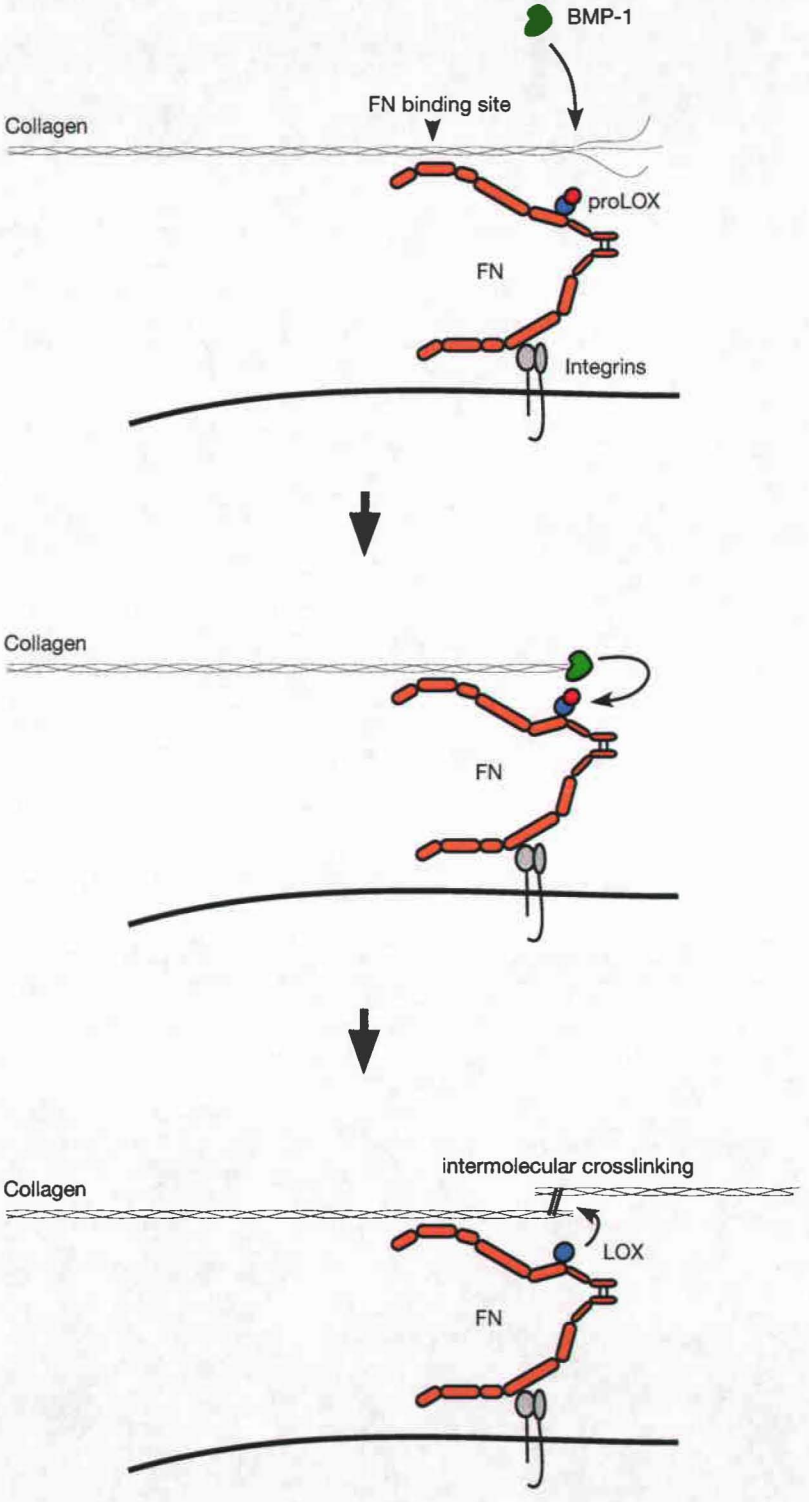

Figure 55. Diagram of our current working hypothesis to explain the complex interactions between FN, LOX, collagen, and BMP-1. The FN protein regulates the assembly of the collagen matrix by allowing proteolytic cleavage of proLOX and providing a scaffolding for its activity against other ECM molecules. Proteins are drawn approximately to scale.

Implications for human disease

As reviewed in Chapter 1, there are several diseases that are associated with an upregulation of LOX activity, including cardiovascular diseases, fibrosis, and tumor invasion. In cardiovascular diseases such as atherosclerosis and restenosis, the accumulation of crosslinked ECM molecules contributes greatly to the irreversibility of the diseases [160, 170]. Increased LOX activity has been shown to cause increased migration of vascular smooth muscle cells [115], which migrate into the neointima during the progression of atherosclerosis [168, 407]. Fibrosis, which can affect almost every tissue in the body, is characterized by an abnormal synthesis of ECM components, principally collagen fibers. This cannot occur without a parallel increase in lysyl oxidase enzyme activity [236]. Breast cancer cell invasion is promoted by increased LOX activity [117], although the mechanisms have not been discovered. *If specific inhibitors of the FN-LOX interaction can be designed, they may be useful as molecular therapeutics to prevent the proteolytic activation of the LOX enzyme and/or the guidance of LOX crosslinking activity in these diseases.* If such therapeutics could be applied locally, such as topically to dermal wounds or integrated into drug-eluting stents, then they may avoid problems of widespread toxicity. In addition, by being specifically designed for LOX's proteolytic activation, the non-specific inhibition of LOX-like enzymes and other amine oxidases would be avoided.

Perhaps some of the consequences of the increased or reduced FN observed in physiological and pathological conditions may be attributed to the resultant change in LOX activity. Decreased cFN has been shown to cause defective wound healing [288, 408, 409], malignant transformation [288, 355], and impaired vasculogenesis [296, 297]. In contrast, increased levels of FN have been shown to occur following such pathologies as myocardial infarctions [410], rheumatic diseases [411], fibrotic diseases of the kidney [412] and lung [413], and in vascular diseases [289]. It would be beneficial to determine the downstream effects of these pathologic changes in FN levels on the activation of the LOX enzyme. In addition, in diseases where alternative FN splicing may play a role, such as the oncofetal FN form present in

certain cancers and fibrotic diseases, it will be important to investigate the effects on the interaction with LOX and LOX's proteolytic activation.

The discovery of this FN-LOX interaction has the potential to lead us to understand the mechanism by which LOX contributes to a range of heritable and acquired human diseases and provide avenues to explore promising new molecular therapies for many serious human diseases. We will continue to characterize this critical relationship, and explore the development of such therapeutics.

REFERENCES

1. Geiger, B.J., H. Steenbock, and H.T. Parsons, *Lathyrism in the rat.* J Nutr, 1933. **6**: p. 427-442.

2. Schilling, E.D. and F.M. Strong, *Isolation, structure, and synthesis of a lathyrus factor from L. odoratus.* J Am Chem Soc, 1954. **76**: p. 2848.

3. Gross, J., C.I. Levene, and S. Orloff, *Fragility and extractable collagen in the lathyritic chick embryo. An assay for lathyrogenic agents.* Proc Soc Exp Biol Med, 1960. **105**: p. 148-51.

4. Levene, C.I. and J. Gross, *Alterations in state of molecular aggregation of collagen induced in chick embryos by beta-aminopropionitrile (lathyrus factor).* J Exp Med, 1959. **110**: p. 771-90.

5. Page, R.C. and E.P. Benditt, *Molecular diseases of connective and vascular tissues. I. The source of lathyritic collagen.* Lab Invest, 1966. **15**(11): p. 1643-51.

6. Tanzer, M.L., *Experimental lathyrism.* Int Rev Connect Tissue Res, 1965. **3**: p. 91-112.

7. Piez, K.A., *Cross-linking of collagen and elastin.* Annu Rev Biochem, 1968. **37**: p. 547-70.

8. Bornstein, P., A.H. Kang, and K.A. Piez, *The nature and location of intramolecular cross-links in collagen.* Proc Natl Acad Sci U S A, 1966. **55**(2): p. 417-24.

9. Kang, A.H., K.A. Piez, and J. Gross, *Characterization of the alpha-chains of chick skin collagen and the nature of the NH2-terminal cross-link region.* Biochemistry, 1969. **8**(9): p. 3648-55.

10. Page, R.C. and E.P. Benditt, *Molecular diseases of connective and vascular tissues. 3. The aldehyde content of normal and lathyritic soluble collagen.* Lab Invest, 1968. **18**(2): p. 124-30.

11. Miller, E.J., et al., *The biosynthesis of elastin cross-links. The effect of copper deficiency and a lathyrogen.* J Biol Chem, 1965. **240**(9): p. 3623-7.

12. O'Dell, B.L., et al., *Inhibition of the biosynthesis of the cross-links in elastin by a lathyrogen.* Nature, 1966. **209**(21): p. 401-2.

13. Miller, E.J., et al., *Investigation of the nature of the intermediates involved in desmosine biosynthesis.* Biochem Biophys Res Commun, 1967. **26**(2): p. 132-7.

14. Hart, E.B., et al., *Iron in nutrition. VII. Copper as a supplement to iron for hemoglobin building in the rat.* J Biol Chem, 1928. **77**: p. 797-812.

15. O'Dell, B.L., et al., *Connective tissue defect in the chick resulting from copper deficiency.* Proc Soc Exp Biol Med, 1961. **108**: p. 402-5.

16. Shields, G.S., et al., *Studies on copper metabolism. 32. Cardiovascular lesions in copper-deficient swine.* Am J Pathol, 1962. **41**: p. 603-21.

17. Coulson, W.F. and W.H. Carnes, *Cardiovascular Studies On Copper-Deficient Swine. V. The Histogenesis Of The Coronary Artery Lesions.* Am J Pathol, 1963. **43**: p. 945-54.

18. Starcher, B., C.H. Hill, and G. Matrone, *Importance Of Dietary Copper In The Formation Of Aortic Elastin.* J Nutr, 1964. **82**: p. 318-22.

19. Savage, J.E., et al., *Comparison of copper deficiency and lathyrism in turkey poults.* J Nutr, 1966. **88**(1): p. 15-25.

20. O'Dell, B.L., et al., *Composition of aortic tissue from copper-deficient chicks.* J Nutr, 1966. **88**(1): p. 9-14.

21. Bird, D.W., J.E. Savage, and B.L. O'Dell, *Effect of copper deficiency and inhibitors on the amine oxidase activity of chick tissues.* Proc Soc Exp Biol Med, 1966. **123**(1): p. 250-4.

22. Chou, W.S., J.E. Savage, and B.L. O'Dell, *Role of copper in biosynthesis of intramolecular cross-links in chick tendon collagen.* J Biol Chem, 1969. **244**(21): p. 5785-9.

23. Kim, C.S. and C.H. Hill, *The interrelationship of dietary copper and amine oxidase in the formation of elastin.* Biochem Biophys Res Commun, 1966. **24**(3): p. 395-400.

24. Yamada, H. and K.T. Yasunobu, *Monoamine oxidase. II. Copper, one of the prosthetic groups of plasma monoamine oxidase.* J Biol Chem, 1962. **237**: p. 3077-82.

25. Hill, J.M. and P.J. Mann, *The inhibition of pea-seedling diamine oxidase by chelating agents.* Biochem J, 1962. **85**: p. 198-207.

26. Buffoni, F. and H. Blaschko, *Benzylamine Oxidase And Histaminase: Purification And Crystallization Of An Enzyme From Pig Plasma.* Proc R Soc Lond B Biol Sci, 1964. **161**: p. 153-67.

27. Pinnell, S.R. and G.R. Martin, *The cross-linking of collagen and elastin: enzymatic conversion of lysine in peptide linkage to alpha-aminoadipic-delta-semialdehyde (allysine) by an extract from bone.* Proc Natl Acad Sci U S A, 1968. **61**(2): p. 708-16.

28. Siegel, R.C. and G.R. Martin, *Collagen cross-linking. Enzymatic synthesis of lysine-derived aldehydes and the production of cross-linked components.* J Biol Chem, 1970. **245**(7): p. 1653-8.

29. Martin, G.R., et al., *Chemistry and molecular biology of the intercellular matrix, Vol 1.*, ed. E.A. Balazs. Vol. 1. 1970, New York: Academic Press.

30. Siegel, R.C., S.R. Pinnell, and G.R. Martin, *Cross-linking of collagen and elastin. Properties of lysyl oxidase.* Biochemistry, 1970. **9**(23): p. 4486-92.

31. Narayanan, A.S., R.C. Siegel, and G.R. Martin, *On the inhibition of lysyl oxidase by -aminopropionitrile.* Biochem Biophys Res Commun, 1972. **46**(2): p. 745-51.

32. Mondovi, B., ed. *Structure and functions of amine oxidases*. 1985, CRC Press, Inc.: Boca Raton.

33. Pietrangeli, P. and B. Mondovi, *Amine oxidases and tumors.* Neurotoxicology, 2004. **25**(1-2): p. 317-24.

34. Massey, V., *The chemical and biological versatility of riboflavin.* Biochem Soc Trans, 2000. **28**(4): p. 283-96.

35. Binda, C., A. Mattevi, and D.E. Edmondson, *Structure-function relationships in flavoenzyme-dependent amine oxidations: a comparison of polyamine oxidase and monoamine oxidase.* J Biol Chem, 2002. **277**(27): p. 23973-6.

36. Hartmann, C. and W.S. McIntire, *Amine-oxidizing quinoproteins.* Methods Enzymol, 1997. **280**: p. 98-150.

37. Buffoni, F. and G. Ignesti, *The copper-containing amine oxidases: biochemical aspects and functional role.* Mol Genet Metab, 2000. **71**(4): p. 559-64.

38. Dove, J.E. and J.P. Klinman, *Trihydroxyphenylalanine quinone (TPQ) from copper amine oxidases and lysyl tyrosylquinone (LTQ) from lysyl oxidase.* Adv Protein Chem, 2001. **58**: p. 141-74.

39. Mure, M., *Tyrosine-derived quinone cofactors.* Acc Chem Res, 2004. **37**(2): p. 131-9.

40. Brazeau, B.J., B.J. Johnson, and C.M. Wilmot, *Copper-containing amine oxidases. Biogenesis and catalysis; a structural perspective.* Arch Biochem Biophys, 2004. **428**(1): p. 22-31.

41. Csiszar, K., *Lysyl oxidases: a novel multifunctional amine oxidase family.* Prog Nucleic Acid Res Mol Biol, 2001. **70**: p. 1-32.

42. Narayanan, A.S., R.C. Siegel, and G.R. Martin, *Stability and purification of lysyl oxidase.* Arch Biochem Biophys, 1974. **162**(1): p. 231-7.

43. Harris, E.D., et al., *Connective tissue amine oxidase. II. Purification and partial characterization of lysyl oxidase from chick aorta.* Biochim Biophys Acta, 1974. **341**(2): p. 332-44.

44. Kagan, H.M., et al., *Catalytic activity of aortic lysyl oxidase in an insoluble enzyme-substrate complex.* Biochim Biophys Acta, 1974. **365**(1): p. 223-34.

45. Stassen, F.L., *Properties of highly purified lysyl oxidase from embryonic chick cartilage.* Biochim Biophys Acta, 1976. **438**(1): p. 49-60.

46. Shieh, J.J. and K.T. Yasunobu, *Purification and properties of lung lysyl oxidase, a copper-enzyme.* Adv Exp Med Biol, 1976. **74**: p. 447-63.

47. Siegel, R.C. and J.C. Fu, *Collagen cross-linking. Purification and substrate specificity of lysyl oxidase.* J Biol Chem, 1976. **251**(18): p. 5779-85.

48. Jordan, R.E., et al., *Studies on lysyl oxidase of bovine ligamentum nuchae and bovine aorta.* Adv Exp Med Biol, 1977. **79**: p. 531-42.

49. Kenyon, K., et al., *A novel human cDNA with a predicted protein similar to lysyl oxidase maps to chromosome 15q24-q25.* J Biol Chem, 1993. **268**(25): p. 18435-7.

50. Kim, Y., C.D. Boyd, and K. Csiszar, *A new gene with sequence and structural similarity to the gene encoding human lysyl oxidase.* J Biol Chem, 1995. **270**(13): p. 7176-82.

51. Saito, H., et al., *Regulation of a novel gene encoding a lysyl oxidase-related protein in cellular adhesion and senescence.* J Biol Chem, 1997. **272**(13): p. 8157-60.

52. Jourdan-Le Saux, C., et al., *The human lysyl oxidase-related gene (LOXL2) maps between markers D8S280 and D8S278 on chromosome 8p21.2-p21.3.* Genomics, 1998. **51**(2): p. 305-7.

53. Jang, W., et al., *Comparative sequence of human and mouse BAC clones from the mnd2 region of chromosome 2p13.* Genome Res, 1999. **9**(1): p. 53-61.

54. Maki, J.M. and K.I. Kivirikko, *Cloning and characterization of a fourth human lysyl oxidase isoenzyme.* Biochem J, 2001. **355**(Pt 2): p. 381-7.

55. Huang, Y., et al., *Cloning and characterization of a human lysyl oxidase-like 3 gene (hLOXL3).* Matrix Biol, 2001. **20**(2): p. 153-7.

56. Jourdan-Le Saux, C., et al., *Central nervous system, uterus, heart, and leukocyte expression of the loxl3 gene, encoding a novel lysyl oxidase-like protein.* Genomics, 2001. **74**(2): p. 211-8.

57. Asuncion, L., et al., *A novel human lysyl oxidase-like gene (LOXL4) on chromosome 10q24 has an altered scavenger receptor cysteine rich domain.* Matrix Biol, 2001. **20**(7): p. 487-91.

58. Maki, J.M., H. Tikkanen, and K.I. Kivirikko, *Cloning and characterization of a fifth human lysyl oxidase isoenzyme: the third member of the lysyl oxidase-related subfamily with four scavenger receptor cysteine-rich domains.* Matrix Biol, 2001. **20**(7): p. 493-6.

59. Hamalainen, E.R., et al., *Molecular cloning of human lysyl oxidase and assignment of the gene to chromosome 5q23.3-31.2.* Genomics, 1991. **11**(3): p. 508-16.

60. Mariani, T.J., et al., *The complete derived amino acid sequence of human lysyl oxidase and assignment of the gene to chromosome 5 (extensive sequence homology with the murine ras recision gene).* Matrix, 1992. **12**(3): p. 242-8.

61. Boyd, C.D., et al., *The size heterogeneity of human lysyl oxidase mRNA is due to alternate polyadenylation site and not alternate exon usage.* Mol Biol Rep, 1995. **21**(2): p. 95-103.

62. Resnick, D., A. Pearson, and M. Krieger, *The SRCR superfamily: a family reminiscent of the Ig superfamily.* Trends Biochem Sci, 1994. **19**(1): p. 5-8.

63. Parsons, M.R., et al., *Crystal structure of a quinoenzyme: copper amine oxidase of Escherichia coli at 2 A resolution.* Structure, 1995. **3**(11): p. 1171-84.

64. Kumar, V., et al., *Crystal structure of a eukaryotic (pea seedling) copper-containing amine oxidase at 2.2 A resolution.* Structure, 1996. **4**(8): p. 943-55.

65. Wilce, M.C., et al., *Crystal structures of the copper-containing amine oxidase from Arthrobacter globiformis in the holo and apo forms: implications for the biogenesis of topaquinone.* Biochemistry, 1997. **36**(51): p. 16116-33.

66. Li, R., J.P. Klinman, and F.S. Mathews, *Copper amine oxidase from Hansenula polymorpha: the crystal structure determined at 2.4 A resolution reveals the active conformation.* Structure, 1998. **6**(3): p. 293-307.

67. Gacheru, S.N., et al., *Structural and catalytic properties of copper in lysyl oxidase.* J Biol Chem, 1990. **265**(31): p. 19022-7.

68. Ryvkin, F. and F.T. Greenaway, *A peptide model of the copper-binding region of lysyl oxidase.* J Inorg Biochem, 2004. **98**(8): p. 1427-35.

69. Kosonen, T., et al., *Incorporation of copper into lysyl oxidase.* Biochem J, 1997. **327**(Pt 1): p. 283-9.

70. Wang, S.X., et al., *A crosslinked cofactor in lysyl oxidase: redox function for amino acid side chains.* Science, 1996. **273**(5278): p. 1078-84.

71. Tang, C. and J.P. Klinman, *The catalytic function of bovine lysyl oxidase in the absence of copper.* J Biol Chem, 2001. **6**: p. 6.

72. Levene, C.I., *Structural requirements for lathyrogenic agents.* J Exp Med, 1961. **114**: p. 295-310.

73. Williamson, P.R., et al., *Reactivity of a functional carbonyl moiety in bovine aortic lysyl oxidase. Evidence against pyridoxal 5'-phosphate.* Biochem J, 1986. **235**(2): p. 597-605.

74. Williamson, P.R., et al., *Evidence for pyrroloquinolinequinone as the carbonyl cofactor in lysyl oxidase by absorption and resonance Raman spectroscopy.* J Biol Chem, 1986. **261**(35): p. 16302-5.

75. Wang, S.X., et al., *Characterization of the native lysine tyrosylquinone cofactor in lysyl oxidase by Raman spectroscopy.* J Biol Chem, 1997. **272**(46): p. 28841-4.

76. Stites, T.E., A.E. Mitchell, and R.B. Rucker, *Physiological importance of quinoenzymes and the O-quinone family of cofactors.* J Nutr, 2000. **130**(4): p. 719-27.

77. Akagawa, M. and K. Suyama, *Characterization of a model compound for the lysine tyrosylquinone cofactor of lysyl oxidase.* Biochem Biophys Res Commun, 2001. **281**(1): p. 193-9.

78. Bazan, J.F., *Structural design and molecular evolution of a cytokine receptor superfamily.* Proc Natl Acad Sci U S A, 1990. **87**(18): p. 6934-8.

79. Kucha, J.A. and D.M. Dooley, *Cloning, sequence analysis, and characterization of the 'lysyl oxidase' from Pichia pastoris.* J Inorg Biochem, 2001. **83**(2-3): p. 193-204.

80. Lee, M., et al., *Crystallization of Pichia pastoris lysyl oxidase.* Acta Crystallogr D Biol Crystallogr, 2002. **58**(Pt 12): p. 2177-9.

81. Duff, A.P., et al., *The crystal structure of Pichia pastoris lysyl oxidase.* Biochemistry, 2003. **42**(51): p. 15148-57.

82. Trackman, P.C., et al., *Post-translational glycosylation and proteolytic processing of a lysyl oxidase precursor.* J Biol Chem, 1992. **267**(12): p. 8666-71.

83. Krebs, C.J. and S.A. Krawetz, *Lysyl oxidase copper-talon complex: a model.* Biochim Biophys Acta, 1993. **1202**(1): p. 7-12.

84. Uzel, M.I., et al., *Molecular events that contribute to lysyl oxidase enzyme activity and insoluble collagen accumulation in osteosarcoma cell clones.* J Bone Miner Res, 2000. **15**(6): p. 1189-97.

85. Cronshaw, A.D., L.A. Fothergill-Gilmore, and D.J. Hulmes, *The proteolytic processing site of the precursor of lysyl oxidase.* Biochem J, 1995. **306**(Pt 1): p. 279-84.

86. Panchenko, M.V., et al., *Metalloproteinase activity secreted by fibrogenic cells in the processing of prolysyl oxidase. Potential role of procollagen C- proteinase.* J Biol Chem, 1996. **271**(12): p. 7113-9.

87. Kessler, E., et al., *Bone morphogenetic protein-1: the type I procollagen C-proteinase.* Science, 1996. **271**(5247): p. 360-2.

88. Uzel, M.I., et al., *Multiple bone morphogenetic protein 1-related mammalian metalloproteinases process pro-lysyl oxidase at the correct physiological site and control lysyl oxidase activation in mouse embryo fibroblast cultures.* J Biol Chem, 2001. **276**(25): p. 22537-43.

89. Borel, A., et al., *Lysyl oxidase-like protein from bovine aorta. Isolation and maturation to an active form by bone morphogenetic protein-1.* J Biol Chem, 2001. **276**(52): p. 48944-9.

90. Siegel, R.C., *Biosynthesis of collagen crosslinks: increased activity of purified lysyl oxidase with reconstituted collagen fibrils.* Proc Natl Acad Sci U S A, 1974. **71**(12): p. 4826-30.

91. Siegel, R.C., *Collagen cross-linking. Synthesis of collagen cross-links in vitro with highly purified lysyl oxidase.* J Biol Chem, 1976. **251**(18): p. 5786-92.

92. Siegel, R.C., J.C. Fu, and Y. Chang, *Collagen cross-linking: the substrate specificity of lysyl oxidase.* Adv Exp Med Biol, 1976. **74**: p. 438-46.

93. Kagan, H.M., *Characterization and regulation of lysyl oxidase*, in *Biology of Extracellular Matrix*, R.P. Mecham, Editor. 1986, Academic Press: Orlando. p. 321-389.

94. Reiser, K., R.J. McCormick, and R.B. Rucker, *Enzymatic and nonenzymatic cross-linking of collagen and elastin.* Faseb J, 1992. **6**(7): p. 2439-49.

95. Knott, L. and A.J. Bailey, *Collagen cross-links in mineralizing tissues: a review of their chemistry, function, and clinical relevance.* Bone, 1998. **22**(3): p. 181-7.

96. Kagan, H.M. and P. Cai, *Isolation of active site peptides of lysyl oxidase.* Methods Enzymol, 1995. **258**: p. 122-32.

97. Gibson, M.A., et al., *Further characterization of proteins associated with elastic fiber microfibrils including the molecular cloning of MAGP-2 (MP25).* J Biol Chem, 1996. **271**(2): p. 1096-103.

98. Ramirez, F., *Pathophysiology of the microfibril/elastic fiber system: introduction.* Matrix Biol, 2000. **19**(6): p. 455-6.

99. Kielty, C.M., et al., *Fibrillin-rich microfibrils: elastic biopolymers of the extracellular matrix.* J Muscle Res Cell Motil, 2002. **23**(5-6): p. 581-96.

100. Trask, T.M., et al., *Interaction of tropoelastin with the amino-terminal domains of fibrillin-1 and fibrillin-2 suggests a role for the fibrillins in elastic fiber assembly.* J Biol Chem, 2000. **275**(32): p. 24400-6.

101. Kozel, B.A., C.H. Ciliberto, and R.P. Mecham, *Deposition of tropoelastin into the extracellular matrix requires a competent elastic fiber scaffold but not live cells.* Matrix Biol, 2004. **23**(1): p. 23-34.

102. Kagan, H.M. and K.A. Sullivan, *Lysyl oxidase: preparation and role in elastin biosynthesis.* Methods Enzymol, 1982. **82**(Pt A): p. 637-50.

103. Bedell-Hogan, D., et al., *Oxidation, cross-linking, and insolubilization of recombinant tropoelastin by purified lysyl oxidase.* J Biol Chem, 1993. **268**(14): p. 10345-50.

104. Rosenbloom, J., W.R. Abrams, and R. Mecham, *Extracellular matrix 4: the elastic fiber.* Faseb J, 1993. **7**(13): p. 1208-18.

105. Kagan, H.M. and W. Li, *Lysyl oxidase: properties, specificity, and biological roles inside and outside of the cell.* J Cell Biochem, 2003. **88**(4): p. 660-72.

106. Molnar, J., et al., *Structural and functional diversity of lysyl oxidase and the LOX-like proteins.* Biochim Biophys Acta, 2003. **1647**(1-2): p. 220-4.

107. Li, W., et al., *Localization and activity of lysyl oxidase within nuclei of fibrogenic cells.* Proc Natl Acad Sci U S A, 1997. **94**(24): p. 12817-22.

108. Nellaiappan, K., et al., *Fully processed lysyl oxidase catalyst translocates from the extracellular space into nuclei of aortic smooth-muscle cells.* J Cell Biochem, 2000. **79**(4): p. 576-82.

109. Hayashi, K., et al., *Comparative immunocytochemical localization of lysyl oxidase (LOX) and the lysyl oxidase-like (LOXL) proteins: changes in the expression of LOXL during development and growth of mouse tissues.* J Mol Histol, 2004. **in press**.

110. Li, P.A., et al., *Up-regulation and altered distribution of lysyl oxidase in the central nervous system of mutant SOD1 transgenic mouse model of amyotrophic lateral sclerosis.* Brain Res Mol Brain Res, 2004. **120**(2): p. 115-22.

111. Kagan, H.M., et al., *Histone H1 is a substrate for lysyl oxidase and contains endogenous sodium borotritide-reducible residues.* Biochem Biophys Res Commun, 1983. **115**(1): p. 186-92.

112. Giampuzzi, M., R. Oleggini, and A. Di Donato, *Demonstration of in vitro interaction between tumor suppressor lysyl oxidase and histones H1 and H2: definition of the regions involved.* Biochim Biophys Acta, 2003. **1647**(1-2): p. 245-51.

113. Mello, M.L., et al., *Modulation of ras transformation affecting chromatin supraorganization as assessed by image analysis.* Exp Cell Res, 1995. **220**(2): p. 374-82.

114. Lazarus, H.M., et al., *Induction of human monocyte motility by lysyl oxidase.* Matrix Biol, 1995. **14**(9): p. 727-31.

115. Li, W., et al., *Hydrogen peroxide-mediated, lysyl oxidase-dependent chemotaxis of vascular smooth muscle cells.* J Cell Biochem, 2000. **78**(4): p. 550-7.

116. Nelson, J.M., R.F. Diegelmann, and I.K. Cohen, *Effect of beta-aminopropionitrile and ascorbate on fibroblast migration.* Proc Soc Exp Biol Med, 1988. **188**(3): p. 346-52.

117. Kirschmann, D.A., et al., *A molecular role for lysyl oxidase in breast cancer invasion.* Cancer Res, 2002. **62**(15): p. 4478-83.

118. Giampuzzi, M., et al., *Lysyl oxidase activates the transcription activity of human collagene III promoter. Possible involvement of Ku antigen.* J Biol Chem, 2000. **275**(46): p. 36341-9.

119. Jeay, S., et al., *Lysyl oxidase inhibits ras-mediated transformation by preventing activation of NF-kappa B.* Mol Cell Biol, 2003. **23**(7): p. 2251-63.

120. Li, W., et al., *Lysyl oxidase oxidizes basic fibroblast growth factor and inactivates its mitogenic potential.* J Cell Biochem, 2003. **88**(1): p. 152-64.

121. Hornstra, I.K., et al., *Lysyl oxidase is required for vascular and diaphragmatic development in mice.* J Biol Chem, 2002. **7**: p. 7.

122. Maki, J.M., et al., *Inactivation of the lysyl oxidase gene Lox leads to aortic aneurysms, cardiovascular dysfunction, and perinatal death in mice.* Circulation, 2002. **106**(19): p. 2503-9.

123. Olivares, M. and R. Uauy, *Copper as an essential nutrient.* Am J Clin Nutr, 1996. **63**(5): p. 791S-6S.

124. Klevay, L.M., *Cardiovascular disease from copper deficiency--a history.* J Nutr, 2000. **130**(2S Suppl): p. 489S-492S.

125. Strausak, D., et al., *Copper in disorders with neurological symptoms: Alzheimer's, Menkes, and Wilson diseases.* Brain Res Bull, 2001. **55**(2): p. 175-85.

126. Brewer, G.J., *Copper in medicine.* Curr Opin Chem Biol, 2003. **7**(2): p. 207-12.

127. Tapiero, H., D.M. Townsend, and K.D. Tew, *Trace elements in human physiology and pathology. Copper.* Biomed Pharmacother, 2003. **57**(9): p. 386-98.

128. Bertinato, J. and M.R. L'Abbe, *Maintaining copper homeostasis: regulation of copper-trafficking proteins in response to copper deficiency or overload.* J Nutr Biochem, 2004. **15**(6): p. 316-22.

129. Barceloux, D.G., *Copper.* J Toxicol Clin Toxicol, 1999. **37**(2): p. 217-30.

130. Hotz, C., et al., *Assessment of the trace element status of individuals and populations: the example of zinc and copper.* J Nutr, 2003. **133**(5 Suppl 1): p. 1563S-8S.

131. Gaetke, L.M. and C.K. Chow, *Copper toxicity, oxidative stress, and antioxidant nutrients.* Toxicology, 2003. **189**(1-2): p. 147-63.

132. Shim, H. and Z.L. Harris, *Genetic defects in copper metabolism.* J Nutr, 2003. **133**(5 Suppl 1): p. 1527S-31S.

133. Keen, C.L., et al., *Effect of copper deficiency on prenatal development and pregnancy outcome.* Am J Clin Nutr, 1998. **67**(5 Suppl): p. 1003S-1011S.

134. Uauy, R., M. Olivares, and M. Gonzalez, *Essentiality of copper in humans.* Am J Clin Nutr, 1998. **67**(5 Suppl): p. 952S-959S.

135. Prohaska, J.R., *Development of copper deficiency in neonatal mice.* J Nutr Biochem, 1990. **1**(8): p. 415-9.

136. Allen, K.G. and L.M. Klevay, *Copper: an antioxidant nutrient for cardiovascular health.* Curr Opin Lipidol, 1994. **5**(1): p. 22-8.

137. Nath, R., *Copper deficiency and heart disease: molecular basis, recent advances and current concepts.* Int J Biochem Cell Biol, 1997. **29**(11): p. 1245-54.

138. Rucker, R.B., et al., *Copper, lysyl oxidase, and extracellular matrix protein cross-linking.* Am J Clin Nutr, 1998. **67**(5 Suppl): p. 996S-1002S.

139. Saari, J.T. and D.A. Schuschke, *Cardiovascular effects of dietary copper deficiency.* Biofactors, 1999. **10**(4): p. 359-75.

140. Saari, J.T., *Copper deficiency and cardiovascular disease: role of peroxidation, glycation, and nitration.* Can J Physiol Pharmacol, 2000. **78**(10): p. 848-55.

141. Hunsaker, H.A., M. Morita, and K.G. Allen, *Marginal copper deficiency in rats. Aortal morphology of elastin and cholesterol values in first-generation adult males.* Atherosclerosis, 1984. **51**(1): p. 1-19.

142. Hamilton, I.M., W.S. Gilmore, and J.J. Strain, *Marginal copper deficiency and atherosclerosis.* Biol Trace Elem Res, 2000. **78**(1-3): p. 179-89.

143. Smith-Mungo, L.I. and H.M. Kagan, *Lysyl oxidase: properties, regulation and multiple functions in biology.* Matrix Biol, 1998. **16**(7): p. 387-98.

144. Kuo, Y.M., et al., *The copper transporter CTR1 provides an essential function in mammalian embryonic development.* Proc Natl Acad Sci U S A, 2001. **98**(12): p. 6836-41.

145. Lee, J., J.R. Prohaska, and D.J. Thiele, *Essential role for mammalian copper transporter Ctr1 in copper homeostasis and embryonic development.* Proc Natl Acad Sci U S A, 2001. **98**(12): p. 6842-7.

146. Vulpe, C., et al., *Isolation of a candidate gene for Menkes disease and evidence that it encodes a copper-transporting ATPase.* Nat Genet, 1993. **3**(1): p. 7-13.

147. Mercer, J.F., et al., *Isolation of a partial candidate gene for Menkes disease by positional cloning.* Nat Genet, 1993. **3**(1): p. 20-5.

148. Tanzi, R.E., et al., *The Wilson disease gene is a copper transporting ATPase with homology to the Menkes disease gene.* Nat Genet, 1993. **5**(4): p. 344-50.

149. Bull, P.C., et al., *The Wilson disease gene is a putative copper transporting P-type ATPase similar to the Menkes gene.* Nat Genet, 1993. **5**(4): p. 327-37.

150. Das, S., et al., *Similar splicing mutations of the Menkes/mottled copper-transporting ATPase gene in occipital horn syndrome and the blotchy mouse.* Am J Hum Genet, 1995. **56**(3): p. 570-6.

151. Dierick, H.A., et al., *Immunocytochemical localization of the Menkes copper transport protein (ATP7A) to the trans-Golgi network.* Hum Mol Genet, 1997. **6**(3): p. 409-16.

152. Francis, M.J., et al., *A Golgi localization signal identified in the Menkes recombinant protein.* Hum Mol Genet, 1998. **7**(8): p. 1245-52.

153. Iwase, T., et al., *Localization of Menkes gene expression in the mouse brain; its association with neurological manifestations in Menkes model mice.* Acta Neuropathol (Berl), 1996. **91**(5): p. 482-8.

154. Barnes, N., et al., *The Copper-transporting ATPases, Menkes and Wilson Disease Proteins, Have Distinct Roles in Adult and Developing Cerebellum.* J Biol Chem, 2005. **280**(10): p. 9640-5.

155. Royce, P.M., J. Camakaris, and D.M. Danks, *Reduced lysyl oxidase activity in skin fibroblasts from patients with Menkes' syndrome.* Biochem J, 1980. **192**(2): p. 579-86.

156. Gacheru, S., et al., *Expression and accumulation of lysyl oxidase, elastin, and type I procollagen in human Menkes and mottled mouse fibroblasts.* Arch Biochem Biophys, 1993. **301**(2): p. 325-9.

157. Kuivaniemi, H., L. Peltonen, and K.I. Kivirikko, *Type IX Ehlers-Danlos syndrome and Menkes syndrome: the decrease in lysyl oxidase activity is associated with a corresponding deficiency in the enzyme protein.* Am J Hum Genet, 1985. **37**(4): p. 798-808.

158. Royce, P.M. and B. Steinmann, *Markedly reduced activity of lysyl oxidase in skin and aorta from a patient with Menkes' disease showing unusually severe connective tissue manifestations.* Pediatr Res, 1990. **28**(2): p. 137-41.

159. Tyagi, S.C., *Vasculogenesis and angiogenesis: extracellular matrix remodeling in coronary collateral arteries and the ischemic heart.* J Cell Biochem, 1997. **65**(3): p. 388-94.

160. Newby, A.C. and A.B. Zaltsman, *Fibrous cap formation or destruction--the critical importance of vascular smooth muscle cell proliferation, migration and matrix formation.* Cardiovasc Res, 1999. **41**(2): p. 345-60.

161. Arteaga-Solis, E., B. Gayraud, and F. Ramirez, *Elastic and collagenous networks in vascular diseases.* Cell Struct Funct, 2000. **25**(2): p. 69-72.

162. Raines, E.W., *The extracellular matrix can regulate vascular cell migration, proliferation, and survival: relationships to vascular disease.* Int J Exp Pathol, 2000. **81**(3): p. 173-82.

163. Jacob, M.P., et al., *Extracellular matrix remodeling in the vascular wall.* Pathol Biol (Paris), 2001. **49**(4): p. 326-32.

164. Camejo, G., et al., *The extracellular matrix on atherogenesis and diabetes-associated vascular disease.* Atheroscler Suppl, 2002. **3**(1): p. 3-9.

165. Barnes, M.J. and R.W. Farndale, *Collagens and atherosclerosis.* Exp Gerontol, 1999. **34**(4): p. 513-25.

166. Toborek, M. and S. Kaiser, *Endothelial cell functions. Relationship to atherogenesis.* Basic Res Cardiol, 1999. **94**(5): p. 295-314.

167. Taddei, S., et al., *Endothelial dysfunction in hypertension.* J Nephrol, 2000. **13**(3): p. 205-10.

168. Kraemer, R., *Regulation of cell migration in atherosclerosis.* Curr Atheroscler Rep, 2000. **2**(5): p. 445-52.

169. Poredos, P., *Endothelial dysfunction in the pathogenesis of atherosclerosis.* Int Angiol, 2002. **21**(2): p. 109-16.

170. Ruberg, F.L., J.A. Leopold, and J. Loscalzo, *Atherothrombosis: plaque instability and thrombogenesis.* Prog Cardiovasc Dis, 2002. **44**(5): p. 381-94.

171. Milewicz, D.M., Z. Urban, and C. Boyd, *Genetic disorders of the elastic fiber system.* Matrix Biol, 2000. **19**(6): p. 471-80.

172. Miller, F.J., Jr., *Aortic aneurysms: It's all about the stress.* Arterioscler Thromb Vasc Biol, 2002. **22**(12): p. 1948-9.

173. Daugherty, A. and L.A. Cassis, *Mouse models of abdominal aortic aneurysms.* Arterioscler Thromb Vasc Biol, 2004. **24**(3): p. 429-34.

174. Ruigrok, Y.M., G.J. Rinkel, and C. Wijmenga, *Genetics of intracranial aneurysms.* Lancet Neurol, 2005. **4**(3): p. 179-89.

175. Kagan, H.M., et al., *Ultrastructural immunolocalization of lysyl oxidase in vascular connective tissue.* J Cell Biol, 1986. **103**(3): p. 1121-8.

176. Baccarani-Contri, M., et al., *Localization of human placenta lysyl oxidase on human placenta, skin and aorta by immunoelectronmicroscopy.* Matrix, 1989. **9**(6): p. 428-36.

177. Wakasaki, H. and A. Ooshima, *Immunohistochemical localization of lysyl oxidase with monoclonal antibodies.* Lab Invest, 1990. **63**(3): p. 377-84.

178. Rodriguez, C., et al., *Low density lipoproteins downregulate lysyl oxidase in vascular endothelial cells and the arterial wall.* Arterioscler Thromb Vasc Biol, 2002. **22**(9): p. 1409-14.

179. Bank, R.A. and V.W. van Hinsbergh, *Lysyl oxidase: new looks on LOX.* Arterioscler Thromb Vasc Biol, 2002. **22**(9): p. 1365-6.

180. Raposo, B., et al., *High levels of homocysteine inhibit lysyl oxidase (LOX) and downregulate LOX expression in vascular endothelial cells.* Atherosclerosis, 2004. **177**(1): p. 1-8.

181. Herrera, V.M., et al., *Differential regulation of functional gene clusters in overt coronary artery disease in a transgenic atherosclerosis-hypertensive rat rodel.* Mol Med, 2002. **8**(7): p. 367-75.

182. Spears, J.R., et al., *Modulation by beta-aminopropionitrile of vessel luminal narrowing and structural abnormalities in arterial wall collagen in a rabbit model of conventional balloon angioplasty versus laser balloon angioplasty.* J Clin Invest, 1994. **93**(4): p. 1543-53.

183. Nuthakki, V.K., et al., *Lysyl oxidase expression in a rat model of arterial balloon injury.* J Vasc Surg, 2004. **40**(1): p. 123-9.

184. Bissell, M.J., et al., *The organizing principle: microenvironmental influences in the normal and malignant breast.* Differentiation, 2002. **70**(9-10): p. 537-46.

185. Ingber, D.E., *Cancer as a disease of epithelial-mesenchymal interactions and extracellular matrix regulation.* Differentiation, 2002. **70**(9-10): p. 547-60.

186. Radisky, D., J. Muschler, and M.J. Bissell, *Order and disorder: the role of extracellular matrix in epithelial cancer.* Cancer Invest, 2002. **20**(1): p. 139-53.

187. Stupack, D.G. and D.A. Cheresh, *Apoptotic cues from the extracellular matrix: regulators of angiogenesis.* Oncogene, 2003. **22**(56): p. 9022-9.

188. Shekhar, M.P., R. Pauley, and G. Heppner, *Host microenvironment in breast cancer development: extracellular matrix-stromal cell contribution to neoplastic phenotype of epithelial cells in the breast.* Breast Cancer Res, 2003. **5**(3): p. 130-5.

189. Stewart, D.A., C.R. Cooper, and R.A. Sikes, *Changes in extracellular matrix (ECM) and ECM-associated proteins in the metastatic progression of prostate cancer.* Reprod Biol Endocrinol, 2004. **2**(1): p. 2.

190. Sund, M., L. Xie, and R. Kalluri, *The contribution of vascular basement membranes and extracellular matrix to the mechanics of tumor angiogenesis.* Apmis, 2004. **112**(7-8): p. 450-62.

191. Sottile, J., *Regulation of angiogenesis by extracellular matrix.* Biochim Biophys Acta, 2004. **1654**(1): p. 13-22.

192. Kuivaniemi, H., et al., *Deficient production of lysyl oxidase in cultures of malignantly transformed human cells.* FEBS Lett, 1986. **195**(1-2): p. 261-4.

193. Contente, S., et al., *Expression of gene rrg is associated with reversion of NIH 3T3 transformed by LTR-c-H-ras.* Science, 1990. **249**(4970): p. 796-8.

194. Kenyon, K., et al., *Lysyl oxidase and rrg messenger RNA.* Science, 1991. **253**(5021): p. 802.

195. Giampuzzi, M., et al., *Down regulation of lysyl oxidase induced tumorigenic transformation in NRK-49F cells characterized by constitutive activation of Ras proto-oncogene.* J Biol Chem, 2001. **25**: p. 25.

196. Hamalainen, E.R., et al., *Quantitative polymerase chain reaction of lysyl oxidase mRNA in malignantly transformed human cell lines demonstrates that their low lysyl oxidase activity is due to low quantities of its mRNA and low levels of transcription of the respective gene.* J Biol Chem, 1995. **270**(37): p. 21590-3.

197. Ren, C., et al., *Reduced lysyl oxidase messenger RNA levels in experimental and human prostate cancer.* Cancer Res, 1998. **58**(6): p. 1285-90.

198. Perou, C.M., et al., *Molecular portraits of human breast tumours.* Nature, 2000. **406**(6797): p. 747-52.

199. Kaneda, A., et al., *Identification of silencing of nine genes in human gastric cancers.* Cancer Res, 2002. **62**(22): p. 6645-50.

200. Csiszar, K., et al., *Somatic mutations of the lysyl oxidase gene on chromosome 5q23.1 in colorectal tumors.* Int J Cancer, 2002. **97**(5): p. 636-42.

201. Giampuzzi, M., R. Oleggini, and A. Di Donato, *Altered adhesion features and signal transduction in NRK-49F cells transformed by down-regulation of lysyl oxidase.* Biochim Biophys Acta, 2003. **1647**(1-2): p. 239-44.

202. Kirschmann, D.A., et al., *Differentially expressed genes associated with the metastatic phenotype in breast cancer.* Breast Cancer Res Treat, 1999. **55**(2): p. 127-36.

203. Kaneda, A., et al., *Lysyl oxidase is a tumor suppressor gene inactivated by methylation and loss of heterozygosity in human gastric cancers.* Cancer Res, 2004. **64**(18): p. 6410-5.

204. Palamakumbura, A.H., et al., *The propeptide domain of lysyl oxidase induces phenotypic reversion of ras-transformed cells.* J Biol Chem, 2004. **279**(39): p. 40593-600.

205. Zatterstrom, U.K., et al., *Collagen XVIII/endostatin structure and functional role in angiogenesis.* Cell Struct Funct, 2000. **25**(2): p. 97-101.

206. Debelle, L. and A.M. Tamburro, *Elastin: molecular description and function.* Int J Biochem Cell Biol, 1999. **31**(2): p. 261-72.

207. Tassabehji, M., et al., *An elastin gene mutation producing abnormal tropoelastin and abnormal elastic fibres in a patient with autosomal dominant cutis laxa.* Hum Mol Genet, 1998. **7**(6): p. 1021-8.

208. Zhang, M.C., et al., *Cutis laxa arising from frameshift mutations in exon 30 of the elastin gene (ELN).* J Biol Chem, 1999. **274**(2): p. 981-6.

209. Rodriguez-Revenga, L., et al., *A novel elastin gene mutation resulting in an autosomal dominant form of cutis laxa.* Arch Dermatol, 2004. **140**(9): p. 1135-9.

210. Loeys, B., et al., *Homozygosity for a missense mutation in fibulin-5 (FBLN5) results in a severe form of cutis laxa.* Hum Mol Genet, 2002. **11**(18): p. 2113-8.

211. Markova, D., et al., *Genetic heterogeneity of cutis laxa: a heterozygous tandem duplication within the fibulin-5 (FBLN5) gene.* Am J Hum Genet, 2003. **72**(4): p. 998-1004.

212. de Schepper, S., et al., *Cutis laxa of the autosomal recessive type in a consanguineous family.* Eur J Dermatol, 2003. **13**(6): p. 529-33.

213. Liu, X., et al., *Elastic fiber homeostasis requires lysyl oxidase-like 1 protein.* Nat Genet, 2004. **36**(2): p. 178-82.

214. Khakoo, A., et al., *Congenital cutis laxa and lysyl oxidase deficiency.* Clin Genet, 1997. **51**(2): p. 109-14.

215. Safdar, K. and E.R. Schiff, *Alcohol and hepatitis C.* Semin Liver Dis, 2004. **24**(3): p. 305-15.

216. Gabele, E., D.A. Brenner, and R.A. Rippe, *Liver fibrosis: signals leading to the amplification of the fibrogenic hepatic stellate cell.* Front Biosci, 2003. **8**: p. d69-77.

217. Chatziantoniou, C., et al., *Progression and regression in renal vascular and glomerular fibrosis.* Int J Exp Pathol, 2004. **85**(1): p. 1-11.

218. Klahr, S., *Progression of chronic renal disease.* Heart Dis, 2001. **3**(3): p. 205-9.

219. Moncrieff, J., M.M. Lindsay, and F.G. Dunn, *Hypertensive heart disease and fibrosis.* Curr Opin Cardiol, 2004. **19**(4): p. 326-31.

220. Bouros, D., et al., *Association of malignancy with diseases causing interstitial pulmonary changes.* Chest, 2002. **121**(4): p. 1278-89.

221. Khalil, N. and R. O'Connor, *Idiopathic pulmonary fibrosis: current understanding of the pathogenesis and the status of treatment.* Cmaj, 2004. **171**(2): p. 153-60.

222. Thannickal, V.J., et al., *Mechanisms of pulmonary fibrosis.* Annu Rev Med, 2004. **55**: p. 395-417.

223. Denton, C.P. and C.M. Black, *Scleroderma--clinical and pathological advances.* Best Pract Res Clin Rheumatol, 2004. **18**(3): p. 271-90.

224. Steen, V.D., *Occupational scleroderma.* Curr Opin Rheumatol, 1999. **11**(6): p. 490-4.

225. Harris, M.L. and A. Rosen, *Autoimmunity in scleroderma: the origin, pathogenetic role, and clinical significance of autoantibodies.* Curr Opin Rheumatol, 2003. **15**(6): p. 778-84.

226. Marek, A., et al., *TGF-beta (transforming growth factor-beta) in chronic inflammatory conditions - a new diagnostic and prognostic marker?* Med Sci Monit, 2002. **8**(7): p. RA145-51.

227. Branton, M.H. and J.B. Kopp, *TGF-beta and fibrosis.* Microbes Infect, 1999. **1**(15): p. 1349-65.

228. Trivedy, C., et al., *The upregulation of lysyl oxidase in oral submucous fibrosis and squamous cell carcinoma.* J Oral Pathol Med, 1999. **28**(6): p. 246-51.

229. Desmouliere, A., et al., *Extracellular matrix deposition, lysyl oxidase expression, and myofibroblastic differentiation during the initial stages of cholestatic fibrosis in the rat.* Lab Invest, 1997. **76**(6): p. 765-78.

230. Di Donato, A., et al., *Lysyl oxidase expression and collagen cross-linking during chronic adriamycin nephropathy.* Nephron, 1997. **76**(2): p. 192-200.

231. Decitre, M., et al., *Lysyl oxidase-like protein localizes to sites of de novo fibrinogenesis in fibrosis and in the early stromal reaction of ductal breast carcinomas.* Lab Invest, 1998. **78**(2): p. 143-51.

232. Streichenberger, N., et al., *Constrictive bronchiolitis obliterans. Characterisation of fibrogenesis and lysyl oxidase expression patterns.* Virchows Arch, 2001. **439**(1): p. 78-84.

233. Tzortzaki, E.G., et al., *Expression of FACIT collagens XII and XIV during bleomycin-induced pulmonary fibrosis in mice.* Anat Rec, 2003. **275A**(2): p. 1073-80.

234. Tsuda, T., et al., *Post-ischemic myocardial fibrosis occurs independent of hemodynamic changes.* Cardiovasc Res, 2003. **59**(4): p. 926-33.

235. Franklin, T.J., *Therapeutic approaches to organ fibrosis.* Int J Biochem Cell Biol, 1997. **29**(1): p. 79-89.

236. Kagan, H.M., *Intra- and extracellular enzymes of collagen biosynthesis as biological and chemical targets in the control of fibrosis.* Acta Trop, 2000. **77**(1): p. 147-52.

237. Luban, J. and S.P. Goff, *The yeast two-hybrid system for studying protein-protein interactions.* Curr Opin Biotechnol, 1995. **6**(1): p. 59-64.

238. Young, K.H., *Yeast two-hybrid: so many interactions, (in) so little time.* Biol Reprod, 1998. **58**(2): p. 302-11.

239. Fashena, S.J., I. Serebriiskii, and E.A. Golemis, *The continued evolution of two-hybrid screening approaches in yeast: how to outwit different preys with different baits.* Gene, 2000. **250**(1-2): p. 1-14.

240. Toby, G.G. and E.A. Golemis, *Using the yeast interaction trap and other two-hybrid-based approaches to study protein-protein interactions.* Methods, 2001. **24**(3): p. 201-17.

241. Serebriiskii, I. and J.K. Joung, *Yeast and bacterial two-hybrid selection systems for studying protein-protein interactions*, in *Protein-protein interactions*, E. Golemis, Editor. 2002, Cold Spring Harbor Laboratory Press: Cold Spring Harbor. p. 93-142.

242. Joung, J.K., E.I. Ramm, and C.O. Pabo, *A bacterial two-hybrid selection system for studying protein-DNA and protein-protein interactions.* Proc Natl Acad Sci U S A, 2000. **97**(13): p. 7382-7.

243. Shioda, T., et al., *A green fluorescent protein-reporter mammalian two-hybrid system with extrachromosomal maintenance of a prey expression plasmid: application to interaction screening.* Proc Natl Acad Sci U S A, 2000. **97**(10): p. 5220-4.

244. Goodyear, C.S. and G.J. Silverman, *Phage-display approaches for the study of protein-protein interactions*, in *Protein-protein interactions*, E. Golemis, Editor. 2002, Cold Spring Harbor Laboratory Press: Cold Spring Harbor. p. 143-165.

245. James, P., J. Halladay, and E.A. Craig, *Genomic libraries and a host strain designed for highly efficient two-hybrid selection in yeast.* Genetics, 1996. **144**(4): p. 1425-36.

246. Hieber, A.D., et al., *Detection of elastin in the human fetal membranes: proposed molecular basis for elasticity.* Placenta, 1997. **18**(4): p. 301-12.

247. Casey, M.L. and P.C. MacDonald, *Lysyl oxidase (ras recision gene) expression in human amnion: ontogeny and cellular localization.* J Clin Endocrinol Metab, 1997. **82**(1): p. 167-72.

248. Hein, S., et al., *Lysyl oxidases: expression in the fetal membranes and placenta.* Placenta, 2001. **22**(1): p. 49-57.

249. Legrain, P., J. Wojcik, and J.M. Gauthier, *Protein--protein interaction maps: a lead towards cellular functions.* Trends Genet, 2001. **17**(6): p. 346-52.

250. Handwerger, S., *Clinical counterpoint: the physiology of placental lactogen in human pregnancy.* Endocr Rev, 1991. **12**(4): p. 329-36.

251. Walker, W.H., et al., *The human placental lactogen genes: structure, function, evolution and transcriptional regulation.* Endocr Rev, 1991. **12**(4): p. 316-28.

252. Gertler, A. and J. Djiane, *Mechanism of ruminant placental lactogen action: molecular and in vivo studies.* Mol Genet Metab, 2002. **75**(3): p. 189-201.

253. Barrera-Saldana, H.A., *Growth hormone and placental lactogen: biology, medicine and biotechnology.* Gene, 1998. **211**(1): p. 11-8.

254. Handwerger, S. and M. Freemark, *The roles of placental growth hormone and placental lactogen in the regulation of human fetal growth and development.* J Pediatr Endocrinol Metab, 2000. **13**(4): p. 343-56.

255. Corbacho, A.M., G. Martinez De La Escalera, and C. Clapp, *Roles of prolactin and related members of the prolactin/growth hormone/placental lactogen family in angiogenesis.* J Endocrinol, 2002. **173**(2): p. 219-38.

256. Forsyth, I.A. and M. Wallis, *Growth hormone and prolactin--molecular and functional evolution.* J Mammary Gland Biol Neoplasia, 2002. **7**(3): p. 291-312.

257. Takeda, T., et al., *Participation of JAK, STAT and unknown proteins in human placental lactogen-induced signaling: a unique signaling pathway different from prolactin and growth hormone.* J Endocrinol, 1997. **153**(1): p. R1-3.

258. Goffin, V. and P.A. Kelly, *The prolactin/growth hormone receptor family: structure/function relationships.* J Mammary Gland Biol Neoplasia, 1997. **2**(1): p. 7-17.

259. Yamauchi, T., et al., *Growth hormone and prolactin stimulate tyrosine phosphorylation of insulin receptor substrate-1, -2, and -3, their association with p85 phosphatidylinositol 3-kinase (PI3-kinase), and concomitantly PI3-kinase activation via JAK2 kinase.* J Biol Chem, 1998. **273**(25): p. 15719-26.

260. Biener, E., et al., *Ovine placental lactogen-induced heterodimerization of ovine growth hormone and prolactin receptors in living cells is demonstrated by fluorescence resonance energy transfer microscopy and leads to prolonged phosphorylation of signal transducer and activator of transcription (STAT)1 and STAT3.* Endocrinology, 2003. **144**(8): p. 3532-40.

261. Harper, M.E., H.A. Barrera-Saldana, and G.F. Saunders, *Chromosomal localization of the human placental lactogen-growth hormone gene cluster to 17q22-24.* Am J Hum Genet, 1982. **34**(2): p. 227-34.

262. Barsh, G.S., P.H. Seeburg, and R.E. Gelinas, *The human growth hormone gene family: structure and evolution of the chromosomal locus.* Nucleic Acids Res, 1983. **11**(12): p. 3939-58.

263. Hirt, H., et al., *The human growth hormone gene locus: structure, evolution, and allelic variations.* DNA, 1987. **6**(1): p. 59-70.

264. Elkins, P.A., et al., *Ternary complex between placental lactogen and the extracellular domain of the prolactin receptor.* Nat Struct Biol, 2000. **7**(9): p. 808-15.

265. van Garderen, E. and J.A. Schalken, *Morphogenic and tumorigenic potentials of the mammary growth hormone/growth hormone receptor system.* Mol Cell Endocrinol, 2002. **197**(1-2): p. 153-65.

266. Latham, C., et al., *Frequent co-amplification of two different regions on 17q in aneuploid breast carcinomas.* Cancer Genet Cytogenet, 2001. **127**(1): p. 16-23.

267. Argraves, W.S., et al., *Fibulin, a novel protein that interacts with the fibronectin receptor beta subunit cytoplasmic domain.* Cell, 1989. **58**(4): p. 623-9.

268. Timpl, R., et al., *Fibulins: a versatile family of extracellular matrix proteins.* Nat Rev Mol Cell Biol, 2003. **4**(6): p. 479-89.

269. Chu, M.L. and T. Tsuda, *Fibulins in development and heritable disease.* Birth Defects Res C Embryo Today, 2004. **72**(1): p. 25-36.

270. Zhang, H.Y., M. Lardelli, and P. Ekblom, *Sequence of zebrafish fibulin-1 and its expression in developing heart and other embryonic organs.* Dev Genes Evol, 1997. **207**(5): p. 340-351.

271. Barth, J.L., et al., *Identification of chicken and C. elegans fibulin-1 homologs and characterization of the C. elegans fibulin-1 gene.* Matrix Biol, 1998. **17**(8-9): p. 635-46.

272. Spence, S.G., et al., *Fibulin is localized at sites of epithelial-mesenchymal transitions in the early avian embryo.* Dev Biol, 1992. **151**(2): p. 473-84.

273. Zhang, H.Y., et al., *The extracellular matrix glycoproteins BM-90 and tenascin are expressed in the mesenchyme at sites of endothelial-mesenchymal conversion in the embryonic mouse heart.* Differentiation, 1993. **52**(3): p. 211-20.

274. Miosge, N., et al., *The extracellular matrix proteins fibulin-1 and fibulin-2 in the early human embryo.* Histochem J, 1996. **28**(2): p. 109-16.

275. Roark, E.F., et al., *The association of human fibulin-1 with elastic fibers: an immunohistological, ultrastructural, and RNA study.* J Histochem Cytochem, 1995. **43**(4): p. 401-11.

276. Zhang, H.Y., et al., *Fibulin-1 and fibulin-2 expression during organogenesis in the developing mouse embryo.* Dev Dyn, 1996. **205**(3): p. 348-64.

277. Argraves, W.S., et al., *Fibulin is an extracellular matrix and plasma glycoprotein with repeated domain structure.* J Cell Biol, 1990. **111**(6 Pt 2): p. 3155-64.

278. Kluge, M., et al., *Characterization of a novel calcium-binding 90-kDa glycoprotein (BM-90) shared by basement membranes and serum.* Eur J Biochem, 1990. **193**(3): p. 651-9.

279. Kostka, G., et al., *Perinatal lethality and endothelial cell abnormalities in several vessel compartments of fibulin-1-deficient mice.* Mol Cell Biol, 2001. **21**(20): p. 7025-34.

280. Visconti, R.P., et al., *Codistribution analysis of elastin and related fibrillar proteins in early vertebrate development.* Matrix Biol, 2003. **22**(2): p. 109-21.

281. Sasaki, T., et al., *Tropoelastin binding to fibulins, nidogen-2 and other extracellular matrix proteins.* FEBS Lett, 1999. **460**(2): p. 280-4.

282. Tran, H., et al., *Human fibulin-1D: molecular cloning, expression and similarity with S1-5 protein, a new member of the fibulin gene family.* Matrix Biol, 1997. **15**(7): p. 479-93.

283. Pan, T.C., et al., *Sequence of extracellular mouse protein BM-90/fibulin and its calcium-dependent binding to other basement-membrane ligands.* Eur J Biochem, 1993. **215**(3): p. 733-40.

284. Adam, S., et al., *Binding of fibulin-1 to nidogen depends on its C-terminal globular domain and a specific array of calcium-binding epidermal growth factor-like (EG) modules.* J Mol Biol, 1997. **272**(2): p. 226-36.

285. Debeer, P., et al., *The fibulin-1 gene (FBLN1) is disrupted in a t(12;22) associated with a complex type of synpolydactyly.* J Med Genet, 2002. **39**(2): p. 98-104.

286. Toren, A., et al., *MYH9 spectrum of autosomal-dominant giant platelet syndromes: unexpected association with fibulin-1 variant-D inactivation.* Am J Hematol, 2003. **74**(4): p. 254-62.

287. Mosher, D.F., *Fibronectin*. Biology of Extracellular Matrix: A Series. 1989, San Diego: Academic Press.

288. Hynes, R.O., *Fibronectins*. 1990, New York: Springer-Verlag.

289. Magnusson, M.K. and D.F. Mosher, *Fibronectin: structure, assembly, and cardiovascular implications.* Arterioscler Thromb Vasc Biol, 1998. **18**(9): p. 1363-70.

290. Pankov, R. and K.M. Yamada, *Fibronectin at a glance.* J Cell Sci, 2002. **115**(Pt 20): p. 3861-3.

291. Wierzbicka-Patynowski, I. and J.E. Schwarzbauer, *The ins and outs of fibronectin matrix assembly.* J Cell Sci, 2003. **116**(Pt 16): p. 3269-76.

292. Williams, E.C., et al., *Conformational states of fibronectin. Effects of pH, ionic strength, and collagen binding.* J Biol Chem, 1982. **257**(24): p. 14973-8.

293. Erickson, H.P. and N.A. Carrell, *Fibronectin in extended and compact conformations. Electron microscopy and sedimentation analysis.* J Biol Chem, 1983. **258**(23): p. 14539-44.

294. Rocco, M., et al., *Dependence of the shape of the plasma fibronectin molecule on solvent composition. Ionic strength and glycerol content.* J Biol Chem, 1983. **258**(23): p. 14545-9.

295. Johnson, K.J., et al., *The compact conformation of fibronectin is determined by intramolecular ionic interactions.* J Biol Chem, 1999. **274**(22): p. 15473-9.

296. George, E.L., et al., *Defects in mesoderm, neural tube and vascular development in mouse embryos lacking fibronectin.* Development, 1993. **119**(4): p. 1079-91.

297. George, E.L., H.S. Baldwin, and R.O. Hynes, *Fibronectins are essential for heart and blood vessel morphogenesis but are dispensable for initial specification of precursor cells.* Blood, 1997. **90**(8): p. 3073-81.

298. ffrench-Constant, C., *Alternative splicing of fibronectin--many different proteins but few different functions.* Exp Cell Res, 1995. **221**(2): p. 261-71.

299. Kosmehl, H., A. Berndt, and D. Katenkamp, *Molecular variants of fibronectin and laminin: structure, physiological occurrence and histopathological aspects.* Virchows Arch, 1996. **429**(6): p. 311-22.

300. Asaga, H., S. Kikuchi, and K. Yoshizato, *Collagen gel contraction by fibroblasts requires cellular fibronectin but not plasma fibronectin.* Exp Cell Res, 1991. **193**(1): p. 167-74.

301. Wilson, C.L. and J.E. Schwarzbauer, *The alternatively spliced V region contributes to the differential incorporation of plasma and cellular fibronectins into fibrin clots.* J Cell Biol, 1992. **119**(4): p. 923-33.

302. Saren, A., et al., *The cellular form of human fibronectin as an adhesion target for the S fimbriae of meningitis-associated Escherichia coli.* Infect Immun, 1999. **67**(5): p. 2671-6.

303. Sakai, T., et al., *Plasma fibronectin supports neuronal survival and reduces brain injury following transient focal cerebral ischemia but is not essential for skin-wound healing and hemostasis.* Nat Med, 2001. **7**(3): p. 324-30.

304. Zand, L., et al., *Differential effects of cellular fibronectin and plasma fibronectin on ovarian cancer cell adhesion, migration, and invasion.* In Vitro Cell Dev Biol Anim, 2003. **39**(3-4): p. 178-82.

305. Schwarzbauer, J.E., et al., *Multiple sites of alternative splicing of the rat fibronectin gene transcript.* Embo J, 1987. **6**(9): p. 2573-80.

306. Peters, J.H., et al., *Expression of the alternatively spliced EIIIB segment of fibronectin.* Cell Adhes Commun, 1995. **3**(1): p. 67-89.

307. Matsui, S., et al., *Expression, localization and alternative splicing pattern of fibronectin messenger RNA in fibrotic human liver and hepatocellular carcinoma.* J Hepatol, 1997. **27**(5): p. 843-53.

308. Manabe, R., N. Oh-e, and K. Sekiguchi, *Alternatively spliced EDA segment regulates fibronectin-dependent cell cycle progression and mitogenic signal transduction.* J Biol Chem, 1999. **274**(9): p. 5919-24.

309. Sechler, J.L., et al., *A novel RGD-independent fibronectin assembly pathway initiated by alpha4beta1 integrin binding to the alternatively spliced V region.* J Cell Sci, 2000. **113 (Pt 8)**: p. 1491-8.

310. Fukuda, T., et al., *Mice lacking the EDB segment of fibronectin develop normally but exhibit reduced cell growth and fibronectin matrix assembly in vitro.* Cancer Res, 2002. **62**(19): p. 5603-10.

311. Komoriya, A., et al., *The minimal essential sequence for a major cell type-specific adhesion site (CS1) within the alternatively spliced type III connecting segment domain of fibronectin is leucine-aspartic acid-valine.* J Biol Chem, 1991. **266**(23): p. 15075-9.

312. Humphries, M.J., et al., *Identification of an alternatively spliced site in human plasma fibronectin that mediates cell type-specific adhesion.* J Cell Biol, 1986. **103**(6 Pt 2): p. 2637-47.

313. Mould, A.P., et al., *The CS5 peptide is a second site in the IIICS region of fibronectin recognized by the integrin alpha 4 beta 1. Inhibition of alpha 4 beta 1 function by RGD peptide homologues.* J Biol Chem, 1991. **266**(6): p. 3579-85.

314. Jongewaard, I.N., P.M. Tsai, and J.W. Smith, *The type III connecting segment of fibronectin contains an aspartic acid residue that regulates the rate of binding to integrin alpha 4 beta 1.* Cell Adhes Commun, 1996. **3**(6): p. 487-95.

315. Mostafavi-Pour, Z., et al., *Identification of a novel heparin-binding site in the alternatively spliced IIICS region of fibronectin: roles of integrins and proteoglycans in cell adhesion to fibronectin splice variants.* Matrix Biol, 2001. **20**(1): p. 63-73.

316. Matsuura, H. and S. Hakomori, *The oncofetal domain of fibronectin defined by monoclonal antibody FDC-6: its presence in fibronectins from fetal and tumor tissues and its absence in those from normal adult tissues and plasma.* Proc Natl Acad Sci U S A, 1985. **82**(19): p. 6517-21.

317. Loridon-Rosa, B., et al., *Distribution of oncofetal fibronectin in human mammary tumors: immunofluorescence study on histological sections.* Cancer Res, 1990. **50**(5): p. 1608-12.

318. Nicolo, G., et al., *Expression of tenascin and of the ED-B containing oncofetal fibronectin isoform in human cancer.* Cell Differ Dev, 1990. **32**(3): p. 401-8.

319. Inufusa, H., et al., *Localization of oncofetal and normal fibronectin in colorectal cancer. Correlation with histologic grade, liver metastasis, and prognosis.* Cancer, 1995. **75**(12): p. 2802-8.

320. Midulla, M., et al., *Source of oncofetal ED-B-containing fibronectin: implications of production by both tumor and endothelial cells.* Cancer Res, 2000. **60**(1): p. 164-9.

321. Matsuura, H., T. Greene, and S. Hakomori, *An alpha-N-acetylgalactosaminylation at the threonine residue of a defined peptide sequence creates the oncofetal peptide epitope in human fibronectin.* J Biol Chem, 1989. **264**(18): p. 10472-6.

322. Matsuura, H., et al., *The oncofetal structure of human fibronectin defined by monoclonal antibody FDC-6. Unique structural requirement for the antigenic specificity provided by a glycosylhexapeptide.* J Biol Chem, 1988. **263**(7): p. 3314-22.

323. Velling, T., et al., *Polymerization of type I and III collagens is dependent on fibronectin and enhanced by integrins alpha 11beta 1 and alpha 2beta 1.* J Biol Chem, 2002. **277**(40): p. 37377-81.

324. Sottile, J. and D.C. Hocking, *Fibronectin polymerization regulates the composition and stability of extracellular matrix fibrils and cell-matrix adhesions.* Mol Biol Cell, 2002. **13**(10): p. 3546-59.

325. Engvall, E. and E. Ruoslahti, *Binding of soluble form of fibroblast surface protein, fibronectin, to collagen.* Int J Cancer, 1977. **20**(1): p. 1-5.

326. Taliana, L., et al., *Vitronectin or fibronectin is required for corneal fibroblast-seeded collagen gel contraction.* Invest Ophthalmol Vis Sci, 2000. **41**(1): p. 103-9.

327. Nakamura, Y., et al., *Permissive effect of fibronectin on collagen gel contraction mediated by bovine trabecular meshwork cells.* Invest Ophthalmol Vis Sci, 2003. **44**(10): p. 4331-6.

328. Woodley, D.T., et al., *Collagen telopeptides (cross-linking sites) play a role in collagen gel lattice contraction.* J Invest Dermatol, 1991. **97**(3): p. 580-5.

329. Redden, R.A. and E.J. Doolin, *Collagen crosslinking and cell density have distinct effects on fibroblast-mediated contraction of collagen gels.* Skin Res Technol, 2003. **9**(3): p. 290-3.

330. Hedman, K., et al., *Structure of the pericellular matrix: association of heparan and chondroitin sulfates with fibronectin-procollagen fibers.* Cell, 1982. **28**(3): p. 663-71.

331. Li, S., et al., *Vascular smooth muscle cells orchestrate the assembly of type I collagen via alpha2beta1 integrin, RhoA, and fibronectin polymerization.* Am J Pathol, 2003. **163**(3): p. 1045-56.

332. Engvall, E., E. Ruoslahti, and E.J. Miller, *Affinity of fibronectin to collagens of different genetic types and to fibrinogen.* J Exp Med, 1978. **147**(6): p. 1584-95.

333. Chiquet-Ehrismann, R., et al., *Tenascin variants: differential binding to fibronectin and distinct distribution in cell cultures and tissues.* Cell Regul, 1991. **2**(11): p. 927-38.

334. Mumby, S.M., G.J. Raugi, and P. Bornstein, *Interactions of thrombospondin with extracellular matrix proteins: selective binding to type V collagen.* J Cell Biol, 1984. **98**(2): p. 646-52.

335. Taipale, J., et al., *Latent transforming growth factor-beta 1 and its binding protein are components of extracellular matrix microfibrils.* J Histochem Cytochem, 1996. **44**(8): p. 875-89.

336. Yamada, K.M., et al., *Characterization of fibronectin interactions with glycosaminoglycans and identification of active proteolytic fragments.* J Biol Chem, 1980. **255**(13): p. 6055-63.

337. Fushida-Takemura, H., et al., *Detection of lysyl oxidase gene expression in rat skin during wound healing.* Arch Dermatol Res, 1996. **288**(1): p. 7-10.

338. Siegel, R.C., *Lysyl oxidase.* Int Rev Connect Tissue Res, 1979. **8**: p. 73-118.

339. Feres-Filho, E.J., G.B. Menassa, and P.C. Trackman, *Regulation of lysyl oxidase by basic fibroblast growth factor in osteoblastic MC3T3-E1 cells.* J Biol Chem, 1996. **271**(11): p. 6411-6.

340. Shanley, C.J., et al., *Transforming growth factor-beta 1 increases lysyl oxidase enzyme activity and mRNA in rat aortic smooth muscle cells.* J Vasc Surg, 1997. **25**(3): p. 446-52.

341. Hong, H.H., et al., *Regulation of lysyl oxidase, collagen, and connective tissue growth factor by TGF-beta1 and detection in human gingiva.* Lab Invest, 1999. **79**(12): p. 1655-67.

342. Ravid, K., et al., *Upregulation of lysyl oxidase in vascular smooth muscle cells by cAMP: role for adenosine receptor activation.* J Cell Biochem, 1999. **75**(1): p. 177-85.

343. Hong, H.H. and P.C. Trackman, *Cytokine regulation of gingival fibroblast lysyl oxidase, collagen, and elastin.* J Periodontol, 2002. **73**(2): p. 145-52.

344. Palamakumbura, A.H., P. Sommer, and P.C. Trackman, *Autocrine growth factor regulation of lysyl oxidase expression in transformed fibroblasts.* J Biol Chem, 2003. **278**(33): p. 30781-7.

345. Harlow, C.R., et al., *Lysyl Oxidase Gene Expression and Enzyme Activity in the Rat Ovary: Regulation by Follicle-Stimulating Hormone, Androgen, and Transforming Growth Factor-beta Superfamily Members in Vitro.* Endocrinology, 2003. **144**(1): p. 154-62.

346. Botney, M.D., et al., *Extracellular matrix protein gene expression in atherosclerotic hypertensive pulmonary arteries.* Am J Pathol, 1992. **140**(2): p. 357-64.

347. Farhadian, F., et al., *Fibronectin and basement membrane in cardiovascular organogenesis and disease pathogenesis.* Cardiovasc Res, 1996. **32**(3): p. 433-42.

348. Naito, M., et al., *Substrate-bound fibrinogen, fibrin and other cell attachment-promoting proteins as a scaffold for cultured vascular smooth muscle cells.* Atherosclerosis, 1992. **96**(2-3): p. 227-34.

349. Thyberg, J. and A. Hultgardh-Nilsson, *Fibronectin and the basement membrane components laminin and collagen type IV influence the phenotypic properties of subcultured rat aortic smooth muscle cells differently.* Cell Tissue Res, 1994. **276**(2): p. 263-71.

350. Thyberg, J., et al., *Phenotypic modulation of smooth muscle cells after arterial injury is associated with changes in the distribution of laminin and fibronectin.* J Histochem Cytochem, 1997. **45**(6): p. 837-46.

351. Labat-Robert, J., et al., *Comparative distribution patterns of type I and III collagens and fibronectin in human arteriosclerotic aorta.* Pathol Biol (Paris), 1985. **33**(4): p. 261-5.

352. Dubin, D., et al., *Balloon catheterization induced arterial expression of embryonic fibronectins.* Arterioscler Thromb Vasc Biol, 1995. **15**(11): p. 1958-67.

353. Gabler, U., et al., *Matrix remodelling in dilated cardiomyopathy entails the occurrence of oncofetal fibronectin molecular variants.* Heart, 1996. **75**(4): p. 358-62.

354. Kim, S., et al., *Angiotensin II type 1 receptor blockade inhibits the expression of immediate-early genes and fibronectin in rat injured artery.* Circulation, 1995. **92**(1): p. 88-95.

355. Vaheri, A., J. Keski-Oja, and T. Vartio, *Fibronectin and malignant transformation*, in *Fibronectin*, D. Mosher, Editor. 1989, Academic Press, Inc.: San Diego. p. 255-271.

356. Yamada, K.M., S.H. Ohanian, and I. Pastan, *Cell surface protein decreases microvilli and ruffles on transformed mouse and chick cells.* Cell, 1976. **9**(2): p. 241-5.

357. Yamada, K.M., S.S. Yamada, and I. Pastan, *Cell surface protein partially restores morphology, adhesiveness, and contact inhibition of movement to transformed fibroblasts.* Proc Natl Acad Sci U S A, 1976. **73**(4): p. 1217-21.

358. Vaheri, A., et al., *Fibronectin and the pericellular matrix of normal and transformed adherent cells.* Ann N Y Acad Sci, 1978. **312**: p. 343-53.

359. Labat-Robert, J., *Fibronectin in malignancy.* Semin Cancer Biol, 2002. **12**(3): p. 187-95.

360. De Petro, G., et al., *Transformation-enhancing activity of gelatin-binding fragments of fibronectin.* Proc Natl Acad Sci U S A, 1981. **78**(8): p. 4965-9.

361. Vartio, T., et al., *Fibronectin and its proteolytic fragments. Potential as cancer markers.* Invasion Metastasis, 1983. **3**(3): p. 125-38.

362. McCarthy, J.B., S.T. Hagen, and L.T. Furcht, *Human fibronectin contains distinct adhesion- and motility-promoting domains for metastatic melanoma cells.* J Cell Biol, 1986. **102**(1): p. 179-88.

363. Zardi, L., et al., *Transformed human cells produce a new fibronectin isoform by preferential alternative splicing of a previously unobserved exon.* Embo J, 1987. **6**(8): p. 2337-42.

364. Karelina, T.V. and A.Z. Eisen, *Interstitial collagenase and the ED-B oncofetal domain of fibronectin are markers of angiogenesis in human skin tumors.* Cancer Detect Prev, 1998. **22**(5): p. 438-44.

365. Kaczmarek, J., et al., *Distribution of oncofetal fibronectin isoforms in normal, hyperplastic and neoplastic human breast tissues.* Int J Cancer, 1994. **59**(1): p. 11-6.

366. Smith, D.B. and K.S. Johnson, *Single-step purification of polypeptides expressed in Escherichia coli as fusions with glutathione S-transferase.* Gene, 1988. **67**(1): p. 31-40.

367. Mould, P., *Solid phase assays for studying ECM protein-protein interactions*, in *Extracellular Matrix Protocols*, C.H. Streuli and M. Grant, Editors. 2000, Humana Press: Totowa, NJ. p. 295-299.

368. Jung, S.T., et al., *Purification of enzymatically active human lysyl oxidase and lysyl oxidase-like protein from Escherichia coli inclusion bodies.* Protein Expr Purif, 2003. **31**(2): p. 240-6.

369. Einarson, M.B. and J.R. Orlinick, *Identification of protein-protein interactions with glutathione-S-transferase fusion proteins*, in *Protein-protein interactions*, E. Golemis, Editor. 2002, Cold Spring Harbor Laboratory Press: Cold Spring Harbor. p. 37-57.

370. Adams, P.D., S. Seeholzer, and M. Ohh, *Identification of associated proteins by coimmunoprecipitation*, in *Protein-protein interactions*, E. Golemis, Editor. 2002, Cold Spring Harbor Laboratory Press: Cold Spring Harbor. p. 59-74.

371. Ouzzine, M., A. Boyd, and D.J. Hulmes, *Expression of active, human lysyl oxidase in Escherichia coli.* FEBS Lett, 1996. **399**(3): p. 215-9.

372. Blackwood, E.M. and R.N. Eisenman, *Max: a helix-loop-helix zipper protein that forms a sequence-specific DNA-binding complex with Myc.* Science, 1991. **251**(4998): p. 1211-7.

373. Kaelin, W.G., Jr., et al., *Expression cloning of a cDNA encoding a retinoblastoma-binding protein with E2F-like properties.* Cell, 1992. **70**(2): p. 351-64.

374. Yamada, K., *Fibronectin domains and receptors*, in *Fibronectin*, D. Mosher, Editor. 1989, Academic Press, Inc.: San Diego. p. 48-121.

375. Mosher, D.F. and P.E. Schad, *Cross-linking of fibronectin to collagen by blood coagulation Factor XIIIa.* J Clin Invest, 1979. **64**(3): p. 781-7.

376. Mosher, D.F., P.E. Schad, and H.K. Kleinman, *Inhibition of blood coagulation factor XIIIa-mediated cross-linking between fibronectin and collagen by polyamines.* J Supramol Struct, 1979. **11**(2): p. 227-35.

377. Trackman, P.C. and H.M. Kagan, *Nonpeptidyl amine inhibitors are substrates of lysyl oxidase.* J Biol Chem, 1979. **254**(16): p. 7831-6.

378. Trackman, P.C., C.G. Zoski, and H.M. Kagan, *Development of a peroxidase-coupled fluorometric assay for lysyl oxidase.* Anal Biochem, 1981. **113**(2): p. 336-42.

379. Palamakumbura, A.H. and P.C. Trackman, *A fluorometric assay for detection of lysyl oxidase enzyme activity in biological samples.* Anal Biochem, 2002. **300**(2): p. 245-51.

380. Atkins, P.W., *Molecules*. 1987, New York: W.H. Freeman and Company.

381. Kagan, H.M., et al., *Purification and properties of four species of lysyl oxidase from bovine aorta.* Biochem J, 1979. **177**(1): p. 203-14.

382. Erickson, H.P., N. Carrell, and J. McDonagh, *Fibronectin molecule visualized in electron microscopy: a long, thin, flexible strand.* J Cell Biol, 1981. **91**(3 Pt 1): p. 673-78.

383. Fischer, H., I. Polikarpov, and A.F. Craievich, *Average protein density is a molecular-weight-dependent function.* Protein Sci, 2004. **13**(10): p. 2825-8.

384. Saoncella, S., et al., *Syndecan-4 signals cooperatively with integrins in a Rho-dependent manner in the assembly of focal adhesions and actin stress fibers.* Proc Natl Acad Sci U S A, 1999. **96**(6): p. 2805-10.

385. Kostin, S., et al., *The internal and external protein scaffold of the T-tubular system in cardiomyocytes.* Cell Tissue Res, 1998. **294**(3): p. 449-60.

386. Hagg, P., et al., *Type XIII collagen: a novel cell adhesion component present in a range of cell-matrix adhesions and in the intercalated discs between cardiac muscle cells.* Matrix Biol, 2001. **19**(8): p. 727-42.

387. Forastieri, H. and K.C. Ingham, *Fluid-phase interaction between human plasma fibronectin and gelatin determined by fluorescence polarization assay.* Arch Biochem Biophys, 1983. **227**(2): p. 358-66.

388. Leighton, M. and K.E. Kadler, *Paired basic/Furin-like proprotein convertase cleavage of Pro-BMP-1 in the trans-Golgi network.* J Biol Chem, 2003. **278**(20): p. 18478-84.

389. Takahara, K., G.E. Lyons, and D.S. Greenspan, *Bone morphogenetic protein-1 and a mammalian tolloid homologue (mTld) are encoded by alternatively spliced transcripts which are differentially expressed in some tissues.* J Biol Chem, 1994. **269**(51): p. 32572-8.

390. Noblesse, E., et al., *Lysyl oxidase-like and lysyl oxidase are present in the dermis and epidermis of a skin equivalent and in human skin and are associated to elastic fibers.* J Invest Dermatol, 2004. **122**(3): p. 621-30.

391. Rennard, S.I. and R.G. Crystal, *Fibronectin in human bronchopulmonary lavage fluid. Elevation in patients with interstitial lung disease.* J Clin Invest, 1982. **69**(1): p. 113-22.

392. Bae, E., T. Sakai, and D.F. Mosher, *Assembly of exogenous fibronectin by fibronectin-null cells is dependent on the adhesive substrate.* J Biol Chem, 2004. **279**(34): p. 35749-59.

393. Shi, Y., *Caspase activation, inhibition, and reactivation: a mechanistic view.* Protein Sci, 2004. **13**(8): p. 1979-87.

394. Philchenkov, A., *Caspases: potential targets for regulating cell death.* J Cell Mol Med, 2004. **8**(4): p. 432-44.

395. Balbona, K., et al., *Fibulin binds to itself and to the carboxyl-terminal heparin-binding region of fibronectin.* J Biol Chem, 1992. **267**(28): p. 20120-5.

396. Roman, J. and J.A. McDonald, *Fibulin's organization into the extracellular matrix of fetal lung fibroblasts is dependent on fibronectin matrix assembly.* Am J Respir Cell Mol Biol, 1993. **8**(5): p. 538-45.

397. Godyna, S., D.M. Mann, and W.S. Argraves, *A quantitative analysis of the incorporation of fibulin-1 into extracellular matrix indicates that fibronectin assembly is required.* Matrix Biol, 1995. **14**(6): p. 467-77.

398. Akiri, G., et al., *Lysyl oxidase-related protein-1 promotes tumor fibrosis and tumor progression in vivo.* Cancer Res, 2003. **63**(7): p. 1657-66.

399. Rost, T., et al., *Reduction of LOX- and LOXL2-mRNA expression in head and neck squamous cell carcinomas.* Anticancer Res, 2003. **23**(2B): p. 1565-73.

400. Johansson, S. and M. Hook, *Heparin enhances the rate of binding of fibronectin to collagen.* Biochem J, 1980. **187**(2): p. 521-4.

401. Cidadao, A.J., *Interactions between fibronectin, glycosaminoglycans and native collagen fibrils: an EM study in artificial three-dimensional extracellular matrices.* Eur J Cell Biol, 1989. **48**(2): p. 303-12.

402. Mosher, D.F., *Cross-linking of plasma and cellular fibronectin by plasma transglutaminase.* Ann N Y Acad Sci, 1978. **312**: p. 38-42.

403. Mosher, D.F. and R.B. Johnson, *Specificity of fibronectin--fibrin cross-linking.* Ann N Y Acad Sci, 1983. **408**: p. 583-94.

404. Matsuka, Y.V., M.M. Migliorini, and K.C. Ingham, *Cross-linking of fibronectin to C-terminal fragments of the fibrinogen alpha-chain by factor XIIIa.* J Protein Chem, 1997. **16**(8): p. 739-45.

405. Prockop, D.J., A.L. Sieron, and S.W. Li, *Procollagen N-proteinase and procollagen C-proteinase. Two unusual metalloproteinases that are essential for procollagen processing probably have important roles in development and cell signaling.* Matrix Biol, 1998. **16**(7): p. 399-408.

406. Dzamba, B.J., et al., *Fibronectin binding site in type I collagen regulates fibronectin fibril formation.* J Cell Biol, 1993. **121**(5): p. 1165-72.

407. Lusis, A.J., *Atherosclerosis.* Nature, 2000. **407**(6801): p. 233-41.

408. Colvin, R.B., *Fibronectin in wound healing*, in *Fibronectin*, D. Mosher, Editor. 1989, Academic Press, Inc.: San Diego. p. 213-254.

409. Muro, A.F., et al., *Regulated splicing of the fibronectin EDA exon is essential for proper skin wound healing and normal lifespan.* J Cell Biol, 2003. **162**(1): p. 149-60.

410. Knowlton, A.A., et al., *Rapid expression of fibronectin in the rabbit heart after myocardial infarction with and without reperfusion.* J Clin Invest, 1992. **89**(4): p. 1060-8.

411. Carsons, S., B.B. Lavietes, and H.S. Diamond, *Role of fibronectin in rheumatic diseases*, in *Fibronectin*, D. Mosher, Editor. 1989, Academic Press, Inc.: San Diego. p. 327-361.

412. Oberley, T.D. and J. Murphy-Ullrich, *Fibronectin and the kidney*, in *Fibronectin*, D. Mosher, Editor. 1989, Academic Press, Inc.: San Diego. p. 309-326.

413. McDonald, J.A., *Fibronectin in the lung*, in *Fibronectin*, D. Mosher, Editor. 1989, Academic Press, Inc.: San Diego. p. 363-393.